DYNAMIC MODELLING OF ROCK FRACTURING BY DESTRESS BLASTING

By
Mani Ram Saharan
Department of Mining, Metals and Materials Engineering
McGill University, Montreal
May 2004

A thesis submitted to McGill University in partial fulfilment of the requirements of the degree of Doctor of Philosophy in Mining Engineering

Your file Votre référence
ISBN: 0-612-98370-6
Our file Notre référence
ISBN: 0-612-98370-6

"Greater skill is needed to avoid high rock loading than to oppose it."

Rziha*, 1872

* - The renowned 19th century German tunnelling engineer

Abstract

Rockburst control measures have been in practice with continued efforts for improvements since the beginning of the 20^{th} century. The thesis concentrates on the evaluation of destress blasting, which is an important pro-active rockburst control measure. The concept of destress blasting is based on the fracturing of highly stressed rock mass by detonating explosive charge within it. The concept has been carried out ever since the first reported use in a Canadian coal mine circa in the early 1930s. Since then, many mines across the continents have applied this technique using a trial-and-error approach with mixed successes. To date, the application lacks scientific base.

The aim of this thesis is to identify the governing mechanisms associated with destress blasting applications. A holistic approach is undertaken, which involves a critical analysis of the reported field evidences, development of a numerical procedure and detailed investigations at the micro-mechanical level to investigate the fracturing of rock under confinement by different types and magnitudes of explosive energy.

A numerical procedure is developed in the thesis that carries promising potential to improve the understanding on rock fracturing by explosive energy as well as provides a platform to develop means for enhancing explosive energy utilization. The procedure is validated with reported field observations.

Analyses of destress blasting is made through dynamic modelling by simulating discrete fractures using the developed procedure. A normalized parameter ℓ_{ci} is introduced to investigate fracturing extent after destress blasts. The investigations revealed that destress blasting produces limited fractures aligned along the principal stresses. The fracturing extent reduces with the increase in the confinement. The study indicates that the current practice of destress blasting seemingly provides more psychological benefits than factual benefits from the desired destressing.

The study also introduces a non-dimensional parameter, β_{ij}, which characterizes destressing effects. The parameter not only adequately explains destressing phenomenon, but also offers clarifications to seemingly inexplicable reported field observations of destress blasting. Local fractures around the boreholes aligned along the principal stresses are found to be the cause of reported local stress concentration and rock stiffening post to destress blasting against the desired stress relaxation and softening.

Sommaire

Les mesures de contrôle de coup de terrain sont utilisées depuis le début du 20ème siècle grâce aux efforts continus pour les améliorer. Cette thèse se concentre sur l'évaluation de la méthode tirs de relaxation, qui est une mesure de contrôle proactive importante contre le coup de terrain. Ce concept est basé sur la rupture du massif rocheux, qui est soumis aux fortes contraintes, en détonant une charge explosive. La première utilisation documentée de cette technique à la mine de charbon canadienne Circa date des années 30. Depuis lors, beaucoup de mines à travers le monde ont appliqué la technique en utilisant une approche par essai et erreur qui a donné des résultats mitigés. À_ce jour, la base scientifique du tirs de relaxation n'existe pas.

Cette thèse vise à identifier les mécanismes impliqués dans les tirs de relaxation. Une approche holistique est utilisée, celle ci comporte l'analyse critique de données de terrain, le développement d'un procédé expérimental et d'investigations détaillées, au niveau micromécanique, pour étudier la rupture de la roche sous confinement pour différents types d'explosifs et de niveaux d'énergie.

Une procédure numérique est développée dans la thèse. Celle-ci offre le potentiel d'améliorer la compréhension de la fracturation de la roche par l'énergie d'explosif ainsi que fournir une plateforme pour développer des moyens d'augmenter l'utilisation del'énergie explosive. La procédure est validée par des observations de terrain disponibles dans la littérature.

L'analyse de tirs de relaxation est faite par modélisation dynamique de ruptures discrètes en utilisant la procédure numérique développée dans le cadre de cette recherche. Un paramètre normalisé ℓ_{ci} est introduit pour étudier la fracturation lors d'un tir de relaxation. Les investigations ont indiqué que les tirs de relaxation produisent des ruptures qui sont alignées le long des contraintes principales. La longueur de ces ruptures

diminue avec l'augmentation du confinement. L'étude indique également que la pratique en vigueur des tirs de relaxation semble donner des avantages plutôt psychologiques que physiques.

Dans le cadre de cette étude, un nouveau paramètre non dimensionnel, β_{ij}, est présenté; il permet de caractériser les effets de relaxation. Le paramètre explique non seulement en juste proportion le phénomène de relaxation des contraintes mais offre également des éclaircissements sur certaines observations de terrain qui semblaient en apparence inexplicables. Lors d'un essai de tir de relaxation, les ruptures localisées se forment autour du forage. Elles-ci sont aligne le long des contraintes principales et sont la cause de concentrations des contraintes localisées, ce qui induit l'effet raidissant du massif rocheux, le tout a l'encontae de l'objectif vis par les tirs de relaxation.

Acknowledgements

It is my great pleasure to express my sincerest gratitude to all individuals and institutions, whom extended their kind support during my research work. The thesis is the product of their good wishes, kind support and able supervision. The support I received was so mighty that I am finding it very difficult to express their kindness in such a tiny place; still a humble attempt is made through the following paragraphs.

The thesis is an extension of consistent hard work of several years by Professor Hani S. Mitri, the thesis supervisor. Not only, did he furnish all relevant publications from his collection of several years, but was also involved at every moment to assure that the work was accomplished in an accurate and efficient manner. I feel privileged to learn from a personality who has a distinct academic knack. His teachings on several aspects of numerical modelling and rock mechanics will remain with me as a treasure.

The work done in the thesis is financially supported from many organisations. It would not have been possible to finish the work without their generous support. I express my sincerest gratitude for their benevolence. The organisations those extended their generosity are as follows: Central Mining Research Institute, India (CMRI); Natural Sciences and Engineering Research Council of Canada (NSERC); James Douglas Foundation, Canada; Faculty of Graduate Studies and Research, McGill University, Canada (FGSR, now Graduate and Postdoctoral Studies Office, GPSO) and J.W. McConnel Foundation, McGill University, Canada.

Finally, I express my sincerest gratitude to the Academic Staff of the Department for their kind encouragement throughout my studies. I would especially like to mention Professor Ferri P. Hassani, Director of the Mining Program, for his care during the studies. Kindness and cordial support extended by the administrative staff (Mrs. Carol Rousseau, Ms. Barbara Hanley, Ms. Norma Procyshyn and Ms. Marina Rosati) will always be in my memory and I am thankful to them. Assistance provided by the McGill's Library Staff in numerous forms is thankfully acknowledged.

It would be remiss on my part should I forget my parent organisation, Central Mining Research Institute, India (CMRI), and its highly qualified scientists. I will ever remain indebted to the Director General, Council of Scientific and Industrial Research, India (for granting me the permission to do this work); the Director CMRI (for forwarding my application to DG-CSIR with his kind consent); Professor Bharat B. Dhar, former Director CMRI (for providing a platform to work for Rock Mechanics problems); Dr P.R. Sheorey, former Assistant Director and Scientist of International Repute (for kindling interest for Numerical Modelling). Encouragement provided by Dr. P.K Singh, Dr. M. Verman, J.C. Jhanwar, Dr. R.K. Goel and G.M. Mohan will ever remain a treasure for me. At this moment, I cannot forget benevolence of Dr. J.L. Jethwa, former Assistant Director CMRI, and another Scientist of International Repute from the institute. This energetic personality and my mentor has always remained with me as a strong pillar and introduced me with several practical aspects of rock mechanics. His following words are always a source of inspiration and encouragement for me.

> "*Mr. Saharan, being a scientist you should not see what others are seeing, but you must see which others cannot see*".

I passed through a wonderful experience during the thesis. I received generous support from learned personalities across continents. None of these kind figures is concerned with the thesis and to most of them I never met. Even then, I received overwhelming immediate support from them despite their busy schedule. The world could have been a better place to live should it had more kind persons like mentioned here. I would like to extend special thanks to Professor James Nemes, McGill University (for providing help with Abaqus Modelling and introducing his students to extend the help); Professor P. Bettess, Professor A. Selby and Dr. C.L. Ramshaw, all from the University of Durham, UK (for furnishing important documents on Abaqus Modelling); Professor H. Einstein, MIT, USA (for sending thesis on rockburst); Professor C. Romanel from Brazil (for furnishing his publication); Professor L. Mishnaevsky Jr., University of Stuttgart, Germany (for providing valuable hints for Abaqus Modelling and resolving difficulties);

Professor Fourney, University of Maryland, USA (for furnishing his valuable publications); Professor S. Bhandari (for teaching blasting, always encouraging for higher studies and furnishing valuable documents); Professor B. Mohanty, University of Toronto, Canada (for evaluating some parts of the thesis and suggesting valuable tips for blasting input parameters); Mr. Daniel Roy, Dynonobel, Montreal (for providing borehole pressure profiles); Professor S. Sharan, Laurentian University, Canada (for providing help in resolving Numerical Modelling difficulties); Mr. Zafer Toper, CSIR Miningtek, South Africa (for furnishing destress blasting documents); Mr. J. Dunn and Mr. Sourabh Bahuguna, both from ABAQUS Great Lakes, Inc., USA (for keeping patience with my nonsense and resolving many difficulties during ABAQUS Modelling); Dr. C. Ryu, Korea Institute of Geoscience and Mineral Resources, Korea (for furnishing valuable publications); Dr. Jung, National Institute of Advanced Industrial Science and Technology, Japan (for furnishing important laboratory data); Professor J. Podgorski, Technical University of Lublin, Poland (for providing important data on rock failure criteria); Dr. Ken Liu, Noranda Technology Centre, Canada (for providing data on blasthole pressure measurements); Dr. B. Tang (for translating a Chinese publication in English), Dr. J.P. Aglawe, Acres International Ltd., Canada (for furnishing his thesis) and Professor Ravichandran, California Institute of Technology, USA (for furnishing valuable material on brittle rock failure). Assistance provided by Ben Yahia Faycal, ROI Eng, Canada, needs separate mentioning. It was due to his advise and support that ultimately proved a breakthrough in difficult time periods. This kind figure was even sitting beside me during early hours to resolve difficulties. I have never met such an expert of dynamic modelling and still too modest. It was a great pleasure to listen to his valuable tips.

Encouragement is also provided by friends at McGill: Afshin Mantegh, Shahe Shnorhokian, Afsaneh Hosseini, Raja Bhattacharya and friend of all seasons: Ravi. I thank them for providing help in many respects. Mr. Arun is thankfully acknowledged for the financial loan.

The period passed through the thesis proved to be very hard for my spouse and child. They were forced into a situation, which neither one deserves nor they were habitual. I regret for the sufferings. Also, this thesis is one of the milestones in the journey of my parents. They started their journey from a tiny village, which still lacks rudimental facilities. They worked hard so their kids can have a decent life. The thesis is dedicated to their dreams and hard efforts.

At the last, if there is any, whom I have not mentioned and they happens to and read this thesis, feel left out, I offer my sincerest apologies in advance.

Table of Contents

Abstract i
Sommaire iii
Acknowledgements v
Table of Contents ix
List of Figures xiii
List of Tables xviii
Notations xix

CHAPTER 1

INTRODUCTION 1

1.1 BACKGROUND - OVERVIEW OF ROCKBURST PHENOMENA 1

1.2 STATEMENT OF THE PROBLEM 4

1.2.1 LOCAL STRESS TRANSFER BY FRACTURING 5
1.2.2 MODIFYING ROCK MASS PROPERTIES 12
1.2.3 ROCKBURSTS TRIGGERING SIMULTANEOUS TO DESTRESS BLASTING AS A SUCCESS MEASURE 16
1.2.4 DESTRESSING AS A TRANSIENT PHENOMENON 18
1.2.5 SUITABLE EXPLOSIVE FOR EFFECTIVE DESTRESSING 19

1.3 OBJECTIVES OF THE RESEARCH 20

1.4 SCOPE OF THE RESEARCH 22

1.5 THESIS ORGANIZATION 22

CHAPTER 2

DESTRESS BLASTING – EVOLUTION, CONCEPTS AND PRACTICES IN UNDERGROUND MINES 24

2.1 DEFINITION 24

2.2 HISTORICAL BACKGROUND 24

2.3 MECHANISMS OF DESTRESS BLASTING 30

2.4 APPLICATION AREAS FOR DESTRESS BLASTING 33

2.5 BENEFITS OF DESTRESS BLASTING 35
2.6 LIMITATIONS OF DESTRESS BLASTING 35
2.7 CRITICAL REVIEW OF THREE CASE HISTORIES 36
2.7.1 STRATHCONA MINE, FALCONBRIDGE, CANADA 36
2.7.2 STAR MINE, COEUR D'ALENE MINING DISTRICT, IDAHO, USA 39
2.7.3 BRUNSWICK MINE, CANADA 44
2.8 SUMMARY 50

CHAPTER 3

FRACTURES INITIATION AND PROPAGATION IN ROCK BY EXPLOSIVE ENERGY 51

3.1 OVERVIEW 51
3.2 DYNAMIC ROCK FRACTURE MECHANISMS 52
3.3 QUANTIFICATION OF ROCK FRACTURING BY EXPLOSIVE ENERGY 66
3.4 ROCK – EXPLOSIVE ENERGY INTERACTION STUDIES 72
3.5 DYNAMIC FRACTURES INITIATION AND PROPAGATION UNDER IN-SITU STRESS FIELD 75
3.6 SUMMARY 79

CHAPTER 4

DEVELOPMENT OF A NUMERICAL PROCEDURE FOR INVESTIGATING ROCK FRACTURING BY EXPLOSIVE ENERGY 81

4.1 OVERVIEW 81
4.1.1 REVIEW OF PREVALENT PRACTICES FOR ROCK BLASTING SIMULATION 84
4.1.2 CONCLUDING REMARKS 88
4.2 DEVELOPMENT OF A NEW PROCEDURE FOR THE SIMULATION OF EXPLICIT FRACTURE NETWORK DUE TO BLASTING 94
4.2.1 SELECTION OF A PROPER NUMERICAL MODELLING TOOL 94
4.2.2 SELECTION OF AN APPROPRIATE TECHNIQUE FOR MODELLING OF ROCK FRACTURES BY EXPLOSIVE ENERGY USING ABAQUS 99
4.2.3 SETTING-UP NUMERICAL MODEL PARAMETERS SUITABLE FOR DYNAMIC ROCK FRACTURING BY THE EXPLOSIVE ENERGY 107
4.3 SAMPLE MODEL ANALYSES AND THEIR VERIFICATION 134
4.4 SUMMARY 149

CHAPTER 5

ANALYSIS OF DESTRESS BLASTING THROUGH DYNAMIC MODELLING OF DISCRETE FRACTURES 150

5.1 OVERVIEW 150

5.2 "ℓ_{ci}" – A NEW FRACTURE ZONE CHARACTERIZATION PARAMETER 153

5.3 EVALUATION OF THE EXTENT OF ROCK FRACTURING BY DESTRESS BLASTING 155

5.3.1 EFFECT OF CONFINEMENT....................155
5.3.2 EFFECT OF STRESS ANISOTROPY 160
5.3.3 EFFECT OF STRESS LEVEL 165
5.3.4 EFFECT OF BOREHOLE SPACING 168
5.3.5 EFFECT OF YOUNG'S MODULUS 175
5.3.6 EFFECT OF STATIC TENSILE STRENGTH 180
5.3.7 EFFECT OF EXPLOSIVE ENERGY CHARACTERISTICS 183
5.3.8 EFFECT OF EXPLOSIVE ENERGY MAGNITUDE 186
5.3.9 EFFECT OF DE-COUPLING OF EXPLOSIVE CHARGE 192
5.3.10 DIRECTIONAL FRACTURES GROWTH BY NOTCHED BOREHOLE 195

5.4 SUMMARY 198

CHAPTER 6

A NOVEL METHOD FOR CHARACTERIZING DESTRESSING 199

6.1 OVERVIEW 199

6.2 "β_{ij}" – THE NEW STRESS RELAXATION PARAMETER 202

6.3 SUMMARY 214

CHAPTER 7

VALIDITY AND LIMITATIONS OF THE SIMULATIONS 215

7.1 VALIDITY....................215

7.2 LIMITATIONS OF THE STUDY 219

CHAPTER 8

CONCLUSIONS **221**

8.1 CONCLUSIONS 221

8.2 LIMITATIONS 225

8.3 SCOPE OF THE FUTURE RESEARCH 226

STATEMENT OF CONTRIBUTIONS **227**

REFERENCES **229**

List of Figures

Figure 1.1 – Flowchart illustrating the classification of rockburst mechanisms 2
Figure 1.2 – Destress blasting as a rockburst control measure 3
Figure 1.3 – Idealized cross-section through a stope showing the fracture patterns that develop near stopes in deep gold mines 6
Figure 1.4- Plan-view showing eight petroscopic holes and the lateral extent of the extensional type fractures zones 7
Figure 1.5 – Damage zone identification with the pre- and post- destress blast seismic tomography in the Brunswick Mine, Canada..8
Figure 1.6 – Phase 2 preconditioning, 7900 level, Star Mine 10
Figure 1.7 – Average axial stress as a function of the average axial strain for the simulation of a biaxial test 11
Figure 1.8 – Strain gauge measurements of a test destress blast 14
Figure 1.9 – Modulus of elasticity obtained before and after a destress blasting............15
Figure 1.10 – Daily microseismicity for stope 'A', Coeur d'Alene mining district, Idaho, USA...17

Figure 2.1 - Geomechanical effects of destress blasting..26
Figure 2.2 – Current destress blasting practice in the gold mines of South Africa 28
Figure 2.3 – Typical narrow vein destress blasting applications in North American mines 29
Figure 2.4 – Applications of destress blasting 34
Figure 2.5 – Destress blasting in drifting at the Strathcona Mine...................................38
Figure 2.6 – Destressing hole pattern at the Star Mine 41
Figure 2.7 – Mining geometry, stope preconditioning and pillar destressing at the Star Mine 42
Figure 2.8 – Phase 2 preconditioning, 7900 level, Star Mine..43
Figure 2.9 – Schematic Plan view of destress blasting pillar (29-9 pillar) 46
Figure 2.10 – Schematic Longitudinal section of destress blasting pillar 47
Figure 2.11 – Schematic drilling pattern for destress blasting and instrumentation of the 29-9 pillar..47
Figure 2.12 – Stress cell measurements from the uphole and the downhole 48
Figure 2.13 - MPBX measurements from the downhole 48
Figure 2.14 – Seismic tomography of the destress blasting zone 49

Figure 3.1 – Engineering systems for rock blasting..53
Figure 3.2 – Detonation process of an explosive in a borehole 54
Figure 3.3 – Pressure pulse shapes for two categories of detonation 56
Figure 3.4 – Action of an explosive in a rock mass 58

Figure 3.5 – Radius of fractures by different explosives in different rocks....................68
Figure 3.6 – Estimated peak particle velocity as a function of distance for different linear charge densities, kg/m borehole length....................70
Figure 3.7 – Reported damage threshold with respect to peak particle velocity 71
Figure 3.8 – Explosive energy released during different phases of rock blasting 72
Figure 3.9 – Schematic energy utilization for hard and soft rocks with high order and low order detonation 74
Figure 3.10. - Photographs of marble plates after blasting. 76
Figure 3.11 – Dynamic fractures propagation under uni-axial stress field....................76
Figure 3.12 –Cross-cutting fractures concept 77
Figure 3.13 – Effect of the differential stress on the fractures length, including cross-cutting fractures....................78
Figure 3.14 – Estimated penny- and cone-shaped crack extent in rock....................78
Figure 3.15 – Dynamic fractures initiation and propagation in rocks under the confinement....................80

Figure 4.1 – Mining induced excavation stresses 108
Figure 4.2 – Schematic of the proposed plane stress 2D models with one central 38 mm diameter hole....................109
Figure 4.3 – Stresses created by an explosion pressure 111
Figure 4.4 – Rankine criterion in the deviatoric stress (S) space....................113
Figure 4.5 – Rankine criterion in plane stress space....................114
Figure 4.6 – Comparison of the different methods for approximation of the blast pressure-time profile 120
Figure 4.7 – Schematic optimized pressure-time profile of different explosives used in the study for 38 mm diameter borehole 126
Figure 4.8 – Constant stress elements used in the present study 131
Figure 4.9 – Schematic of plane stress model details for the convergence analysis......133
Figure 4.10 – Convergence analysis results....................133
Figure 4.11 – FE mesh and model boundary conditions used for the validation tests for the developed procedure 136
Figure 4.12 – Zoom-in view of the model mesh central zone showing 38 mm diameter blasthole 137
Figure 4.13 – Fractures initiation load magnitude....................138
Figure 4.14 – Fracture pattern at the peak load magnitude....................139
Figure 4.15 – Final fracture pattern 140
Figure 4.16 – The fracture pattern at the end of the calculations (2 millisecond) 141
Figure 4.17 – Kinetic, Internal and Artificial energy plots....................142
Figure 4.18 – Peak particle velocity plots (PPV in the X-axis direction)....................143
Figure 4.19 – PPV trend for two types of explosives characteristics 144

Figure 5.1 – Measurement of normalized fractures length (Schematic)........................154
Figure 5.2 – Effect of confinement level on the extent of fractures 156
Figure 5.3 – Fracture pattern with no confinement for emulsion type explosive 157
Figure 5.4 – Fracture pattern with the 200 MPa confinement for emulsion type explosive 157
Figure 5.5 – Fracture pattern with no confinement for ANFO type explosive..............158
Figure 5.6 – Fracture pattern with 200 MPa confinement for ANFO type explosive 158
Figure 5.7 – Effect of stress anisotropy on the extent of fractures (for σ_v= 100 MPa) ..161
Figure 5.8 – Fracture pattern with emulsion type explosive (σ_v = 100 MPa; σ_h = 50 MPa)...162
Figure 5.9 – Fracture pattern with emulsion type explosive (σ_v = 50 MPa; σ_h = 100 MPa)...162
Figure 5.10 – Fracture pattern with ANFO type explosive (σ_v = 100 MPa; σ_h = 50 MPa) 163
Figure 5.11 – Fracture pattern with ANFO type explosive (σ_v = 50 MPa; σ_h = 100 MPa) 163
Figure 5.12 – Fracture pattern with σ_h = 150 MPa for the emulsion type explosive......166
Figure 5.13 – Fracture pattern with σ_h = 300 MPa for the emulsion type explosive......166
Figure 5.14 – Fracture pattern with σ_h = 150 MPa for the ANFO type explosive 167
Figure 5.15 – Fracture pattern with σ_h = 300 MPa for the ANFO type explosive 167
Figure 5.16 – Schematic arrangement for the two-borehole models studies 170
Figure 5.17 – Fracture pattern from the two-borehole model aligned with the major principal stress direction for emulsion type explosive 171
Figure 5.18 – Fracture pattern from two-borehole model aligned with the intermediate principal stress direction for emulsion type explosive 172
Figure 5.19 – Fracture pattern from two-borehole model aligned with the major principal stress direction for ANFO type explosive..173
Figure 5.20 – Fracture pattern from two-borehole model aligned with the intermediate principal stress direction for ANFO type explosive..............................174
Figure 5.21 – Fracture pattern with Young's modulus = 60 GPa for emulsion type explosive 176
Figure 5.22 – Fracture pattern with Young's modulus = 50 GPa for emulsion type explosive 176
Figure 5.23 – Fracture pattern with Young's modulus = 40 GPa for emulsion type explosive 177
Figure 5.24 – Fracture pattern with Young's modulus = 30 GPa for emulsion type explosive 177
Figure 5.25 – Fracture pattern with Young's modulus = 60 GPa for ANFO type explosive 178
Figure 5.26 – Fracture pattern with Young's modulus = 50 GPa for ANFO type explosive 178
Figure 5.27 – Fracture pattern with Young's modulus = 40 GPa for ANFO type explosive 179
Figure 5.28 – Fracture pattern with Young's modulus = 30 GPa for ANFO type explosive 179

Figure 5.29 – Fracture pattern with static tensile strength = 15 MPa for emulsion type explosive 181
Figure 5.30 – Fracture pattern with static tensile strength = 5 MPa for emulsion type explosive 181
Figure 5.31 – Fracture pattern with static tensile strength = 15 MPa for ANFO type explosive 182
Figure 5.32 – Fracture pattern with static tensile strength = 5 MPa for ANFO type explosive 182
Figure 5.33 – Fracture pattern from emulsion type explosive in 38 mm diameter borehole 184
Figure 5.34 – Fracture pattern from ANFO type explosive in 38 mm diameter borehole 184
Figure 5.35 – Effect of explosive energy magnitude on the fracturing extent 187
Figure 5.36 – Fracture pattern from emulsion type explosive in 38 mm diameter borehole 188
Figure 5.37 – Fracture pattern from emulsion type explosive in 55 mm diameter borehole 188
Figure 5.38 – Fracture pattern from emulsion type explosive in 76 mm diameter borehole 189
Figure 5.39 – Fracture pattern from emulsion type explosive in 89 mm diameter borehole 189
Figure 5.40 – Fracture pattern from ANFO type explosive in 38 mm diameter borehole 190
Figure 5.41 – Fracture pattern from ANFO type explosive in 55 mm diameter borehole 190
Figure 5.42 – Fracture pattern from ANFO type explosive in 76 mm diameter borehole 191
Figure 5.43 – Fracture pattern from ANFO type explosive in 89 mm diameter borehole 191
Figure 5.44 – The concept of de-coupling 193
Figure 5.45 – Fracture pattern from fully coupled 55 mm diameter borehole by emulsion type explosive 193
Figure 5.46 – Fracture pattern from 70 per cent coupled 55 mm diameter borehole by emulsion type explosive 194
Figure 5.47 – Fracture pattern from 50 per cent coupled 55 mm diameter borehole by emulsion type explosive 194
Figure 5.48 – Initial configuration of 55 mm diameter borehole with two notches 196
Figure 5.49 – Fracture pattern by 55 mm diameter borehole with no notch and simulated with emulsion types explosive 197
Figure 5.50 – Fracture pattern by 55 mm diameter notched borehole simulated with emulsion type explosive 197

Figure 6.1 – Damage zone identification with the pre- and post- destress blast seismic tomography in the Brunswick Mine, Canada (Longitudinal-section).....200
Figure 6.2 – Measurements for the Stress Relaxation parameter, β_{ij} (Schematic, not to the scale) 204
Figure 6.3 – Stress relaxation to the σ_1 with fracture pattern generated by emulsion type explosive destress blast in 38 mm dia borehole........205
Figure 6.4 – Stress relaxation to the σ_2 with fracture pattern generated by emulsion type explosive destress blast in 38 mm dia borehole........206
Figure 6.5 – Stress relaxation to the σ_1 with fracture pattern generated by emulsion type explosive destress blast in 38 mm dia borehole........207
Figure 6.6 – Stress relaxation to the σ_2 with fracture pattern generated by emulsion type explosive destress blast in 38 mm dia borehole........208
Figure 6.7 – Stress relaxation to the σ_1 with fracture pattern generated by ANFO type explosive destress blast in 38 mm dia borehole........209
Figure 6.8 – Stress relaxation to the σ_2 with fracture pattern generated by ANFO type explosive destress blast in 38 mm dia borehole........210
Figure 6.9 – Stress relaxation to the σ_1 with fracture pattern generated by ANFO type explosive destress blast in 38 mm dia borehole........211
Figure 6.10 – Stress relaxation to the σ_2 with fracture pattern generated by ANFO type explosive destress blast in 38 mm dia borehole........212

List of Tables

TABLE 3.1 – BLASTING THEORIES AND THEIR BREAKAGE MECHANISMS...59

TABLE 3.2 – LABORATORY STUDIES FOR DYNAMIC ROCK FRACTURES MECHANISMS 61

TABLE 3.3 – PILOT FIELD STUDIES FOR DYNAMIC ROCK FRACTURES MECHANISMS 64

TABLE 3.4 – INDIRECT TECHNIQUES FOR STUDYING DYNAMIC ROCK FRACTURES MECHANISMS....................65

TABLE 4.1(A) – CONTINUUM APPROACH FOR NUMERICAL SIMULATION OF BLASTING....................89

TABLE 4.1(B) – DISCONTINUUM APPROACH FOR NUMERICAL SIMULATION OF BLASTING....................91

TABLE 4.2 – ROCK FRACTURES SIMULATION BY NUMERICAL MODELLING 105

TABLE 4.3 – TYPICAL GRANITE ROCK PROPERTIES FOR NUMERICAL MODELLING....................115

TABLE 4.4 – CHOICES FOR EXPLOSION PRESSURE-TIME PROFILE AS A NUMERICAL MODELLING INPUT PARAMETER....................118

TABLE 4.5 – DETAILS OF EXPLOSIVE PROPERTIES FOR BOREHOLE PRESSURE CALCULATIONS 122

TABLE 4.6 – ESTIMATED BOREHOLE PRESSURE VALUES 122

TABLE 4.7 - DETAILS OF FRACTURES ZONE CALCULATIONS FOR EMULSION TYPE EXPLOSIVES....................123

TABLE 4.8 - DETAILS OF FRACTURES ZONE CALCULATIONS FOR ANFO TYPE EXPLOSIVES....................124

Notations

β_{ij} = Stress relaxation parameter (i = 1,2,3; j =x,y,z)

[B] = Strain-displacement matrix

[C] = Damping matrix

[D] = Constitutive matrix

C_p, C_d, P = Longitudinal wave velocity

C_s, S = Transverse wave velocity

ε =Strain

E = Young's modulus of elasticity

ϕ, d_b =Borehole diameter

γ = Adiabatic exponent

k = Stress ratio

[K] = Stiffness matrix

$\hat{\lambda}$ and $\hat{\mu}$ = Effective Lame constants

ℓ_{cri} = Fractures length along the major principal stresses (i = 1,2,3)

ℓ_{ci} = Normalized fractures length along the major principal stresses (i =1,2,3)

[M] = Mass matrix

ν = Poisson's ratio

[N] = Shape function matrix

P_b = Borehole pressure

P_d = Detonation pressure

P_e = Explosion pressure

PPV = Peak particle velocity

q =Explosive weight, TNT equivalent

Q = Rock quality designation

Q = Heat of explosion of the explosive

R = Rayliegh wave velocity

r_c = Coupling ratio

r_{cr} = Crushed zone radius

r_f = Fracture zone radius

r_s = Seismic zone radius

RMR = Rock mass rating

S_i = Deviatoric stresses (i = 1,2,3)

ρ = Mass density

σ_i = The principal stresses (i =1,2,3)

σ_v = The vertical principal stress

σ_H = The horizontal principal stress

UCS, σ_c = Uniaxial compressive strength

σ_t = Tensile strength

VOD, V_d = Velocity of detonation

u = Displacement

$\dot{u}$ = Velocity

$\ddot{u}$ = Acceleration

CHAPTER 1

INTRODUCTION

1.1 BACKGROUND - OVERVIEW OF ROCKBURST PHENOMENA

The mining industry is still facing problems of rockbursts since they first reported it in an Indian gold mine at the end of the 19th century (Morrison, 1942, Blake, 1972a). Since then, there has been a worldwide increase in the reported incidences of rockbursts as mining operations reached deeper ore deposits with higher extraction ratios due to economic pressures. Geologic conditions affecting local stresses can create rockburst hazards at any mining depth (Johnston and Einstein, 1990) and rockbursts have been recorded at depths as shallow as 30 to 50m (Brauner, 1994). However, the severity, frequency and intensity of rockbursts increase with the depth (Brauner, 1994, Nakajima and Watanabe, 1981).

Intensive research has been carried out to identify the root causes and to develop means of controlling or eliminating rockbursts. The studies resulted in a better understanding of brittle rock failure characteristics as well as formulation and implementation of energy theories (e.g. see Simon, 1999 and Tang, 2000 for the detailed review). Such studies have led to a better understanding of the different types of rockbursts and their causative mechanisms. Figure 1.1 presents rockburst classification as proposed by Brown (1984) and later accepted by the Canada Rockburst Research Program (CRRP, 1996).

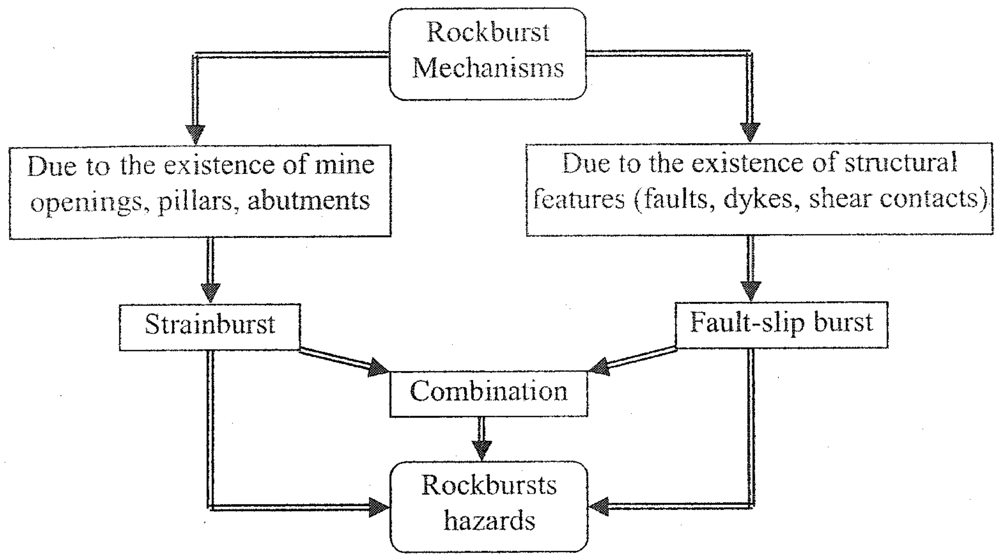

Figure 1.1 – Flowchart illustrating the classification of rockburst mechanisms (CRRP, 1996)

While much has been learn about rockbursts, their prediction is still a mystery. Contributory factors to rockbursts (high stresses, stiff rock strata, rapid mining cycles and larger excavation area) are known but their triggering mechanism and likelihood of triggering time period cannot be predicted. Therefore, much attention has and is being paid to the development of rockburst control and containment measures (Figure 1.2). However, it appears that the application of rockburst control measures seemingly provide only psychological advantages as rockburst triggering mechanisms are hitherto unknown. It has always been a challenge to guarantee that a rockburst control measure application will achieve the desired objectives and it is to date elusive to deterministically claim that the rockburst control measure has achieved the desired objectives. Rockbursts continue to occur despite the improvements in the rockburst control measures application.

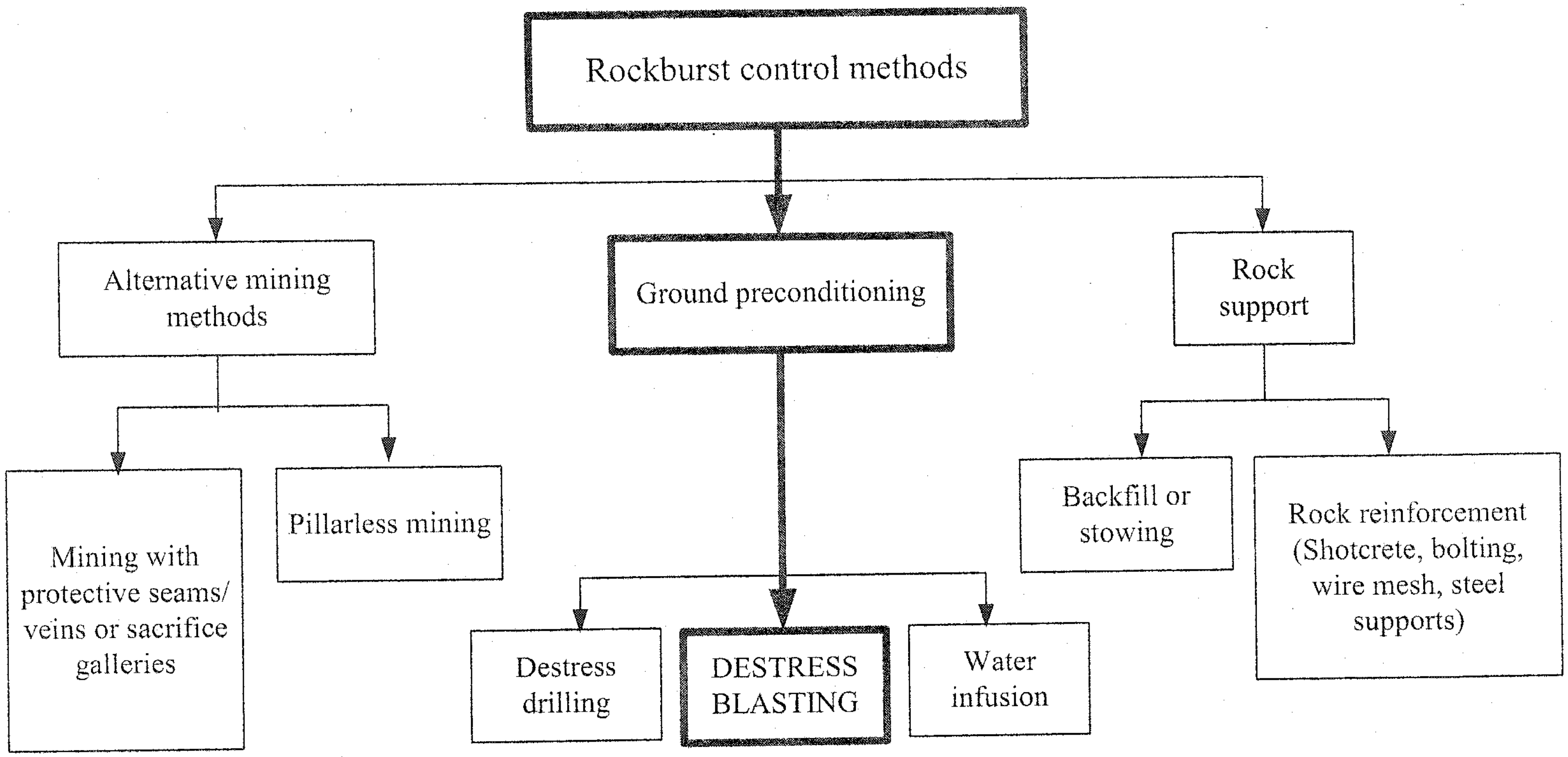

Figure 1.2 – Destress blasting as a rockburst control measure
(Modified after Mitri, 2000)

Figure 1.2 indicates that destress blasting is one of the important pro-active rockburst control measures. The method was conceived and first applied to a Canadian coal mine (McInnes et al., 1959). Since then, the method has been applied (with modifications to suit various mining environments) and is currently being practiced in several underground mines around the world.

The current research aims to evaluate destress blasting mechanism(s). The focus of the research is the application of destress blasting to contain the strain bursting phenomenon. Also, the focus is only concentrated on destress blasting applications used for drift development cases of hard rock underground mines in the Canadian Shield. However, The thesis reviews destress blasting practice as applied to other parts of deep underground hard rock mines.

1.2 STATEMENT OF THE PROBLEM

Field application of destress blasting is full of contradictions even after over 80 years of the first reported application in the early 1930s for Springhill colliery, Canada (McInnes et al., 1959). The lack of knowledge related to the governing mechanisms together with an effective assessment tool resulted in the abandonment of the destress blasting practice by the Swedish (Taube et al., 1991), re-thinking its use and concepts by the South Africans (Toper et al., 1997), mining method transformation in the silver producing mines, Idaho, USA (Williams and Cuvellier, 1988) and using it only as a last resort measure in Canada. The contradictions associated with the apparent success stories are appraised through the following sub-sections.

1.2.1 Local Stress Transfer by Fracturing

It is postulated that destress blasting induces fractures in the rock mass (Roux et al., 1957). This fracturing results in local readjustment of stresses by transferring them to a non-fractured zone ahead of the destressing zone. However, the field application is full of contradictory evidence.

Studies done along with the revival of destress blasting in South Africa could neither reveal new fractures nor an effective extensions of the existing fractures (Adams and Jager, 1980; Brummer and Rorke, 1984). These studies indicate changes in the characteristics of the pre-existing fractures (more gouge filling after the blasting) rather than the extension. Their finding is limited to the near face extensional failures (Napier et al., 1997), a universal failure characteristic around an underground opening due to the bi-axial mining induced stresses. Figures 1.3 and 1.4 depict systematic fracture patterns around the stope face as per the South African experiences. Systematic investigations including RQD (Rock Quality Designation, a measure to characterize the rock mass by measuring fracturing with the core logs) measurements and petroscopy in Pyhäsalmi Mine, Finland also indicate no radial fractures created by destress blasting beyond 1.4m lateral to 89 mm diameter holes charged up to 60 kg of explosives (Hakami et al., 1990). The most recent, well documented, Canadian experience based on borehole endoscopy and cross-examination done with seismic tomography could not identify the fracturing even from 165 mm diameter borehole destress blasting in the Brunswick Mine (Andrieux et al., 2003). Figure 1.5 presents outcome of the study based on seismic tomography. Brauner (1994) indicates the inapplicability of destress blasting to higher stresses due to its inability to generate sufficient fractures under such conditions for underground coal mine workings. Karwoski et al. (1979) reported similar observations for hard rock mines and expressed doubt about enough fracturing by small diameter closely spaced boreholes.

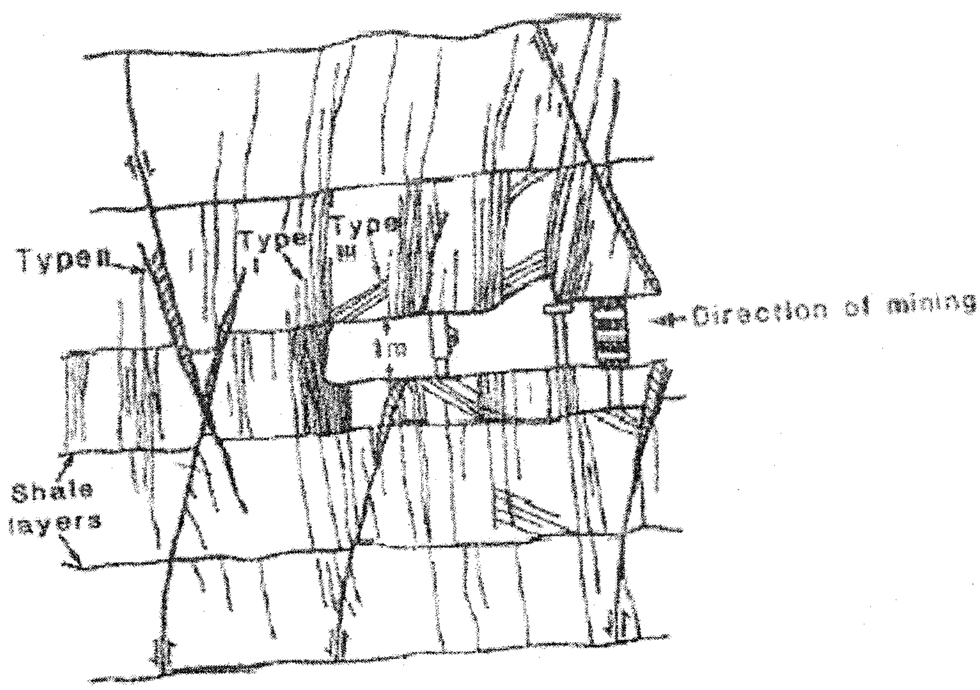

Figure 1.3 – Idealized cross-section through a stope showing the fracture patterns that develop near stopes in deep gold mines
(Brummer and Rorke, 1984)

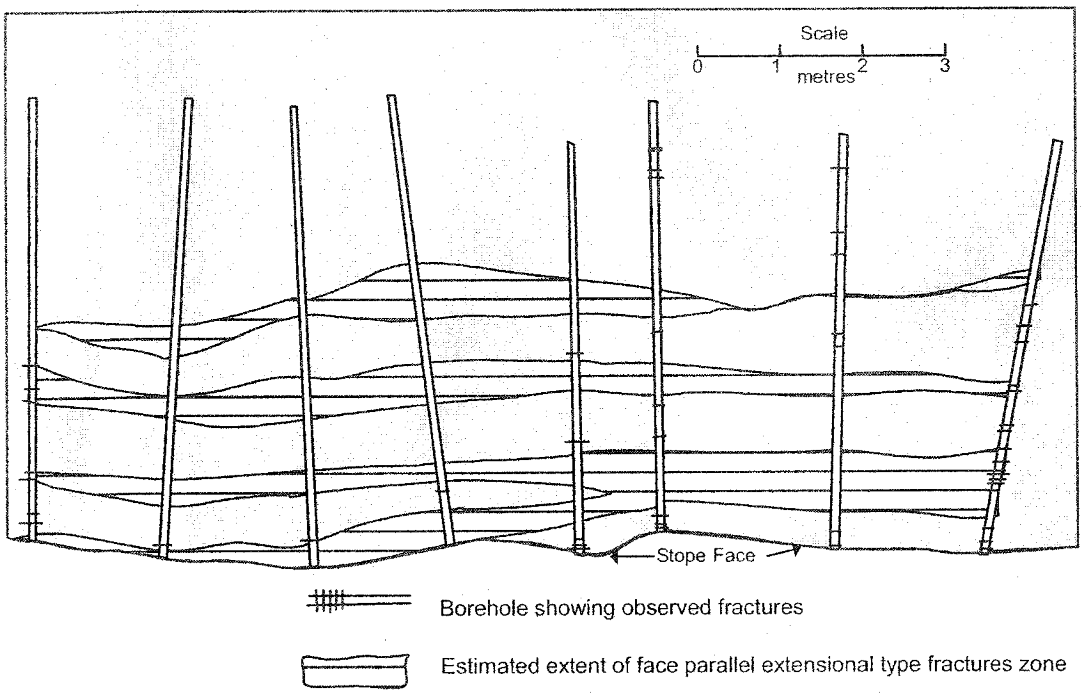

Figure 1.4- Plan-view showing eight petroscopic holes and the lateral extent of the extensional type fractures zones
(Adams and Jager, 1980)

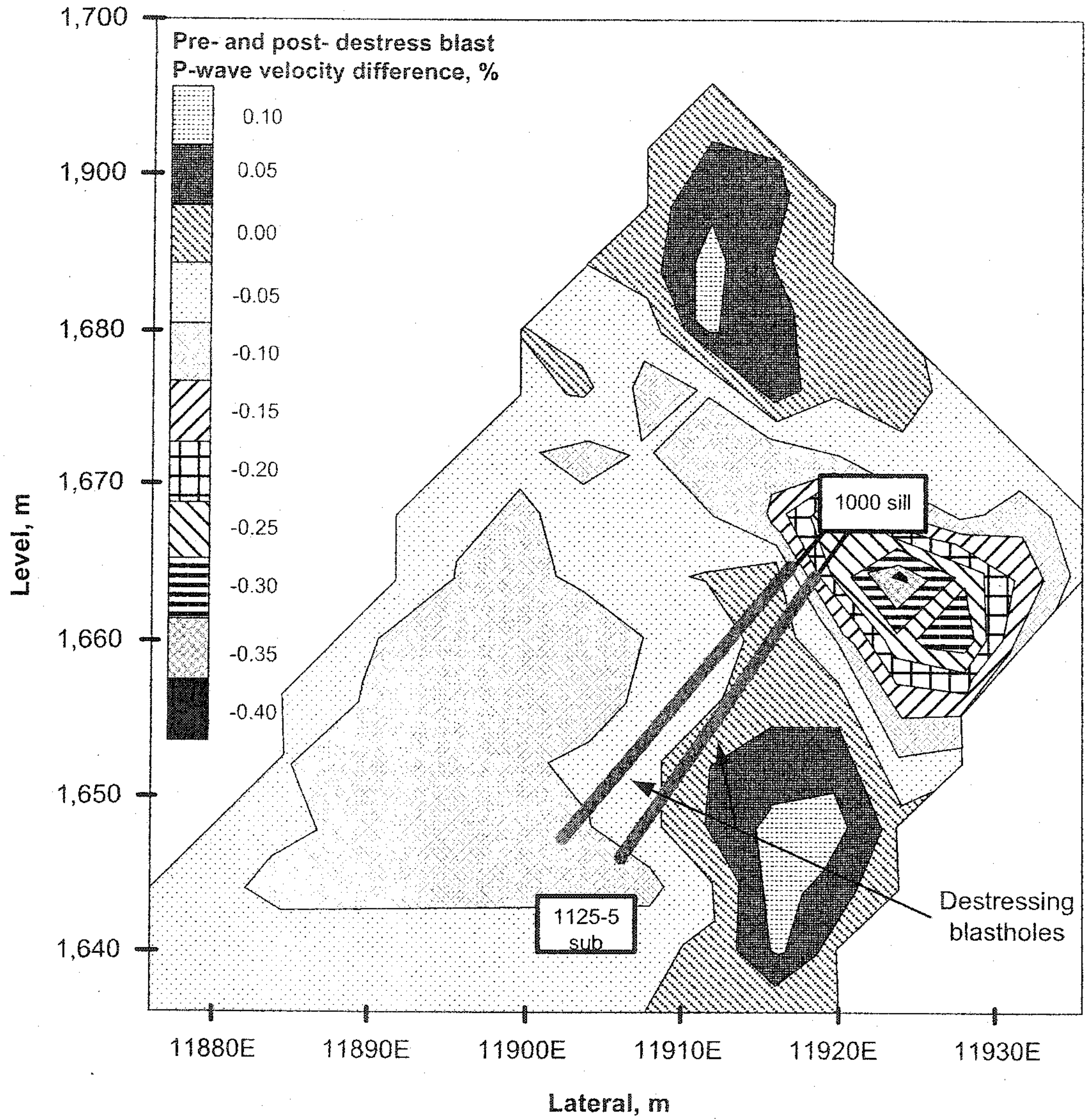

Figure 1.5 – Damage zone identification with the pre- and post- destress blast seismic tomography in the Brunswick Mine, Canada

(Longitudinal-section)
(Andrieux et al., 2003)

In contrast, North American experiences with destress blasting are entangled in ground control problems. The ground control problems caused by destress blasting application led to its experimentation in the walls instead of into the vein (Corp, 1981), change of the mining method from overhand cut-and-fill to underhand cut-and-fill (Board & Fairhurst, 1983) and abandoning a portion of the stope (Blake, 1998). Figure 1.6 depicts a ground control problem area in Coeur d'Alene Mining District, Idaho, USA.

The following fundamental state emerges about the fracturing by the explosives in the confined rock mass on the basis of well-established rock mechanics principles and explosive engineering hypotheses.

> *"Detonation of a borehole in stressed rock medium will most likely induce few cracks in the major principal stress direction. This directional crack generation is not able to produce any rock movement hence stress relaxation or local stress transfer or yielding rock failure mode".*

Only one laboratory study can be traced which supports the above assertion but only to the part that the fracture growth is more along the major principal stress (Schatz et al., 1987a). Van De Steen et al. (2001) simulated fracturing in rock blocks under bi-axial confinement using the displacement discontinuity boundary element method and observed that no-stress-relaxation can be achieved with a tensile failure criterion (Rankine failure criterion) generating an extensional fracture pattern in the rock blocks. They observed that a shear failure mode and criterion (Coulomb failure criterion) are necessary for the stress relaxation (Figure 1.7). The study indicates that the extensional type fractures observed in South Africa (see Figures 1.3 and 1.4) cannot lead to the desired rock destressing.

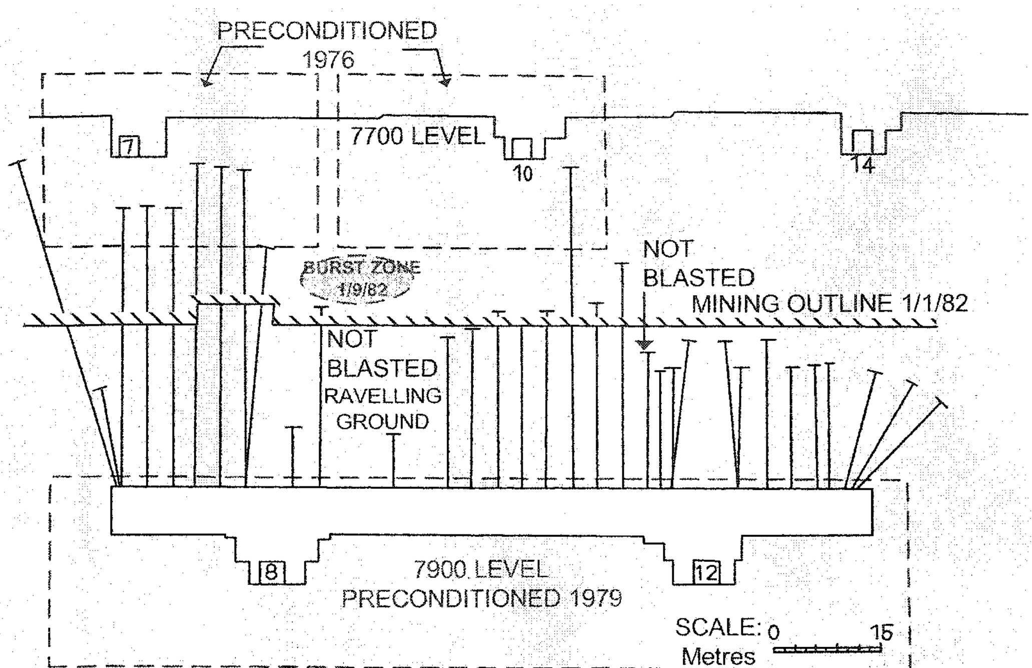

Figure 1.6 – Phase 2 preconditioning, 7900 level, the Star Mine

(Longitudinal –section)

(Blake, 1982)

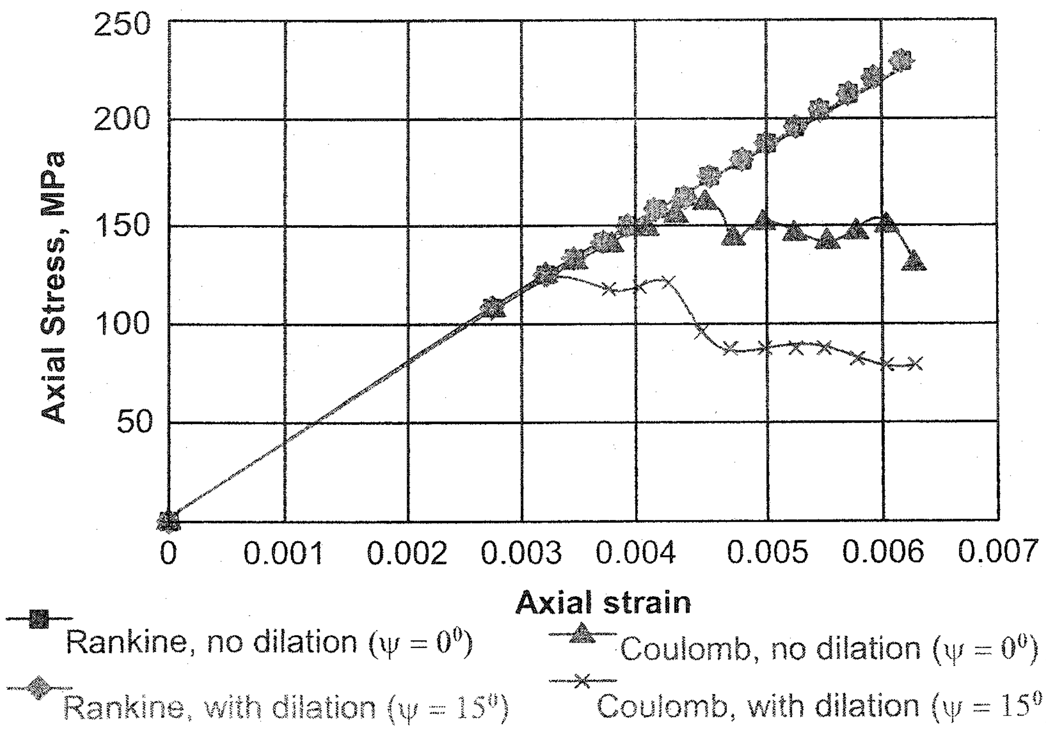

Figure 1.7 – Average axial stress as a function of the average axial strain for the simulation of a biaxial test

(Van De Steen et al., 2001)

1.2.2 Modifying Rock Mass Properties

It is conceived that fracturing by destress blasting reduces the load-carrying ability of the rock apparently by reducing the confined rock mass strength and the modulus of elasticity (Blake, 1972a; Board and Fairhurst, 1983). However, up untill now no study has been made to present a plausible explanations for the nature of fractures growth after a destress blast under confinement and resultant changes associated with it. More evidence is against the notion of effective fracturing by destress blasting.

Transient relief of destress blasting in South African mines since the first systematic observations of the technique in the early 1950s reflects no change in the rock mass properties, particularly fracturing and associated strength reduction. The rock should not experience stress concentration up to the perilous level in a short duration should it attain the reduced stiffness properties due to destress blasting. Toper et al. (1998) report rockburst incidences of 1.1 ML on the Richter scale in a panel preconditioned 15 days earlier. The current belief for destress blasting application in South Africa is now based on the concept that the purpose of destress blasting is to activate existing fracture networks rather than to create new ones (Toper et al., 1998). Scoble et al. (1987) validate this concept with the borehole endoscopy measurements in the Campbell Red Lake Mine, Canada. Their studies found only extension of the pre-existing fractures, which were limited only up to 1.4 m from the 45 mm diameter boreholes. Fractures were observed only near to the borehole collars in the most recent Canadian experiment in the Brunswick Mine (Andrieux et al., 2003). Hakami et al. (1990) reports similar observations. Extension of the premise set in the preceding section lead to the following scenario with respect to the extension of the new fracture networks.

"It can be argued that if the new fracture sets have to grow in the unfavourable direction with respect to the stress relaxation under confinement (as discussed in the preceding section), then the existing fracture networks will also follow the same path under the same environment, thus being not amenable to the desired destressing".

Further, Toper (1995) presents laboratory tested rock properties and mentions no perceptible change in the rock properties (uniaxial compressive strength and the Young's modulus) for before and after destress blasting measurements. It is noteworthy to mention that Toper et al. (1994) report an increase in the major principal stress magnitude and a reduction in the minor principal stress magnitude due to destress blasting based on the measurements with strain gauges (Figure 1.8). Hakami et al. (1990) point out similar observations for the local reduction in strength and modulus properties limited to the plane of boreholes and even an increase beyond some distance away from the holes plane (Figure 1.9). It is interesting enough to point out again that load cell measurements in the studies done by Hakami et al. (1990) indicated a significant increase in the compressive principal stresses parallel to the fractures plane. Only stress relaxation observed in the order of 11 MPa for the principal stress perpendicular to the fractures plane, which is identical to the observations by Toper et al. (1994). Labrie et al. (1997) also reports an increase in the modulus properties in the order of 11 per cent after an experimental destress blast in the Sigma I Mine, Canada.

No plausible explanation can be put forward to explain the increase in the major principal stress and the stiffness of the rock mass after destress blasting application which was aimed at reduction in the major principal stress magnitude and stiffness properties. This poses a perplexing complexity on part of the practical application of destress blasting but it also provides an intriguing research challenge to solve.

The perplexity to the issue of rock fracturing by destress blasting increases more should one assume a diametric assumption to the fundamental position which indicates that the fractures align along the principal stresses. The following scenario emerges with conjectures that the blasting in the confined rock medium produces radial fracturing enough for the effective destressing (Taube et al., 1991).

> "*If radial cracks growth due to detonation of borehole is presumed, this will mean an increase in rock volume hence increase in the modulus properties. An increase in the modulus properties will lead to more stress concentration instead of desired stress relaxation or local stress transfer and will ultimately contribute in violent brittle rock failure*".

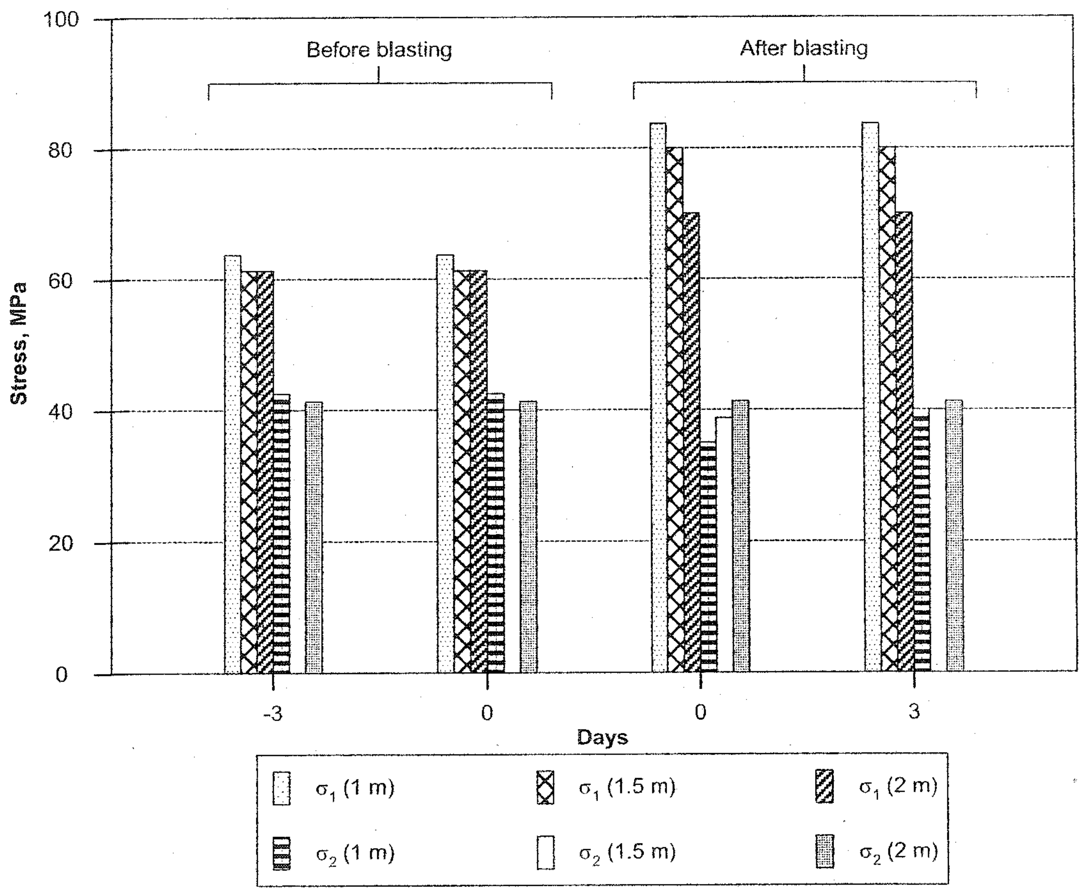

Figure 1.8 – Strain gauge measurements of a test destress blast

(Toper at al., 1994)

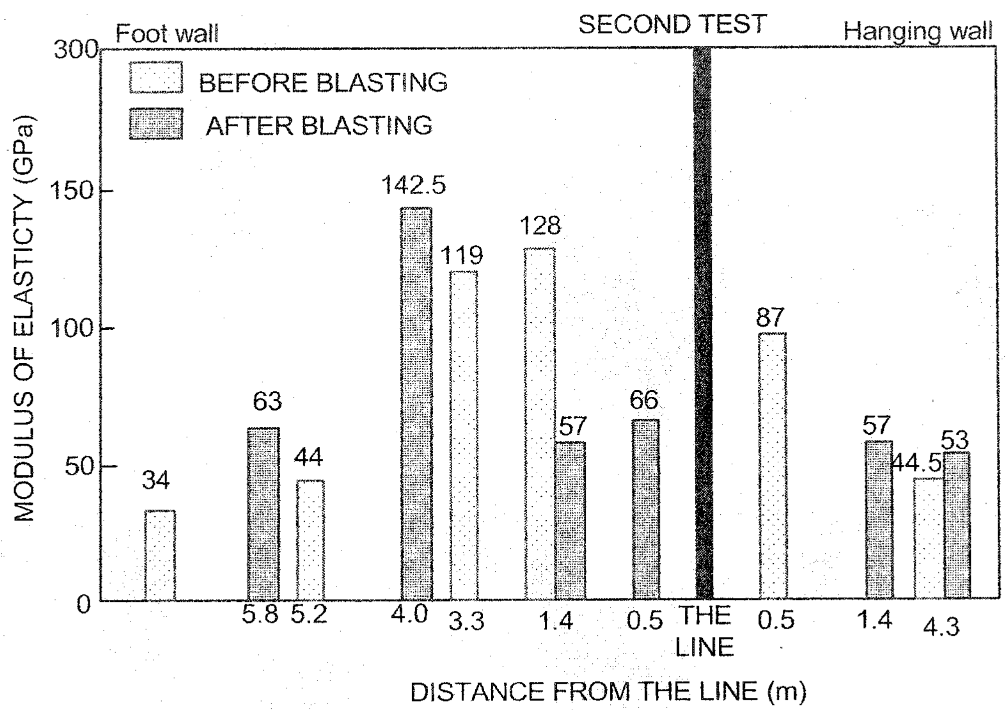

Figure 1.9 – Modulus of elasticity obtained before and after a destress blasting (Hakami et al., 1990)

1.2.3 Rockbursts Triggering Simultaneous to Destress Blasting as a Success Measure

The objective of destressing is to reduce the stress in the rock immediately ahead of the mining face and to maintain the fracture zone in a state of stable equilibrium. However, in practice, most of the time the most inappropriate way to achieve this objective is undertaken by trying to generate fracture networks in the rock ahead of the face by a heavy blasting (clearly, the practitioners believe that it will generate radial fractures). Willan et al. (1985) conducted a survey of 30 case studies and reported that the explosive energy applied was as high as 219 kcal/m^3 for destress blasting. Brummer and Andrieux (2002) report explosive energy as high as 1350 kcal/m^3 and suggest the same level for the application (converting mass into volume by rock density = 2.7 t/m^3 to the given data). These explosive energy consumption figures reach close to the production blasting requirements. Cook et al. (1966), based on the calculations of energy theories, reported that a successful destress blast should release more energy than contained by the explosive itself, i.e., a successful destress blast should trigger a rockburst simultaneous to it. It is important to note here is that each blasting is a seismic event that can easily be recorded with microseismic monitoring equipment.

The majority of the rockbursts in underground mines are simultaneous with production blasting. The incidences of rockburst occurrences with production blasts are so high that they cannot be termed a mere coincidence. Rienferg (1991) reports that 91 per cent of rockburst incidences are associated with blasting, without differentiating between destress blasting and routine blasting (Figure 1.10). Gay et al. (1984) report similar observations for gold mine destressing. Lightfoot et al. (1996) report seismic activities associated with destress blasts as well as spaced out up to a few hours post to destress blasting.

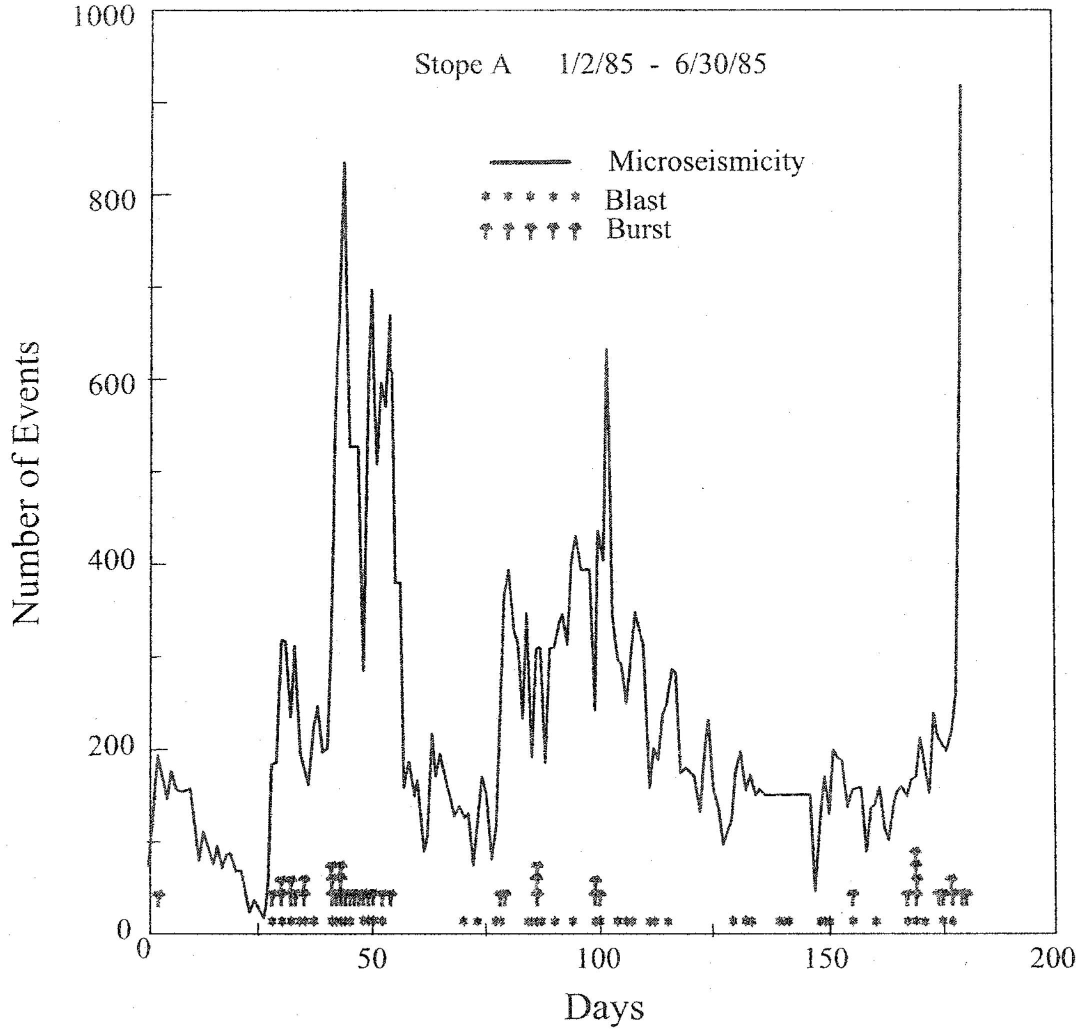

Figure 1.10 – Daily microseismicity for stope 'A', Coeur d'Alene mining district, Idaho, USA

(Rienferg, 1991)

Further, there should be calculations as well as control with release of the amount of the explosive energy if triggering a burst with destress blasting is the success. Sadly, it is not the case with the available field experience. Macasa Mine, Canada triggered a severe rockburst on April 3, 1982 with a routine blasting operation (Cook, 1982; Cook and Bruce, 1983). On the other hand, Strathcona Mine, Canada had experienced a rockburst of 2.7 Nuttli magnitude simultaneously with destress blasting (with no apparent stress relief signs in underground), which resulted in support damage (Hanson et al., 1992).

1.2.4 Destressing as a Transient Phenomenon

Experience gained in South African mines for destress blasting indicate that the effect of destress blasting is transient in nature (Lightfoot et at., 1996; Roux et al., 1957 and Toper et al., 1998). It is not surprising that efforts are made to incorporate destress blasting into the daily schedule of stoping operations in South African gold mines.

However, experience gained in the Coeur d'Alene Mining District, Idaho, USA indicates that the benefits from carefully planned destress blasting operations can be enjoyed over a longer period of time (Blake, 1972a & b, 1982, 1987, 1998, Board and Fairhurst, 1983, Corp, 1981, Karwoski et al., 1979). Recent experiments in Canadian mines (Andrieux et al., 2003; Brummer and Andrieux, 2002) also aimed for long-term stress relief by destress blasting. Further, if the destressing involves a permanent change in the material properties (strength and modulus) then such changes should yield long term effects.

No reasonable logic exists to dispel either of the beliefs.

1.2.5 Suitable Explosive for Effective Destressing

It is frequently mentioned that an explosive with higher gas content (ANFO types) is good for destress blasting (Blake, 1972a & b, 1982, 1998, Board and Fairhurst, 1983, Brummer, 1988, Lightfoot et at., 1996, Toper et al., 1998). It is argued that higher gas content will help in extending the fracture networks.

However, in the same references, explosives with lower gas content (emulsion and slurry) were used and the application termed as success. A review made in the thesis (section 3.2, Chapter 3.0) indicates that high order detonation products or ideal detonation products like emulsion and slurry explosives are required for fractures generation and propagation in hard rocks. Also, higher shock wave energy is required (can be attained from larger borehole diameter blasting using emulsion type explosives) with an increase in confinement due to higher in-situ stress regime at deeper workings.

Further, controversies exist for the precise role of gas pressure and shock wave energy parts of an explosive in rock fracturing. Recent experiments of Brinkmann et al. (1987) and Nie and Olsson (2000) were also unable to find out the role of gas energy in fractures generation and extension.

The above untenable destress blasting mechanisms; its contradictory explanation and seemingly unguided field application is due to lack of knowledge on destress blasting mechanisms. Certainly there is a need to look beyond the existing representation of destress blasting fractures zone by crude approximation of the modulus reduction as reported by Karwoski et al. (1979), Hedley (1992), Tang (2000) and Andrieux et al. (2003).

1.3 OBJECTIVES OF THE RESEARCH

The analyses made in the preceding section pose the following four issues which need to be answered before further advances can be made with the effective destress blasting application.

(i) *What is the nature of the fractures growth by rock blasting under confinement? It is important to know whether the fractures propagate radially or directional growth takes place.*

(ii) *What is the extent of the fracture network due to rock blasting under confinement? It is important to ascertain that the fractures extent is appropriate enough for the desired effect of destressing.*

(iii) *What amount of stress relaxation or stress redistribution is attained due to fractures induced by rock blasting under confinement? Most important factor in the entire exercise of destress blasting is to ascertain the changes created with the magnitudes of the principal stresses.*

(iv) *What type of explosive energy (shock versus quasi-static energy) is more appropriate for hard rock mines for the purpose of effective destressing? It is equally important to gain knowledge on the explosive energy utilization for effective application of destress blasting.*

Destress blasting is essentially an application of explosive energy to rock subjected to high stress levels. Therefore, an experimental technique, suitable for dynamic rock fracturing studies, is needed to resolve the aforementioned uncertainties. The outcome of the analysis for a study conducted in this thesis (Chapter 3) to assess the quantifiable role of explosive energy in rock fracturing further compounds the complexities. No suitable experimental technique exists to study the dynamic rock fracturing. The prevalent laboratory scale experimental techniques suffer from the scale effect and the field scale studies are prohibitive. Therefore, it is first required to develop an experimental procedure in order to study issues related with destressing blasting.

The following specific objectives are targeted and obtained with the thesis.

(1) Development of an experimental procedure to study the dynamic rock fracturing by explosive energy. A numerical procedure is developed which fully accounts for the explosive characteristics, rock properties and unrestricted growth of the discrete fractures. The procedure is validated with the existing empirical knowledge base.

(2) Identification of the nature of the fractures growth due to rock blasting under confinement. The confinement levels commensurate to the deep hard rock mines in the Canadian Shield are considered for the dynamic numerical modelling simulations.

(3) Identification of the extent of the fracture networks under the variable bi-axial confinements with different spatial location of the boreholes. Critical examination is made in order to understand the stress relaxation phenomenon associated with fractures growth in such environment.

(4) Improving the understanding of the role of rock properties on extent and nature of the fractures. The simulations are conducted to identify the effect of change in the rock properties on the fractures growth.

(5) Identification of the role of the explosive energy on extent of the fracturing. The characteristics and magnitude of the explosive energy are both evaluated with the studies.

(6) Exploration for the enhancement of explosive energy utilization for the effective application with minimal detrimental effect to the host rock. Few simulations are conducted to assess the potential of smooth blasting techniques in the effective explosive energy utilization.

1.4 SCOPE OF THE RESEARCH

The research described in this thesis is undertaken in order to improve the understanding of destress blasting mechanisms through a series of micro-mechanical dynamic numerical modelling. Endeavours are made in analyzing the importance of confinement levels, variable differential stress levels, rock properties, explosive characteristics and blasting parameters on destress blasting program. The scope of the study is limited to the evaluation of destress blasting mechanisms and possible stress relaxation phenomena in underground hard rock mines through numerical modelling exercises only. The scope of the research made in the thesis is limited to destress blasting cases related to the drift developments where a few short length holes (about 7 m) of small diameter (38 to 89 mm) are practiced. Primary numerical models are standardized and verified against reported empirical knowledge bases, wherever possible, and then a detailed parametric study is undertaken from the primary models with due consideration of the confinement level. Results of such detailed studies are also compared with reported field observations.

1.5 THESIS ORGANIZATION

Chapter 1 starts with brief background information on rockburst phenomenon. The chapter also presents a critical examination of destress blasting mechanisms in order to define the problem. Scope of the research is also defined in this introductory chapter. Chapter 2 reviews reported field destress blasting practices. Analyses of three case studies are also presented in the chapter. Chapter 3 addresses issues pertaining to rock fracturing by explosive energy. Explanations are put forward to explain rock fracturing mechanisms and experimental techniques used to obtain such information. Studies made to quantify the fracturing and the role of confinement in rock fracturing are also discussed and analysed in the chapter. Chapter 4 is concerns the development of a new numerical procedure to study rock fracturing by explosive energy. The chapter also presents an analysis of the attempted procedures to study rock blasting employed elsewhere. Validation of the new procedure is also made in the chapter. Chapter 5 addresses core issues of destress blasting. A detailed parametric study is undertaken to understand the dynamic rock fracturing process at the micro-mechanical level. The chapter introduces a non-dimensional parameter, ℓ_{ci}, to characterize fracturing extent as well as destressing. Investigations in the chapter provide answers to the questions (i), (ii) and (iv) posed in Section 1.3. Chapter 6 introduces a novel stress relaxation parameter β_{ij}. This parameter provides an answer to the question (iii) posed in Section 1.3. The parameter not only adequately describes destressing but also offers an explanation to the inexplicable field observations mentioned in Section 1.3. Chapter 7 provides discussion on the validity of the modelling and limitations. Chapter 8 summarises the outcome of the research. Limitations of the study as well as the scope of future research are also delineated in the chapter. A Summary is presented at the end of each chapter. References cited in the thesis are presented in the last part of the thesis.

CHAPTER 2

DESTRESS BLASTING – EVOLUTION, CONCEPTS AND PRACTICES IN UNDERGROUND MINES

2.1 DEFINITION

A ground preconditioning method, performed by drilling and blasting in highly stressed rock to relax the zones of high stress. The peak load in the blasted zone is thus transferred deeper into the undisturbed rock and a protective barrier is formed (Mitri, 2000).

Various terminologies used over time include concussion blasting, volley firing, shake blasting, camouflet blasting and precondition blasting, to name a few. The thesis uses only destress blasting, which is a widely accepted term for the technique.

2.2 HISTORICAL BACKGROUND

Destress blasting was conceived as a rock fracturing technique to shift high abutment pressure away from an active face, which is one of the causes of rockbursts in mines. A common notion is permeated that destress blasting was conceived and first applied to the gold mines of South Africa (Rorke and Brummer, 1990; Roux et al., 1957; Tang and Mitri, 2001). Contrary to this permeation, literature indicates that Springhill Colliery, Nova Scotia, Canada (McInnes et al., 1959) introduced and applied destress blasting as a rockburst control measure in the early 1930s. Christian (1939) reported the first application of destress blasting for hard rock mines in Teck-Hughes Mines, Canada. The mines of Kirkland Lake - Ontario, Canada, used destress blasting in the 1930's on a trial and error basis (Hanson et al., 1987).

However, the first systematic observations of destress blasting and its benefits are documented with the detailed experiments conducted in the early 1950's for the gold mines of the Witswatersrand area, South Africa (Roux et al., 1957, Gay et al., 1984, Hill and Plewman, 1957). The concept of destress blasting evolved from the observation that the zone of highly fractured rock immediately surrounding some deep underground openings seems to offer some shielding to both the occurrence of and damage from rockbursts. It was argued that both the occurrence and effects of rockbursts could be reduced by extending and maintaining this zone of the fractured rock ahead of a face (Figure 2.1). In fact, the observations were an extension of the dome theory proposed by Morrison (1942). Effectiveness of the concept was tested in the field and involved destress blasting of 32 stopes over a 19 month period at the East Rand Proprietary Mines Ltd. The results were encouraging. The incidence of rockbursts, severity of rockbursts, time of rockbursts (relative to shifts) and causalities were among the parameters monitored before and after destress blasting. Improvements ranged from 34 per cent for the first parameter to 100 per cent for the last (Roux et al., 1957).

Destress blasting was again re-evaluated for South African gold mines in the late 1980s (Brummer and Rorke, 1988; Rorke et al. 1990; Adams et al., 1981; Adams, et al., 1993; Lightfoot et al., 1996; Toper, et al., 1997). The current practice has many notable departures from the original concepts of destress blasting. The following is a summary of the beliefs (based on the references cited above) associated with the current practice adopted after the re-evaluation of destress blasting.

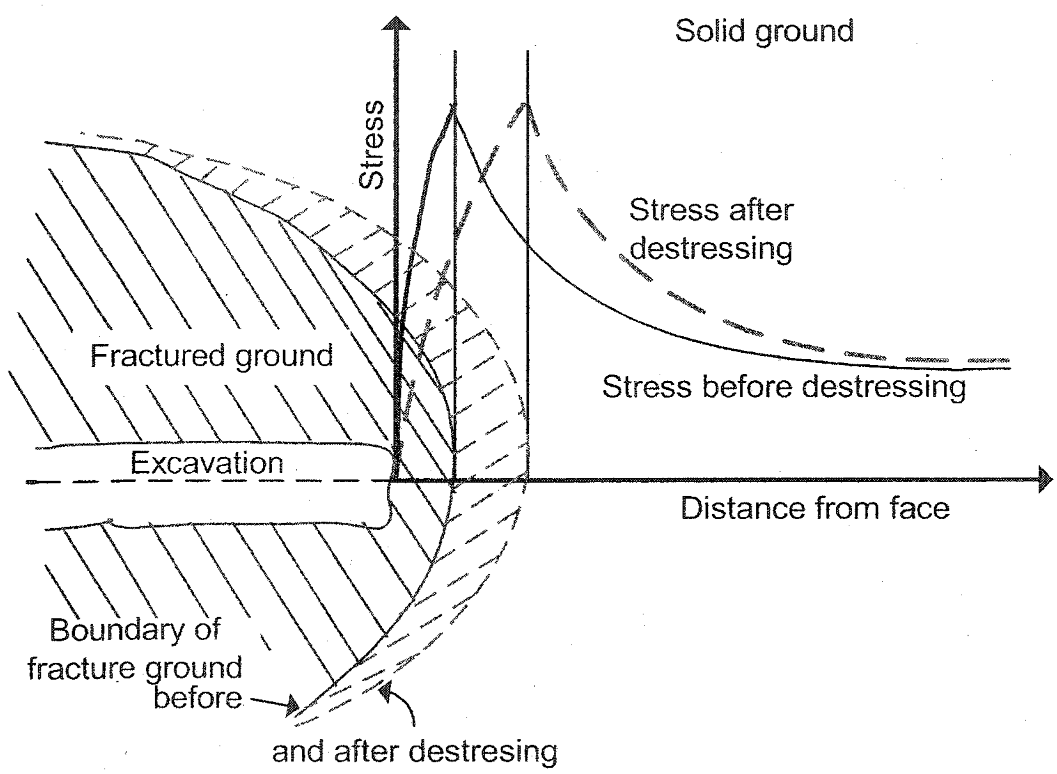

Figure 2.1 - Geomechanical effects of destress blasting

(Roux et al., 1957)

(a) The main objective of destress blasting is to activate already existing tightly closed fractures rather than to initiate and propagate new ones.

(b) The position and depth of destress blast holes should be confined to the already fractured zone for an effective application.

(c) The aim of destress blasting is to shift stress concentrations and associated seismic activities deeper into the rock. Extent of the already fractured zone is generally 3-5 m from the active face. Therefore, destress blasting should be part of a regular production cycle to be effective in continuously transferring the seismic activities away from the face.

(d) A low shock and high gas energy explosive (ANFO types) has a better effect in the opening and extending pre-existing fractures, hence should be employed.

(e) Destress boreholes should be equally far from the walls (hangingwall and footwall) to avoid damage to the walls in order to minimize ground control problems. The borehole spacing of 3.0 m is established for the 38 mm diameter boreholes.

Figure 2.2 illustrates two different schemes for destress blasting application in the South African gold mines.

In North American mines, destressing is more widely practiced (Dickhout, 1962; Hedley, 1992; Mitri, 2000; Moruzi and Pasieka, 1969). Detressing of sill pillar was done on a regular basis in the Coeur d'Alene mining district of northern Idaho. Several publications reported instrumented field trials for the mines (Blake, 1972a and b; Corp, 1981; Board and Fairhurst, 1983). It was reported that destressing significantly reduces seismic activity during the mining (Blake, 1982). It seems that the cooperative efforts by the United States Bureau of Mines and the mining companies showed that for certain mining geometries, sill pillars in particular, destress blasting could be effective in improving rockbursts control (Mitri, 2000). Figure 2.3 illustrates two schemes of destress blasting, which indicates its application in two different areas of deep hard rock mines in the North American Continent.

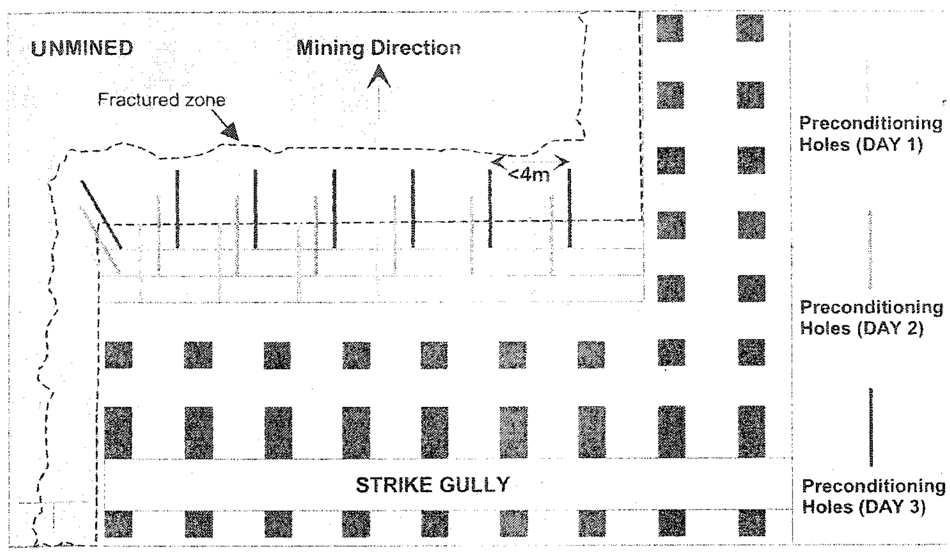

(a) Face parallel destress blasting with 38 mm diameter borehole

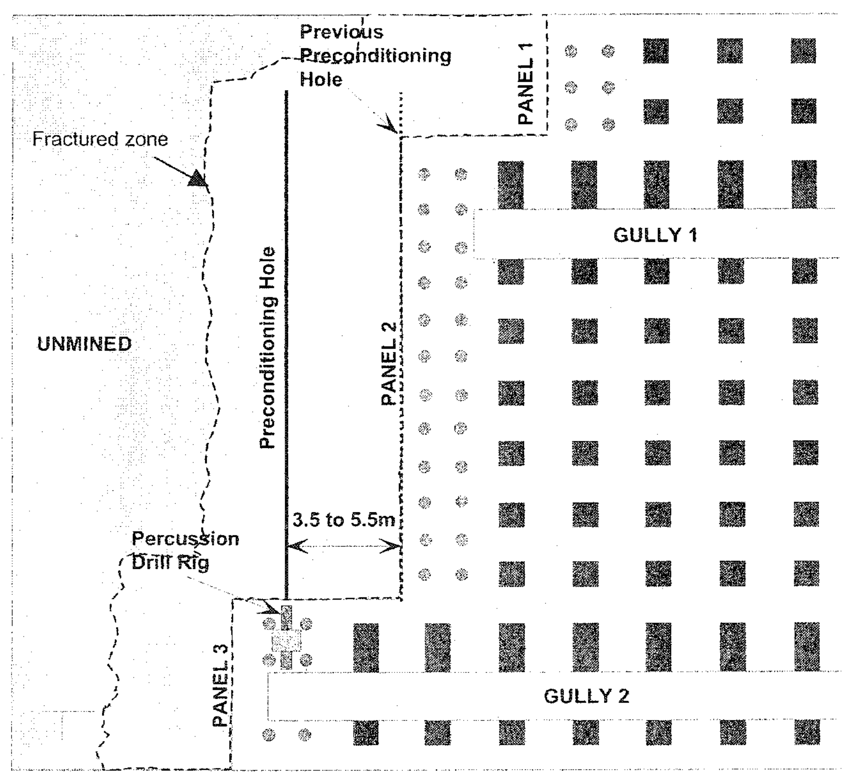

(b) Face perpendicular destress blasting with 89 mm diameter borehole

Figure 2.2 – Current destress blasting practice in the gold mines of South Africa (Adams et al., 1993; Lightfoot et al., 1996; Toper et al., 1997)

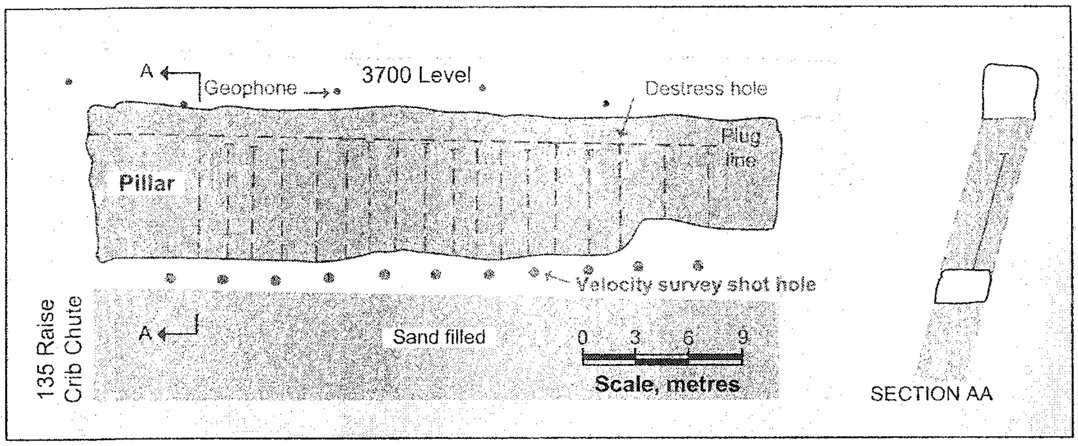

(a) Crown/ sill pillar destressing practice at Galena Mine, ID, USA

(Longitudinal and cross - section)

(Blake, 1972b)

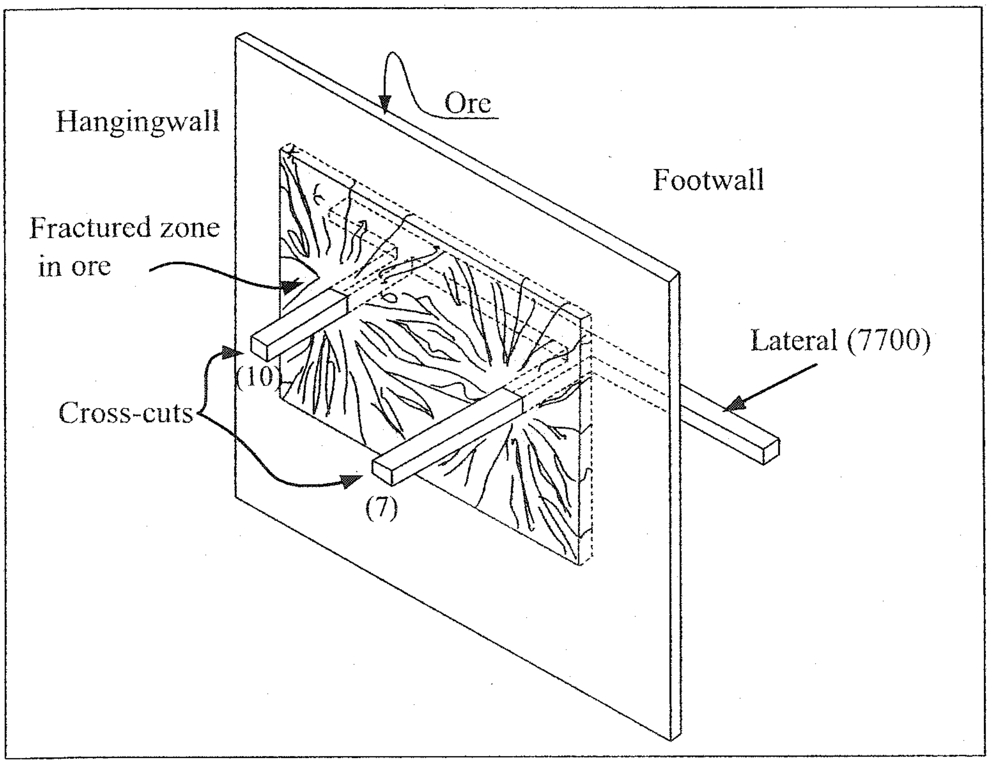

(b) Prospective of stope preconditioning at the Star Mine

(Corp, 1981)

Figure 2.3 – Typical narrow vein destress blasting applications in North American mines

In Canadian mines, destressing is normally practiced in crown/sill pillars in thin, steeply dipping ore bodies such as those at Campbell Red Lake Mine, Dickenson Mine (now Red Lake Mine), Falconbridge Mine (Moruzi and Pasieka, 1969), and Kirkland Lake (Cook and Bruce, 1983; Hanson, et al, 1987). Labrie et al. (1997) and Mitri (1996) also report experimental destress blasting for the Val d'Or's Sigma Mine I, Quebec, Canada. At Inco's Creighton Mine, destress blasting is in regular use in driving development openings, and in pillars, which is a form of preconditioning (MacDonald, et al., 1988; O'Donnell, 1992; Oliver, et al., 1987). The most recent application of destress blasting is reported for the Brunswick Mine, Canada (Liu et al., 2003, Andrieux et al., 2003).

Destress blasting practice on the North American continent involves beliefs that are altogether different from the South African practice. The following summarizes prevalent notions for destress blasting particularly applied to pillars and stopes of the steeply dipping veins of hard rock mines.

(a) The main objective of destress blasting is to fracture highly stressed stiff rocks. The resultant effect of such exercises is to transfer mining induced stresses to other parts of the mine. Destressing involves a change in the rock properties and its benefits can be enjoyed over a longer period of time.

(b) The borehole depth is a function of the desired destressing area, the magnitude of the mining induced stresses, the mining method and the available mechanization in the mine. Boreholes of 9-10 m depth for crown/sill pillars have been reported (Blake, 1972b). Higher magnitude of the induced stresses may necessitate destressing for the whole stope in advance with 20-25 m deep boreholes (Karwoski et al., 1979; Andrieux et al., 2003).

(c) The aim of destress blasting is to fracture overly stiff homogenous rock. Therefore, more blasting energy is preferred. Explosive energy levels close to production blasting have been suggested and implemented (Brummer and Andrieux, 2002).

(d) Emulsion type explosives as well as ANFO type explosives are equally reported in use (Willan et al., 1985).

(e) Destress blastholes should preferably be shifted towards the footwall side to minimise the ground control problems during crown/ sill pillar destressing (Blake, 1972b). The most recent application involved the use of 165 mm diameter boreholes (Andrieux et al., 2003).

Although destress blasting is considered one of the best techniques of controlling rockbursts (Blake, 1982; Roux et al., 1957; Oliver et al., 1987; William and Cuvellier, 1988; etc.), it has achieved mixed success in its application. Apart from the apparent success stories, the ground control problems resulted by destress blasting application lead to experiment it in the walls instead of in the vein (Corp, 1981), change of the mining method from overhand cut-and-fill to underhand cut-and-fill (Board & Fairhurst, 1983) and abandoning a portion of the stope (Blake, 1998) in the silver producing mines of Coeur d'Alene Mining District, Idaho, USA. Lately, the mines in the area switched to the underhand longwall mining method (Williams and Cuvellier, 1988). Further, fracturing of confined rocks remained doubtful. Scoble et al. (1987) with borehole endoscopy measurements in Campbell Red Lake Mine, Canada, reported that destress blasting involved only the extension of pre-exisiting fractures and that too upto a limit of 1.4 m from the 45 mm diameter boreholes. The most recent Canadian experiment in the Brunswick Mine, Canada could only find the fractures near to the borehole collars (Andrieux et al., 2003). Measurements by Labrie et al. (1997) in the Sigma I Mine, Canada, add complexity to the problem as they report an increase in the modulus properties in the order of 11 per cent after an experimental destress blast. Hanson et al. (1992) report extensive damage to drifts after a destress blast in the Strathcona Mine, Falconbridge, Canada. The destress blast triggered rockbursts of 2.7 on the Nuttli magnitude.

Depth, stress and rock conditions in many deep mines are conducive to severe bursting on an almost daily basis. It is a fact that bursting is infrequent and associated only with particular geometries and geological conditions. It shows that a considerable amount of natural self-destressing accompanies to mining (Roux, et al., 1957, Corp, 1981). Destress blasting is mostly applied as a last resort, i.e., when the natural or self-destressing of strainburst prone structures cannot be induced by the design of the mining geometry and mining sequence (Blake, 1998).

2.3 MECHANISMS OF DESTRESS BLASTING

The destressing by blasting is conceived to shift away high stress concentration near to the active face (Brauner, 1994; see Fig. 2.1 also). In hard rock mines, destress blasting is thought to be a means of maintaining and extending natural fracturing around an excavation. It is perceived that inducing fractures by blasting in the rock ahead of the face produces the following effects (Blake, 1972a and 1998; Board and Fairhurst, 1983; Brauner, 1994; Brummer, 1988; Corp, 1981; Kowarski et al., 1979; Mitri, 2000; Roux et al., 1957; Toper et al., 1997).

(a) **Local stress transfer by fracturing** – Destress blasting induces a set of fractures in the rock mass. This fracturing results in local readjustment of stresses by transferring them to a non-fractured zone ahead of the destressing zone. The benefit to the mining personnel is that a low stressed "cushion" of rock is produced in the immediate stope face.

(b) **Modifying rock mass properties** – The fracturing by destress blasting reduces the load-carrying ability of the rock apparently by reducing the confined rock mass strength and modulus of elasticity. The collective result of change in the properties is stress decrease in the fractured zone.

(c) **Modifying rock mass failure mechanism** – Rockburst is normally associated with brittle elastic rock failure. Fractures induced by destress blasting provoke yielding characteristics of rock mass and hence change its failure mechanism from brittle elastic to yielding type. Successive destress blasting applications develop a progressive yielding to maintain the cushion as the face advances. Furthermore, continued yielding dissipates continued loading of the destressed zone. Therefore, the destressed zone yields gradually rather than fails suddenly and violently.

2.4 APPLICATION AREAS FOR DESTRESS BLASTING

Destress blasting is a pro-active control measure against the strain bursting phenomena. Therefore, destress blasting can be applied to any area in the mines which is susceptible to the strainbursts. Mitri (2000) summarises various scenarios susceptible to strainbursts due to different mining activities (Figure 2.4). These scenarios can be broadly grouped into the following three places.

(a) **Drifts/raises/shafts**: Strainbursting is attributed to rapid changes in the opening geometry as initial mining of the stope begins. The rapid change in geometry does not allow the rock to self-destress, and burst-prone geometries are created on a daily basis. They also occur when the opening intersects dykes, faults or hard lenses of siliceous quartzite. Bursts in these types of situation are usually small in magnitude. Application of destress blasting can transfer high abutment stresses farther from the face.

(b) **Pillars:** A large excavation area is created as mining progresses away from the starting point. The larger excavation area generates larger mining induced stresses in the pillars, which are formed due to the mining operations. High pillar stressing may also be the result of narrowing a pillar size by two excavation areas approaching each other. Application of destress blasting in such cases is aimed to weaken the pillars and by doing so, stress transfer is achieved.

(b) **Stopes:** Pillar size or geometry becomes immaterial as stoping operations approach deeper and deeper in stiff strata with the principal stress perpendicular to the larger excavation area. The whole stope area may require destressing (or preconditioning) prior to taking up the stoping operations.

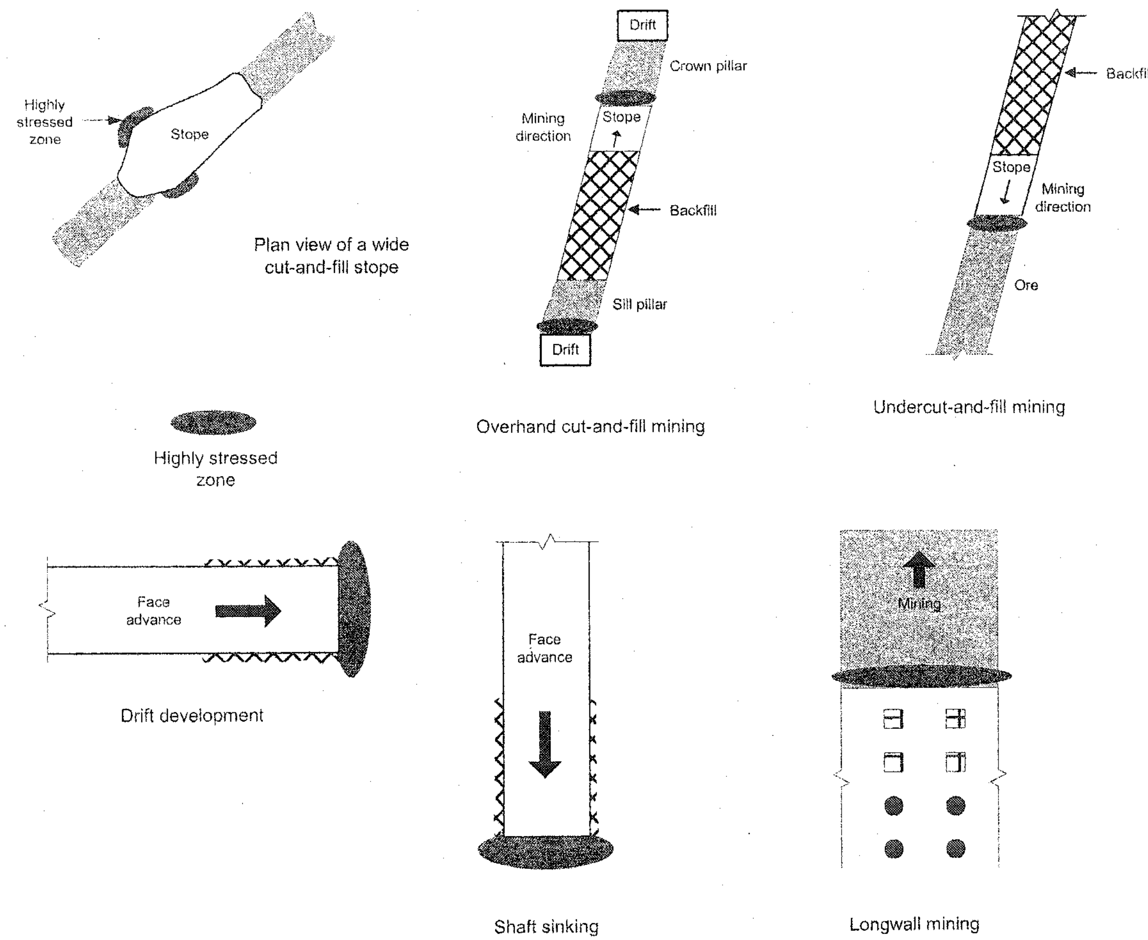

Figure 2.4 – Applications of destress blasting

(Mitri, 2000)

2.5 BENEFITS OF DESTRESS BLASTING

A successfully conducted destressing blast should alleviate high stress related difficulties, primarily strainbursting. The following additional benefits could be achieved once the targeted area is destressed (Mitri, 2000).

(a) Improved rock fragmentation from production blasting.

(b) Improved productivity due to faster stoping operations.

(c) Increased mine workers safety.

(d) Reduction in rockburst incidences.

(e) Reduction in rockburst severity.

2.6 LIMITATIONS OF DESTRESS BLASTING

Despite the apparent success stories reported earlier, destress blasting applications involve certain limitations. The followings are limitations reported by researchers (Blake, 1998; Boler and Swanson, 1993; Karwoski et al., 1979; Neuman et al., 1987; Toper et al. 1997).

(a) Limited space at working face, particularly in narrow vein mining, restricts the size of drilling equipment. Smaller size drilling equipment means that one has to wait until the situation becomes critical. This increases the risk for on-shift bursting.

(b) Any misfire can be hazardous for subsequent mining.

(c) Too early destressing can result into subsequent on-shift bursting.

(d) Production delays invariably result because of the time required to drill the destress holes and carry out the destressing.

(e) Destresssing is a slow and costly process while the results obtained have not been entirely predictable.

(f) The destressing holes, even on 1.5 m spacing, may not be loaded heavily enough to accomplish complete destressing.

(g) Destressing, like mining, often shifts the stresses to the adjacent areas unless it is done in a planned and controlled sequence.

(h) It is currently not possible to guarantee that a destress blast will achieve the desired objectives, nor it is possible to tell whether the destress blast has achieved the desired objective until a sufficient time has passed without a damaging event.

2.7 CRITICAL REVIEW OF THREE CASE HISTORIES

Three typical case studies are presented in order to illustrate complexities associated with destress blasting in the field. The first case study brings out the damage inflicted to the drifts supported with wire-mesh plus rockbolts. The study clearly indicates that the notion of measuring success with the release of more seismic energy than contained by explosives is a dangerous proposition. The second case study distinctly reports transfer of stresses to other parts of the mine and causing damages there as well as ground control problems in the destressing stope. The study indicates the need for careful planning before the application of destress blasting. The last case study poses questions on the ability of fracturing by destress blasting. The study involves 165 mm diameter blastholes and even then fracturing is not apparent. The study also emphasizes that more insight for data analysis is required when costly instrumentation is involved. In summary, these case studies underline the fact that destress blasting is hitherto poorly understood in spite of involvement of the best available technical skills and a generous investment for sophisticated equipment.

2.7.1 Strathcona Mine, Falconbridge, Canada

(Hanson et al., 1992)

- **Mine** – Strathcona, Falconbridge, Canada
- **Mining Method** – Cut-and-Fill
- **Problem** - Sill pillars rock bursting
  - at cross-cuts and the large excavation area in footwall. Stress fractures were observed in the backs and walls at a depth of 1.2 m, with fracturing more pronounced near the footwall contact. Based on the numerical modelling results, areas considered to be critically overstressed were attempted for destressing after re-supporting the critical areas with 2.4 m bolts plus wire-mesh (area A, B and D shown in Figure 2.5). Destress blastholes were 5.5 m long.

- **Properties**
  - **Rock** – good quality feldspathic gneiss (Q= 25, RMR=73, UCS=300 MPa, E=40 GPa, m=10, s=0.05). Three joint sets with the predominant joint set has rough undulating surface having chlorite talc alteration with 2-4 m spacing and 3-10 m in persistence.
  - **Ore** – softer nickel sulphide (UCS=110 MPa, E=55 GPa)
  - **Mining induced stresses** - in excess of 100 MPa near F/W contact as estimated by numerical modelling
- **Destress blasting parameters**– 5.5 m long, 63 mm diameter 66 holes in 2.1 m burden and spacing and 1.2 m stemming were fired with Magnafrac3000 explosive (Emulsion) in footwall drifts (Figure 2.5). Powder factor ranged from 0.11 to 0.16 kg/m^3.
- **Destress blasting result** – 0.5 m skin rock displaced with mesh and bolt plate necking in the line of blast holes. Craters of 0.3 m were also left behind at some places. Seismic activity of 2.7 on the Nuttli magnitude was observed by microseismic as well as regional seismic observations.
- **Review** – The problem of rock bursting centred in the region of a larger excavation area in the footwall and an area that falls in between the excavation zones. Destress blasting triggered a rockburst of 2.7 on the Nuttli magnitude scale and also resulted in support damage. It appears that the place of destressing was in stress relaxation zones, which was in the sidewalls based on the assumption of regional stress pattern in North America (high horizontal stresses as the major principal stress, which are perpendicular to the veins).

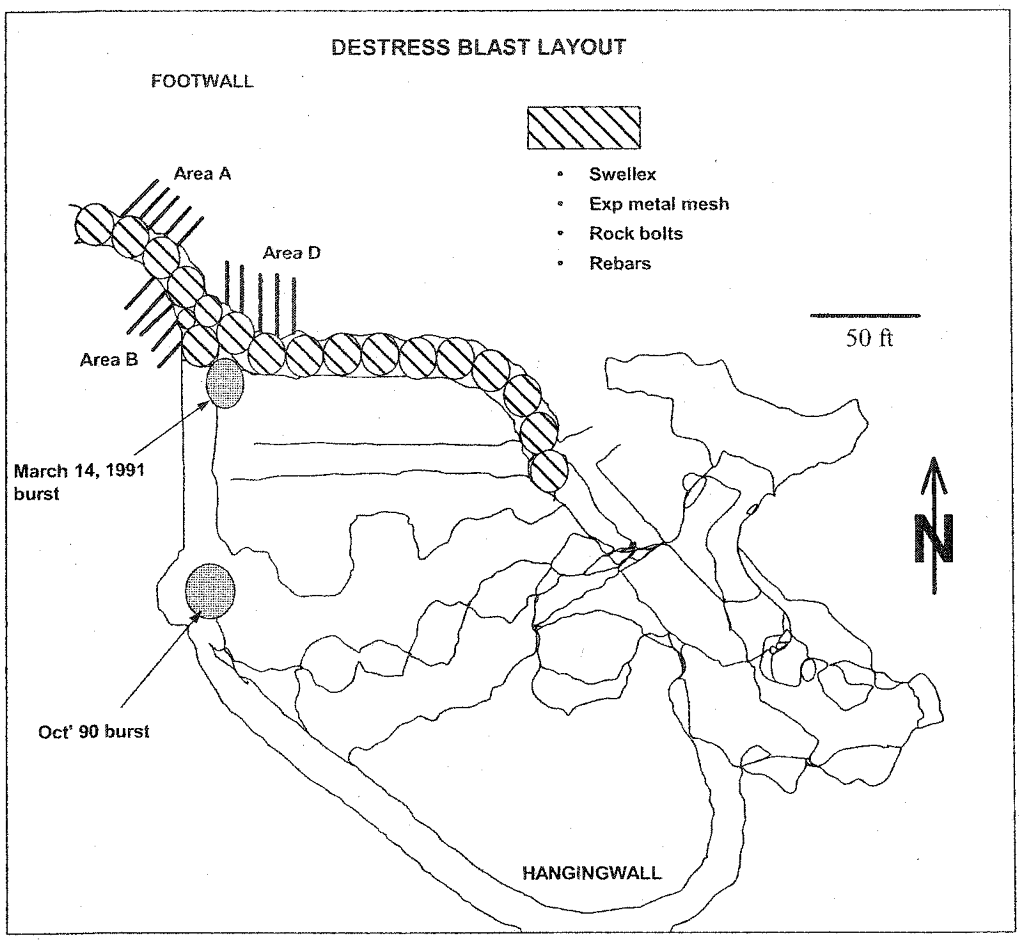

Figure 2.5 – Destress blasting in drifting at the Strathcona Mine

(Hanson et al., 1992)

2.7.2 Star Mine, Coeur d'Alene Mining District, Idaho, USA

(Blake, 1982, Corp, 1981, Karwoski et al., 1979)

- **Mining district** – Half the silver and a majority of lead and zinc production for the US is extracted from the district in Idaho and the mining depth is more than 2000 m. Ground control became the major mining problem in the district because of the mining depth, major faulting and folding, and the hardness and brittleness of the rock. As a result of these problems, the Coeur d'Alene district has become one of the most extensively studied mining areas in the world.
- **Mine** – Star Mine, Burke, Idaho, USA
- **Mining Method** – Cut-and-Fill
- **Mining depth** – approx. 2400 m
- **Problems** -

  Beyond 2000 m depth, all the stopes were under risks of bursting, irrespective of the pillar size (formed due to cut-and-fill mining).
- **Ground conditions** – Vertical stress is comparable with what might be expected from gravity loading. The horizontal stress, however, often exceeds the vertical (1.5 times at 2000 m depth). Estimated tensile strength of rocks varies from 8.3 to 26 MPa, UCS from 85 to 289 MPa and the modulus of elasticity ranges from 13.8 to 69 GPa. The wall rocks are a series of thin- and thick– bedded quartzites with argillaceous interbeds.
- **Destress blasting parameters**–

  Two blocks of ground, 76 m long by 12.5 m above and 12.5 m below the 7700 level by 1.5 m wide, in the plane of the vein were drilled with a fan-shaped pattern up to 30 m long, 100 mm diameter. A total number of 66 holes, 33 in each block, were drilled (Figure 2.6). The calculated powder factor is 0.28 kg//m^3. At the 7900 level, fan-shaped holes were drilled in 140 m strike length and 15 m above and below to the level. Holes were fired from Tovex 5000 (Emulson) with a charge density of 0.22 kg/m^3.

- **Destress blasting results review** –

  Figure 2.7 illustrates the perspective of stope destressing exercises conducted around the 7700 level. Destressing at the 7700 level, through seismic velocity measurements, showed that both the vein and wall rock had lower velocities after blasting- indicating reduced stiffness that should prevent high stress build-up. As mining progressed beyond the preconditioned zone, the release of seismic energy increased and rock bursting occurred, and some 20 incidences of bursts were observed. Closure measurements also show reduced stope closure – indicating a stiffer, more burst-prone vein and wall rock. Microseismic data showed that seismic activity in the non-preconditioned rock lasts longer after a stope round is blasted. Entire stopes in the vicinity were extracted without any significant seismic danger and it was made possible due to the destressing at the 7900 level. However, stress transfer due to this destressing caused a rockburst of 2.6 M_L on the Richter scale below the 7500 level (Figure 2.7 area marked 3 and details are also given in Figure 2.8). Figure 2.7 also illustrates an axis of rockbursts, which indicates about the axis where majority of the rockbursts occurred in the particular area at the different levels and in the time scale.

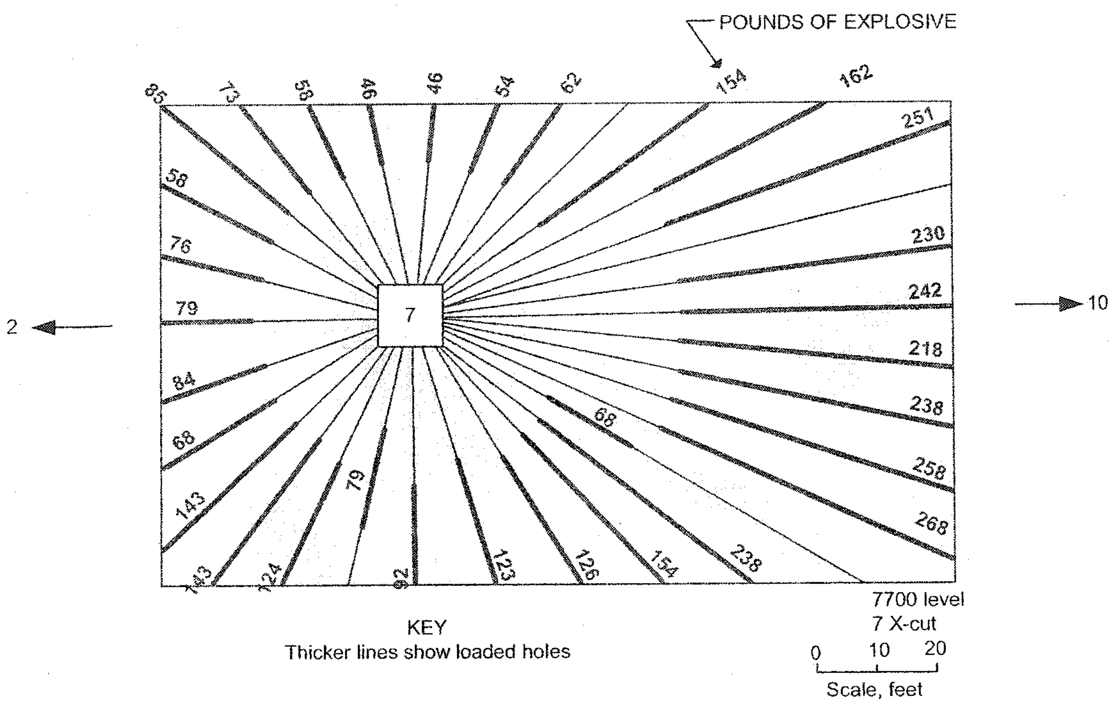

Figure 2.6 – Destressing hole pattern at the Star Mine

(Longitudinal - section)
(Corp, 1981, Karwoski et al., 1979)

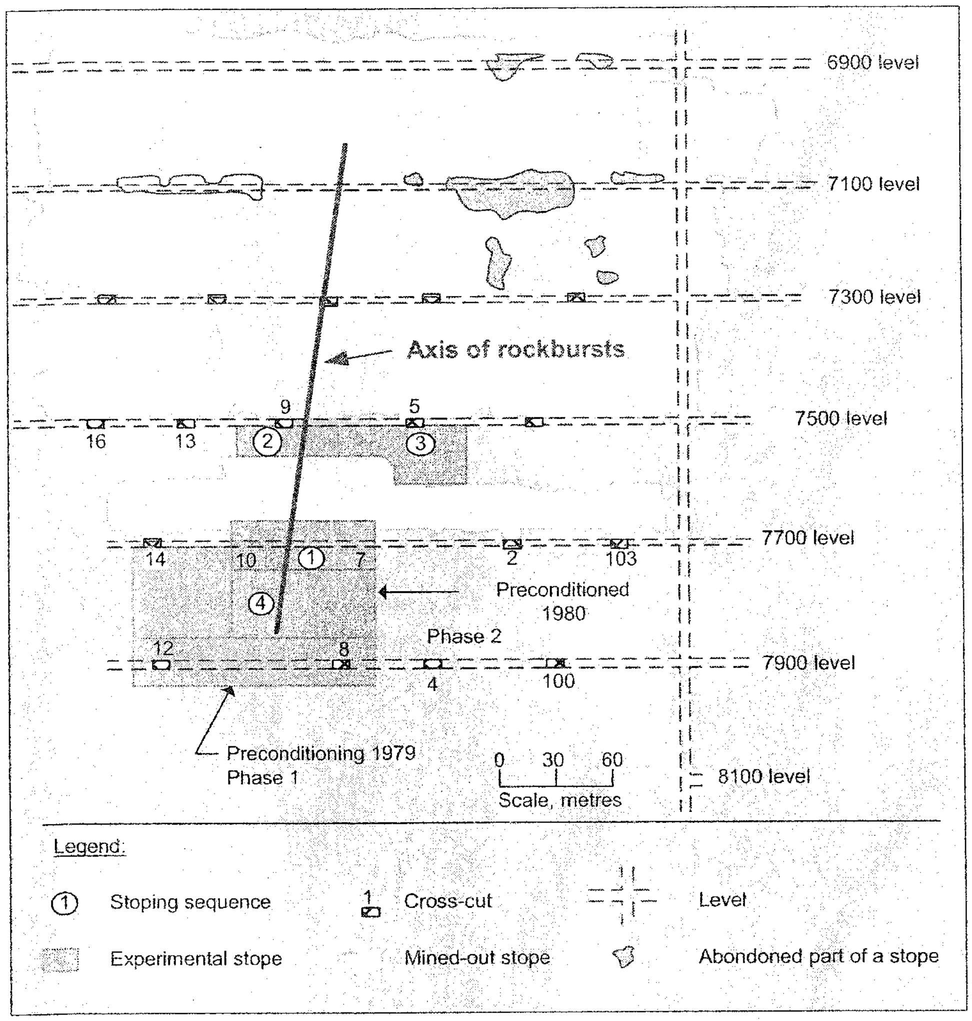

Figure 2.7 – Mining geometry, stope preconditioning and pillar destressing at the Star Mine

(Longitudinal section)
(Blake, 1982)

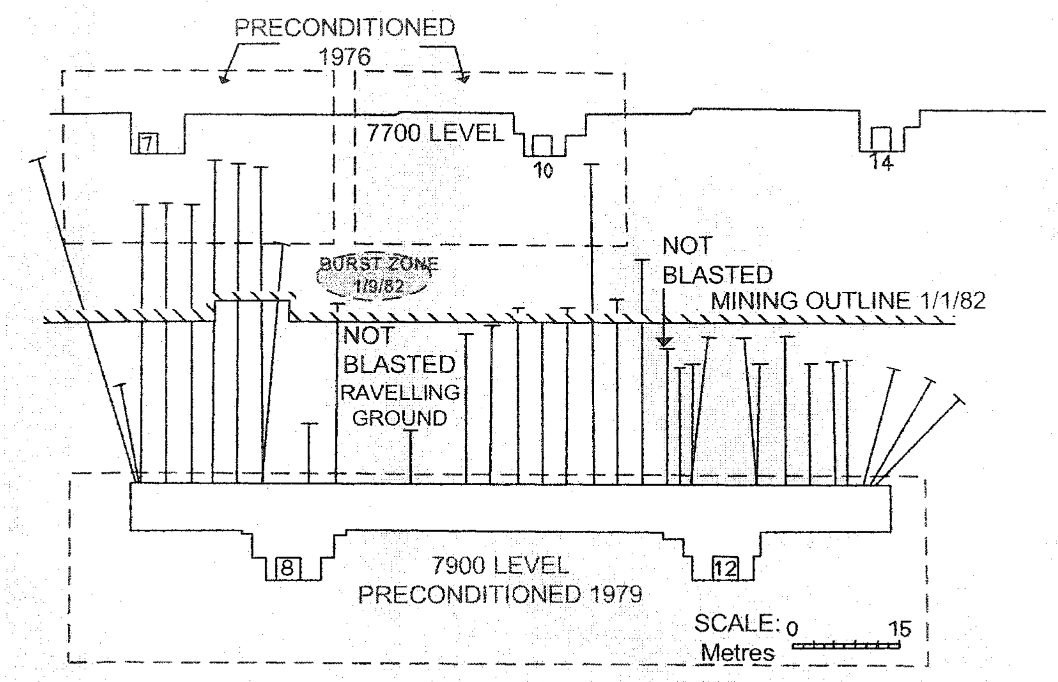

Figure 2.8 – Phase 2 preconditioning, 7900 level, Star Mine

(Longitudinal –section)
(Blake, 1982)

2.7.3 Brunswick Mine, Canada

(Andrieux et al., 2003; Liu et al., 2003)

- **Mine** – Brunswick Mine, Canada
- **Mining Method** –Open stope stoping with delayed backfill
- **Problem** - Difficult mining due to high stresses.

  The particular pillar of the case study, 29-9, is a squat pillar comprising massive, strong and stiff low-grade sulphides (Figure 2.9 and 2.10). The mine management called for an exercise to weaken the pillar so that stress shadow could be provided to the parallel vein pillars where high-grade ores are situated.
- **Ore properties** - massive stiff sulhpides (UCS=200 MPa, E=70 GPa, ρ =4.3 t/m^3).
- **Destress blasting parameters**– 165 mm diameter boreholes with an average charge length of 20 m were at a 2.4 m by 2.4 m grid at the toe (Figure 2.11). Emulsion explosive with a total of 17100 kg was used with no free face available to any of the holes. The powder factor ranged from 0.11 to 0.16 kg/m^3.
- **Destress blasting result** – The access drift from where destress blastholes were drilled showed the drift closure was due to the material ejection post the destress blast. It is important to note that in addition to the normal confinement, additional confinement was provided by pastefill spread in the drift.
- **Review** – The study involves the extensive use of an array of sophisticated equipment and techniques (Figure 2.11). Results obtained from the stress cells (Figure 2.12) do not match well either with the multi-point borehole extensometer (MPBX) observations presented (Figure 2.13) or with the expected response due to concurrent mining in the adjacent stopes. It is not clear why the stress cell in the uphole was showing higher stress relaxation while the mining in the adjacent stopes should have resulted in the stress concentration. Also, the downhole stress cell was placed only 4.5

m deep from the collar and therefore was too far from the blasting zone to provide any meaningful information. This load cell was located in the zone that experienced collar failure after destress blasting. Further, MPBX was not showing any response except a single value and the stress cells also seemed to be dead after the blasting. MPBX observations could not be corroborated from the seismic tomography results. Only two observations corroborate each other, borehole endoscopy and seismic tomography (Figure 2.14) indicate that the charged section did not induce effective fracturing in the rockmass.

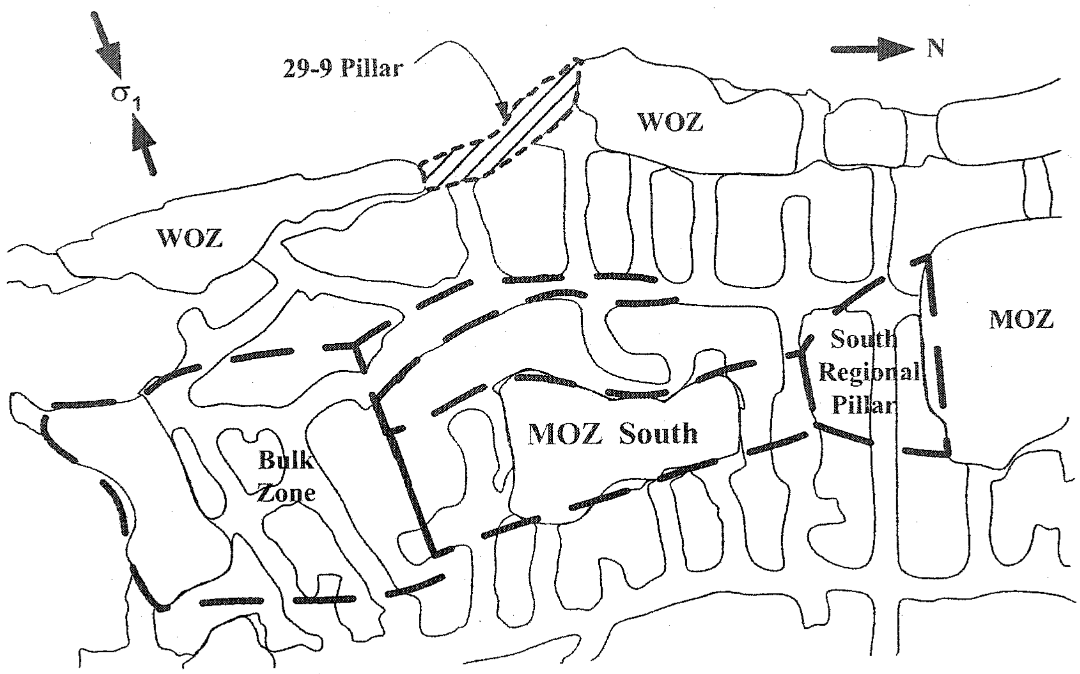

Figure 2.9 – Schematic Plan view of destress blasting pillar (29-9 pillar)
(Andrieux et al., 2003)

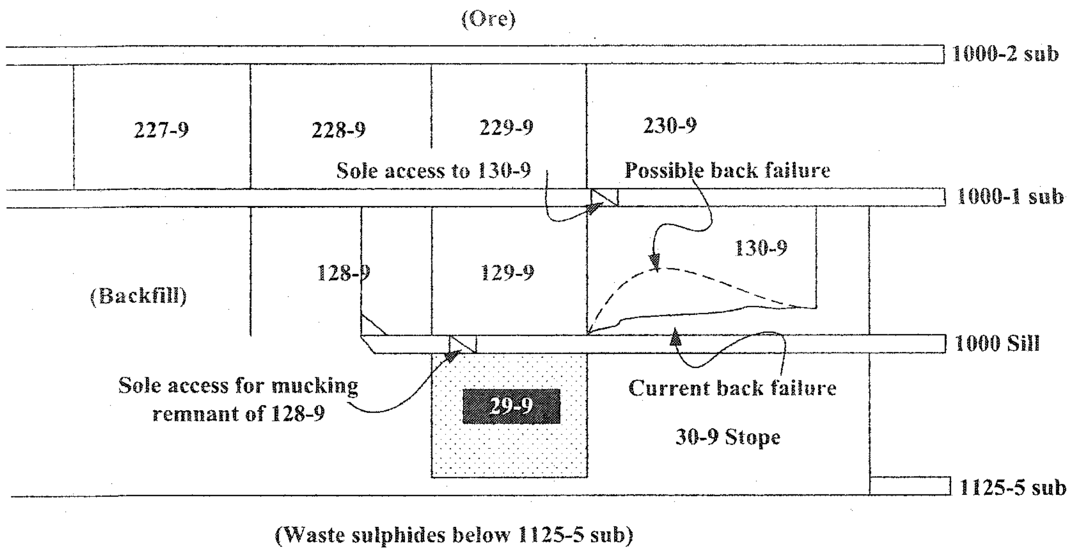

Figure 2.10 – Schematic Longitudinal section of destress blasting pillar

(Andrieux et al., 2003)

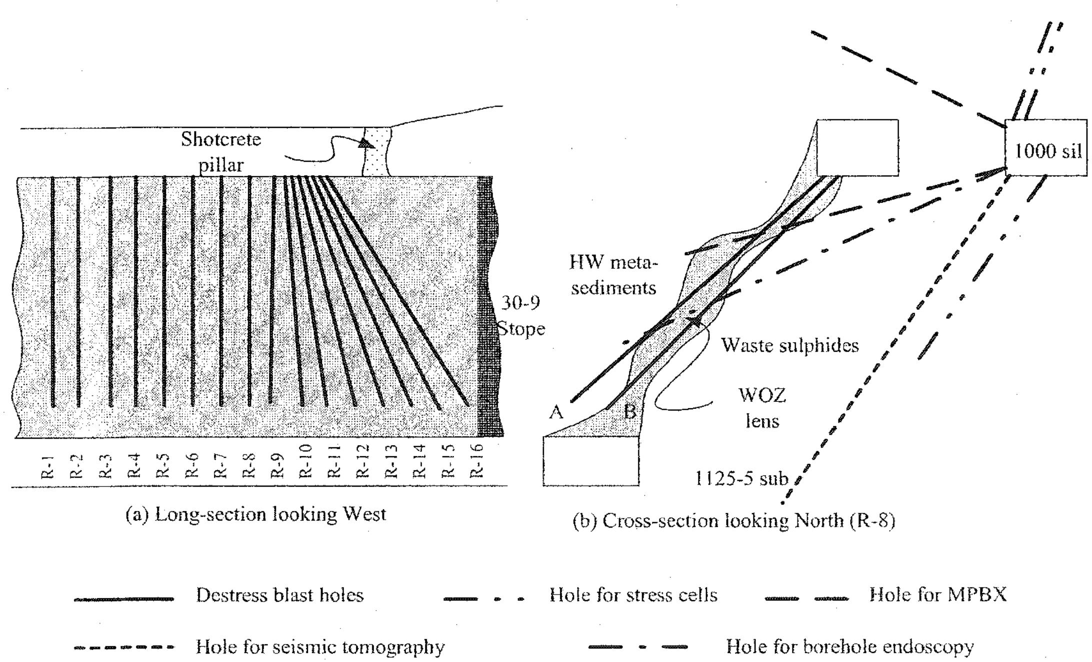

Figure 2.11 – Schematic drilling pattern for destress blasting and instrumentation of the 29-9 pillar

(Andrieux et al., 2003)

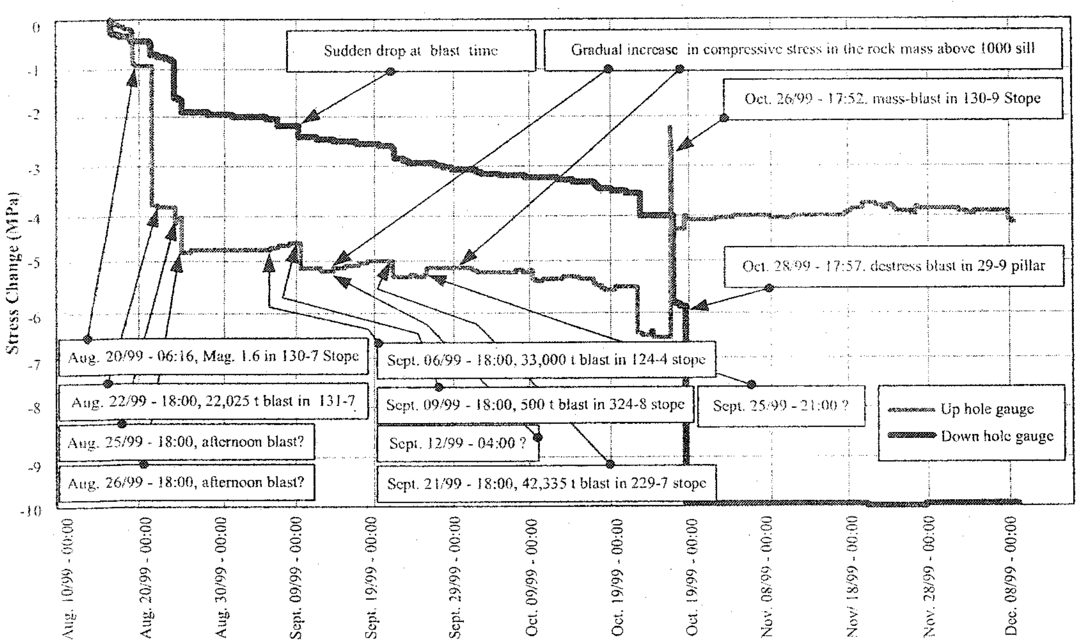

Figure 2.12 – Stress cell measurements from the uphole and the downhole (Andrieux et al., 2003)

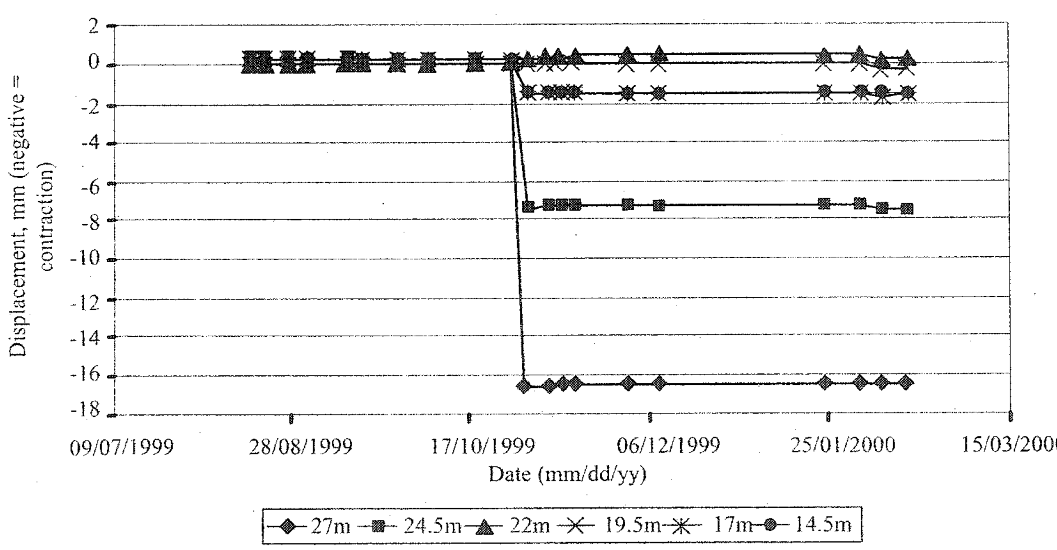

Figure 2.13 - MPBX measurements from the downhole (Andrieux et al., 2003)

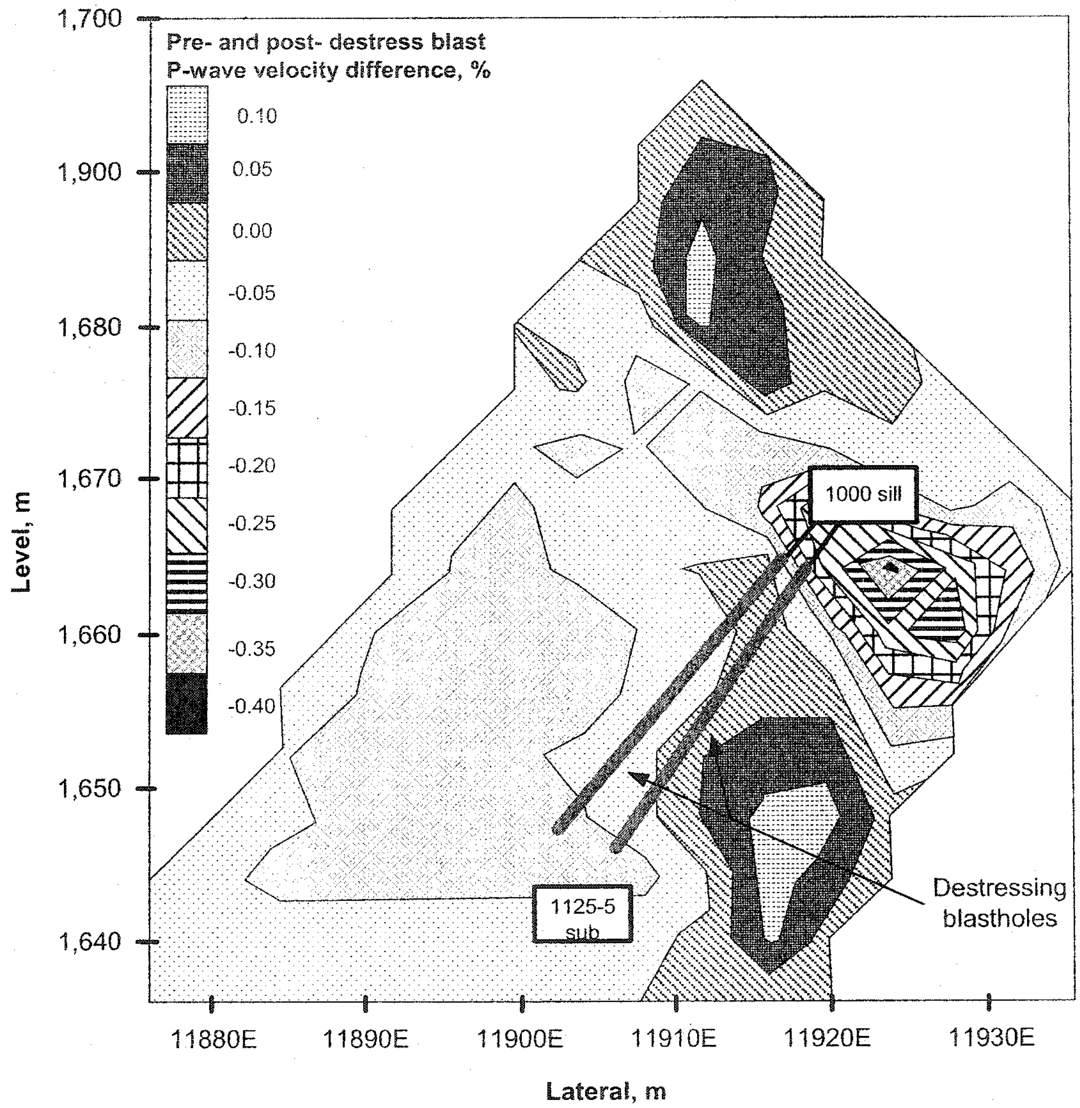

Figure 2.14 – Seismic tomography of the destress blasting zone
(Andrieux et al., 2003)

2.8 SUMMARY

The analysis presented in the chapter indicates that different governing operating mechanisms are involved in the field destress blasting program. It is not known which operative mechanism is involved in a particular scenario. An active face of any underground excavation susceptible to strainbursting needs destressing. The active face may be a drift, a pillar or the complete stope. A successful destress blasting should have significant technical and economical benefits for the mines suffering from strain bursting phenomena. The case studies evaluated indicate that the field application of destress blasting is very complicated; it needs a thorough understanding of in situ stress regimes as well as mining induced stresses and may involve an extensive or sophisticated instrumentation program. Even then, the success of destress blasting cannot be guaranteed. This suggests that a better understanding is required about stress transfer mechanisms as well as the way explosive energy is transmitted to the rock. This requires investigation to understand rock fracturing by explosive energy and propagation of the fractures under in-situ stress regimes. An attempt is made towards this direction in the following chapter.

CHAPTER 3

FRACTURES INITIATION AND PROPAGATION IN ROCK BY EXPLOSIVE ENERGY

3.1 OVERVIEW

The study of fracture initiation and propagation in rocks due to explosive energy is of great engineering importance. This knowledge has many practical applications for mining engineering, civil engineering and petroleum engineering. The knowledge in mining engineering is required for efficient rock breakage, limiting damage to the host rock mass and effective destressing of a rockburst prone area.

A system engineering approach is required for a better understanding of the phenomena governing a dynamic fractures initiation and propagation study. Figure 3.1 illustrates three main systems involved in the study, namely, rock, explosive and boundary conditions. The study is influenced by numerous sub-systems and their mutual interaction. A detailed investigation on the role of various systems and sub-systems on rock fractures initiation and propagation is discussed in the subsequent sections.

A theoretical analysis is presented here for a better understanding of dynamic fracture initiation and propagation mechanisms as well as rock-explosive energy interaction studies. The analysis is also made in order to find out a suitable experimental procedure for destress blasting as well as to identify the role of in-situ stresses on the dynamic fractures initiation and propagation. This will assist in evaluating destress blasting mechanisms as well as its effective field implementation.

3.2 DYNAMIC ROCK FRACTURE MECHANISMS

Explanation of the detonation process can be found in many publications related to blasting engineering (e.g. Bhandari, 1997; Clark, 1987; Fourney, 1993, etc.). According to these explanations, detonation of an explosive charge, confined within a borehole, initiates a very rapid chemical reaction at a velocity between 2000 to 7000 m/s (VOD or V_d, velocity of detonation). The chemical reaction is exothermic (temperature in the range of 3000 to 4000 K) and converts the solid mass of explosive into gaseous products. The very rapid conversion of chemical energy into thermal and gaseous energy develops a detonation pressure (P_d) in the range of 0.5 to 50 GPa. The detonation pressure generates an explosion pressure (P_e) in the reacted portion of the explosive column. The actual pressure on the boundary of the borehole (P_b, borehole pressure) depends on the rock mass stiffness properties, amount of gas produced, temperature, velocity of detonation, borehole volume, etc. (Figure 3.2).

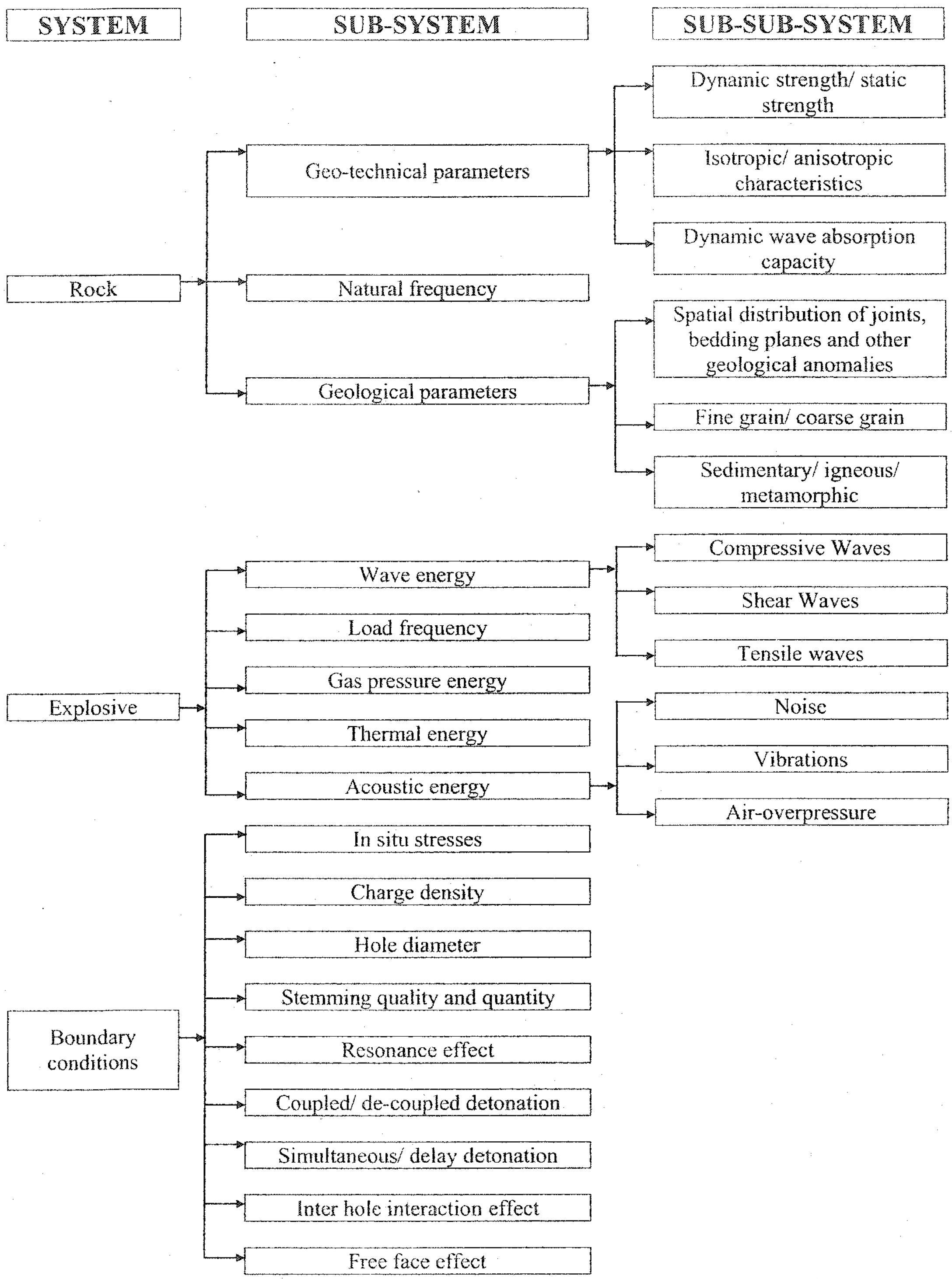

Figure 3.1 – Engineering systems for rock blasting

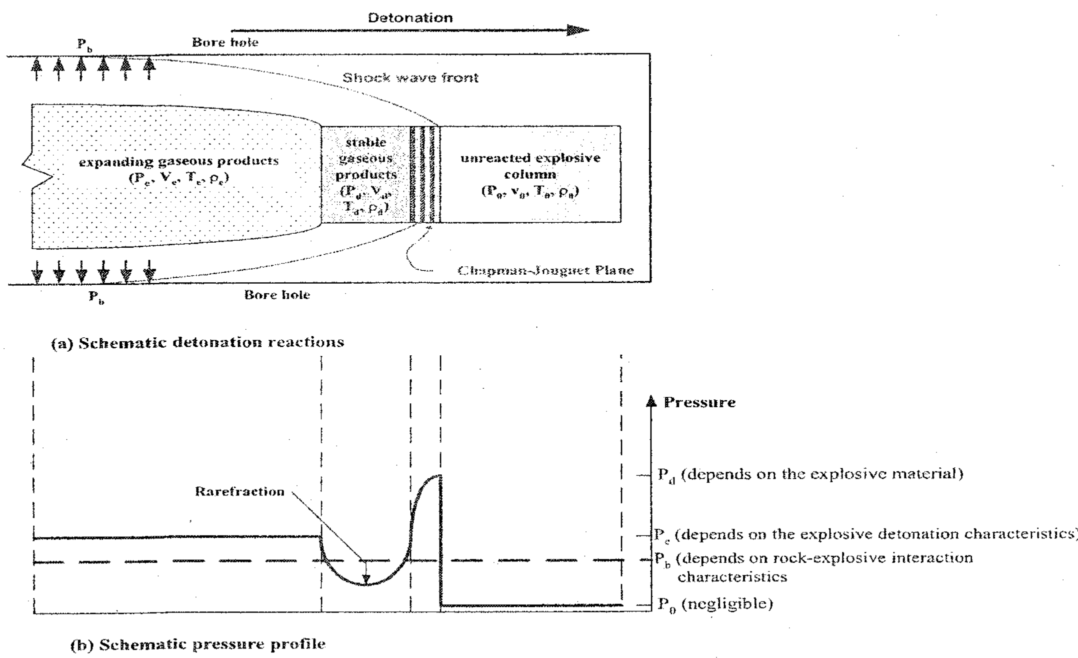

Figure 3.2 – Detonation process of an explosive in a borehole
(Atlas, 1987; Bhandari, 1997; Clark, 1987; Khoshrou, 1996)

The following simplified equations are in use for the estimation of P_d, P_e and P_b (Atlas, 1987; Clark, 1987; Nie and Olsson, 2000).

$$\text{Detonation Pressure, } P_d = \rho \frac{V_d^2}{4}, \text{Pa} \quad \text{......(3.1)}$$

$$\text{Explosion Pressure, } P_e = \frac{P_d}{2} = \rho \frac{V_d^2}{8}, \text{Pa} \quad \text{......(3.2)}$$

$$\text{Bore Hole Pressure, } P_b = P_e\left(r_c^{2\gamma}\right), \text{Pa} \quad \text{......(3.3)}$$

where, ρ = explosive density, kg/m^3

V_d = Velocity of detonation, m/s

$$r_c = \text{coupling ratio} = \frac{\text{explosive diameter}}{\text{bore hole diameter}}$$

γ = adiabatic exponent = 1.5 (Persson et al., 1994)

$$= \sqrt{1 + \frac{V_d^2}{Q}} \quad \text{(Fickett and Davis, 1979) ......(3.4)}$$

Q = heat of explosion of the explosive, KJ/kg

The borehole pressure has two distinct characteristics for two general categories of detonation, namely, high order detonation (also termed ideal detonation) and low order detonation (also termed non-ideal detonation). The high order detonation has a higher peak pressure as well as a steep drop in the pressure wave whereas the low order detonation has a lower peak pressure, which attenuates in a longer duration (Aimone, 1992; Olsson et al., 2001) (Figure 3.3). One can find contradicting in-borehole pressure measurements with regards to the time needed to attain the peak-pressure values. However, the complete duration time for the borehole pressure-time profile is similar in these contradicting measurements. The peak-pressure time profile falls to stand-off pressure in a couple of milliseconds (stand-off pressure is a pressure much less than the tensile strength of most of the rocks). Many publications cite explosive peak-pressure attainment time in the order of milliseconds (Holloway et al., 1986; Nakayama, et al., 2001; Schatz et al., 1987a) but there are also in-borehole measurements suggesting the peak pressure rise time is in between 20-150 microseconds depending on the explosive types and confinement (Daniel, 2003; Frantzos, 1989; Jung et al., 2001; McHugh and Keough, 1982; Olsson et al., 2001).

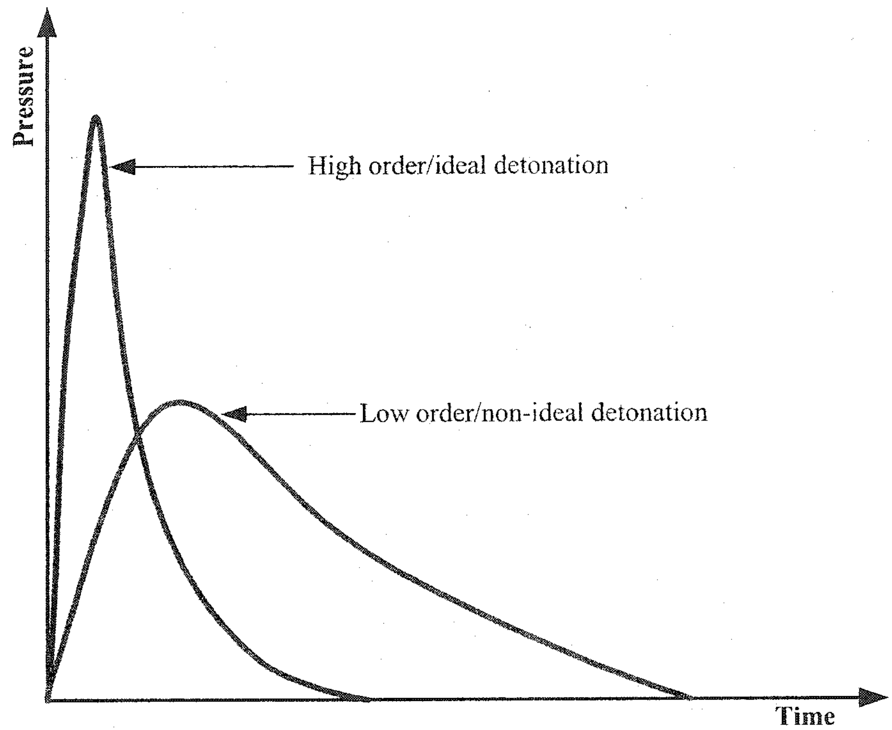

Figure 3.3 – Pressure pulse shapes for two categories of detonation (Aimone, 1992; Olsson et al., 2001)

The action of detonation in the rock mass is shown in Figure 3.4. According to Figure 3.4, impingement of the transient borehole pressure on the borehole boundary generates shock waves into the rock. Primarily, shock waves are compressive but they associate tensile waves due to hoop stresses during the process of rock fracturing. Part of the shock wave energy is reflected where it meets either with a discontinuity (showed as interface in between rock 1 and rock 2 in Figure 3.4) or media with changed properties (showed as free face at the borehole collar and at the bench slope in Figure 3.4). The reflected shock wave acts as a new source of shock wave energy propagation (secondary shock wave) and may be compressional or tensile in primary nature, depending on the characteristic acoustic impedance difference at the interface of the original and new media or discontinuity. The stress waves, through their interaction with existing microflaws, are the dominant force in fragmenting the rock (Winzer et al., 1983). Fractures generation, propagation and coalescence at a point of consideration continues untill superimposed values of the primary and secondary shock waves attenuate to a value lower than the tensile strength of the rock at that point under the existing state of stress.

Considerable efforts were made in the last four decades to understand rock fracture mechanisms by explosive energy. The work done so far has only led to general agreement on the development of stress waves and gas pressure by explosive loading. Controversies still exist regarding their respective roles and mechanisms (see Table 3.1).

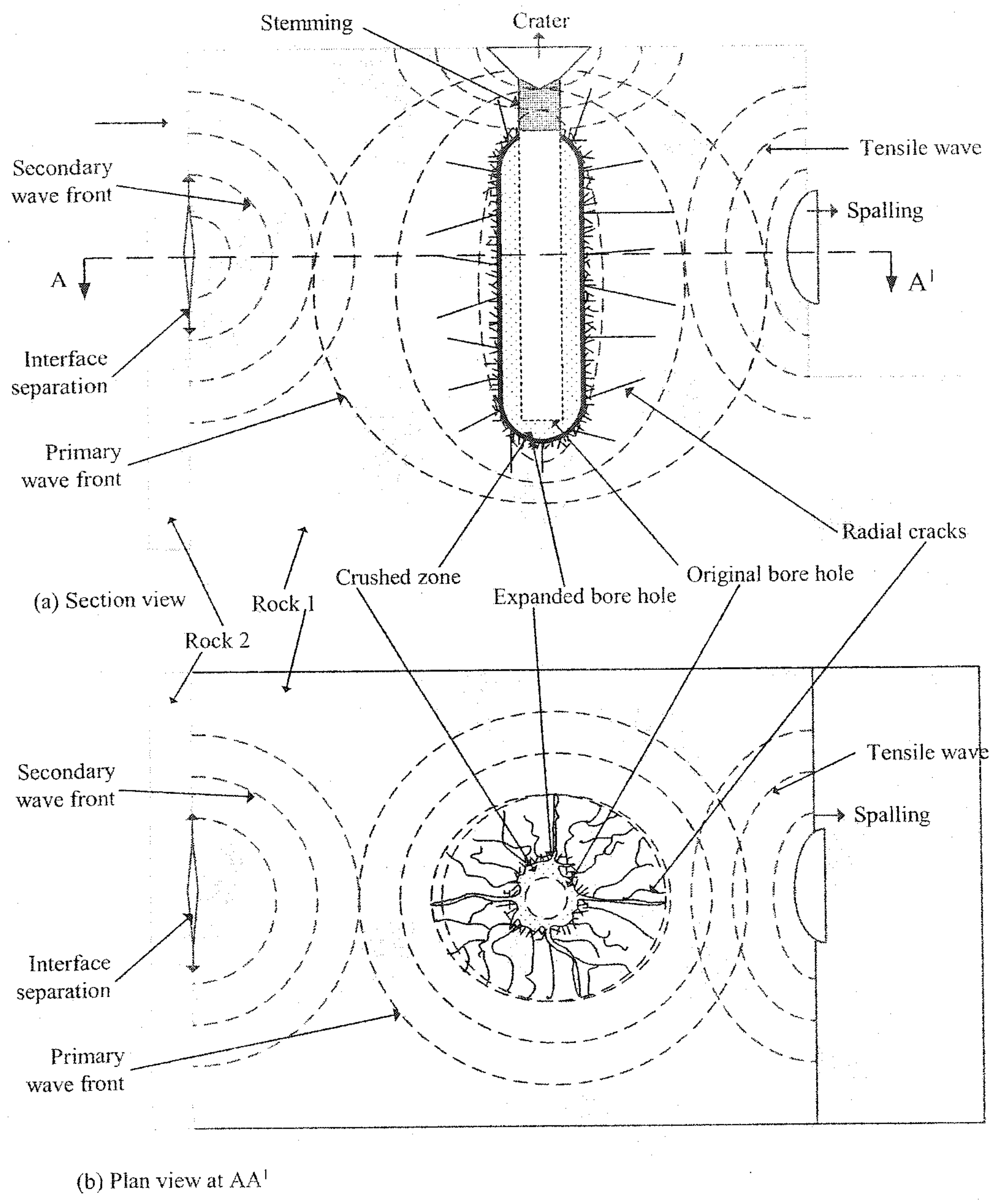

Figure 3.4 – Action of an explosive in a rock mass

(Atchison, 1968; Bhandari, 1997; Mosinets and Garbocheva, 1972; Scott et al., 1996)

TABLE 3.1 – Blasting theories and their breakage mechanisms

(Revised after Atlas, 1987)

Reference	Breakage mechanism				
	Tensile reflected waves	Compressional stress waves	Gas pressure	Flexural rupture	Nuclie stress flow
Obert & Duval, 1949	X				
Hino, 1956	X				
Duval & Atchison, 1957	X				
Rinehart, 1958	X				
Langefors & Kihlstrom, 1963		X	X		
Starfield, 1966	X				
Porter & Fairhurst, 1970		X	X		
Persson et al., 1970		X			
Kutter & Fairhurst, 1971		X	X		
Field & Ladegarrd-Pederson, 1971		X	X		
Johansson & Persson, 1972	X		X		
Lang & Favreau, 1972	X	X	X		X
Ash, 1973			X	X	
Bhandari and Vutukuri, 1974	X	X	X		
Hagan & Just, 1974		X			
Barker et al., 1978					X
Winzer et al., 1983					X
Margolin & Adams et al., 1983					X
McHugh, 1983					X
Brinkmann 1987		X			
Daehnke et al., 1996			X		
Nie & Olsson, 2000		X			

Propounders of the gas pressure breakage theory put forth differences in the shock wave velocity and the crack propagation speed (shock wave velocity is three times greater than crack propagation speed) (Edgeston and Barstow, 1941; Shockey et al., 1974) in favour of their arguments (Daehnke et al., 1997) but at the same time ignore interaction between the primary and the secondary waves (emanated from pre-existing flaws in the rock mass). Expounders of stress wave theories put forth larger number of cracks formation near a borehole in favour of their point of view (quasi-static pressure should form only a couple of cracks rather than numerous cracks) (McHugh, 1983).

Various experimental methods have been employed to understand rock fracturing by explosive energy. The experimental methods involved laboratory studies (summarized in Table 3.2), pilot field studies (summarized in Table 3.3), and other indirect techniques like the Hopkinson split pressure bar technique (summarized in Table 3.4) for the identification of dynamic fracture mechanisms. None of these methods are suitable for the research proposed in this thesis. The laboratory experimental methods suffer from the scale effect and the field scale studies are prohibitive due to the cost involved. Further, none of the existing experimental methods provides full control on the experiments (the dynamic load needs to be applied at a much reduced level with the laboratory level methods, and boundary effects can not be avoided in both the field and the laboratory methods) and a rapid fracturing process also poses observational difficulties. However, barring the controversies of the respective roles of stress wave and gas pressure in rock fracturing and limitations of the different experimental procedures, the following conclusive observations can be made with the studies done so far.

TABLE 3.2 – Laboratory studies for dynamic rock fractures mechanisms

RESEARCHER (S)	PURPOSE OF EXPERIMENTS	BRIEF DESCRIPTION	REPORTED RESULTS
Olsson et al. (2001)	Investigations for fundamental rock breakage phenomena	Two steel lined holes of 43 mm dia. at 0.8 m simultaneously fired with 17 mm dia. Pipe charges (dynamite and emulsion) in 2-4 m^3 granite blocks without stemming. Stemmed hole of 38 mm without liners were also tried.	Shock wave is responsible for rock breakage and gas pressure helps in movement of broken rock. Low velocity of detonation (VOD) explosives works gently on rock while high VOD gives more impact shock.
Ayres et al. (2000)	Safe boulder blasting	Water filled 5/8" holes in 1 ft^3 blocks were blasted with 8 No. cap + c4 explosive (RDX, cyclotrimethylemetrinitramine, based)	Water filled boulder blasting fragmented blocks in large pieces without fly-rock.
Daehnke et al. (1997)	Investigate dynamic fractures mechanisms	Cylinderical PbZ_3 charge used in PMMA (Polymethyl methacrylate, an amorphous brittle material) blocks. Numerical modeling analysis employing fracture mechanics principles also performed.	Majority of fracturing occurs due to pressurization of detonation gases.
Bhandari, S. and Badal, R. (1990)	Effect of joint pattern on bench blasting	Bench blasting was simulated with 750 mm x 500 mm x 500 mm sandstone blocks. Holes were blasted with detonating cords.	Reflected tensile waves further extend fractures already created by compressive waves.

Singh, D.P. and Sastry, V.R. (1986)	Effect of joint material on fragmentation in bench blasting	Bench shaped models (700 mm x 400 mm x 150 mm) of Chunar Sandstone were blasted with a single 50 mm deep and 6.5 mm dia. hole with detonating cord. A single 3 mm wide joint running parallel to the face and filled with four different types of materials was incorporated in the study.	Size and shape of bench crater is more controlled by burden than by the jointing material itself. Strain energy dominates fragmentation mechanism at smaller burden but for larger burden both, gaseous and strain energy, play role.
McHugh and Keough (1982) McHugh (1983) Schatz et al. (1987a and b)	Study oil well stimulation technique	Cylinderical tuff blocks of 12" dia. and 12 " long 0.5" central stemmed hole were blasted with PETN. The blocks were hydrostatically pressurized to 6.9 MPa.	Gas pressure acts dynamically rather than quasi-statically and increases the crack length in order of 5 to 10 times than the dynamic pressure without the gases. Lower amplitude pressure with the low frequency produces smaller crushed zone and longer radial fractures. Confinement reduces the crack length by a factor of 2 to 3.
Worsey et al. (1981)	Investigating pre-split mechanism	Detonating cords used in 2.5 mm to 25 mm dia. holes for 150 x 150 x 75 mm Plexiglas blocks. Tests are also conducted on larger sandstone blocks with discontinuous planes.	The majority of cracks are exclusively caused by quasi-static gas pressure. Pre-splitting is primarily caused by the interaction of tensile stresses induced by quasi-static gas pressure.

Dally et al. (1978)	Investigating pre-split mechanisms	70 mg charge placed in 8.75 mm diameter holes and simultaneously fired in 6.4 x 450 x 610 mm Homolite sheets	Notched holes are the best for the control of fractures direction in comparison to simultaneous firing and dummy hole practice
Dally et al. (1975)	Investigating effect of gas pressure on crack generation	70 mg of PbN_6 was blasted in 0.344" holes made in transparent Homalite100 2D sheets (16" x 16" & ¼" thick). Some holes were contained for comparative gas pressure effect	Gas pressure helps in extending cracks in blasthole vicinity. Containment of gaseous products increases amplitude of tensile wave and results in more fractures and fractures length. There is no difference in compressional waves.
Bhandari, S. & Vutukuri, V.S. (1974)	Investigating bench blasting parameters	Granite blocks of 300 mm x 300 mm x 230 mm and bigger mortar blocks were blasted with detonating cord (5.3g/m) in hole dia. 4.8 mm to 7.9 mm	Near blast hole fractures are formed by quasi-static gas pressure while fractures near free face are formed by stress waves reflection.

TABLE 3.3 – Pilot field studies for dynamic rock fractures mechanisms

RESEARCHER (S)	PURPOSE OF EXPERIMENTS	BRIEF DESCRIPTION	REPORTED RESULTS
Olsson et al. (2001)	Investigation for fundamental rock breakage phenomena	Commercial pipe charges (dynamite based and emulsion based) of 17 mm to 22 mm dia. are used in 51 mm to 64 mm dia. Holes on 5 m high granite benches with 1.0 m burden and 0.8m spacing. Some holes were stemmed; some unstemmed and in some steel liner was inserted (swellex bolt). Holes were simultaneously fired.	Shock wave generates cracks and gas pressure helps in moving fragmented rock but the phenomena are explosives dependant
Liu and Katsabanis (1996)	Investigating effect of air-decking on fragmentation	30 gm high explosive (Detasheet C) is blasted with and without airdecking in a 22 mm dia. , 240 mm long hole in granite	Air-decked hole produced larger crater and longer radial cracks around blasthole
Brinkmann (1987 and 1990)	To establish the influence of important blasting variables on blasting results	Dynamite, ANFO, watergel and emulsion explosives were used in 0.9 m to 1.5 m long and 28 mm to 42 mm diameter holes with a burden of 0.4 to 0.8m in a 185m deep gold mine of less than 1m thick coarse grained Kimberely quartzite (but stope width is 1 to 1.4 m) in between fine grained Witswatersrand quartzite	Blast hole liner experiments suggest that break-out is controlled by gas penetration and fragment sizes are governed by shock
Bhandari, S. (1979)	Investigation for quasi-static gas pressure on fragmentation	25 mm dia. holes were blasted with slurry explosive (0.5 kg/ per hole) on 1m high benches in granite with varying spacing and burden	Change in blasting parameters changes fragmentation mechanism from quasi-static gas pressure to strain energy.

TABLE 3.4 – Indirect techniques for studying dynamic rock fractures mechanisms

RESEARCHER (S)	PURPOSE OF EXPERIMENTS	BRIEF DESCRIPTION	REPORTED RESULTS
Zhang, Z.X., Yu, J. Kou, S.Q. and Lindqvist, P.A. (2001)	Investigate effect of loading rate and temperature on dynamic fractures of rock	Hopkinson Split Pressure Bar used on 30 mm dia. And 44 mm long gabbro and marble samples	Better energy utilization is possible with slow loading rate no matter whether a high temperature is available or not.
Bohloli, B. (1997)	Study of fines generation due to dynamic loading	Hopkinson Split Pressure Bar used on 42 mm dia., 25 mm long diabase and gneiss samples	Rock structure plays an important role in fines generation. Rock containing brittle and granular mineral like quartz and feldspar generates more fines than the elongated minerals like amphiboles and pyroxenes.
Shockey et al. (1974)	Predict fragment size distributions for rock under dynamic loading conditions	Impact experiments carried out with gas gun using flat projectile impact technique on cylindrical quartzite specimens of 0.635 cm thick and 1.27 to 3.81 cm dia.	Fragmentation mechanism consists of four stages: (a) Activation of pre-existing flaws. (b) Radially outward propagation of flaws (c) Coalescence and bifurcation of propagating flaws, and (d) Isolation of individual flaws from one another An FDM model using fracture mechanics principles also confirms the above mechanism in their study.
Kutter & Fairhust (1971)	Dynamic fracture mechanism	Electro hydraulically dynamic loads (high voltage electric under water spark) were provided to 2D samples (plates/ discs) of Plexiglas, glass, marble, granite, basalt and slate.	Fractures process starts with wave action but extended by gas pressure. Fractures by wave action is dependant on wave velocity, tensile strength of rock, borehole pressure, velocity of detonation and energy absorption by rock mass. Both wave and gas generated fractures propagate preferentially in the direction of maximum principal stress. This effect has strong effect and can even eliminate the influence of pre-existing fractures.

(a) Reduction in unwanted damage to the host rock by an explosive action can be achieved by hydrofrac action rather than dynamic action. This hydrofrac action can be achieved by de-coupling and non-ideal detonation of low energy explosives and prolonged action of the reduced pressure level (see also Barkley et al., 2001).

(b) Further reduction in the crushing zone and intense fracturing zone can be achieved by air-decking techniques (see also Bussey and Borg, 1989; Worsey et al., 1981).

(c) Insertion of a viscous medium (such as water or sand) or a material with a different impedance than the rock also helps in reducing the crushing zone as well as reducing the number of radial fractures. Bhandari and Rathore (2002) suggest the use of cardboard liners to reduce damage to the host rock.

(d) Rock structure plays an important role in the fracturing of rock. Granular minerals produce more fines than elongated minerals.

(e) The fractures propagation needs to be specified in the borehole should directional fracture growth be needed. The notched borehole technique and shaped charges can be employed for such effects.

3.3 QUANTIFICATION OF ROCK FRACTURING BY EXPLOSIVE ENERGY

The pressure from the borehole is transmitted as shock waves (the primary shock waves) in the rock mass. Transmission of the shock waves in the rock mass creates a crushed zone (up to 4 borehole radii), a fractured zone (up to 50 borehole radii) and a seismic zone beyond these two zones, respectively, starting from the borehole boundary (Bhandari, 1997). Mosinets and Garbacheva (1972) proposed the following equations for the identification of the crushed zone, fractured zone and seismic zone, respectively, based on large diameter borehole blasting studies.

$$\text{Crushed zone radius, } r_{cr} = \sqrt{\frac{C_s}{C_p}} \cdot \sqrt[3]{q} \qquad (3.5)$$

$$\text{Fracture zone radius, } r_f = \sqrt{\frac{C_p}{C_s}} \cdot \sqrt[3]{q} \qquad (3.6)$$

$$\text{Seismic zone radius, } r_s = \frac{\sqrt{C_p}}{10} \cdot \sqrt[3]{q} \qquad (3.7)$$

where, q = explosive weight in TNT equivalent, kg

C_p = longitudinal shock wave velocity, m/s

C_s = transverse shock wave velocity, m/s

The above equations can be validated from the ground penetrating radar (GPR) studies made by Grodner (2001) in South African gold mines. He identified a seismic zone, which is in remarkably good aggrement with Equation 3.7 above.

In another study for deep coal mines in China, Kexin (1995) reports the following equation for the identification of the fractures zone radius. The fractures zone radius predicted by Equation 3.8 differs by 1.3 to 2.6 times the predictions made by Equation 3.6.

$$\text{fractures zone radius, } r = 96\left(\frac{G}{10\sigma_c}\right)^{\frac{1}{8}} (10E)^{\frac{1}{6}} \qquad (3.8)$$

where, r is the fractures zone radius(mm), σ_c is the uniaxial compressive strength (MPa), E is the elastic modulus(MPa) and G is the unit charge length (kg/m) (TNT equivalent).

Calder (1977) presents a nomogram for the fractures zone estimation based on several experiments involving different rocks and explosives (Figure 3.5). The nomogram appears to be in good agreement with Equations 3.7 and 3.8 as well as with the field study by Grodner (2001).

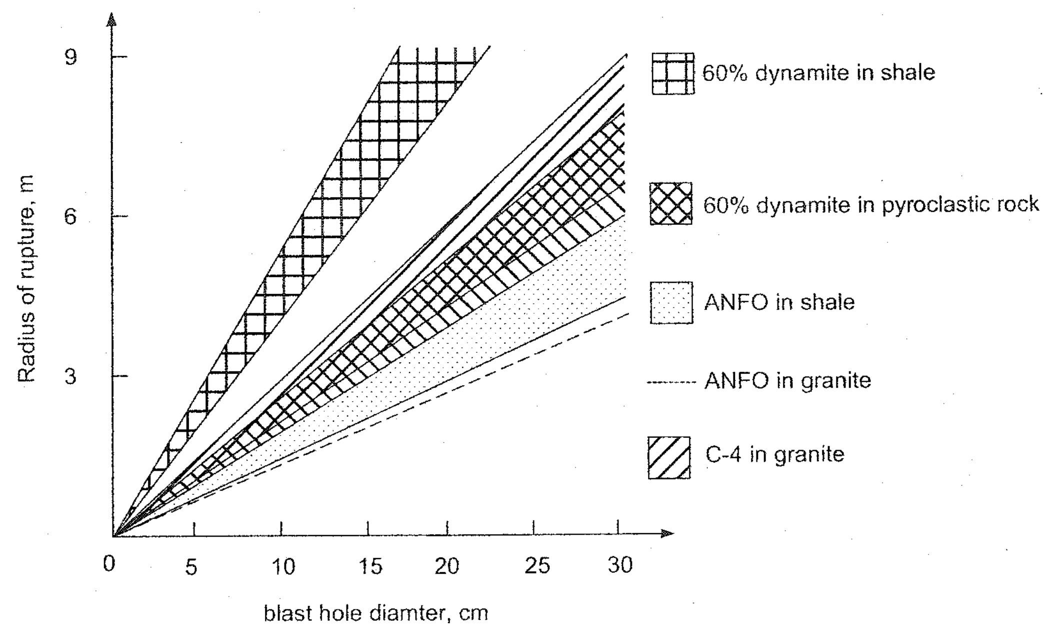

Figure 3.5 – Radius of fractures by different explosives in different rocks (Calder, 1977)

Holmberg and Persson (1979) proposed the following equation for damage assessment due to small and large diameter blasting in hard rock mines. The minimum peak particle velocity of 700 mm/sec. is assessed as the damage initiation level (Figure 3.6).

The peak particle velocity, $$v = k\, l^{\alpha} \left[\int_0^H \frac{dx}{\left[R_0^2 + \left(R_0 \tan\theta - x \right)^2 \right]^{\beta/2\alpha}} \right]^{\alpha} \qquad \text{.............(3.9)}$$

where, R_0 = perpendicular distance from borehole to the point of observation, m

θ = the angle of elevation to the point of observation from the end of explosive charge

k, α, β = constants (700, 0.7 and 1.5 for the hard rocks, respectively)

H = Explosive charge column height, m

l = charge concentration in kg/m normalized with respect to the weight strength of ANFO (1.05) as given below

$$s_{ANFO} = \frac{\left(Q + \frac{V_g}{0.85} \right)}{5.04} \qquad \text{...(3.10)}$$

Q = heat of explosion, MJ/kg

V_g = released gas volume at STP, m^3/kg

Brinkmann et al. (1987) summarize different criteria of rock fracturing predictions based on peak particle velocity (PPV) measurements, which are presented in Figure 3.7.

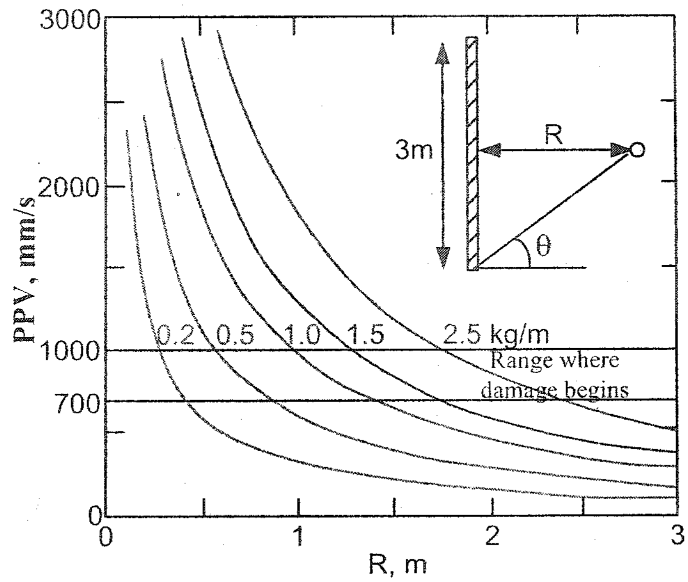

(a) Small diameter tunnel blasting

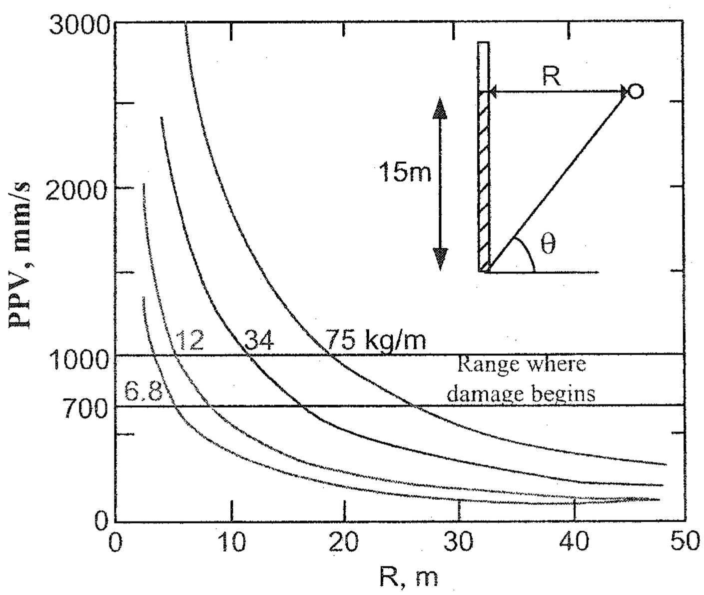

(b) Large diameter open pit blasting

Figure 3.6 – Estimated peak particle velocity as a function of distance for different linear charge densities, kg/m borehole length

(Holmberg and Persson, 1979)

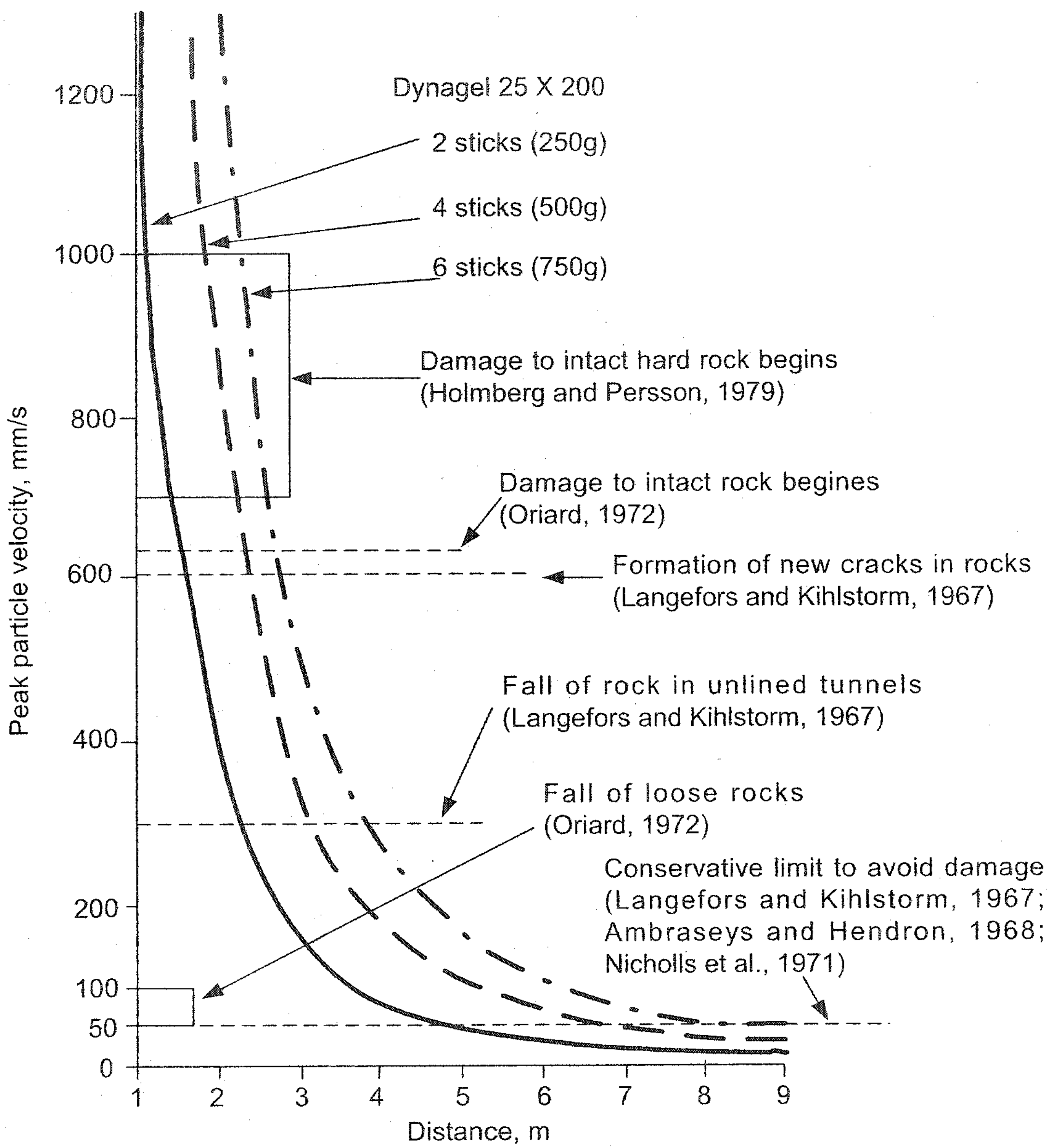

Figure 3.7 – Reported damage threshold with respect to peak particle velocity (Brinkmann et al., 1987)

3.4 ROCK – EXPLOSIVE ENERGY INTERACTION STUDIES

A mechanistic model is in use to describe the rock-explosive interaction using pressure-volume curves of explosion gases by blasting (Lownds, 1986; Lownds and Du Plessis, 1984; Kirby and Lieper, 1985; Udy and Lownds, 1990; Scott et al., 1996; Whittaker, 1992). According to the model, the area under the curve between borehole pressure and volume of expanding explosive gases represents explosive energy utilization. The concept is shown in Figure 3.8 with the assumed partition of the explosive energy.

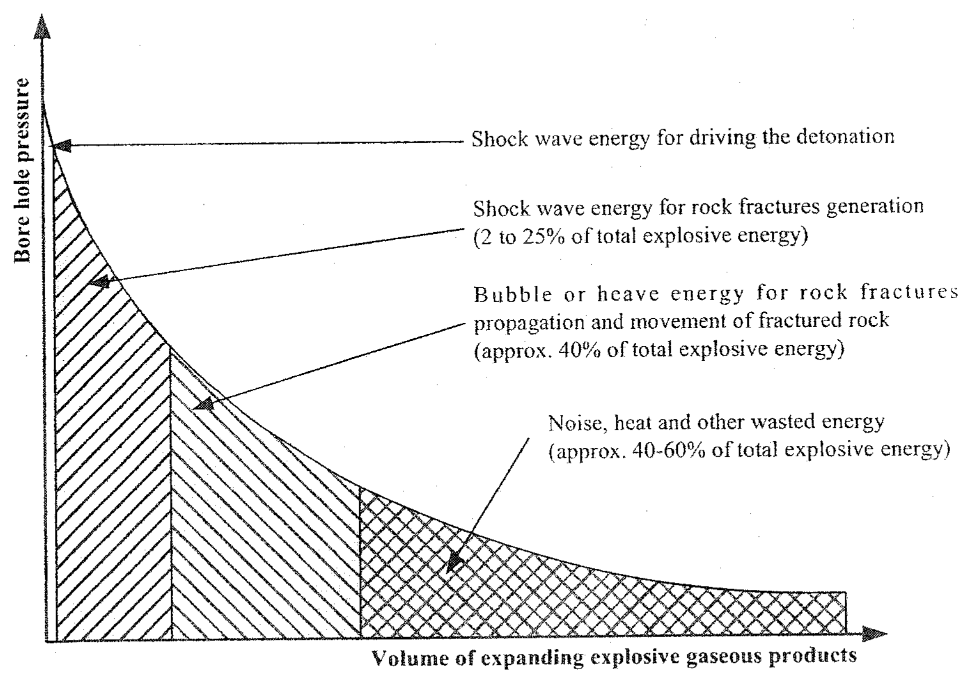

Figure 3.8 – Explosive energy released during different phases of rock blasting (Lownds, 1986; Lownds and Du Plessis, 1984; Scott et al., 1996; Whittekar, 1992)

Fogelson et al. (1959) concluded that energy in the form of a shock wave is about 9 per cent of the total energy for a high energy explosive. Langefors and Kihlstorm (1978) theoretically estimated and found that shock wave energy is between 5 to 15 per cent of the total explosive energy. Lownds and Du Plessis (1984) assume shock wave energy as 2 to 20 per cent of the total explosive energy. Brinkmann (1990), during his experiments in the deep underground gold mines of South Africa, estimated shock wave energy as 25 per cent of the total explosive energy for emulsion explosives. The work by Brinkmann indicates a greater role (and possibly more generation) of shock wave energy under confinement. This observation corroborates findings of Fogelson et al. (1959) where they identified 10-18 per cent of the total energy with the wave energy by test blasts in granite (stiffer rock), whereas Nicholls and Hooker (1962) observed only 2-4 per cent in salt rocks (softer rock). Therefore, the utilisation of explosive energy is dependent on the explosive properties as well as rock properties. It is also evident from Figure 3.9 that high detonation energy explosives are better for hard rocks where destress blasting is needed.

Several studies suggest different means for the enhancement of explosive energy utilization. A low VOD and non-ideal detonation is reported to produce longer radial fractures generation (Zhang et al., 2001; Brinkmann, 1990; McHugh & Keough, 1982). Applications of de-coupling (Hudson, J.A., 1993; Worsey et al., 1981) and air-decking (Liu and Katsabanis, 1996) techniques are also found to enhance the radial fractures growth. Controlled fractures growth can also be achieved with notched holes (Holloway et al., 1986), shaped charges (Holloway et al., 1986), slotted tubes (Ladegaard-Pedersen et al., 1974) and even with a change of media separating explosive and rock (Ayres et al., 2000). A rise in the peak pressure is found with the insertion of a steel liner (Olsson et al., 2001), whereas discontinuity or free surface reflects wave propagation and thus deflects fractures direction (Worsey et al., 1981). Therefore, these can have deleterious affects on the energy utilization. Directional fractures growth by the pre-split pattern is found to be not only dependant on the discontinuity plane but also on the inter hole distance (Olsson et al., 2001; Worsey et al., 1981) as well as on the delay (Olsson et al.; 2001). Bhandari and Rathore (2002) suggest cardboard liners for enhancing energy utilization in pre-split blasting.

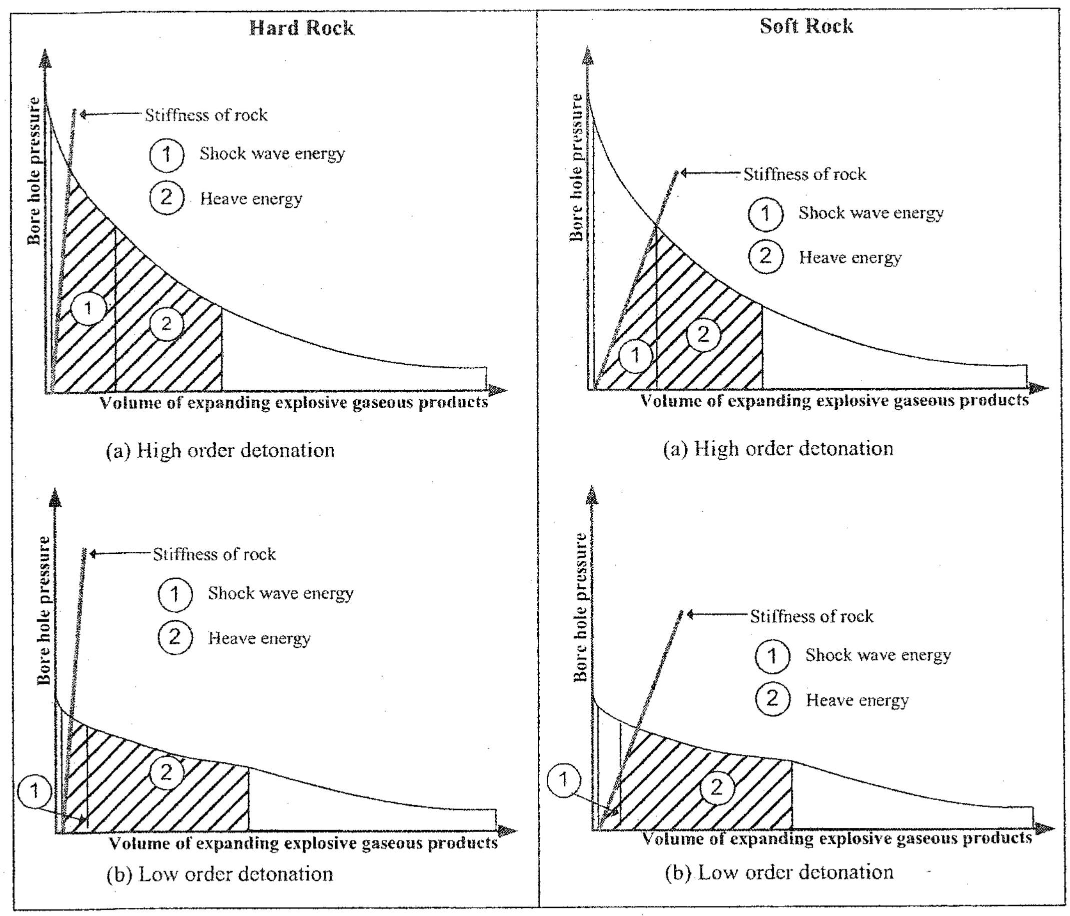

Figure 3.9 – Schematic energy utilization for hard and soft rocks with high order and low order detonation

(Brinkmann, 1990; Lownds and Du Plessis, 1984)

3.5 DYNAMIC FRACTURES INITIATION AND PROPAGATION UNDER IN-SITU STRESS FIELD

The influence of the in-situ stress field on dynamic fractures initiation and propagation is of prime importance for underground blasting in general and destress blasting in particular. Such a stress regime causes a non-uniform stress concentration around the borehole. Radial cracks from the borehole grow towards the least resistance path (either the least tensile strength or the least tensile stress). Obert (1962) observed with core drilling that micro and macro cracks align with the major principal stress direction. Kutter and Fairhust (1971) and Jung et al. (2001) experimentally validated that the preferred fractures path align with the maximum principal stress direction (Figure 3.10). Donze et al. (1997) numerically validated this trend (Figure 3.11). Kutter and Fairhurst (1971) further observed that the fracture growths in the principal stress direction are so strong that they ignores pre-existing flaws.

However, Schatz et al. (1987a and b) numerically showed that the fracture lengths of up to 50 times the borehole radius in a plane perpendicular to the principal stress direction (cross-cutting fractures) is not inconceivable, and that a typical length of 10 times the borehole radius can easily be achieved (Figure 3.12). Stress anisotropy effects on such fracture growths are insignificant (Figure 3.13). Such fractures can be generated with non-ideal detonation and the prolonged action of the borehole pressure. However, their laboratory experiments did not validate the numerical simulations prediction of the cross-cutting fracture lengths of more than 10 times the borehole length.

Further, McHugh (1983) numerically observed that the primary effect of a confining pressure of 6.9 MPa is to reduce the crack lengths by a factor of 2 to 3. Daehnke et al. (1997), by employing the fracture mechanics principle and closed-form integral equations, provide similar observations and state that the fracture growths due to gas pressure is inhibited with the increase in the stress field (Figure 3.14).

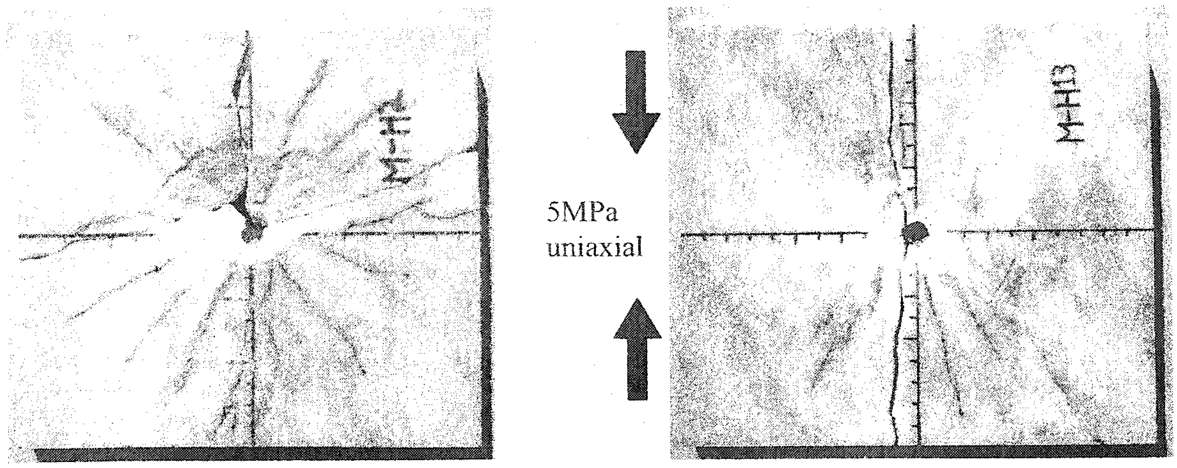

(a) Without pressure on the side of the sample

(b) With pressure of 5 MPa

Figure 3.10. - Photographs of marble plates after blasting.

(Size: 200 mm × 200 mm × 23 mm)
(Jung et al., 2001)

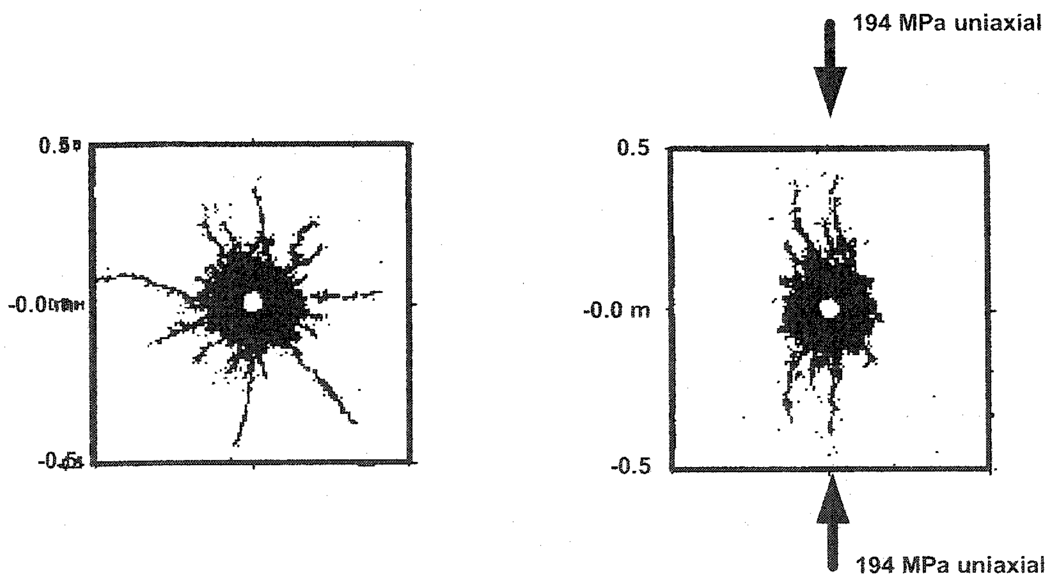

(a) Blasting without external stress field

(b) Blasting under external stress field

Figure 3.11 – Dynamic fractures propagation under uni-axial stress field

(Donze et al., 1997)

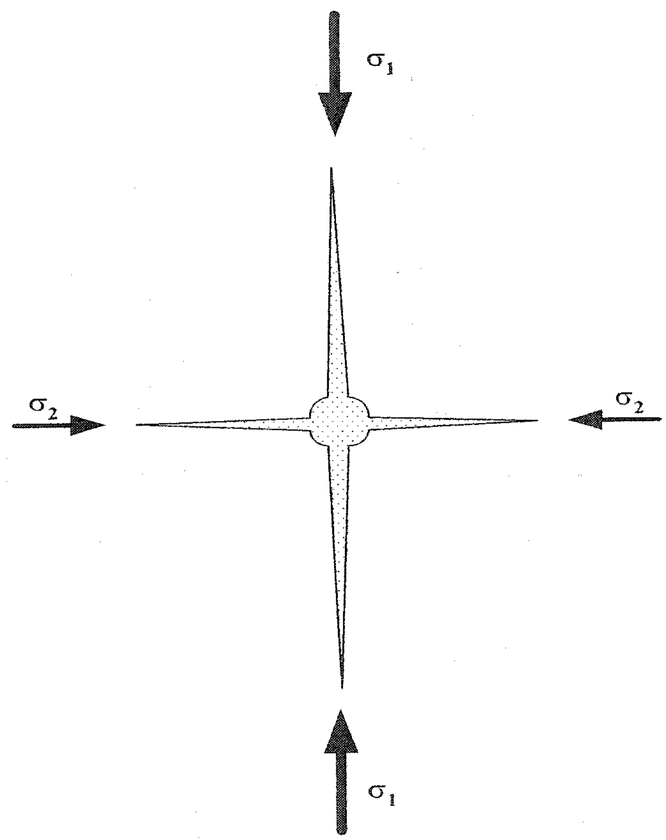

Figure 3.12 –Cross-cutting fractures concept
(Schatz et al., 1987a and b)

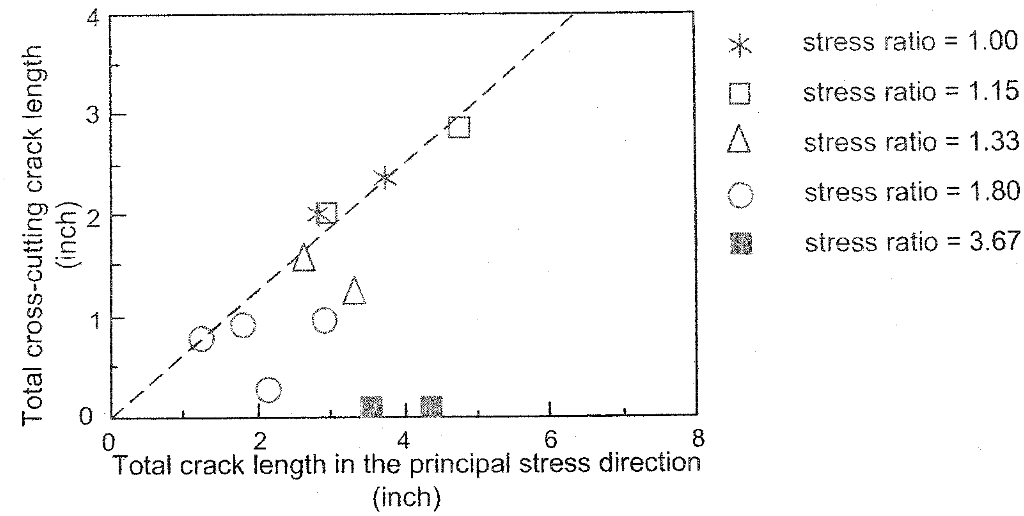

Figure 3.13 – Effect of the differential stress on the fractures length, including cross-cutting fractures.

(Schatz et al., 1987a and b)

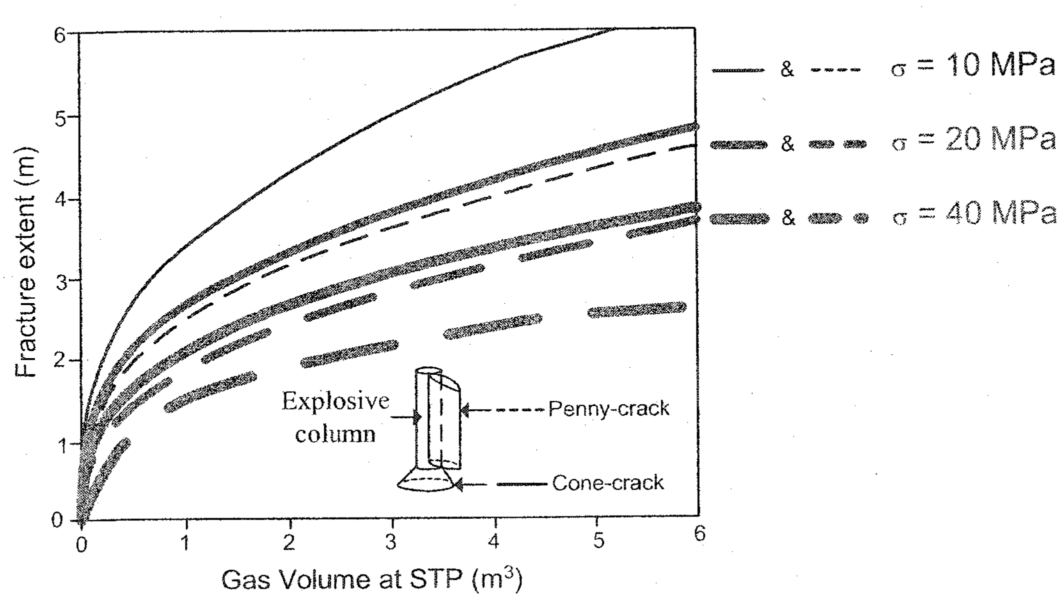

Figure 3.14 – Estimated penny- and cone-shaped crack extent in rock

(Daehnke et al., 1997)

3.6 SUMMARY

Controversies exist for the respective roles of gas pressure and shock wave energy in dynamic fractures initiation and propagation. It is also uncertain what amount of the respective part of the energy is liberated and imparted in the different situations for engineering blasting operations as well as different rock types. Part of this limitation is due to the difficulties associated with the prevalent experimental methods. However, some conclusive evidence is available suggesting the means for enhancing effective explosive energy utilisation. Explosive energy utilization can be enhanced by non-ideal detonation with a prolonged action of the pressure generated. Air-decking, de-coupling, notched holes and liners are a few other means to enhance explosive energy utilization. Hard brittle rocks need higher shock wave energy to initiate and propagate the fractures network. Knowledge of the dynamic fractures propagation under the in–situ stress regime (particularly bi-axial stress field) is a grey area and requires experimental work. Dynamic fractures generation and propagation in rocks can best be summarized as per Figure 3.15 to the best of the present level of knowledge. As per Figure 3.15, longer cracks in the principal stress direction, along with a few smaller cracks in the intermediate principal stress direction should be generated due to the blasting of a isolated hole in confined rock mass. Stiffer rocks in conjunction with confinement will reduce the number of cracks as well as the crack length.

A new experimental procedure is needed to meet the objectives of the research, as prevalent experimental techniques are not suitable to the requirements of the objectives of the research proposed in this thesis. The numerical simulation of dynamic rock fracturing is another possibility and it will be attempted to develop the requisite experimental procedure. The next chapter deals with this endeavour.

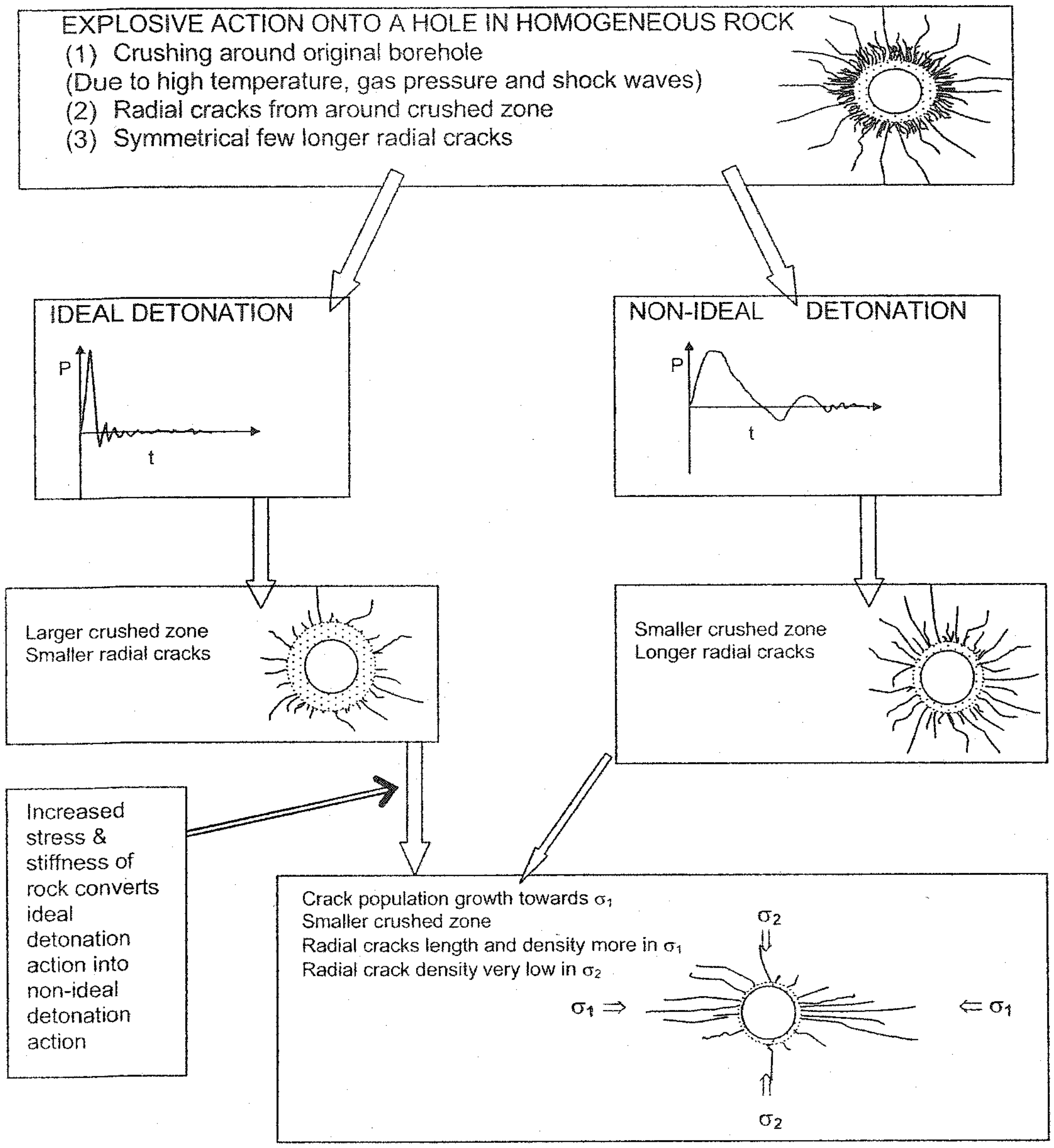

Figure 3.15 – Dynamic fractures initiation and propagation in rocks under the confinement

Chapter 4

DEVELOPMENT OF A NUMERICAL PROCEDURE FOR INVESTIGATING ROCK FRACTURING BY EXPLOSIVE ENERGY

4.1 OVERVIEW

Rapid advances made with numerical modelling tools and the availability of powerful computational resources at affordable costs make numerical simulation a most promising experimental method to study dynamic rock fracturing processes. The use of numerical simulation for dynamic rock fracturing is appealing, essential and most suitable due to the large number of complex variables involved.

There are certain prerequisites to start with numerical simulation of blasting. Part of the pre-requisites is needed to successfully transform a physical phenomenon into a numerical one. This part requires a sound understanding of transient loading characteristics as well as knowledge of the rock failure processes. Apart from the needed transformation, one needs to take care of numerical challenges, which arise due to the transient loading process and the wave propagation phenomena with the numerical modelling. This part requires a good knowledge of the numerical tool adopted for the purpose. The following is a list of prerequisites (not necessarily in the order given) needed for such a simulation job.

(a) Characteristics of transient load in the blasthole. Typically, the explosion pressure in a borehole decays to a stand-off pressure within a few milliseconds. The stand-off pressure is much below the rock's static tensile strength. The rise time of the explosion pressure to its peak value is very short and varies primarily with the explosive characteristics and secondarily with the blast hole diameter, blast hole confinement, rock strength, etc. Generally, the rise time for an emulsion type explosive is around 25 microseconds and 100 microseconds for ANFO type explosives in 38 mm diameter borehole (Frantzos, 1989; Jung et al., 2001 and Daniel, 2003). The subsequent decay in the peak borehole pressure to the stand-off pressure is steep in the case of emulsion type explosives and gentle for ANFO type explosives.

(b) Rock failure model incorporating physical tensile failure mode. Tensile failure (Mode-I) is the primary mode of rock failure. The rock fails due to tensile stresses exceeding the rock's tensile strength during transient dynamic load of blasting. The fractures initiation is Mode-I category as per the fracture mechanics principles but subsequent behaviour also includes Mode-II (in plane shear) behaviour. These considerations should be incorporated into the chosen rock failure criteria for numerical modelling. Also, in numerical modelling parlance, the plastic flow of rock like material is non-associated, which needs to be included in the material model.

(c) Representation of fractures to incorporate stress anisotropy. Numerically, it is critical to consider appropriate representation of the fractures, which should result in stress anisotropy. This stress anisotropy is essential in the fractures propagation. Rocks are heterogeneous in nature and also, fractures created by blasting enhances heterogeneity. This heterogeneity further enhances the stress anisotropy, which ultimately contributes in the fractures propagation.

(d) Numerical model characteristics for wave propagation. Numerical models act as low pass band filters, i.e., they filter out critical low frequency loads. Also, numerical modelling (particularly the finite element method) is based on deformation produced at nodes due to the applied load. Calculated deformations are used for the calculation of strains and stresses. Hence the accuracy of the modelling depends on the element size chosen (bigger elements give a stiffer response and smaller elements result in the softer response). So, a mesh convergence analysis is first required for finding an appropriate element size. Then, the element size should be adjusted to obtain a response from low frequency loads.

(e) Boundary conditions to represent far-field boundaries. One of the serious concerns of any numerical modelling exercise involving wave propagation is the spurious reflection of impending waves from the model boundaries. Suitable measures are needed to address this issue.

(f) Distribution of high transient load rate in the model to avoid numerical singularities. Application of high transient dynamic load rate (in the order of few GPa in microseconds) is generally responsible for unrealistic results from numerical modelling. Often the numerical code doesn't accept such a load rate and results in numerical singularity. Proper load distribution (smearing in numerical parlance) is required to avoid the numerical singularity. The numerical code should be able to smear the high load rate.

(g) Damping of wave propagation in the numerical model. Rock is a inherently good damper. Further damping is provided by energy consumed in the fracturing process (numerically, in plasticity) after blasting. The numerical model should reflect such typical damping characteristics. Also, damping in natural material is hysteretic, so monotonic damping should be avoided to negate the possibility of over damping of critical load frequencies (low modes).

4.1.1 Review of Prevalent Practices for Rock Blasting Simulation

Numerical simulation of rock fracturing by blasting is approached by two broad categories, namely, continuum approach and discontinuum approach. The continuum approach assumes continuity with the fractures representation, while individual cracks are tracked in the discontinuum approach. The primary aim of the continuum approach is to estimate the extent of the weakening in the material around the source; they do not characterize the very local fracture growths.

The popular continuum approach either treats rock material as perfectly elastic or fracturing is treated as a continuous accrual of damage in tension. A scalar damage variable represents fractures in the continuous damage modelling technique and strains larger than the threshold strains represent fracturing phenomena. The scalar damage variable can take values from 0 (corresponding to undamaged material property) to 1 (corresponding to completely damaged material property).

Khoshrou and Mohanty (1996) used the 2D linear elastic finite element analysis technique to evaluate the effect of weak planes on the extent of rock fracturing for smooth-wall blasting. Tensile stresses were used to delineate the fracturing region in their study. Also, blasthole pressure was applied as a static force rather than the dynamic pressure-pulse. This study is one of the few that carefully selected an appropriate approximation of the modelling plane. However, the study suffers from the obvious shortcomings of any static elastic analysis as an approximation of the dynamic phenomenon. Linear elastic analyses are always over-conservative and static analyses inherently represent higher damage levels (unless otherwise load scaling studies are done). No study was conducted to establish a requisite equivalent dynamic load for the static analyses. Fourney et al. (1993) and Szuladzinski (1993) used a similar approach (static 2D linear elastic finite element models) but with pre-placed fractures. The displacement magnitudes were used as indicators of the fracturing extent. Lima et al. (2002) and Sunu et al., (1988) report the use of an implicit algorithm for dynamic pressure application with 2D elastic material models for their continuum modelling. The fracture energy concept (J-integral) was used to extend the pre-placed fractures in the models by Lima et al. (2002) and the principal stress contours were examined by Sunu et al. (1988). Sunu et al. (1988) adopted a wrong plane in the process of idealizing a 3D problem for 2D numerical analysis.

Contrary to the static modelling approach, blast source functions have also been applied and have attempted to solve with time using equations of motion in continuum elastic or continuous damage models. Ryu (2002) reports that the application of exact blast source functions for continuum models (he referred to FLAC, a finite difference code by ITASCA) either results in an unrealistic ground response or in a numerical instability. Donze et al. (2002) reported similar difficulties with a distinct element code and therefore adopted a Gausian function to represent the dynamic load profile. The Gausian function used does not match the pressure-pulse characteristics of the blast load profile. In the popular technique of continuous damage modelling, damage evolution is tracked by a scalar damage variable associated either with the Poisson's ratio (Taylor et al., 1986) or the volumetric strain (Yang et al., 1996; Liu and Katsabanis, 1997; Hoa et al., 1998 and 2002) or the modulus (Curran et. al, 1987 and Thorne et al., 1990) or global energy (Grady and Kipp, 1993). Studies done by Liu and Katsabanis (1997) are considered noteworthy as they investigated fundamentals of air-deck blasting using the continuous damage modelling technique. However, continuum damage theories of fractures and fragmentation suffer from obvious shortcomings. The discrete nature of cracks is lost in these theories. In homogenizing a cracked solid, sweeping assumptions must necessarily be made regarding the distribution and geometry of cracks, which at best are described by a few set of variables and their interactions (Repetto et al., 2000). The determination of the effective properties of a cracked solid under dynamic conditions presents additional difficulties stemming from the finite speed at which signals propagate between cracks (Freund, 1990). However, perhaps the most fundamental objection to continuum theories is that the failure of a brittle specimen is frequently governed by the growth of a few single dominant cracks, a situation that is not amenable to homogenisation (Repetto et al., 2000).

Numerical simulation of blasting is also attempted with the discontinuum approach by using distinct element codes (Hart, 1993; Donze et al., 1997 and 2002; Mortazavi and Katsabanis, 2001), boundary element codes (Toper, 1995) and finite element codes (Cho et al., 2003 and Jung et al., 2001). Results obtained by Donze et al. (1997 and 2002) are overly affected by boundary value problems. The fracturing zone diameter extends to a distance of 1m (which is the model boundary) in the case of 2D modelling (Donze et al., 1997) for an extremely hard rock (tensile strength of 60 MPa) to 7m subgrade or 10 m radially (again the model boundary) for 3D modelling (Donze et al., 2002). The source function used by Donze et al., (1997 and 2002) is a Gausian function which was probably employed to avoid numerical singularity associated with the high load rate of transient blast loads. Mortazavi and Katsabanis (2001) employed a discontinuous deformation analysis code and provided zero cohesion and zero tension as the material parameters for the selected material model. Regrettably, their results are affected from the gross misrepresentation of a 3D problem by 2D plain strain idealization. Their analysis also lacks practical significance due to the limitations associated with the discrete element modelling codes. Unrealistic results from the distinct element codes (including discrete elements and DDA approach) are due to the fact that they need unrealistic material input properties (Hazzard et al., 2000). Ryu (2002) points out that the results are not only affected by how interaction of distinct blocks are characterized (stiffness and damping) but also by the algorithm used to solve the equations of motion (implicit and explicit). Errors also emanate from the lacking of suitable boundary conditions and damping characteristics with these numerical procedures. Distinct element codes with spherical elements (used by Donze et al., 1997 and 2002) also suffer from poor numerical accuracy due to the high pore volume (Malan and Napier, 1995). Toper (1995) presents post-blast fracture networks results from a 500 MPa blasthole pressure in a 93 mm borehole using the static linear elastic boundary element method involving pre-placed fractures in the model. Napier et al. (1997) report that results obtained by pre-placed fractures carry no practical meaning. Results obtained with the static linear elastic modelling are also affected with the shortcomings of static linear elastic analyses as mentioned above. Further, Toper (1995) incorporated bedding planes in his models with zero cohesion. Cho et al. (2003) used a continuum code (finite element method) and simulated discrete fracture network using node release technique. Their analyses use the pressure-pulse similar to the measured blasting pulse but with the reduced peak pressure of 500 MPa to avoid numerical instability associated with the high transient load. Results by Cho et al. (2003) appear to be affected by the boundary value problems, as failure at the free face by reflected pressure-pulse does not confirm observed field behaviour of slabbing. Further, Cho et al. (2003) needed the rock strength variation through a statistical distribution function to introduce stress anisotropy. Studies presented by Jung et al. (2001) only showed a close resemblance with the reported field behaviour. Their modelling involved both the peak-pressure magnitude (about 1GPa for an 8 mm diameter borehole) and the pressure-time profile similar to the observed values. Further, their procedure needed dynamic compressive and tensile strength values, which were 4.5 times the static strength values, as judgement standard for fractures generation. The publication neither provides the procedure for the fractures initiation/ propagation nor discusses the stability of the results.

Most of the above reported simulations were concerned with the simulation of surface blasting phenomena as the borehole size used were ranged from 100 to 200 mm and the effect of the in-situ stress regime was not considered. Only Donze et al. (1997) provide results in terms of uniaxial stress fields but underground excavation faces have biaxial stress fields so the results are not useful to evaluate in this thesis. Other limitations of their results have been discussed above. Only two studies are reported which used biaxial or triaxial stress fields. Toper (1995) used a static linear elastic boundary element code with pre-placed fractures and Schatz et al (1987a) used an explicit finite difference code with pre-placed fractures. Barring the limitations associated with their results, Toper (1995) indicates alignment of the fractures in the principal stress direction and the stress field around the blasthole changes both in magnitude and direction after the blasting. Schatz et al. (1987a) report the achievable fractures length perpendicular to the major principal stress direction amounting to 50 times the borehole diameter. However, their laboratory results do not confirm their numerical modelling results. Further, results by both the studies were contrived with the pre-placing of the fractures network. Therefore, the results were affected either by pre-placed fractures or by homogenization of fractures by continuum theories in all the simulations.

4.1.2 Concluding Remarks

The prevalent practices for rock blasting simulation are summarized in Table 4.1(a) and (b). It is evident that a proper numerical procedure is lacking that takes into account the above-mentioned pre-requisites in order to successfully transform a physical phenomenon in a numerical one. The successful transformation of this physical phenomenon into the numerical platform is still elusive. Such shortcomings encourage the researcher to develop a new procedure for rock blasting problems. This development procedure is described in the following section.

Table 4.1(a) – Continuum approach for numerical simulation of blasting

Reference	Numerical tool	Explosive Loading	Rock material model	Key input parameters and fractures representation	Key results	Remarks
Khosrhou and Mohanty, 1996	Finite element code	Static	Elastic	2 GPa static borehole pressure (radius = 50 mm) applied to elastic rock ($E = 40$ GPa, $\nu = 0.15$, $\rho = 2.5$ t/m^3). Tensile stresses represented fractures extent calculations.	Burden to spacing ratio from 0.8 to 1.2 is appropriate for wall-control blasting. Weak planes act as free faces and their position determine amount of back break.	Plane strain static analyses are presented. Elastic material model, static modelling and continuous modelling presented overly conservative solutions for the rock fracturing.
Sunu et al., 1988	Finite element code	Dynamic	Elastic	2 GPa dynamic concentrated load applied for 0.1 ms on the periphery of 100 mm blasthole diameter to an elastic rock (E=28.3 GPa, $\nu = 0.27$ and $\rho = 2817$ kg/m^3) in 2D plain strain idealization of a 3D problem. The problem solved using implicit finite element procedure using Newmark method. Tensile stresses used for fractures extent identification.	Optimum burden distance depends on elastic modulus and density of rock material. Effect on Poisson's ratio is negligible for such a case.	Plain strain model assumed in wrong plane for a 3D dynamic problem. Material model is elastic. It is inferred from the publication that the blast source function was a constant concentrated force for a period of 0.1 ms which doesn't reflect a real case.

Liu (1997) and Liu and Katsabanis (1997)	Finite element code	Dynamic	Elasto-Plastic	Dynamic load applied using JWL equation of state for 2D axisymmetric models having 100 mm blasthole diameter to elasto-plastic rock obeying metal plasticity rules. Volumetric strain (scalar quantity) apportioned by statistical fractures mechanics principles used for fractures representation.	Results are qualitatively matched with a crater blasting experiment and physics of air-decking is elaborated.	Associated flow rule used to obey a metal plasticity rule for rock like material. Also, sweeping assumptions made to homogenization of fractures due to the demand of the continuous damage modelling.

Table 4.1(b) – Discontinuum approach for numerical simulation of blasting

Reference	Numerical tool	Explosive Loading	Rock material model	Key input parameters and fractures representation	Key results	Remarks
Toper, 1995	Boundary element code	Static	Elastic	500 MPa static pressure is applied to rock (properties not provided) representing at depth of 2700m. Fractures were pre-placed in the model and extended.	Fractures network grows in σ_1 direction and stress field after blasting changed in magnitude as well as direction (90^0)	2D elasto-static analysis results are contrived with pre-placed fractures. Also, static pressure used (500 MPa) is nowhere near to dynamic pressure in 93 mm diameter holes.
Mortazavi and Katsabanis (2001)	Discontinuous deformation analysis code (DDA)	Dynamic	Elastic	1GPa and 2.5 GPa dynamic pressure applied to 100 mm borehole diameter for elastic blocks stacked together with the zero cohesion and tension strength. Separation of distinct blocks represented for fractures.	Muck profile, back break and toe problems are affected by the bench height and bedding orientation.	Unrealistic material input data are accompanied with gross wrong assumption of plain strain modelling for a 3D problem. Results are affected by shortcomings of the numerical tool used.

Lima et al., 2002	Finite element code	Dynamic	Elastic	1 GPa dynamic pressure applied to 508 mm diameter boreholes in granitic rock ($E = 60$ GPa, $\nu = 0.25$, $\rho = 2800$ kg/m^3, $K_{ID} = 1.65$ MPa.m$^{0.5}$, $K_{IID} = 1.03$ MPa.m$^{0.5}$). Fracture mechanics rules used for extension of pre-placed fractures.	The purpose of the exercise was to show that the dynamic rock fracturing modelling can be accomplished with the pre-placed fractures and their extension by using the fracture mechanics principles	Pre-placed fractures grows radially surrounding the boreholes but their growth is inhibited by the presence of already developed fractures from previously blasted surrounding blastholes. Numerical difficulties prevented fractures growth in time and in directions.
Jung et al., 2001	Finite element code	Dynamic	Elasto-plastic	1.04 GPa peak borehole pressure applied to 8 mm diameter borehole. Material the compressive strength of 301.4 MPa and the tensile strength of 28.2 MPa assumed.	Fractures propagates towards the major principal stress direction	The numerical procedure used observed the peak-pressure magnitude and the pressure-time profile. Results also match with the presented laboratory experimentation. Neither the fracturing procedure nor the stability of the results presented.

Cho et al., 2003	Finite element code	Dynamic	Elasto-Plastic	500 MPa dynamic pressure applied to 100 mm diameter blasthole in a rock having E = 56.4 GPa, $\nu = 0.25$, $\rho = 2700\ kg/m^3$, $G_f = 300$ Pa.m. Fractures path determined by fracture mechanics rules using node release technique.	Qualitatively show effect of pressure-pulse on fracturing	Far-field boundaries were placed only at 2-3 m away from the blasthole. Peak pressure of only 500 MPa was used. Results do not confirm failure behaviour from free faces by reflected pressure waves.
Donze et al. 1997	Distinct element code	Dynamic	Elasto-plastic	1 GPa dynamic pressure with gaussian distribution to 50 mm diameter blasthole in a 1 m x 1 m model size representing very hard rock (E = 100 GPa, $\nu = 0.09$, $\rho = 2950\ kg/m^3$, UCS = 340 MPa, Tensile strength = 60 MPa). Separation of cohesive circular discs and plates represented the fractures.	Qualitatively showed that high frequency detonation leads to more crushing with shorter crack length and low frequency detonation to less crushing with longer cracks length. Also, it is showed that cracks align with the principal stress direction	Numerical model boundaries placed only at 0.5m away from the explosion source and fractures reaches to those boundaries representing a very hard material though the material consisted very high self-damping characteristics.

4.2 DEVELOPMENT OF A NEW PROCEDURE FOR THE SIMULATION OF EXPLICIT FRACTURE NETWORK DUE TO BLASTING

It was demonstrated in the preceding section that there is a dearth of proper numerical modelling procedures for the simulation of explicit fracture networks generated due to blasting in rock. This section deals with the development of a new procedure to fulfill the said requirement. The development first requires the selection of a proper numerical modelling tool and then the identification of an appropriate technique to represent the explicit fracture growths, followed by the setting-up a numerical model with the relevant physical parameters. The following sub-sections detail the development procedure.

4.2.1 Selection of a Proper Numerical Modelling Tool

Four basic numerical modelling tools are available which can be looked into for analysing problems of the fractures generation and propagation in rock. A brief description of each tool, including merits and limitations, is presented below.

(a) **Boundary Element Method (BEM)**. The original development and application of BEM in the field of geomechanics is reported by Crouch and Fairhurst (1973), Cruse (1969), Diest (1973), Hocking (1976), Salamon (1963, 1964a, b and c) and Starfield and Crouch (1973). In BEM, only the boundary of the problem requires discretization. The method is particularly appealing as a framework for analysing fractures propagation as it reduces the representational requirements only to the description of the fractures. It is essentially a method for solving partial differential equations and can only be employed when the physical problem can be expressed as such. The essential reformulation of partial differential equations consists of two operations: (i) an integral equation defined at the boundary of the domain, and (ii) an integral equation that relates the solution at the boundary to the solution at any point in the domain. The methos is most accurate amongst all numerical modelling tools as the fundamental solution exactly satifies the differential equations. Also, the method has the advantage for the simulation of rock mechanics problems of unbounded media because the results are not affected by artificial reflection from numerical model boundaries. Further, results obtained with the method are continuous contrary to the other tools (finite elements and finite difference), where point wise approximations are obtained. (Mitri, 2002).

There are two fundamental techniques to the derivation of an integral equation formulation of a partial differential equation (Fotoohi and Mitri, 1996). The first technique is termed the direct method and the integral equations are derived through the application of Green's second theorem. The governing integral equations contain physical variables of the problem. The other technique is termed the indirect method and is based on the assumption that the solution can be expressed in terms of a source density function defined at the boundary. The indirect method is more popular for the simulation of rock mechanics applications due to the fact that such applications need consideration of body forces, for which fundamental solutions do not exists. The method is further divided into two methods, which are the Fictitious Stress Method (FSM) and Displacement Discontinuity Method (DDM) (Crouch and Starfield, 1983; Fotoohi and Mitri, 1996). The FSM uses Kelvin's solution of plane strain problems for a concentrated planar load applied to an infinite elastic solid domain. The DDM, on the other hand, developed to solve rock mechanics problems where discontinuities in vicinity of mine openings have an influence on the stress redistribution around the opening. The DDM is based on analytical solutions of the problem of constant displacement discontinuity over a finite line segment in an infinite solid elastic domain. (Fotoohi and Mitri, 1996).

The boundary element method with linear variation DDM has been demonstrated to be able to model fracture growths and localisation (Crouch and Starfield, 1983; Van de Steen et al., 2001). The simulation of fracture growths can be effected in two ways (Napier et al., 1997). In the first method, explicit growth sites are defined at specified positions in the material. These sites represent positions from which cracks can be initiated and can be located at random points in the initially unfractured parts of the medium or on boundaries or extremities of pre-existing cracks. The second method of the fracture growths simulation procedure is to specify a random population of potential cracks, which are again selectively activated according to a specified failure criterion.

Inherently, the scope of the boundary element method is essentially limited to homogeneous linear elastic problems (Jing and Hudson, 2002; Pande et al., 1990). Further, the accuracy of the method is dependant on the shape functions describing discontinuity values in each crack and run time efficiency is poor when modelling with a good size of elements (Napier et al., 1997). Napier et al. (1997) also report that the explicit fractures modelling procedure is contrived in having to emplace appropriate growth sites at specific positions, and in having to define the growth modes that are to occur.

Therefore, in the light of the above review, it can be said that the BEM in general is not suitable for modelling dynamic rock fractures initiation and propagation since the method can't do so unless the fracture pattern is pre-specified in the model. Since the method is unable to handle fracture growths and subsequent propagation in unspecified directions, the BEM will not be considered for the current research.

(b) **Finite Difference Method (FDM)**. The second tool is the explicit finite difference method that approximates the differential equations of motion using lumped grid point masses from the density of the surrounding zones. The FDM gives a point-wise approximation to the governing equations that discretize the domain into finite difference grid with nodes at intersections of the grid. The method is memory and speed efficient due to the regular grid scheme. The grid system is a convenient means of generating function values at sampling points with small enough intervals between them, so that errors thus introduced are small enough to be acceptable. Accuracy can usually be improved either by increasing the number of grid points or by including 'correction terms' in the approximation for the derivatives or by use of higher order spatial differentiations. It is the most direct and intuitive technique for the solution of the partial differential equations, as the definition of interpolation functions is not needed. (Mitri, 2002).

A major limitation of the method is that a discontinuity must be aligned to a cartesian grid and this makes it inflexible in dealing with fractures, complex boundary conditions and material heterogeneity (Jing and Hudson, 2002; Mishnaevsky and Schmauder, 2001; Napier et al., 1997). This shortcoming is best addressed by the combination of Finite Volume Method (FVM) with the finite difference method (Jing and Hudson, 2002). Still, explicit representation of fractures is not easy in the FDM/FVM because they require continuity of the functions between the neighbouring grid points. In addition, it is not possible to have special 'fracture elements' as in the finite element method. Despite these limitations, Fang and Harrison (2002) and Poliakov (1999) report an indirect approach of fractures modelling by utilizing local stiffness degradation.

The inability of the explicit fractures simulation makes the FDM an inappropriate tool for the current research purpose and hence will not be considered.

(c) **Discrete Element Method (DEM)**. The theoretical foundation of this tool is the formulation and solution of equations of motion of rigid and/or deformable bodies using implicit (based on FEM discretization) and explicit (using FDM/FVM discretization) formulations. The domain of interest is treated as an assemblage of rigid or deformable blocks/particles and the contacts among them need to be identified and continuously updated during the entire deformation/motion process, and are to be represented by appropriate constitutive models. The blocks are sub-divided in a mesh with nodal points to obtain overall response of individual blocks as per the prescribed force-displacement laws. Large deformations and rotations of blocks are permitted. Rock mechanics is one of the disciplines from which the concept of DEM originated (Cundall, 1971). Due mainly to its conceptual attraction in the explicit representation of fractures, the distinct element method has seen a wide application in rock engineering (Jing and Hudson, 2002). Two types of DEM formulations are in practice. One technique treats the modeled domain as an assembly of blocks (or polygons in 2D problems), which can be either rigid or deformable (e.g. Cundall and Hart, 1993). The second technique uses rigid spheres (or discs in 2D problems)(e.g., Donze et al., 1997).

However, a final fragmentation pattern needs to be discretized at the beginning stage in the DEM to predict later stage particle motion (Li and Reed, 1995). This requirement limits the main strength of the tool. It is extremely difficult to know beforehand the fracture size distribution of rocks. Further, the higher pore ratio with spherical elements in the DEM is a cause for mismatch with the field results (Malan and Napier, 1995). Also, the method suffers from an improper assignment of material properties. Arbitrary values (which are significantly different than the tested material properties) need to be assigned for each block and its interaction behaviour with the surrounding blocks (Hazzard et al., 2000). A parametric study is then required to equate the overall response of the model to the established material behaviour. Ryu (2002) points out that the results are not only affected by how the interaction of discrete blocks are characterized (stiffness and damping) but also by the algorithm used to solve the equations of motion (implicit and explicit). Errors also emanate from the lacking of suitable boundary conditions and damping characteristics with the numerical procedures used by the DEM.

Therefore, due to the difficulties associated with the material parameters and the ability to handle fractures only in specified paths is made the use of the DEM unfavourable for the current research and thus will not be used.

(d) **Finite Element Method**. The finite element method (FEM) developed for the analysis of continua has proved a powerful and versatile tool in deformation analysis of continua as well as discontinua. Strength of the method lies in its generality and flexibility in handling all types of loads and complex and irregular geometries. Application areas of FEM include linear and non-linear materials as well as static, quasi-static and dynamic loading conditions. Advances with the tool made it possible to simulate from discrete fractures propagation (e.g., Camacho and Ortiz, 1996) to rock fragmentation (e.g., Potapov and Cambell, 1996).

The method essentially involves dividing the domain in a mesh of finite elements of various shapes held together at nodes that are corners of the elements (mid-side nodes are also possible for some element types). Displacements at the nodes are treated as unknowns and are solved with the system of linear equations. Strains and stresses resulting from calculated displacements are then calculated at one or more points inside each of the elements. Each element can have different material properties.

Contrary to the previous tools discussed, FEM provides much more flexibility, ease and possibilities in handling analysis of fracture growth due to the dynamic loading. The method provides a number of good choices to simulate fracture generation, propagation and coalescence.

Due to the above-mentioned reasons, a general-purpose finite element analysis tool, ABAQUS (Abaqus, 2003), will be employed for the current research. This research tool is available at McGill University.

4.2.2 Selection of an Appropriate Technique for Modelling of Rock Fractures by Explosive Energy using ABAQUS

Continuous damage modelling method (CDM), cohesive zone modelling (CZM), joint element method (JEM), and element elimination technique (EET) are established procedures used to simulate the fractures growth within the framework of the FEM. These methods will be reviewed here in detail for selecting the most suitable procedure for the current research. Other methodologies are also being developed within the framework of FEM to enhance possibilities for the fractures simulation such as element free galerkin methods (Belytscho et al., 1994), manifold methods (Shi, 1992), level set method (Stolarska et al., 2001), computational cell methodologies (Xia et al., 1995), etc. These methods will not be dealt with in this thesis, as their validity for rock blasting applications is unknown to the researcher.

(a) **Continuous Damage Models (CDM)**. There are two ways to treat crack growth using CDM, namely, tracking individual cracks by plasticity based damage models and by indirect simulation of the effect introduced by growing cracks in the body using statistical fracture mechanics principles.

The plasticity based continuous damage models have consistent and physically meaningful constitutive relations originating from the plasticity theory (Lee, 1996) in contrast to the damage models using statistical fracture mechanics principles, which adopts the damage parameter based on the intuition of the practitioner. The models based on plasticity are capable of simulating inelastic strain as well as the stiffness degradation. The advantage of using such a method is that the damage variable is well defined, carries physical meaning and can easily be calibrated with the experimental data. The plasticity based damage model developed by Lee (1996) and adopted in ABAQUS (Abaqus, 2003) has many limitations, which make it unsuitable for the present need. The model cannot be applied with high confinement (which is the main area of interest in this research). Also, element distortion is a big concern as there is no provision for ultimate plastic strain with the model in ABAQUS. This requires adaptive meshing which makes the model computationally very costly.

In the other approach of CDM, fractures are indirectly modelled using continuum damage theories. In this approach it is inherently presumed that the rock material has numerous microcracks and the growth of an individual crack is neither important nor effective. Rather, the effect of the volume of microcracks is studied using scalar damage variables based on statistical fracture mechanics (Liu, 1997). A scalar continuous state variable is introduced in the method, which describes macroscopic damage. The scalar damage variable can take values from 0 (corresponding to undamaged material) to 1 (corresponding to completely damaged material). The appropriate choice of damage laws allows the simulation of many kinds of material deteriorations such as visco-plastic (Nemes and Eftis, 1993), ductile (Lemaitre, 1985), creep (Leckie and Hayhurst, 1974), fatigue (Lemaitre, 1971), etc. Also, fractures are idealized as a degradation of the elasticity of material (Curran et al., 1987) and by recourse to global energy concepts (Grady and Kipp, 1993) for rock-like materials.

However, continuum theories of fractures and fragmentation suffer from obvious shortcomings. The discrete nature of cracks is lost in these theories. In homogenizing a cracked solid, sweeping assumptions must necessarily be made regarding the distribution and geometry of cracks, which at best are described by a few set of variables and their interactions. The determination of the effective properties of a cracked solid under dynamic conditions presents additional difficulties stemming from the finite speed at which signals propagate between cracks (Freund, 1990). However, perhaps the most fundamental objection to continuum theories is that the failure of a brittle specimen is frequently governed by the growth of a few single dominant cracks, a situation that is not amenable to homogenisation (Repetto et al., 2000). Also, the scalar damage variable is intuitively introduced and it carries no physical meaning.

In contrast to approaches based on continuum damage theories, the present study aims to explicitly follow the initiation and propagation of multiple cracks. These cracks can branch and coalesce and may eventually lead to the formation of fragments. So this technique is ruled out for the present study.

(b) **Joint Element Method (JEM)**. Developments with the FEM also made possible the analysis of discontinua. Goodman et al. (1968) introduced a zero-thickness element inserted between two finite elements allowing tangential displacements due to shear stress along the joint. Schaefer (1975) extended the approach and made possible the opening and closing of cracks by normal stress allowing relative normal displacements along the joint. Alternatively, Zienkiewicz and Best (1970) proposed a thin-layer element and the technique was later adopted by Desai and Zaman (1984). The adaptive mesh refinement technique, which makes the mesh denser along a discontinuity and shock front, further enhanced modelling of discontinua with FEM (Baines, 1985).

There are, however, numerical difficulties associated with the use of joint elements. While some of these elements assume the thickness-approaching zero, others assign an arbitrary value to it. In the former case, the problems of ill-conditioning and/or numerical instability may occur, whereas in the latter case the solution is, in general, sensitive to the thickness chosen (Lee and Pande, 1999). Another drawback of the joint-element method is that the locations of the discontinuities must be fixed in advance, whether by insertion of joint elements in the mesh at predetermined locations or by initial discretization of the mesh into discrete blocks (Li and Reed, 1995). The subsequent deformation under loading is therefore dependent upon the pattern of discontinuities introduced. Further, the technique provides only a limited degree of relative displacement and rotation and the mesh essentially remains a fully connected continuum.

Based on the above limitations, the method is not suitable for the current research and so it will not be considered.

(c) **Cohesive zone modelling (CZM).** In the cohesive zone models (Tvergaard, 1997), the fracture path is prescribed and presented as a thin material layer with its own constitutive relation (traction-separation law). The relation is such that with increasing crack opening the traction reaches a maximum, then decreases and eventually vanishes so that complete decohesion occurs. The softening part in the constitutive relation (where the traction reduces from the assumed maximum value to zero) can affect the correctness of the solution, and can result in mesh dependent FE solution (Mishnaevsky Jr et al., 1998). Yet, by introducing length scale parameters into the formulation the dependence of the solution on the element size can be eliminated. (Mishnaevsky Jr and Schmauder, 2001).

The weak point in the CZM is the requirement of prescribing the fractures path. Also, the technique needs the continuous updates of boundary representation and is thus a computationally costly method. Due to the limitations of prescribing the fracture path, the technique is not suitable for the current research.

(d) **Element elimination technique (EET)**. Another technique available within the framework of FEM is the element elimination technique (EET) that is based on the removal of finite elements, which satisfies some failure conditions (which is to be defined for each material to be considered). Using this technique the formation, growth and coalescence of voids or microcracks, and crack growth are simulated. As criteria of local failure, both global (external loads or displacements) and local (i.e., defined for a given element; for instance, plastic strain, etc.) values as well as any combination of these values can be used. To eliminate an element, all components of stress tensors in this element are set to null. As a result, all forces in this element become zero as well, and therefore, this element stops to transmit load to neighbouring non-eliminated elements. The element elimination does not mean that such an element is really removed from the FE mesh, but that stops to interact with neighbouring elements. This is achieved by setting Young's modulus of eliminated elements to zero. In order to avoid numerical problems related to strong local loss of equilibrium, the stress is set equal to zero in several steps (called relaxation steps). The Young's moduli in the eliminated elements are set to zero in the last relaxation step. (Mishnaevsky Jr. and Schmauder, 2001).

EET is incorporated in the general-purpose finite element analysis code ABAQUS. The advantage of the EET is that initiation, growth and coalescence of the crack/ fractures is captured in a real time framework. Further, fractures propagation can be simulated with the same local damage criteria on a micro scale as well as a macroscale (Mishnaevsky Jr and Schmauder, 2001; Mishnaevsky Jr et al., 2001).

Owing to the advantages associated with the EET technique, it is the most suitable procedure for the current research and hence will be selected for the present study.

4.2.2.1 Concluding Remarks

The various merits and limitations of different numerical modelling tools and techniques available are summarized in the Table 4.2. Though several other methods have capabilities of dynamic rock fractures modelling but they are not suitable and have severe limitations in comparison to FEM. All other methods are not appropriate for the current research program either due to the inability in simulation of fractures generation or propagation without pre-specified locations. Therefore, the general purpose FE code ABAQUS (Abaqus, 2003) is selected for the study presented. It is also evident from Table 4.2 that the element elimination technique (EET) is the best recourse for the present study due to its ability to simulate fractures generation and propagation without prior specification of the locations and the paths.

Table 4.2 – Rock fractures simulation by numerical modelling

Simulation Tool	Simulation technique	Working principle	Example application references	Merits of the technique	Limitations of the technique
BEM	Displacement discontinuity method	Partial differential equations are solved at model boundaries (including considered fractures) and influence functions are then used to obtain continuous solution for the rest of the problem domain.	Crouch and Starfield, 1983; Napier et al. 1997; Van de Steen et al., 2001	Reduces problem geometry by one dimension	- Fractures should be emplaced first - Application is limited to homogeneous linear elastic problems - Poor efficiency with larger models
FDM	Finite volume method	A point wise approximation to the governing partial differential equations yields discretization of the domain into finite difference grid with nodes at intersections of the grid.	Fang and Harrison 2002; Poliakov 1999	Large deformations dynamic modelling	- Explicit fractures modelling is not possible
DEM	Solution of equation of motion	The domain of interest is treated as an assemblage of rigid or deformable blocks/ particles and that the contacts between them are identified and continuously updated during the entire deformation/ motion process, and to be represented by appropriate constitutive models.	Hazzard et al., 2000	Element separation modelling is possible	- Final fragment size should be discretized first - Computationally costly - Difficult to evaluate approximate values for material properties

FEM	Continuous damage models (CDM)	Net effect of fracturing is idealized by degradation of material properties and by doing so simulation results represent homogenized damaged solid.	Curran et al., 1987; Grady and Kipp, 1993; Johnson and Holmquist, 1992; Liu, 1997	Damage zone is quantified and simulated	- Discrete fractures simulation is out of the purview of the technique - Discrete nature and effect of fracturing are lost in the technique
	Joint element method (JEM)	Finite elements with an embedded discontinuity line or localization band. Both the traction-separation law and the stress-strain law give the constitutive model of the element with an embedded discontinuity.	Baines, 1985; Desai and Zaman, 1984	Explicit fractures propagation modelling	- Fractures path and locations need to be prespecified
	Cohesive zone model (CZM)	Fractures behaviour is encapsulated by inserting surface-like cohesive elements thus allowing node duplication at otherwise coherent boundaries as well as generation of fractures plane governed by traction-separation law for cohesive surface elements.	Pandolfi and Ortiz (2002); Tvergaard and Hutchinson (1988); Xu and Needleman (1994)	Explicit fractures generation and propagation simulation	- Fractures path needs to be prespecified - Computationally costly
	Element elimination technique (EET)	Crack growth is presented as a weakening or removal of finite elements in which the local stress or damage parameters exceed some critical level	Mishnaevsky Jr and Schmauder, 2001; Mishnaevsky Jr et al., 2001	Explicit fractures generation and propagation simulation	- Relaxation steps are needed to avoid singularity related with strong loss of local equillibrium.

4.2.3 Setting-up Numerical Model Parameters Suitable for Dynamic Rock Fracturing by the Explosive Energy

4.2.3.1 Deciding appropriate type and size of numerical models

Excavation into any mining front creates two simultaneous effects (Saharan and Mitri, 2003). First, stress perpendicular to the excavation face vanishes at the free face and gradually attains the virgin stress value at a certain distance ahead from the face (Figure 4.1c). Second, the two other stresses parallel to the excavation face concentrate at the free face initially increase to some extent and then monotonically decrease to the virgin stress values away from the mining face (Figures 4.1a and b). The process is schematically represented in Figure 4.1. Insignificant out-of-the-plane stress, in-plane bi-axial stress loading and deformation in plane as well as out-of-the-plane in the vicinity of the free face create a situation, which can be idealized as plane stress situation. This idealization is a representation of the situations where destress blasting is applied on a routine basis. Therefore, the present work will employ 2D plane stress models to analyse destress blasting.

It has been proved by elastic analytical solutions that the radius of influence of any excavation is approximately 6 times the excavation size (Obert and Duvall, 1967). The excavation induced stresses beyond this distance attain the virgin stress values and the direction. Therefore, static numerical modelling exercises keep model boundaries 10 times away the excavation size based on such analyses to fairly represent unbounded rock medium (Mitri, 2002). However, such a premise is not sufficient and accurate enough to represent unbounded rock in dynamic simulation due to wave propagation and reflection phenomena. Therefore, it is proposed to place the far-field boundaries at 250 times the excavation size (blasting borehole in the present case). The followings are prime considerations for such placement.

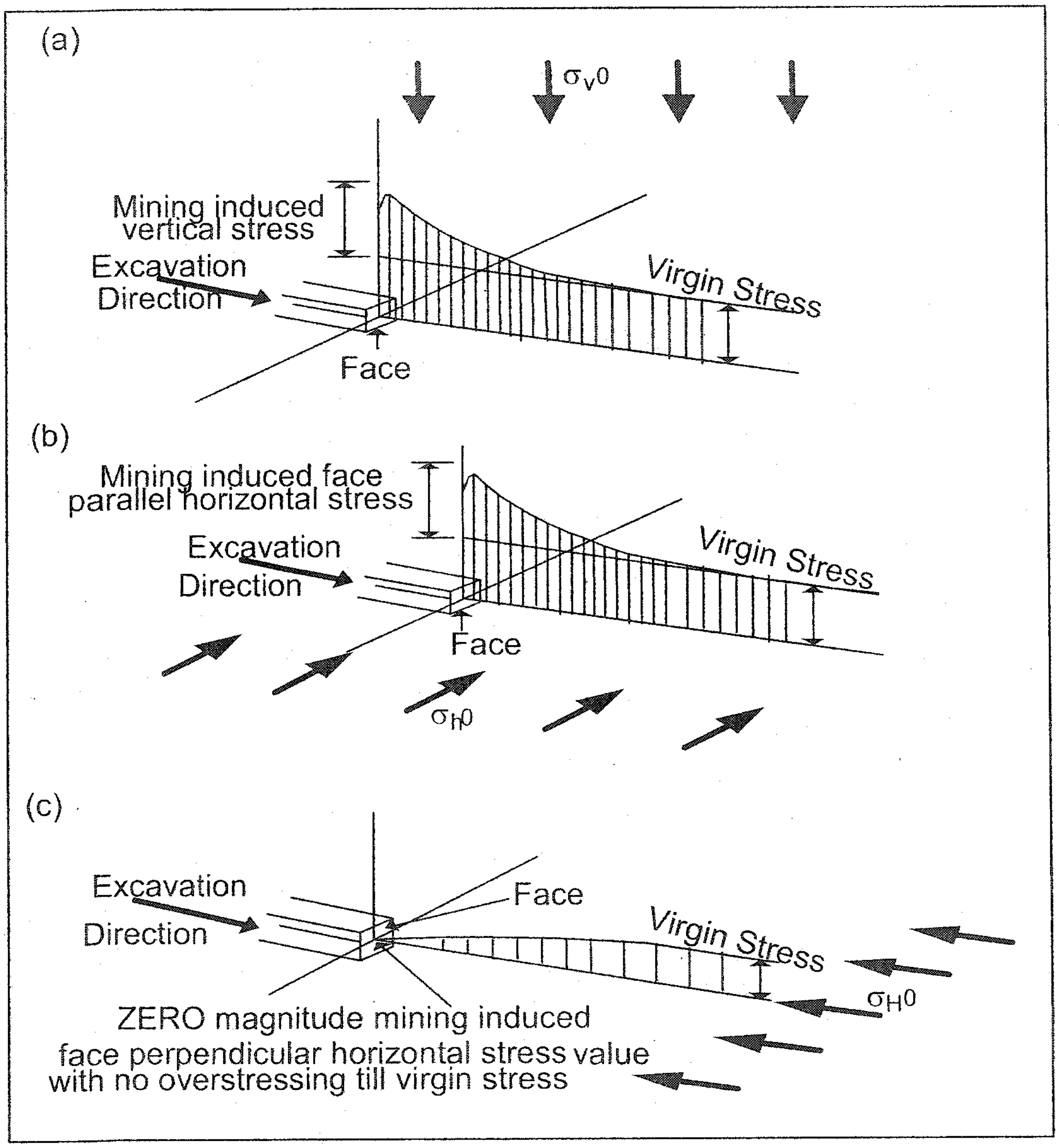

Figure 4.1 – Mining induced excavation stresses

(Saharan and Mitri, 2003)

(a) Avoidance of spurious wave reflections from boundaries and their subsequent deleterious impact on the final model behaviour.

(b) Allocation of sufficient analysis time for fractures propagation due to transient blast wave loadings.

Further, full model domains are proposed. Therefore, model boundary truncation will not be employed by taking advantage of any symmetry plane. This is due to the fact that all symmetry planes vanish once a fracture initiates in the model. Also, the current procedure development doesn't force fractures initiation sites so it is not judicious to impose symmetric plane conditions. Schematic model geometry is shown in Figure 4.2. It is showed in one of the following sections (Section 4.2.5) that the representation of the unbounded rock medium by placing model boundaries at 250 times the excavation size and full model domains are necessary, sufficient and accurate.

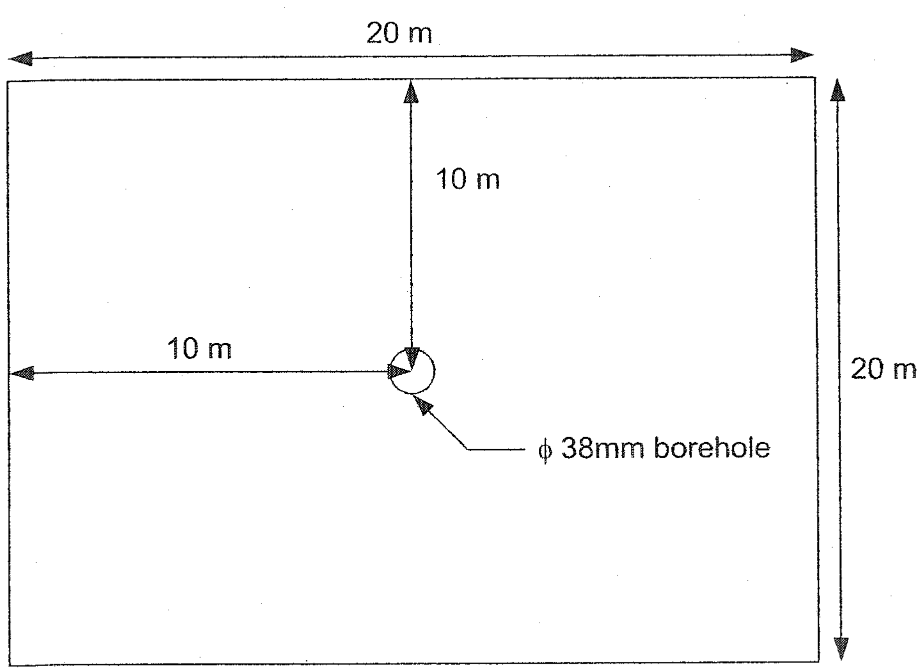

Figure 4.2 – Schematic of the proposed plane stress 2D models with one central 38 mm diameter hole

(Not to the scale)

4.2.3.2 Selection of material model to represent brittle rock behaviour and allocation of rock properties for the modelling purpose

The tensile (or extensile) failure mode is considered to be the basic failure mechanism of rocks (Batzle et al., 1980; Blair and Cook, 1998; Kranz, 1983). Fractures formation in rocks subjected to direct tension is related to the breaking of molecular bonds ahead of the advancing fractures. Fractures generated under compressive stress states are observed to be extensile in nature and follow the direction of maximum compression. The extension and coalescence of these extensile cracks lead to macroscopic failure pattern. Similarly, rock fails where tensile stresses exceed tensile strength of the rock experiencing transient dynamic loading (blasting) (see Figure 4.3). The violation of tensile strength near the blast hole periphery is overwhelming and that leads to a crushing zone. Beyond the crushing zone, the violation results in a discrete fractures network. A detailed discussion on the rock fracturing mechanism by transient dynamic loading can be found in the previous chapter (Chapter 3). Therefore, a material model is needed in the study that identifies rock failure under tension for accurate simulation of the dynamic rock fracturing process. The objectives of the research demand a material model that is able to capture the brittle failure mode of rock in which microcracks coalesce to form discrete macrocracks representing regions of highly localized deformation. Such brittle behaviour is associated with cleavage, shear and mixed mode fracture mechanisms those are observed under tension and tension-compression states of stress and always involve softening of the material.

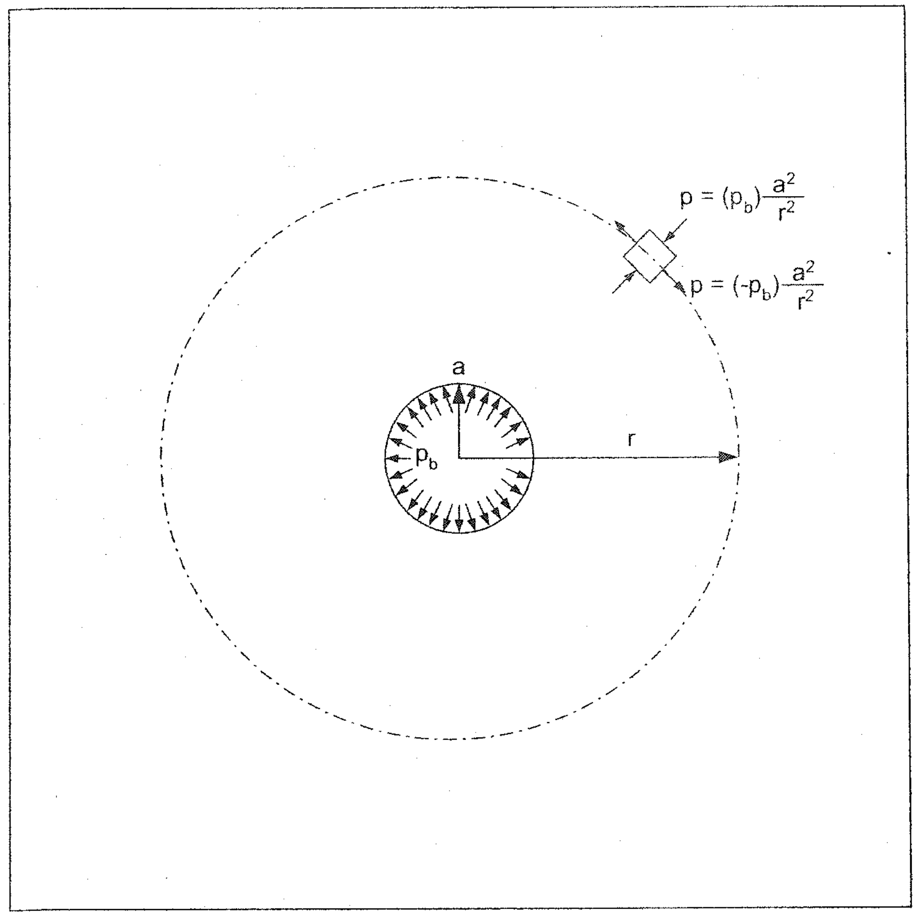

Figure 4.3 – Stresses created by an explosion pressure
(Obert and Duvall, 1967)

ABAQUS provides a brittle cracking model to simulate brittle rock failure processes (Abaqus, 2003). This material model is selected for the research as it fulfills the tensile failure representation requirements mentioned above. The important features of the model are described here and more detailed information of the model can be obtained from ABAQUS manuals (Abaqus, 2003).

The brittle cracking model is intended for applications in which the rocklike brittle material behaviour is dominated by tensile cracking and where compressive failure is not important (the material model ignores hardening and subsequent softening characteristics of compressive failure). The model includes consideration of the anisotropy induced by cracking. In compression, the model assumes elastic behaviour. The brittle cracking model is a smeared crack model in which individual "macro" cracks are not tracked but constitutive calculations are performed independently at each material point of the finite element model. The presence of cracks enters into these calculations by the way in which the cracks affect the stress and material stiffness associated with the material point. The main ingredients of the model are a strain rate decomposition into elastic and cracking strain rates, elasticity, a set of cracking conditions, and a cracking relation (the evolution law for the cracking behaviour). Brief mathematical expressions for the main ingredients of the model are:

(a) <u>strain rate decomposition</u>.

$$d\varepsilon = d\varepsilon^{el} + d\varepsilon^{ck} \qquad \text{............... (4.1)}$$

Where $d\varepsilon$ is the total mechanical strain rate, $d\varepsilon^{el}$ is the elastic strain rate representing the uncracked rock (the continuum between cracks), and $d\varepsilon^{ck}$ is the cracking strain rate associated with any existing cracks. The intact continuum between the cracks is modelled with isotropic, linear elasticity.

(b) <u>Rate constitutive equation</u>.

$$d\boldsymbol{\sigma} = \mathbf{D}^{el}\left(d\varepsilon - \mathbf{T}d\varepsilon^{ck}\right) \qquad \text{............... (4.2)}$$

Where, $d\sigma$ is the rate of stress, $\mathbf{D}^{el}$ is the isotropic linear elasticity matrix and $\mathbf{T}$ is a transformation matrix constructed from the direction cosines of the local coordinate system. $\mathbf{T}$ is constant in the present fixed crack model.

(c) <u>Crack detection</u>

A simple Rankine criterion is used to detect crack initiation. This states that a crack forms when the maximum principal tensile stress exceeds the tensile strength of the brittle material. The Rankine crack detection surface in the deviatoric space and in the plane stress space is shown in Figures 4.4 and 4.5, respectively.

Although crack detection is based purely on Mode I fracture considerations, ensuing cracked behaviour includes both Mode I (tension softening) and Mode II (shear softening/retention) behaviour. The cracked element is removed from the calculations after a certain amount of crack opening displacement, at which it can no longer carry stresses, is attained. A removed element represents a macro crack or fracture in the context of the present research.

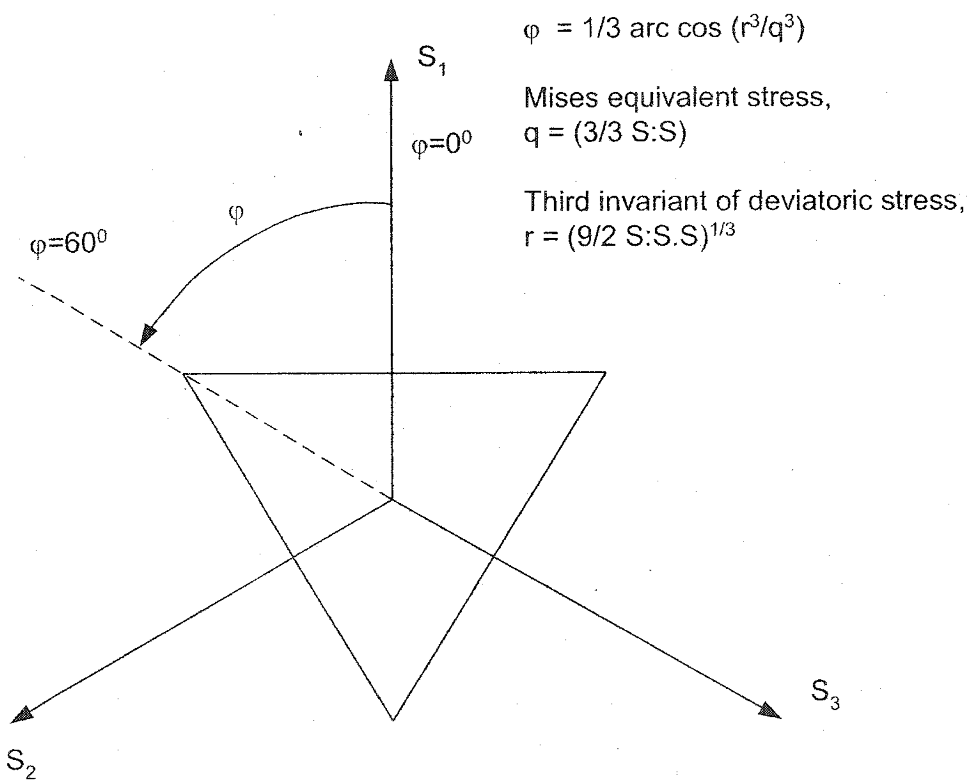

Figure 4.4 – Rankine criterion in the deviatoric stress (S) space.

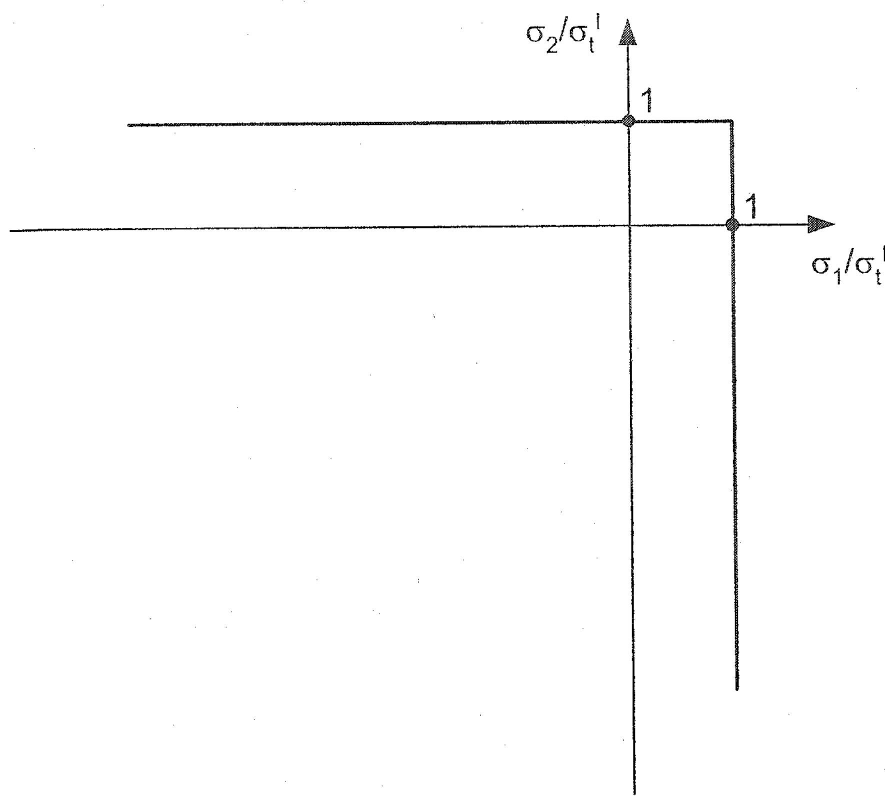

Figure 4.5 – Rankine criterion in plane stress space

(d) Consistency condition.

A consistency condition for cracking (analogous to the yield condition in classical plasticity) written in the crack direction coordinate system has the following form of tensor.

$$\mathbf{C} = \mathbf{C}\,(\mathbf{t}, \boldsymbol{\sigma}^{\mathrm{I,II}}) = \mathbf{0} \qquad \text{........... (4.3)}$$

Where $\mathbf{C} = [C_{nn}C_{tt} \quad C_{ss} \quad C_{nt} \quad C_{ns} \quad C_{ts}]^T$ and $\sigma_{I,II}$ represents a tension softening model (Mode I fracture) in the case of the direct components of stress and a shear softening/retention model (Mode II fracture) in the case of the shear components of stress. The matrices $\partial\mathbf{C}/dt$ and $\partial\mathbf{C}/\partial\sigma_{I,II}$ are assumed to be diagonal.

The brittle cracking model is characterized by a stress-displacement response rather than a stress-strain response. This characterization is based on Hilleborg et al.'s (1976) fracture energy proposal to avoid unreasonable mesh sensitive results. Thus, the crack opening displacement is selected as a criterion of element elimination from the model rather than the plastic strain. The rock material chosen for the current research represents brittle granite whose properties are well tested and known. Table 4.3 gives a summary of the rock properties used for the research as well as the reference of these values. These properties are kept constant in the present research unless otherwise specifically mentioned.

Table 4.3 – Typical granite rock properties for numerical modelling

<table>
<tr><td>Rock property</td><td>Value</td><td>Source reference</td><td>Remarks</td></tr>
<tr><td>Density (ρ), kg/m³</td><td>2650.</td><td rowspan="4">Diederichs, 1999</td><td rowspan="4">Tested and compiled representative values</td></tr>
<tr><td>Young's modulus (E), GPa</td><td>60.</td></tr>
<tr><td>Poisson's ratio (μ)</td><td>0.24</td></tr>
<tr><td>Tensile strength (UTS), MPa</td><td>15.</td></tr>
</table>

4.2.3.3 Appropriate modelling solution scheme for transient loading –explicit integration procedure

Dynamic loading is ideally suited for simulation within an explicit dynamics framework. The explicit dynamics analysis procedure in ABAQUS/Explicit is based upon the implementation of an explicit integration rule together with the use of diagonal or lumped element mass matrices. The method involves solving the equation of motion for a Langrangian mesh, which can be written in the following form using the variational principles (Bickford, 1994),

$$\mathbf{M}\ddot{u} + \mathbf{C}\dot{u} + \mathbf{K}u = \mathbf{P}(t) \quad \ldots\ldots\ldots\ldots\ldots\ldots\ldots\ldots\ldots\ldots\ldots\ldots\ldots \quad (4.4)$$

where,

u = displacement

$$\dot{u} = \text{velocity} = \frac{u(t+\Delta t/2) - u(t-\Delta t/2)}{\Delta t} \quad \text{.......... (4.5)}$$

$$\ddot{u} = \text{acceleration} = \frac{\dot{u}(t+\Delta t/2) - \dot{u}(t-\Delta t/2)}{\Delta t} \quad \text{.......... (4.6)}$$

$$\text{mass matrix, } [M] = \int_V \rho [N]^T [N] dV \quad \text{.......... (4.7)}$$

where, ρ and [N] represent the mass density and shape function matrix.

Damping matrix, [C], for the Rayleigh damping is in the form:

$$[C] = \alpha[M] + \beta[K] \quad \text{.......... (4.8)}$$

where, α and β are the pre-defined constants.

time-dependant stiffness matrix is defined as:

$$[K] = \int_V B^T [D][B] dV \quad \text{.......... (4.9)}$$

where, [D] and [B] represent constitutive and strain-displacement matrix, respectively.

The system nodal force vector due to surface, [q(t)], and body forces, [f(t)], are given by:

$$[P(t)] = \int_S [N]^T [q(t)] dS + \int_V [N]^T [f(t)] dV \quad \text{.......... (4.10)}$$

Equation (4.4) can also be conveniently represented as the equation of momentum, which has the following form:

$$\mathbf{M}\ddot{u} = f^{ext} - f^{int} \quad \text{.......... (4.11)}$$

where, $f^{ext} = \mathbf{P}(t)$ and $f^{int} = \mathbf{C}\dot{u} + \mathbf{K}u$.

Half time step values are used to calculate velocity and acceleration in this method. Both the values are accurate to the order of Δt^2. The values of the derivative at the centre of a time interval are obtained from the difference of the function values at the end of the interval, hence the name central difference scheme. The central difference integration operator is explicit in the kinematic state and it may be advanced using known values of $\dot{u}^{(i-½)}$ and $\ddot{u}^{(i)}$ from the previous increment. The explicit procedure requires no iterations and no tangent stiffness matrices. The key to the computational efficiency of the explicit procedure is the use of diagonal element mass matrices because the inversion of the mass matrix that is used in the computation for the accelerations at the beginning of the increment is triaxial (Abaqus, 2003):

$$\ddot{u} = \mathbf{M}^{-1}(f^{ext} - f^{int}) \quad \text{......} \quad (4.12)$$

The explicit procedure integrates through time by using many small increments. The central difference operator is conditionally stable, and the stability limit for the operator (with no damping) is given in terms of the highest eigenvalue in the system as

$$\Delta t \leq \frac{2}{\omega_{max}} \quad \text{......} \quad (4.13)$$

The current dilatational wave speed in the element is calculated with the following expression:

$$c_d = \sqrt{\frac{(\hat{\lambda} + 2\hat{\mu})}{\rho}} \quad \text{......} \quad (4.14)$$

where, $\hat{\lambda}$ and $\hat{\mu}$ are effective Lame constants and ρ is the material's mass density.

The details of the integration procedures are introduced in the theory manual of ABAQUS/Explicit (Abaqus, 2003).

4.2.3.4 Allocation of explosive properties for the purpose of modelling

Characteristics of blast wave profiles are discussed in detail in Chapter 3 (Section 3.2, Equation 3.3 and Figure 3.3). It may be noted that irrespective of the differences in blast pressure time profile measurements, most researchers arrive at only two broad characteristics profiles, namely, ideal detonation and non-ideal detonation. The ideal detonation profile corresponds to emulsion type explosives where the peak pressure rise time is very short and the fall from peak pressure is steep. The non-ideal detonation profile corresponds to ANFO type explosives where the rise time for the peak blast hole pressure is longer and the fall from the peak pressure is much slower. Numerically, these blast hole pressure profiles can be handled through one of the three procedures, namely, Equation of State (EOS), pressure–decay functions or by using direct input of dynamic pressure as a function of time (Table 4.4).

Table 4.4 – Choices for explosion pressure-time profile as a numerical modelling input parameter

Choice	Equation	Example reference
John-Wilkinson-Lee (JWL) equation	$P = A\left(1-\frac{\omega\rho}{R_1\rho_0}\right)e^{\left(-R_1\frac{\rho_0}{\rho}\right)} + B\left(1-\frac{\omega\rho}{R_2\rho_0}\right)e^{\left(-R_2\frac{\rho_0}{\rho}\right)} + \frac{\omega\rho^2}{\rho_0}E_{m0}$	Liu, 1997
Pressure decay functions	$P=P_0\zeta[e^{-\alpha t} - e^{-\beta t}]$	Cho et al., 2003
	$P=P_0[e^{-\alpha t} - e^{-\beta t}]$	Lima et al., 2002
	$P=P_0e^{-\alpha t}$	Kutter, 1967
Direct input of pressure-time profile	A Gaussian function	Donze et al., 1997
	Triangular load shape	Valliapan et al., 1983
	Optimized pressure profile	Proposed in this thesis

EOS describes material behaviour in the high-rate intense-pressure environment and the equation relates different material quantities as a single valued function of the others, regardless of the deformation prior history. Several EOS relations have been developed and are in use (Braithwaite et al., 1996) but EOS by the Jones-Wilkins-Lee equation (JWL equation) is the most popular in the geomechanics field due to its simple form, experimental basis and ease in use with hydrodynamic calculations (He et al., 2002; Etoh et al., 2002). The JWL EOS contains the parameters describing the relations among the volume, energy and pressure of detonation products. The JWL takes rock-explosive interaction into account (Liu, 1997). However, estimating the correct parameters for non-ideal detonation or in softer rocks poses considerable difficulties (Liu, 1997). The detonation process in most rocks is non-ideal so the accuracy of the JWL equation in its calculations is questionable.

Input in the form of decay equations are also reported (Duvall, 1953; Jung et al., 2001; Lima et al., 2002; Olatidoye et al., 1998; Robertson et al., 1994). These equations are used to replicate exact waveforms. But the use of decay equations requires assumptions of some parameters whose physical significance is unknown.

The dynamic load input as a Gaussian function and as a triangular load function have also been attempted to approximate a measured dynamic-pulse load. However, these procedures are not close to the physical characteristics of the dynamic load and hence carry no physical meaning. The Guassian function is manily introduced to avoid numerical errors associated with the application of a very high magnitude load (in the order of GPa) in a very short duration (in the order of microseconds). Therefore, a new procedure is proposed with this thesis and it is termed as optimized pressure-time profile. The proposition is straightforward and can replicate observed blast hole pressure profiles in a more controlled and simplified way. Therefore, the present study will incorporate application of the direct input of the optimized pressure–time profile considering both the characteristics of blast pressure-time profile mentioned earlier (non- and ideal detonation). The selected procedure has a distinct advantage over the other two methods, Gaussian function and triangular load, as it has a close resemblance to the real load (Figure 4.6).

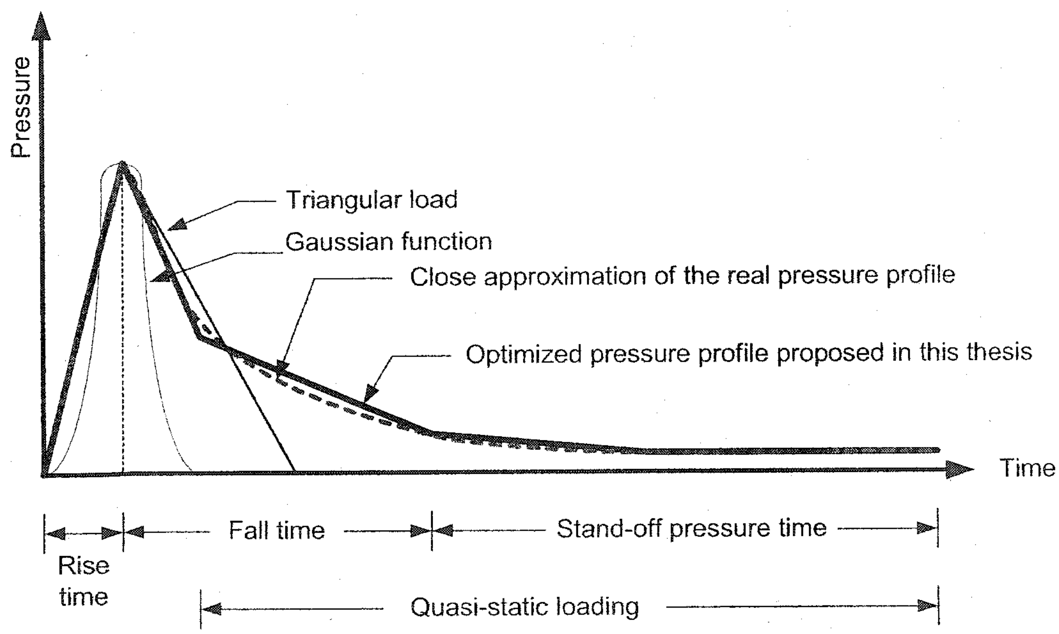

Figure 4.6 – Comparison of the different methods for approximation of the blast pressure-time profile

Two explosive properties, namely, peak borehole pressure and the pressure at different time scales are required to specify the optimized pressure-time profile. The peak borehole pressure can be estimated from Equation 3.3 given in Chapter 3. Values of detonation velocity (VOD), explosive density (ρ) and coupling ratio (r_c, ratio of charge diameter to borehole diameter) are required for estimating the peak borehole pressure. Table 4.5 provides values of VOD and ρ along with source information while Table 4.6 provides typical borehole pressure values obtained from calculations for some borehole diameters and coupling ratio considered in the thesis. The maximum possible fractures zone calculations based on Equations 3.3 and 3.4 using the values provided in Tables 4.3, 4.5 and 4.6 are estimated and compiled in Tables 4.7 and 4.8.

Table 4.5 – Details of explosive properties for borehole pressure calculations

Borehole diameter, mm	Emulsion explosive		ANFO explosive	
	VOD, m/sec.	ρ, kg/m^3	VOD, m/sec.	ρ, kg/m^3
32	4300	1100	2900	1000
Source reference	(Sun et al., 2001; Liu, 2002)	(Brinkmann, 1990)	(Brinkmann, 1990)	(Brinkmann, 1990)
38	4700	1050	3300	950
Source reference	Sun et al., 2001)	(Brinkmann, 1990)	(Mohanty, 2003)	(Brinkmann, 1990)
55	5500	1000	4200	900
Source reference	Extrapolated		Extrapolated	
76 and 89	6000	1000	4700	900
Source reference	Adams et al., 1993	(Brinkmann, 1990)	Adams et al., 1993	(Brinkmann, 1990)

Table 4.6 – Estimated borehole pressure values

Borehole diameter, mm	Peak pressure for emulsion explosive, GPa			Peak pressure for ANFO explosive, GPa
	Fully coupled hole	70 % coupled hole	50 % coupled hole	Fully Coupled hole
38	2.9	0.95	0.35	1.29
55	3.8	1.3	0.47	2.0
76	4.5	1.5	0.6	2.5
89	4.5	1.54	0.56	2.49

Table 4.7 - Details of fractures zone calculations for emulsion type explosives

Borehole diameter, mm	Borehole length, m	Charge length, m	Coupling ratio	Charge volume, x 10^{-3} m^3	Charge wt. in TNT Equivalent, x 10^{-3} t	According to Mosinets and Garbacheva, 1972 (Eqns. 3.5 to 3.7, Chapter 3)			Fractures zone according to Kexin, 1995 (Eq. 1.8, Chapter 3)
						Crushing zone radius, mm	Fractures zone radius, mm	Seismic zone radius, mm	Fractures zone radius, mm
32	3	2	1.0	1.6	2.0	96.7	165.3	908.5	343.2
38	3	2	1.0	2.3	2.7	106.6	182.3	1002.1	356.2
38	3	2	0.7	1.1	1.3	84.3	144.1	791.9	325.8
38	3	2	0.5	0.6	0.7	67.5	115.4	634.2	299.5
55	5	2.5	1.0	5.9	6.8	144.2	246.5	1354.8	388.3
76	6	2.5	1.0	11.4	13.0	178.5	305.1	1677.1	421.0
76	6	2.5	0.70	5.6	6.4	141.0	241.1	1325.4	385.1
76	6	2.5	0.50	2.8	3.3	112.9	193.1	1061.4	354.0
89	7	3	1.0	18.6	21.5	210.3	359.6	1976.8	437.9
89	7	3	0.7	9.1	10.5	166.2	284.2	1562.2	400.6
89	7	3	0.5	4.7	5.4	133.1	227.6	1251.1	368.2

Table 4.8 - Details of Fractures zone calculations for ANFO type explosives

Borehole diameter, mm	Borehole length, m	Charge length, m	Coupling ratio	Charge volume, x 10^{-3} m^3	Charge wt. in TNT Equivalent, x 10^{-3} t	According to Mosinets and Garbacheva, 1972 (Eqns. 3.5 to 3.7, Chapter 3)			Fractures zone according to Kexin, 1995 (Eq. 1.8, Chapter 3)
						Crushing zone radius, mm	Fractures zone radius, mm	Seismic zone radius, mm	Fractures zone radius, mm
32	3	2	1	1.61	1.7	90.9	155.4	854.3	335.3
38	3	2	1	2.27	2.3	100.1	171.2	940.9	347.8
55	5	2.5	1	5.94	5.6	135.1	231.0	1269.8	378.9
76.	6.	2.5	1	11.3	10.7	167.3	286.0	1571.9	410.8
89	7	3	1	18.65	17.6	197.2	337.1	1852.8	427.3

The pressure time profile is constructed with the help of the peak pressure values calculated in Table 4.6 and by applying it over a time period in a magnitude and a manner consistent with the explosive characteristics. The complete process and basis of its construction is briefly described below.

Explosion pressure in a borehole dies down to a stand-off pressure within a couple of milliseconds, which is much below to tensile strength of rocks. The rise time of explosion pressure to its peak is very short and varies primarily according to the explosive characteristics and secondly according to the blast hole diameter, blast hole confinement, rock strength, etc. Generally, the rise time for emulsion type an explosive is around 25 microseconds and 100 microseconds for ANFO type explosives. The subsequent decay in the peak borehole pressure down to stand-off pressure is sharp in the case of the emulsion type explosives and slow for the ANFO type explosives. Therefore, in this study, to construct the optimized pressure-time profile, the peak borehole pressure is applied in its full magnitude (increasing from zero at time zero second) at the respective time mentioned above. The peak pressure magnitude is dropped to 90 per cent, 99 per cent and 99.9 per cent values over a time period consistent with the two types of explosive characteristics, namely, shock type loading of the emulsion type explosives and quasi-static type loading of the ANFO type explosives. The simulation of explosion with de-coupled charges needs additional considerations. Some simplified assumptions are made based on engineering intuition and reported behaviour (Frantzos, 1989). The peak pressure is reduced as per Equation 3.3 (Chapter 3) as summarised in Table 4.5 but the peak stays for some time to give the effect of expansion of the explosion gaseous products in the hole, and then decays according to the explosive characteristics. The complete scenario for the pressure-time profile inputs for different requisite modelling analyses is presented in Figure 4.7. The pressure-time profile selected is in good agreement with the observed profiles by Frantzos (1989), Fourney (1996), Jung et al. (2001) and Daniel (2003).

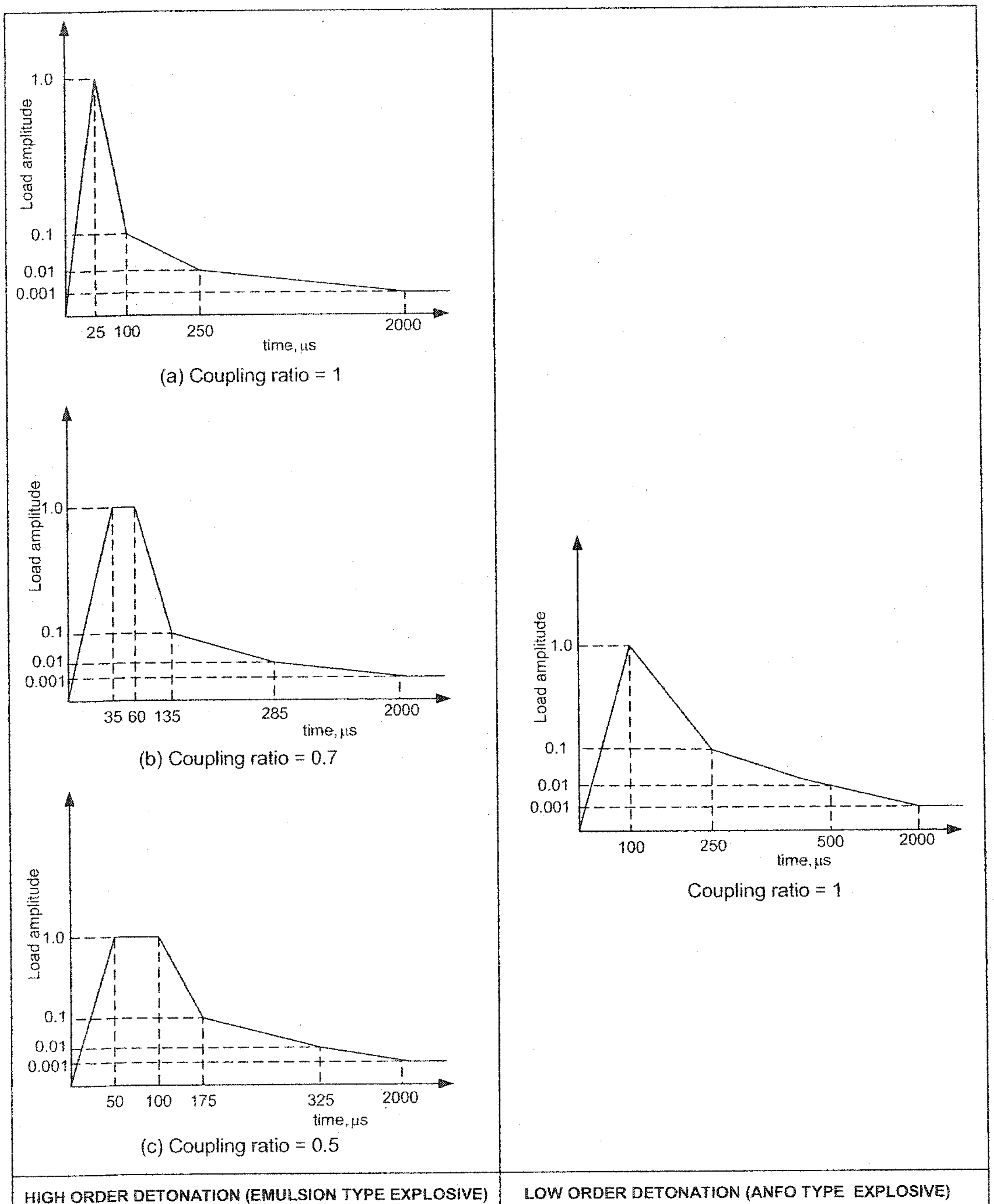

Figure 4.7 – Schematic optimized pressure-time profile of different explosives used in the study for 38 mm diameter borehole

4.2.3.5 Selection of appropriate model and boundary conditions

There are two primary responses of any dynamic loading in a real blasting case. First, the rock undergoes a crushing and fracturing process in response to the dynamic loading. The wave energy dies down due to this fracturing process. Second, the rock mass constitutes an unbounded (infinite) medium to absorb the majority of the remaining wave energy (partly reflected back from the free faces and partly transmitted to the air causing air over-pressure and noise).

Hitherto, the majority of the dynamic modelling analyses were done with elastic material models. This representation leads to two major concerns from a numerical simulation point of view, namely, suitable arrangements at far-field boundaries to represent unbounded medium and spatially damping of the wave energy (in a similar fashion to physical damping). Otherwise oscillations would unabatedly occur in the elastic medium. These two concerns are addressed here in detail in order to establish a valid and representative numerical model.

(a) **Representation of the far-field boundaries**. One of the major concerns of any numerical simulation involving wave propagation in solids of unbounded medium is to avoid the spurious reflection of waves at the model boundaries. Several schemes have been suggested, developed and implemented but all have their own limitations in absorbing outgoing waves.

One of the more popular arrangements is the use of infinite elements to represent the unbounded medium such as developed by Lysmer and Kuhlemeyer (1969). These infinite elements in fact represent infinitesimal dashpots oriented normal and tangential to the boundary. This arrangement works well provided waves impinge on the boundary orthogonally. This means that the boundary should be far enough from the wave source. The wave source should behave like a point source in this case. Further, infinite elements provided by Lysmer and Kuhlemeyer (1969) and adopted in ABAQUS (Abaqus, 2003) absorb almost all of the energy of P (Primary) and S (Secondary) waves but they are less efficient in absorbing R (Rayleigh) wave energy (Ramshaw et al., 1998). These infinite elements represent ‘quiet boundaries’, and not ‘silent boundaries’. The impetus set for the current research is the simulation of an explosive column charge in contrast to the point excitation charge and its effect on the near borehole fracturing process. So it will not be practical to construct computationally unmanageable large model domains to represent the point source for the waves reaching the boundary. Therefore, infinite elements are not suitable and an alternate arrangement needs to be considered.

Another suggested approach is the insertion of a time-damping term in the wave equation and an attenuation boundary zone around the discretization mesh, the wave field goes to zero with time when passing through the zone (Bing and Greenhalgh, 1998). Sochacki et al. (1987) studied five kinds of such damping terms (linear, power, cubic, Gaussian and exponential) for 2D acoustic and elastic modelling in the time domain and concluded that the linear damper reduced the artificial reflections best. The Bing and Greenhalgh’s (1998) study indicates that for effective results from this time damper, a larger mesh and a wider absorbing zone are required. Further, the use of different types of element formulations (one for solid medium and another for wave absorbing zone) may pose numerical instability problems during the dynamic analysis due to mesh incompatibility issues. Therefore, this method will not be used for the present study.

The present study is considering a discrete simulation of fracturing process around the borehole. This means that the model itself should absorb the majority of the energy as it actually occurs in nature. So, prevalent roller boundaries should be accurate enough to represent far-field boundary conditions. However, these boundaries should be far enough (far greater than the established norms for static numerical modelling) to avoid any effect on the fracturing zone after waves reflection as well as to provide enough time for fractures propagation. This will be made possible, in the current development procedure, by considering full models (no truncation of model size due to symmetry planes) with boundaries reasonably far enough from the boreholes to provide enough time for fractures propagation as well as to avoid the effect of reflected waves on the fractures propagation. As per the rock material properties, the estimated maximum primary compressional wave speed is 5166 m/sec (Table 4.5). Also, as per Tables 4.7 and 4.8, the likely maximum radius of the fracturing zone is 0.427 m in the present numerical analyses. Now considering a point 1.0m away from the borehole centre and far-field boundaries placed at 10 m away from the borehole boundary, the fastest wave will take approximately 3.5 milliseconds to reach the point under consideration after reflection from the far-field boundaries. This time is long enough to study the fracturing process by primary waves, as they have peak pressures at 25 microseconds and 100 microseconds, respectively, for emulsion and ANFO type explosive characteristics. So, far-field boundaries can be placed at 10 m away from the central borehole of 38 mm diameter (more than 250 times farther than the excavation size) with prevalent roller boundaries. Further, a numerical solution time of about 2 milliseconds will provide enough time to capture the fracturing process only be the primary waves and hence will be used.

(b) **Damping of the wave energy**. There are two reasons for adding damping to a numerical model: to limit numerical oscillations and to add physical damping to the system (Abaqus, 2003). ABAQUS has provisions for bulk viscosity (in linear and quadratic, both forms) to limit numerical oscillations (Abaqus, 2003). The suggested values for bulk viscosity will be retained during the analysis. Choosing a stiff element (single integration point) will be the other source of damping for the numerical models to take care of numerical oscillations.

The use of Rayleigh damping with elastic material models is common in geo-mechanics applications for adding the effect of physical damping. The damping coefficients are selected either as per the PPV (peak particle velocity) measurements from specific site data or assigned 1 per cent to 15 per cent values (generally 1 per cent-10 per cent for geo-mechanics problems) (Biggs, 1964; Massarsch, 1992). Further, the damping coefficient should not be more than 0.5 per cent if a linear failure criterion (like Mohr-Coulomb) is used (Itasca, 2001). This is due to the reason that the linear failure criterion itself induces early failure or plasticity. Also, in rock and soil, the natural damping is independent of frequency (Gemant and Jackson, 1937) so the use of Rayleigh damping may not be justifiable in such analyses. Another problem reported with frequency dependant damping is misrepresentative results due to sometimes over damping of the low frequency modes (Metzger, 2003), which usually control the solution.

Other types of damping procedures are also reported such as mass proportional damping (Bing and Greenhalch, 1998; Takewaki, 2000), dynamic relaxation damping (Metzger, 2003), etc. But their validity for hysteretic damping medium (such as rock) is not well established. Also, such damping arrangements are mass proportional damping rather than stiffness proportional damping. A physical system like rock has natural frequencies, which are beyond an effective range of the mass proportional damping methods. Stiffness proportional damping is much needed (either in the form of plasticity or by specifying stiffness proportional Rayleigh damping parameter) for such systems. Therefore, arrangements involving mass proportional damping will not be incorporated in this research.

It is reported (Abaqus, 2003) that the energy absorbed by plasticity is significantly higher than it can be absorbed by any artificial damping method like Rayleigh damping. The proposed analysis aims to capture rock fracturing (results of plasticity) on a real time frame as it happens in reality so no artificial damping will be considered in the employed plane stress numerical models. Failed elements estimated by the Rankine failure criterion will be removed from the calculations to give the effect of crack/fracture generation and propagation as a source of plasticity in the analyses.

It is clear from the above discussion that no artificial damping as a material property is needed if the material model considers plasticity. Therefore, the model domain will not consider any artificial material damping.

4.2.3.6 Selecting Element Type and Size for the Analyses

(a) **Element type**. The prerequisite for rock fracture modelling is that the element should provide a rich enough set of possible fracture paths. This issue can be controlled by triangular elements in 2D analysis and by triangular tetrahedra in 3D analysis. Kikuchi (1983) proved the superiority of constant stress-strain triangular elements (CST) over the 4-node isoparametric elements with a reduced integration scheme in 2D analysis for yield modelling. Repetto et al. (2000) also report the suitability of high-order triangles in order to avoid volumetric locking for simulations involving unconstrained plastic flow. However, high-order triangles behave poorly under severe dynamic contact conditions (Abaqus, 2003).

Therefore, first order 3-node triangular plane stress elements will be used in the present study for numerical modelling. The interpolation function for these elements is defined in terms of the element coordinates g and h (Figure 4.8). Since ABAQUS is a Lagrangian code for most applications, these are also material coordinates. They each span a range from 0 to 1 in an element but satisfy the constraint that $g + h \leq 1$ for triangles. The function is calculated as follows.

Displacement, $u = (1 - g - h)\, u_1 + g\, u_2 + h\, u_3$ ....(4.15)

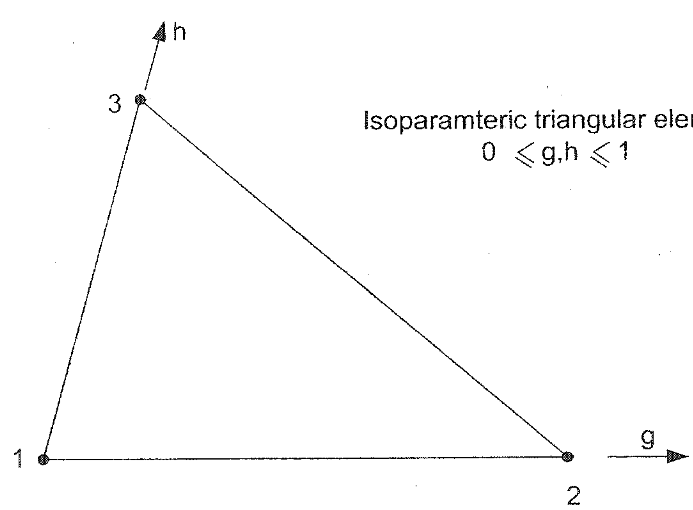

Figure 4.8 – Constant stress elements used in the present study

The first-order triangles are constant stress elements and they use a single integration point for the stiffness calculation when used in stress/displacement applications. A lumped mass matrix is used for such elements, with the total mass divided equally over the nodes. Boundary distributed loads are integrated with two points for first-order triangles. (Abaqus, 2003).

(b) **Elements size.** The structure analysis through finite element analysis is based on the initial configuration of the structure and its deformation throughout the history of loading. The strains and stresses are calculated from the results obtained for deformation. Therefore, a deformation convergence study is required to determine the suitable size of elements. Further, the area of interest is the one surrounding the borehole where the fracturing processes take place. So, suitable size elements will be required for this zone and the rest of the model domain can have larger size elements for computational efficiency. The convergence study is done by employing static analysis with due consideration of elastic material properties and critical load values intended for the research (Figure 4.9). It is evident from the analysis of deformation convergence (Figure 4.10 and Table 4.9) that an element size of 4.59 mm side length for the plane stress analyses is appropriate. But the suitability of the element size chosen is based on static convergence analysis for dynamic modelling should also be evaluated based on the low frequency mode. According to the nomogram provided by Valliapan et al. (1983), the element size of 6.25 mm is required for the critical dynamic pulse of emulsion type explosives with rock material properties as shown in Table 4.2. Therefore, the element size of 4.59 is also suitable for the low frequency modes. Further, numerically 10 nodal points are required within the fastest travelling wave's amplitude for smooth wave propagation through the model (Ramshaw et al., 1998; Abaqus, 2003). The element size of 4.7 mm is required as per this norm for the present analysis with the primary compressional wave speed of 5166 m/sec. Therefore, the element size of 4.59 mm as brought out by static convergence analysis is also appropriate for the dynamic analysis. Elements near the borehole will have a face size of about 4.6 mm and the size will be gradually increased with distance away from the borehole.

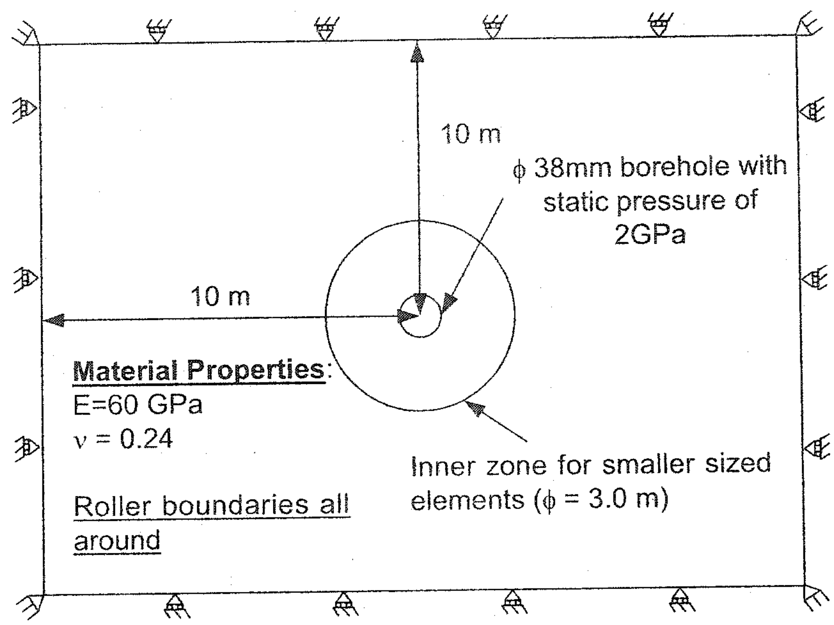

Figure 4.9 – Schematic of plane stress model details for the convergence analysis

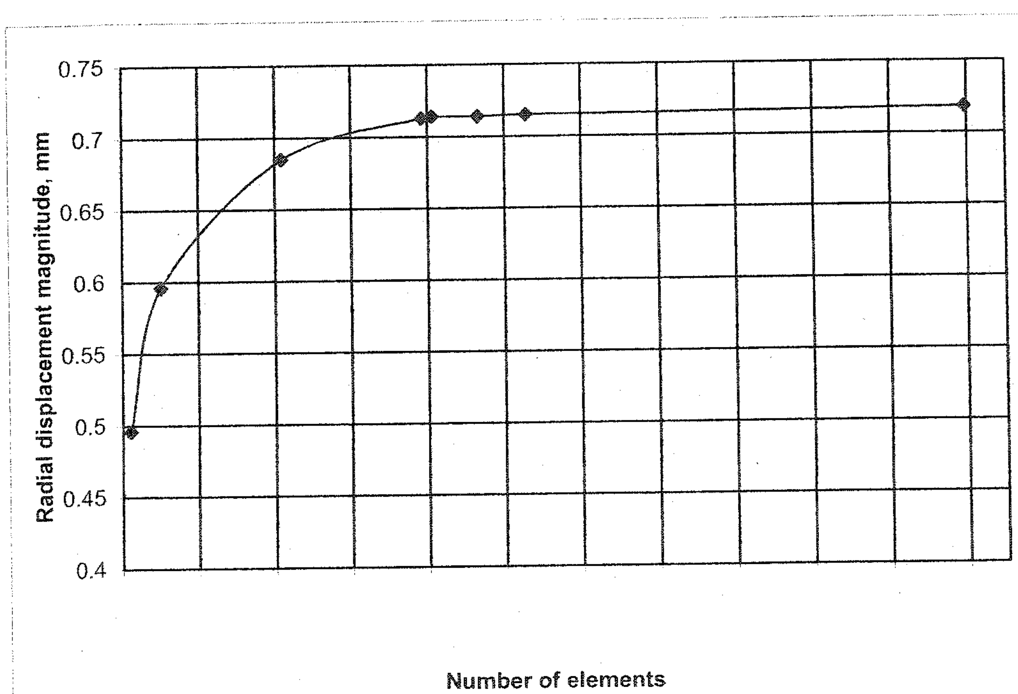

Figure 4.10 – Convergence analysis results

Table 4.9 Convergence analyses for plane stress elements

No. of elements	Side length of borehole skin elements	Radial deformation (mm)
602	21.75	0.496
1676	11.28	0.619
2588	8.5	0.685
4422	4.59	0.713
4560	4.59	0.714
5156	4.59	0.714
5784	4.25	0.715
11474	1.94	0.718

4.3 SAMPLE MODEL ANALYSES AND THEIR VERIFICATION

So far, all the parameters for the new procedure for a dynamic rock fracturing model using element elimination technique available with ABAQUS have been established. This model set-up now needs to be validated against published literature. It is difficult to correlate the model results with exact fracturing behaviour of field scale or laboratory scale reported observations because such a quantifiable knowledge base doesn't exist. This lack of a knowledge base is discussed in Chapter 3, which discusses rock fracturing by explosive energy. The lack of requisite knowledge base is due to the following reasons:

(a) Prevalent experimental techniques have observational difficulties associated with the capturing of growth of fracture networks due to the speed of the detonation process (in the order of a couple of milliseconds), speed of fracture propagation (in the order of a few thousand m/sec.) and visibility hindrance by debris of failed rock material as well as explosion gaseous products, etc.

(b) Prevalent experimental techniques at a laboratory scale are unable to have full control on the experiments due to the stochastic nature of rock material properties. The laboratory scale experiments also suffer from scale effect.

However, enough material is available based on empirical knowledge to verify the developed numerical procedure. Such an empirical knowledge base will be employed to validate the model results. Validation of the model results against more than one type of such a knowledge base will prove its robustness and suitability.

A full model developed and employed for the procedure verification is shown in Figure 4.11. The computational model comprises 4560 first order constant stress triangular elements and 2312 nodes. The spatial distribution of the elements in the mesh is based on the convergence analysis previously made (Fig. 4.10) with the provisions that the elements of desired size and in nearly uniform size are kept in the vicinity of the load plane and then gradually coarsen away from the load plane. Prevalent roller boundaries are used to represent unbounded medium at a distance of 10 m from the central 38 mm diameter borehole. The zoom-in view of the model showing elements around the borehole is shown in Figure 4.12. The central borehole is subjected to peak borehole pressures of 2.9 GPa and 1.29 GPa to represent detonation of emulsion and ANFO type explosives, respectively, using the pressure-time profile depicted in Figure 4.7 for two separate model analyses to evaluate the dynamic fracturing process by distinct explosives characteristics. The material model has values as shown in Table 4.2. The model is solved using an explicit integration scheme with the dynamic load duration of 2 milliseconds. The results of the validation tests for the two types of dynamic loads employed are shown in Figures 4.13 through 4.19.

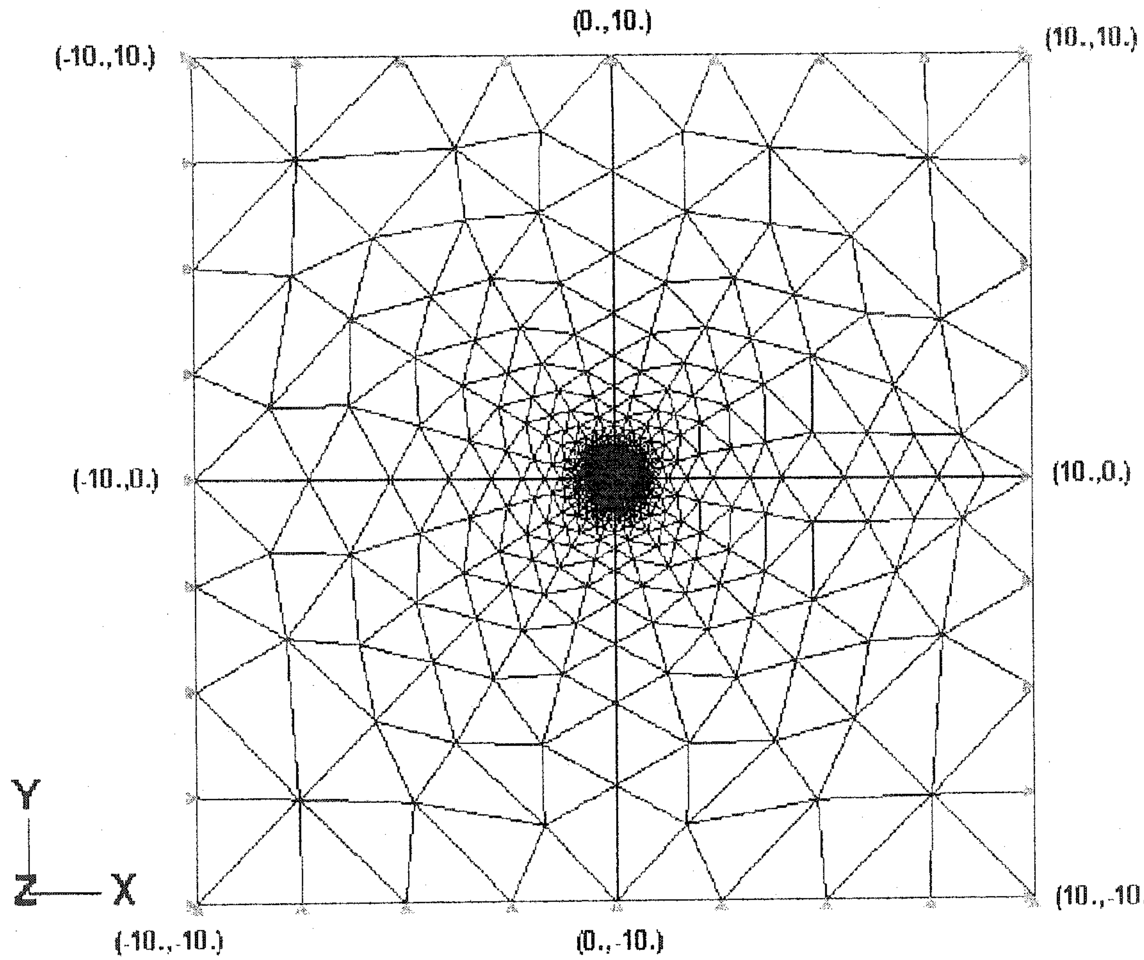

Figure 4.11 – FE mesh and model boundary conditions used for the validation tests for the developed procedure

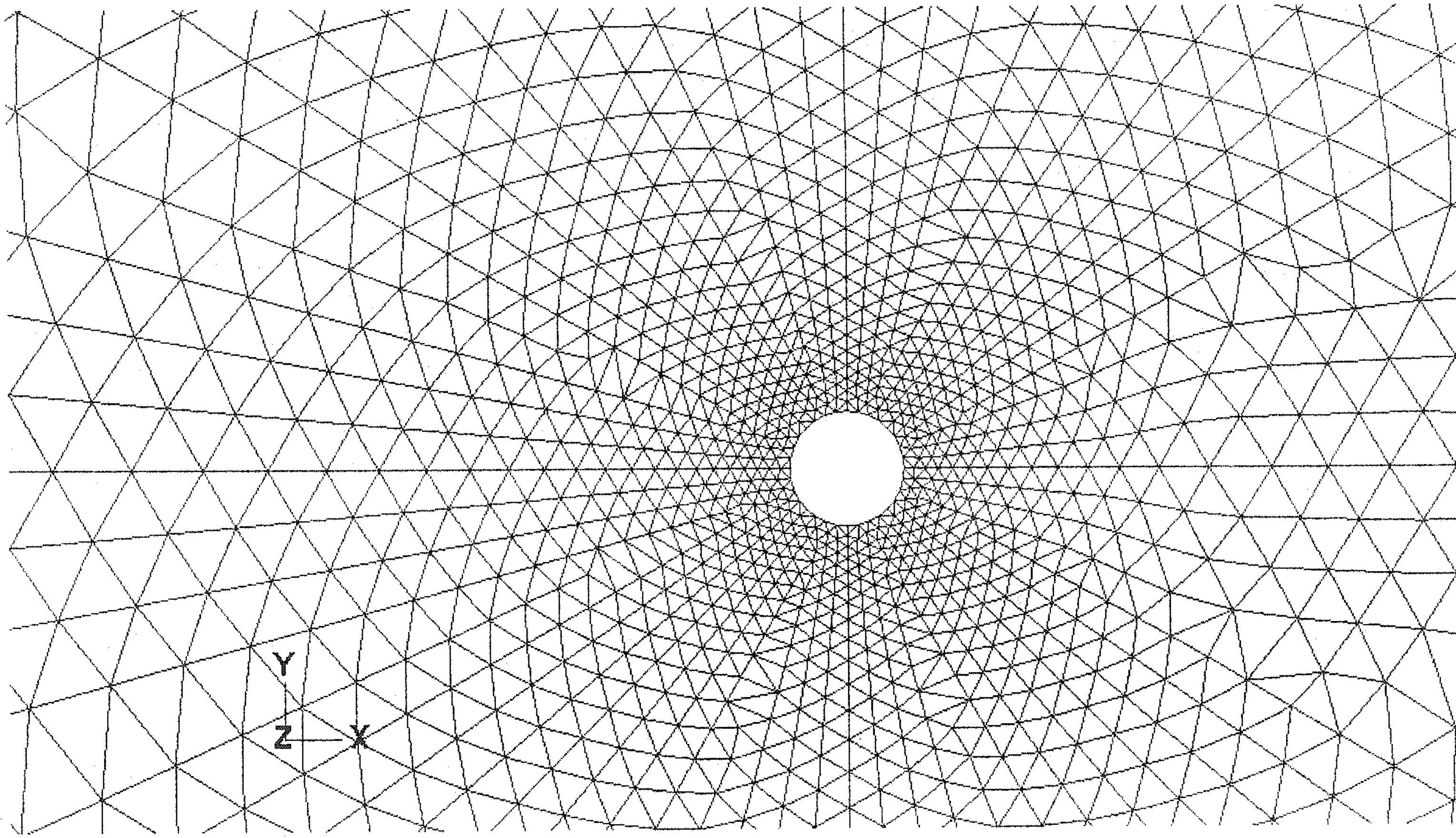

Figure 4.12 – Zoom-in view of the model mesh central zone showing 38 mm diameter blasthole

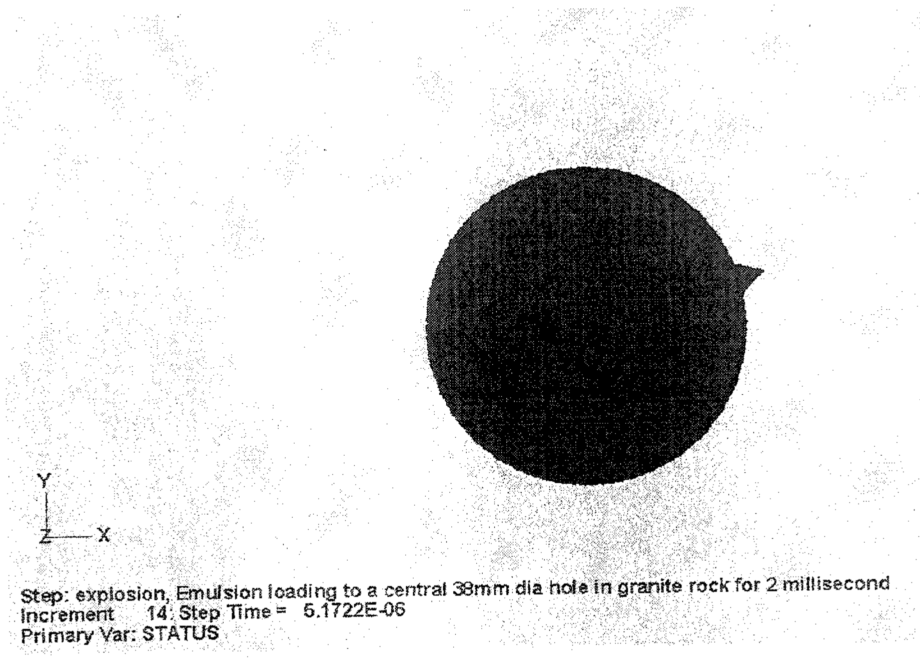

(a) Fractures initiation load magnitude for emulsion types explosive= approx. 600 MPa

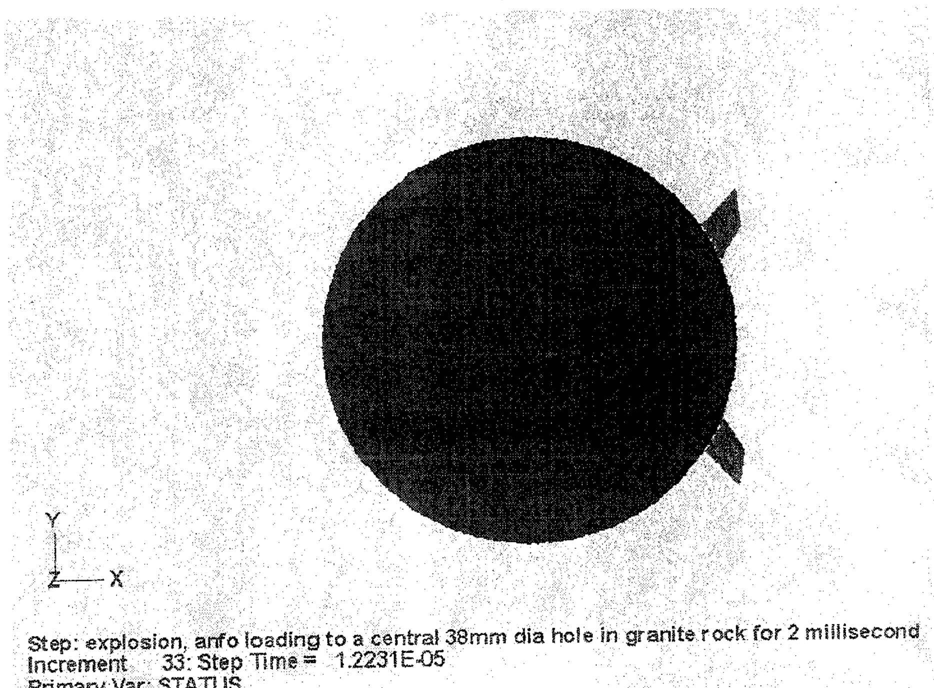

(b) Fractures initiation load magnitude for ANFO types explosive = approx. 159 MPa

Figure 4.13 – Fractures initiation load magnitude

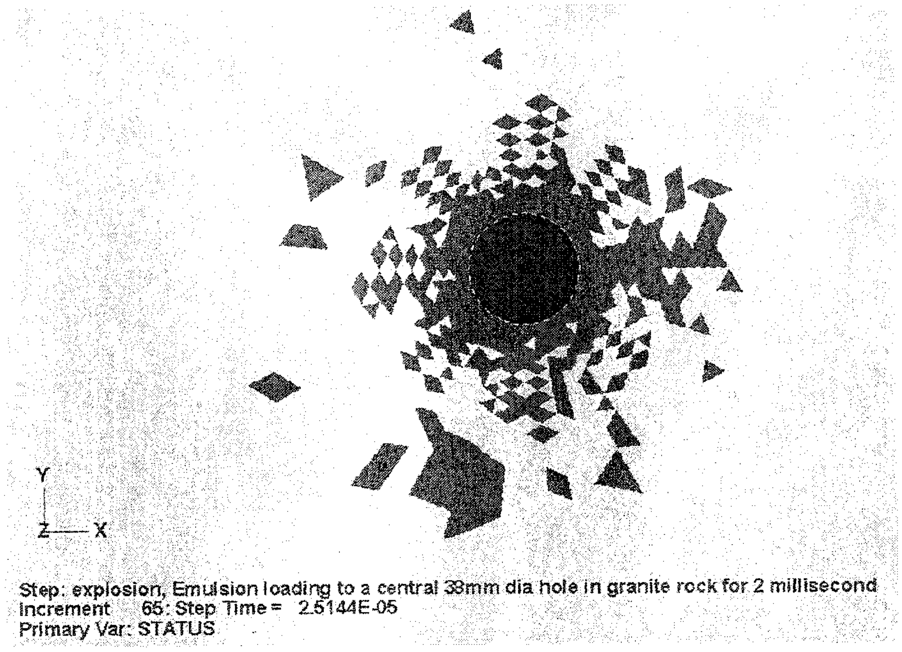

(a) Emulsion types explosive, the peak load = 2.9 GPa

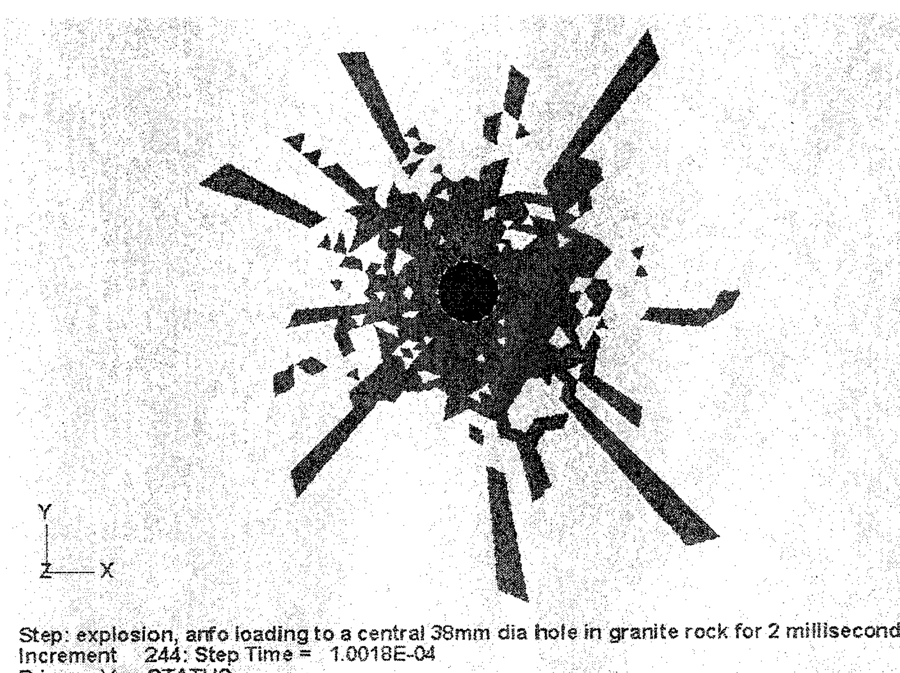

(b) ANFO types explosive, the peak load = 1.29 GPa

Figure 4.14 – Fracture pattern at the peak load magnitude

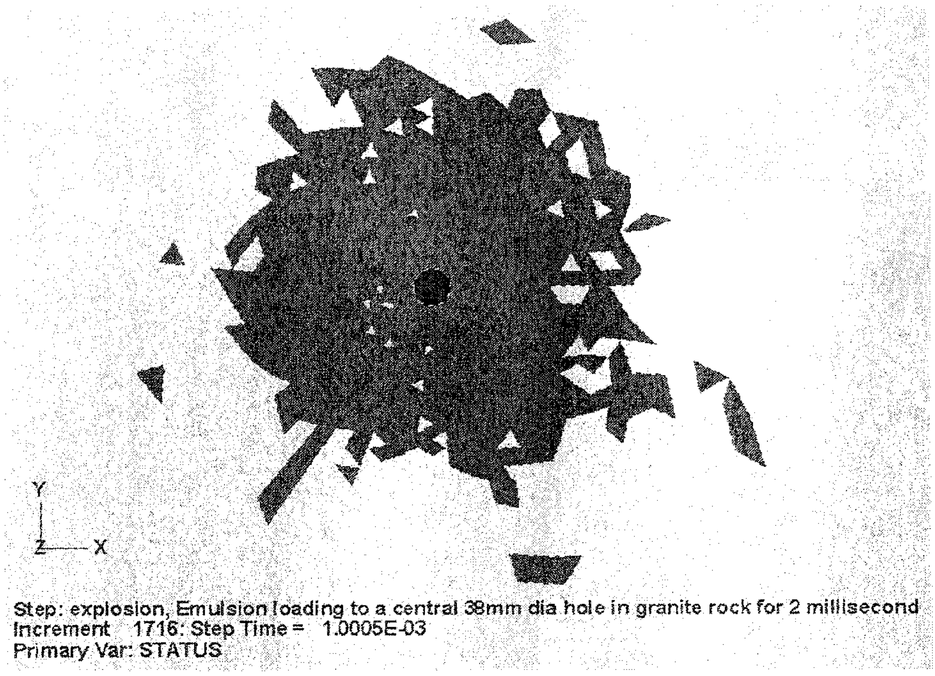

(a) Emulsion types explosive, time = 1 millisecond

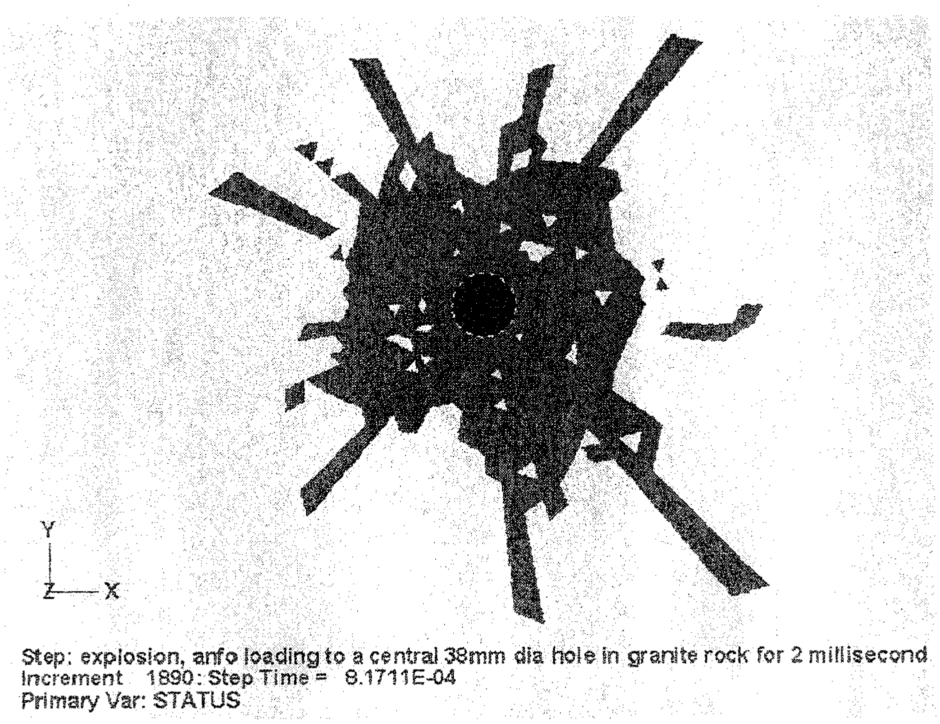

(b) ANFO types explosive, time = 817 microsecond

Figure 4.15 – Final fracture pattern

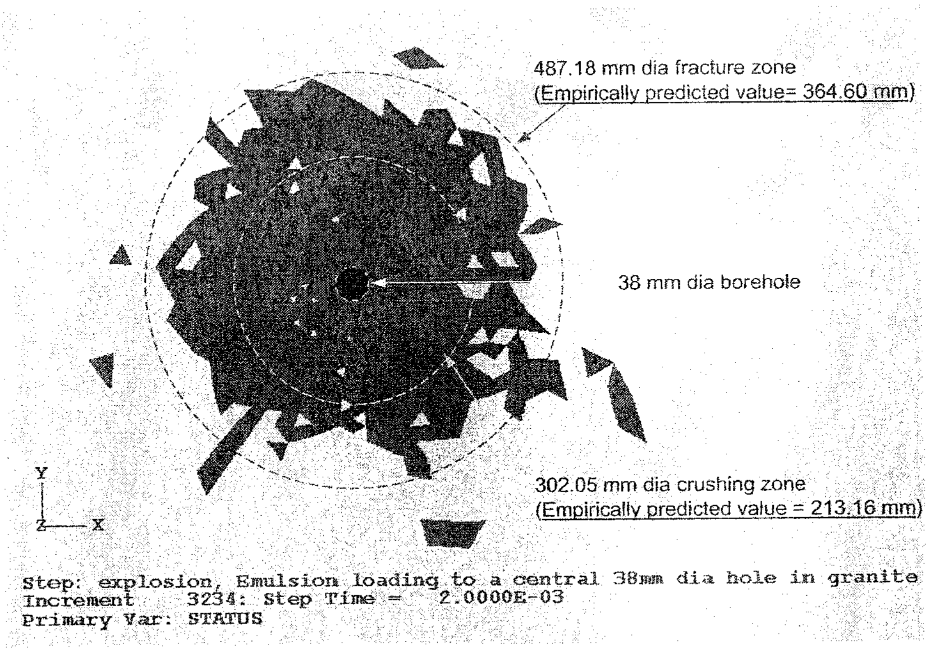

(a) Emulsion types explosive

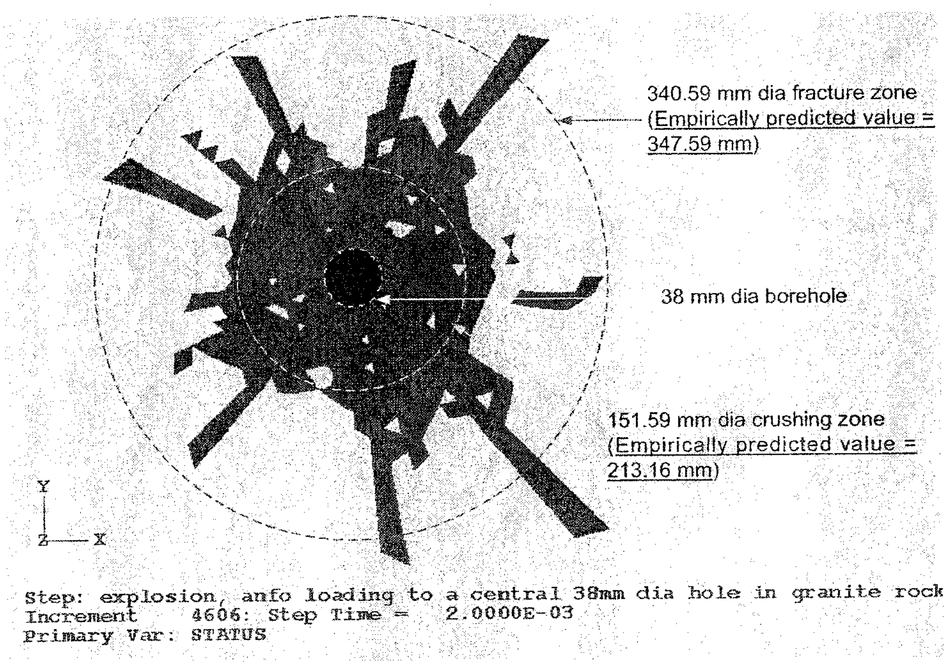

(b) ANFO types explosive

Figure 4.16 – The fracture pattern at the end of the calculations (2 millisecond)

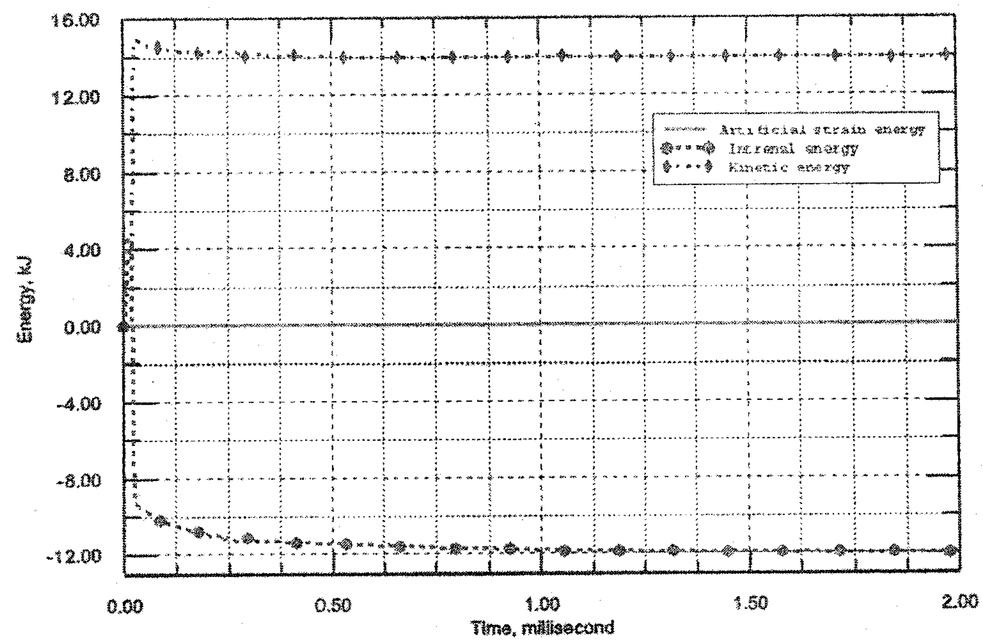

(a) Emulsion types explosive

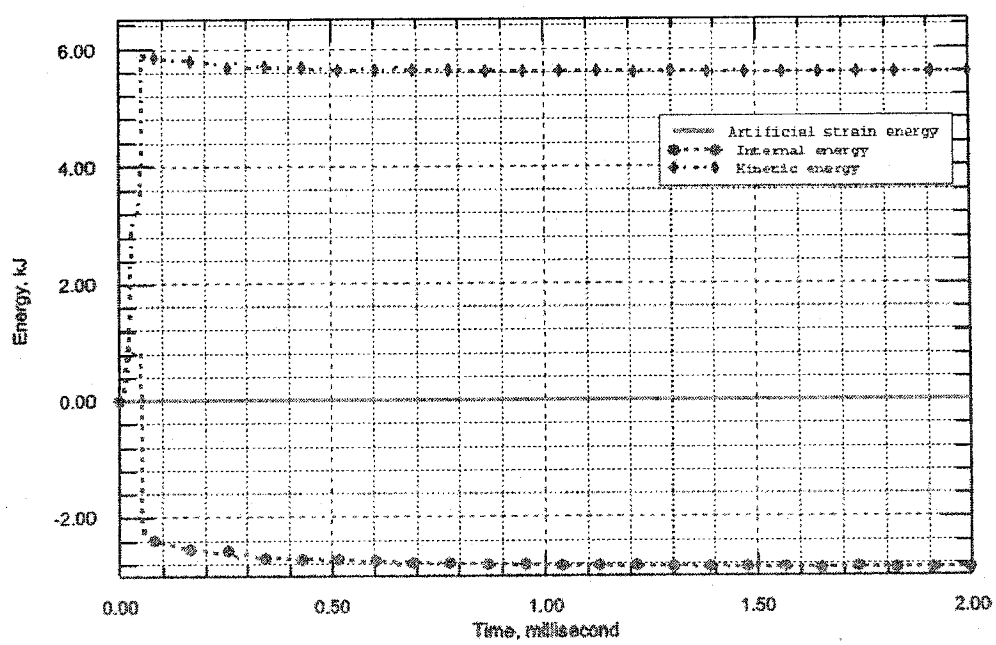

(b) ANFO types explosive

Figure 4.17 – Kinetic, Internal and Artificial energy plots

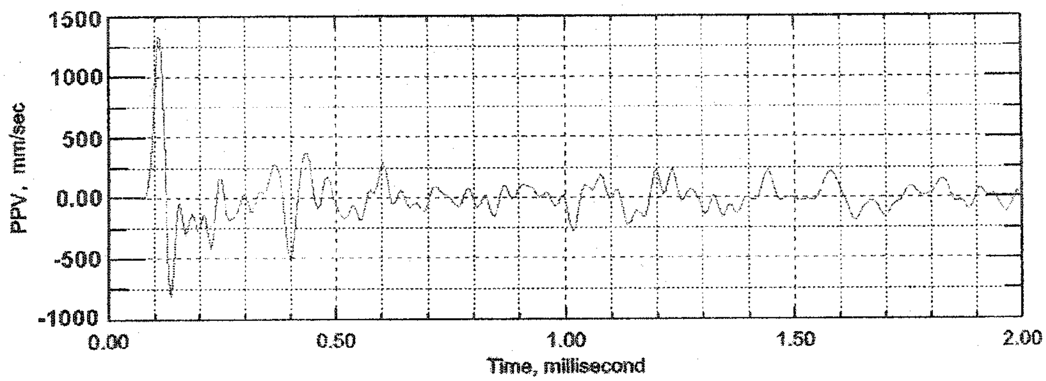

(a) Emulsion types explosive, PPV at 0.5 m from the borehole (point coordinates = 0.5,0.)

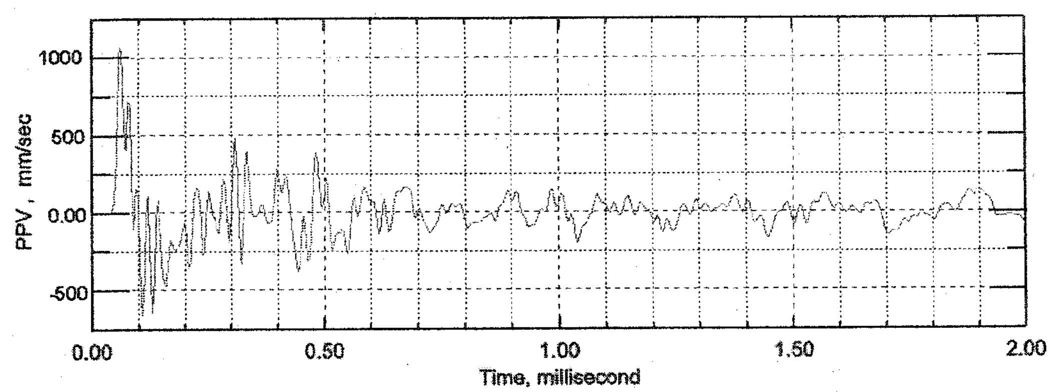

(b) ANFO types explosive, PPV at 0.25m from the borehole (point coordinates = 0.25,0.)

Figure 4.18 – Peak particle velocity plots (PPV in the X-axis direction)

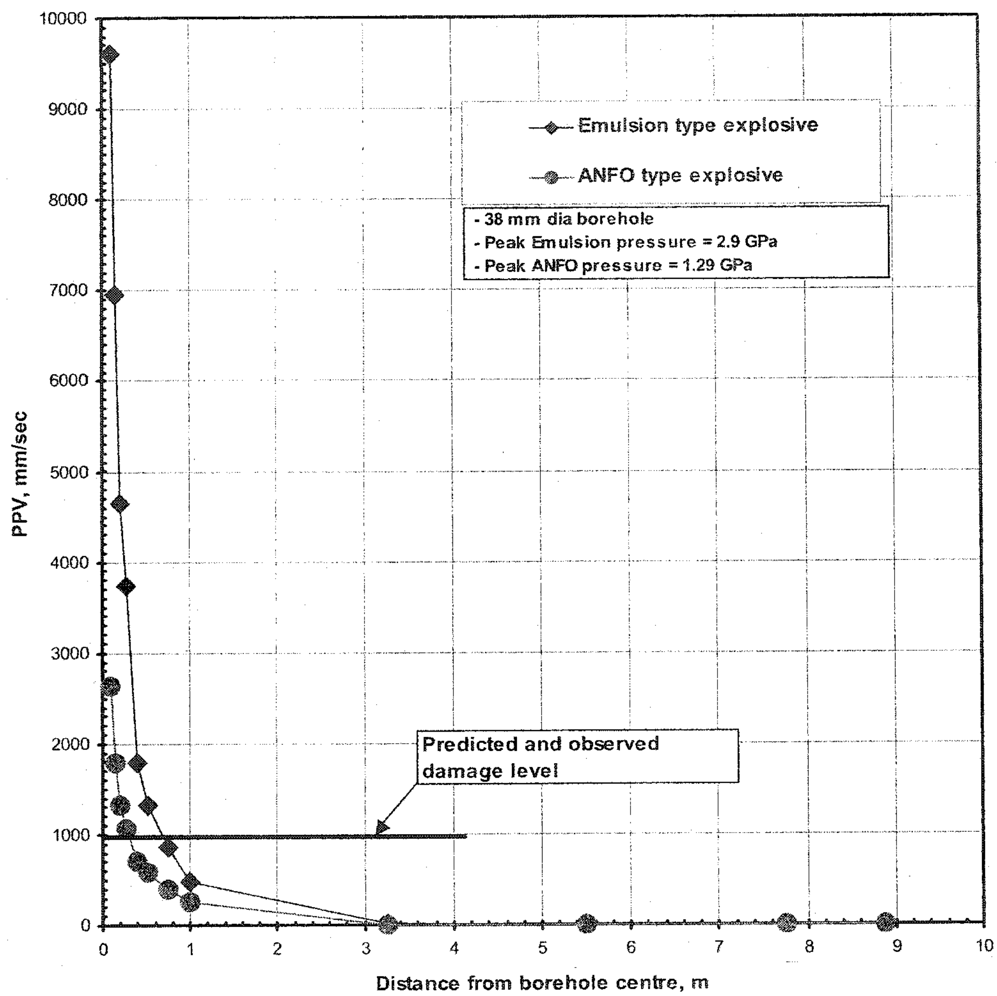

Figure 4.19 – PPV trend for two types of explosives characteristics

The results presented in Figures 4.13 to 4.19 bring out many important phenomena related with the dynamic rock fracturing process. Some significant results are discussed in the following sub-sections.

(a) **Strain rate dependant rock response**: It can be observed from Figure 4.13 that the stress required to open the first crack with a high shock load of the emulsion type explosive characteristics is equivalent to 600 MPa while only 159 MPa is required to open up the first crack in the case of the ANFO type explosive characteristics, having quasi-static loading characteristics.

Several researchers have argued in favour of strain rate dependant rock properties (e.g., Prasad et al., 2000). They advise that the material model used for dynamic numerical modelling should contain provisions for strain rate dependant material properties. It is noteworthy that neither the material behaviour, which remains essentially elastic throughout the calculations nor the brittle failure law using element elimination is rate dependant. The element elimination technique in conjunction with inertia, endows the material with characteristic or intrinsic time scale, an attribute that ultimately accounts for the ability to capture the rate effects accurately.

(b) **Characteristics of fracturing zone**: It has been well observed and documented that the emulsion type explosives lead to more crushing around the borehole which follows large numbers of short length radial cracks (e.g., McHugh and Keough, 1982). In contrast to this, the ANFO type explosives result in a smaller crushing zone followed by a few long radial cracks. Similar results are obtained by the numerical modelling as showed in Figures 4.14 to 4.16. The results shown in these figures demonstrate a good agreement with the published literature.

(c) **Extent of the fracturing zone**: Figure 4.16 presents the extent of such zones predicted by the numerical modelling procedure for the emulsion type and the ANFO type explosives, respectively.

Mosinets and Garbacheva (1972) and Kexin (1995) provide empirical relations to predict the extent of the crushing and fracturing zone. Calculations for these zones are summarized in Tables 4.7 and 4.8, calculated by using the material properties used in the analyses. Numerical results presented herewith are in remarkably good agreement with the empirical predictions. It is noteworthy to mention here that it is out of purview for other numerical tools or techniques, except continuous damage plasticity models capable of tracking failure both in compression and tension (not the continuous damage models based on statistical fractures mechanics), to distinctly reproduce this phenomenon in the first place and accurately simulate in the second place.

(d) **Energy utilisation in the fracturing**: Numerically, the kinetic energy (provided by the explosive energy) supplied in the case of the emulsion type explosive drops from the peak value of 14.994 to 14.00 kJ (Figure 4.17a), while it drops from 5.97 kJ to 5.80 kJ (Figure 4.17b) in the case of the ANFO type explosive. The consumption of kinetic energy amounts to 6.63 per cent in the case of the emulsion type explosive and 2.85 per cent in the case of the ANFO type explosive. The fracturing process is the only source of energy absorption in the numerical models (no artificial damping is used).

It has been reported that a very small amounts of explosive energy are utilised for the intended work of rock fracturing (see Chapter 3, Section 3.4 for the detailed discussion). Most of the energy is lost in terms of heating, crushing, ground vibrations and air-over pressure. It is also reported that emulsion type explosives are better suited for hard rock mines. Energy utilization for the case of emulsion type explosives are reported to be 2-20 per cent of the total energy while ANFO type explosives have a lower rate of energy utilisation. The energy consumption behaviour observed from the numerical modelling simulations is well under the reported values mentioned above. It is important to underline here that a field blasting operation is a thermo-mechanical reaction and in the current numerical formulations, only mechanical reactions are accounted for.

Further, Abaqus (2003) reports that the ratio of kinetic energy to internal energy (includes recoverable strain energy and energy consumed in plastic work) should not be more than 10 per cent. Also, artificial strain energy (a indicator for hourglassing effect) should be negligible to assure accuracy of the dynamic numerical modelling. These conditions are also well complied as can be seen from Figure 4.17.

(e) **Fracturing distance and PPV**: Typical single point PPV observations are plotted in Figure 4.18 for a point 0.5 m away from the borehole in the case of the emulsion type explosive and 0.25 m away for the ANFO type explosive. PPV plots from several distances away from the boreholes are also plotted for the simulation of the two types of explosives in Figure 4.19. These PPV plots are obtained from nodal velocity measurments at points of interest.

Prediction of fracturing based on PPV observations is a common practice in mining. Several predictor equations are based on this concept. Most notably, Homeberg and Persson (1979) predict that fractures are most likely to occur place at a place where the PPV is more than 1000 mm/sec after an explosion. The plots showed in Figure 4.18 are in good resemblance with the routine field PPV measurements where they show a reduction in magnitude with an increase in the distance from the source. This reduction comes from damping of the wave energy by the earth. It is noteworthy here that no artificial damping is used in the present procedure and yet the explosive energy rapidly damps out similarly to field observations.

PPV trends presented in Figure 4.19 not only predict similar trends as reported by Homeberg and Persson (1979) but also the failed zones are limited to a distance where PPV values are more than 1000 mm/sec.

Thus, it can be said that these results are in excellent agreement with the prevalent PPV based fracture zone estimations and that the developed numerical procedure presents a good tool for practical rock blasting research.

Apart from the above-mentioned empirical knowledge bases, the results presented in Figures 4.13 to 4.19 also fulfill prerequisites mentioned in Section 4.1 for a successful transformation of physical phenomena into a numerical platform as well as also validate several proposed model parameters, which are put forth during the development of the new procedure. The following points illustrate these validations.

(a) **Size of the model**: PPV plots presented in Figure 4.18 indicate that the fracture networks obtained are due to the primary shock waves only. The PPV plots do not indicate the secondary loading due to the reflected waves. Therefore, the choice of model domain size was appropriate for such analyses.

(b) **Damping of the wave energy**: PPV plots presented in Figure 4.18 as well as PPV trends obtained by Figure 4.19 illustrate that the material model chosen aptly represents the damping characteristics associated with the natural material. It is noteworthy that no artificial damping was considered in the newly developed procedure. Also, the material model showed enough potential to accurately represent two distinct fracture characteristics, crushing and cracking, with the single parameter of element elimination.

(c) **Duration of the analysis**: Energy plots presented in Figure 4.17 as well as a stable fracture networks illustrated in Figures 4.15 to 4.16 point out that the results obtained are stable in nature. These results also indicate that enough time was provided for fractures propagation. Therefore, the simulation time adopted in the analysis was appropriate to obtain stable fracture networks.

(d) **Model boundary conditions**: Roller boundaries were selected in the new procedure to represent unbounded rock medium. Stable fracture networks, energy plots and PPV plots presented through Figures 4.17 to 4.19 bring out that the results are nowhere affected by spurious waves reflection from the artificial boundaries. Hence, the selection of roller boundaries in the present modelling procedure is justified.

4.4 SUMMARY

An in-depth analysis of the prevalent numerical modelling practice related to rock blasting is made in this chapter. The analysis brings out the need for a procedure to simulate discrete fracture networks emanated due to blasting. Therefore, a new realistic rock fracturing simulation procedure is developed in this chapter. The development of the new procedure involved the selection of an appropriate numerical modelling tool, adoption of a proper numerical modelling technique and setting-up reasonable modelling parameters for the modelling procedure. The development of the procedure includes the selection of a general-purpose finite element analysis code. An element elimination technique (EET) is chosen to simulate generation, growth and propagation of fractures emanated after an explosion. Model set-up for the developed numerical procedure involved the selection of suitable numerical modelling parameters and procedures. The procedure uses tested and observed rock and explosive properties. It is noteworthy that the developed procedure doesn't need pre-specification of fractures growth sites and paths. The fractures grow in an stochastic nature as they do in reality. This is a major departure from the earlier reported numerical exercises where pre-specification of the fractures path was a must whenever it was employed. The results obtained by the new procedure are unique and the first of their kind. The procedure not only captures discrete fracture growths but also provide an easy way to distinctly observe crushing and cracking phenomena. The developed numerical procedure is evaluated against the empirical knowledge base. The developed procedure shows very good agreement with six different empirical knowledge bases. This proves robustness, validity and accuracy of the developed numerical procedure for rock fracturing by explosive energy. Results obtained with the new procedure also validate the accuracy of the selected and proposed model parameters.

Having developed and established the requisite numerical procedure, it can now be extended to look into fracture growths behaviour under high confinement environment where destress blasting is employed. The next chapter deals with this subject, which is the major objective of the thesis.

Chapter 5

ANALYSIS OF DESTRESS BLASTING THROUGH DYNAMIC MODELLING OF DISCRETE FRACTURES

5.1 OVERVIEW

The concept of destress blasting evolved from observations that limited induced fracturing around an excavation front reduces the load carrying capacity of the rock and hence relieves it from a build-up of high stresses up to perilous levels (Roux et al., 1957). Destress blasting is thought of as a means of maintaining and extending this fracturing. However, the success of a destress blasting program is not dependant alone on the amount of fracturing induced. It is more important to know how these fractures will develop in the rock mass under the influence of confinement. Fundamentally, it was challenged in Chapter 1 that the fracture growth caused by an explosion in rock under confinement will propagate in the direction that cannot destress rock. Observations from field experiments indicate that destress blasting is unable to generate new fracture sets (Adams and Jager, 1980). Practitioners of destress blasting in South Africa now believe that the main objective of destress blasting is to activate and propagate the existing fracture networks of rock rather than to create new ones (Toper et al., 1997). However, the argument was continued in Chapter 1 that if the new fracture sets have to grow in the unfavourable direction, with respect to the stress relaxation under high stress confinement, then the existing fracture networks will also follow the same path under the same environment and thus not amenable to the desired destressing. All these complexities make it essential to identify the behaviour of the fracture networks growth in the rock subjected to high levels of confinement. This requires a quantifiable study at the micro level investigating discrete fractures propagation.

A quantifiable database is needed to understand as well as to improve the field application of destress blasting. However, if the quantifiable data pertaining to the nature of fractures due to rock blasting is scarce (see Chapter 3 for a detailed review) then such data for the blasting of rock subjected to high stress confinement is rare. It is no wonder that a majority of the research is targeted to explore rock fragmentation phenomena in open-pit mining due to the bulk economic interests involved. The objective of this research is to provide, through analyses of a series of dynamic numerical modelling exercises, a systematic and quantitative basis for dynamic rock fracturing by destress blasting. The current research is the first initiative to build the necessary knowledge base in order to close the gap between the concepts and practices of destress blasting. Sufficient numbers of simulations are carried out to confer some degree of statistical meaning to the data acquired in order to meet the objectives.

The plane stress models as described in the earlier chapter along with the developed procedure for dynamic rock fracturing simulation are employed in order to accomplish the objectives of the research. The model set-up remains the same unless otherwise specifically mentioned. Initially, mining induced stresses are applied and solved with a static numerical procedure using the Abaqus/Standard. Results of these static analyses provide the confinement to the rock adopted in the simulation, which represented it at great depths (roughly equal to 2000 m below ground surface). These results are then imported to serve as the initial conditions of the models for the dynamic rock fractures modelling. The transient explosive load is then applied and solved with ABAQUS/Explicit as described earlier. The transient load in the form of the two different explosive characteristics, namely - the emulsion and the ANFO type explosive, is used for all of the simulations made. The transient load characteristics has already been described and established in Chapter 3.

The study presented in this chapter evaluates the extent of fracturing. This parameter is evaluated through a series of simulations covering many practical factors affecting the field application of destress blasting. The following is summary of simulations carried out in the study.

a Effect of confinement. For this purpose, isotropic bi-axial stresses (y-axis stress magnitude = x-axis stress magnitude; out of the plane stress is always zero for the plane stress conditions) are applied with different magnitudes to the domains.

b Effect of stress anisotropy. For this purpose, anisotropic bi-axial stresses (stress ratio, k = x-axis stress magnitude/y-axis stress magnitude) are varied and applied to the two different explosive characteristics.

c Effect of stress magnitude. For this purpose, the domain is subjected to two different confinement levels. Stress level magnitudes chosen are commensurate with the stress level encountered at a 2000 m depth in the Canadian Shield. One chosen confinement level is below the uniaxial compressive strength of the rock and the other is near to the bi-axial compressive strength.

d Effect of borehole spacing. For this purpose, blasts are simulated with a 1-millisecond delay in two boreholes placed at spacing commensurate with field practice.

e Effect of Young's modulus. The study is included for assessing effect of rock's stiffness on nature and extent of the fracturing under confinement.

f Effect of static tensile strength. The study is included for assessing effect of the rock's static tensile strength on extent and nature of fracturing under confinement.

g Effect of explosive energy characteristics. The study explores effect of shock versus quasi-static energy on nature of the fracture growths in rock under confinement.

h Effect of explosive energy magnitude. The study explores effect of the explosive energy level on nature of fracture growth in rock under confinement. Explosive energy levels is increased in simulations by increasing the borehole diameter. The chosen borehole diameters are industry standard and are in practice for the underground hard rock mines.

i Effect of de-coupling of explosive charge. The study examines effect of de-coupling in enhancement of the fracture length perpendicular to the far-field major principal stress direction.

j Directional fracture growth by notched borehole. The study examines effect of forced directional growth on the enhancement of the fracture length perpendicular to the far-field major principal stress direction.

5.2 "ℓ_{ci}" – A NEW FRACTURE ZONE CHARACTERIZATION PARAMETER

Introduction of ℓ_{ci} is a major shift from the very premise of fracturing by destress blasting, which seeks fracturing of the entire area ahead of an excavation face. The simulations presented herewith indicate that this is not possible. This representation has evolved from observations of the simulations made in this study, which invariably showed that the fractures align along the principal stresses. The fracture alignment along the principal stresses makes it necessary, in order to effectively study destressing phenomenon, to look into the directional extent of fractures rather than the amount of fracturing induced. Reported field evidences are also in line with the observations made in this study.

Two normalized fractures length parameters, ℓ_{c1} and ℓ_{c2}, are introduced in this study in order to assess the extent of the fractures zone. The ℓ_{c1} and ℓ_{c2} represent non-dimensional parameters obtained by the division of total fracture length along the major principal stress direction and the intermediate principal stress direction, respectively, by the borehole diameter. An increase in the ratio ℓ_{c2}/ℓ_{c1} characterizes longer fractures perpendicular to the major principal stress and thus effective destressing. The entire concept is explained in Figure 5.1. A comprehensive parametric study is presented in order to evaluate the fracturing extent with a range of parameters affecting field destress blasting applications.

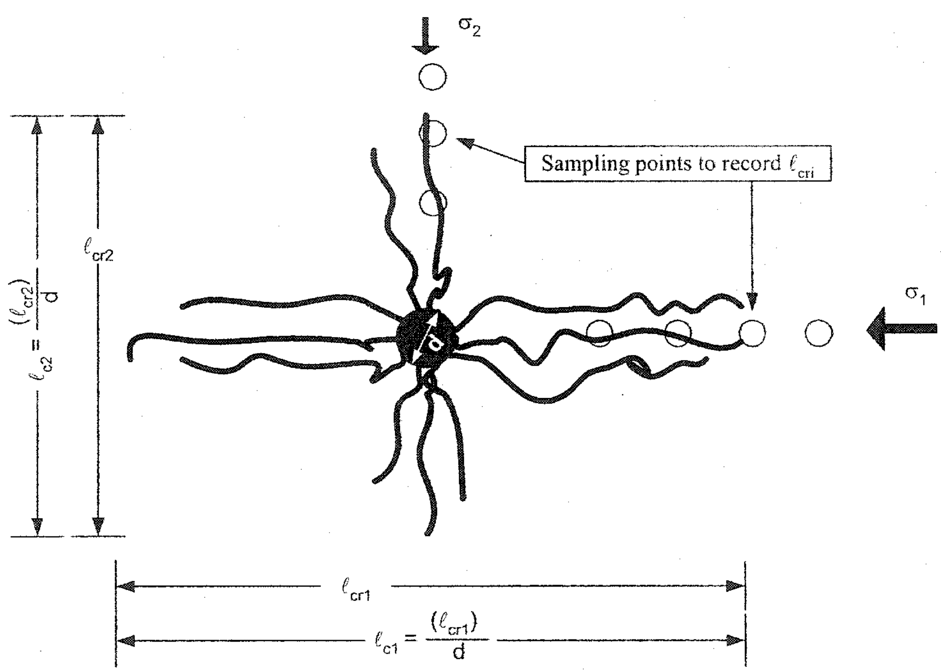

Legend: ℓ_{cr1} = Total fractures length along the major principal stress direction, mm

ℓ_{cr2} = Total fractures length along the intermediate principal stress direction, mm

ℓ_{c1} = Normalized fractures length along the major principal stress direction

ℓ_{c2} = Normalized fractures length along the intermediate principal stress direction

d = Borehole diameter, mm

Figure 5.1 – Measurement of normalized fractures length (Schematic)

5.3 EVALUATION OF THE EXTENT OF ROCK FRACTURING BY DESTRESS BLASTING

5.3.1 Effect of Confinement.

The plane stress models are used, as described in the previous chapter, for the study to investigate growth behaviour of the fracture network in the vicinity of an advancing mining excavation front where destress blasting is applied. Isotropic bi-axial in-plane geostatic stresses are applied to the models with varying magnitudes from 0 MPa to 300 MPa. The results of these analyses are plotted in Figure 5.2 in terms of normalized fracture length. Also, fracture pattern obtained from the analyses carried out is depicted in Figures 5.3 to 5.6.

Analysis of the results

Three studies are traced from the published literature indicating the effect of confinement on the extent of rock fracturing. Studies done by Daehnke et al. (1997), McHugh (1983) and Schatz et al. (1987a) indicate for a reduction in fracture lengths in the order of 2 to 3. This reduction is consistent with the increase of confinement. Schatz et al. (1987a) used two approaches in order to arrive at this conclusion. First, hydrostatic confinements up to 13.8 MPa using flatjacks were provided and second, a numerical modelling code was used based on the finite difference method with pre-placed fractures in the models. It is reported that the loads applied by flatjacks cannot be constant over the contact area so the results obtained do not represent hydrostatic pressure (Hughes and Pritchard, 1994). McHugh (1983) also used laboratory experiments on Plexiglas cylindrical model with 6.9 MPa hydrostatic pressure and one dimensional wave code using CDM (continuous damage modelling technique) in his numerical modelling. Daehnke et al. (1997) used closed form integral equations to study extension of the pre-placed fractures by gas pressure. In all of the numerical modelling simulations, fractures were pre-placed in the models (in terms of numbers as well as positions), which were extended with the progress of the analyses. Therefore, the results were influenced by the pre-placement of fractures. No modelling exercise took full account of the dynamic pressure pulse.

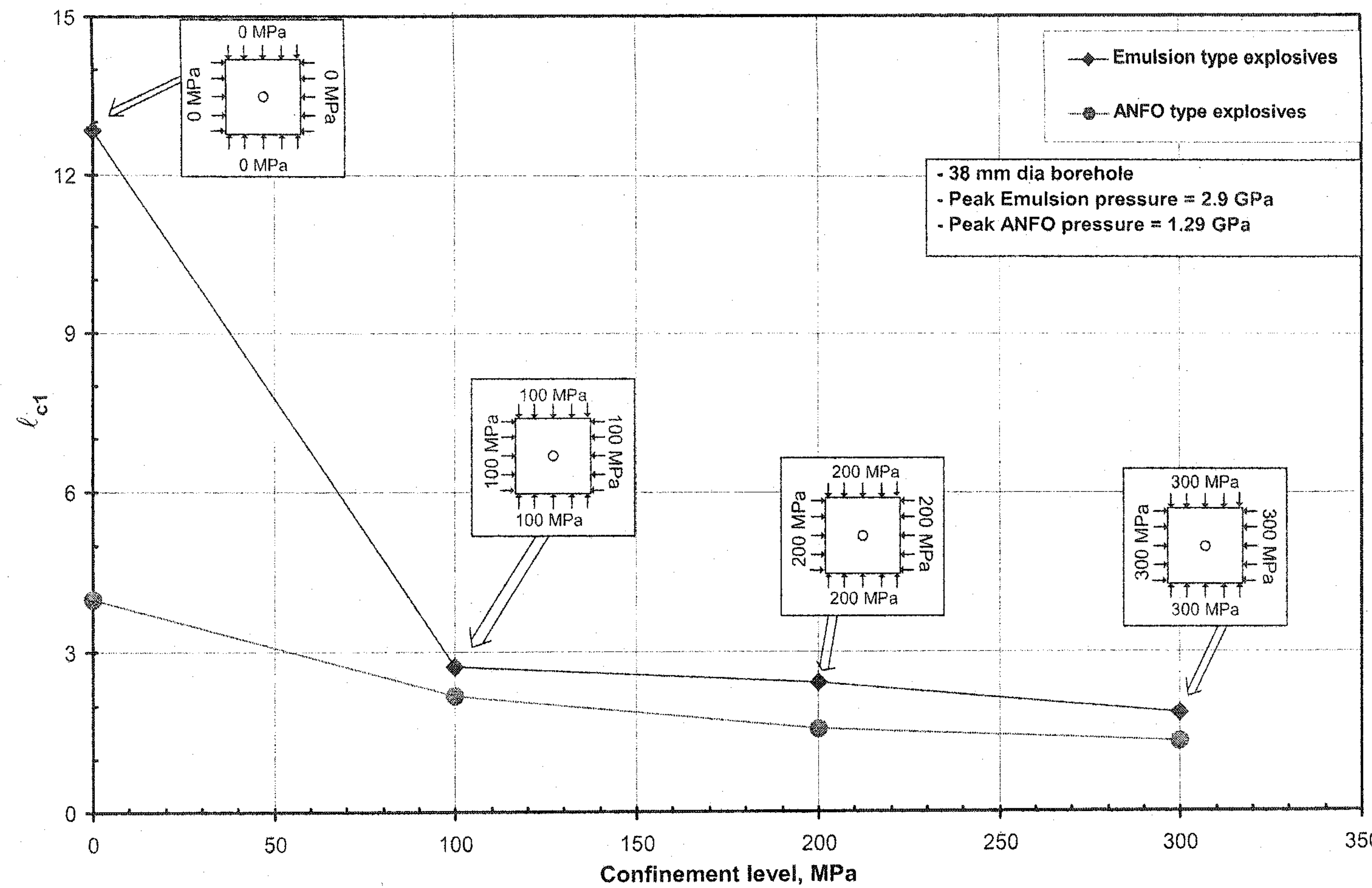

Figure 5.2 – Effect of confinement level on the extent of fractures

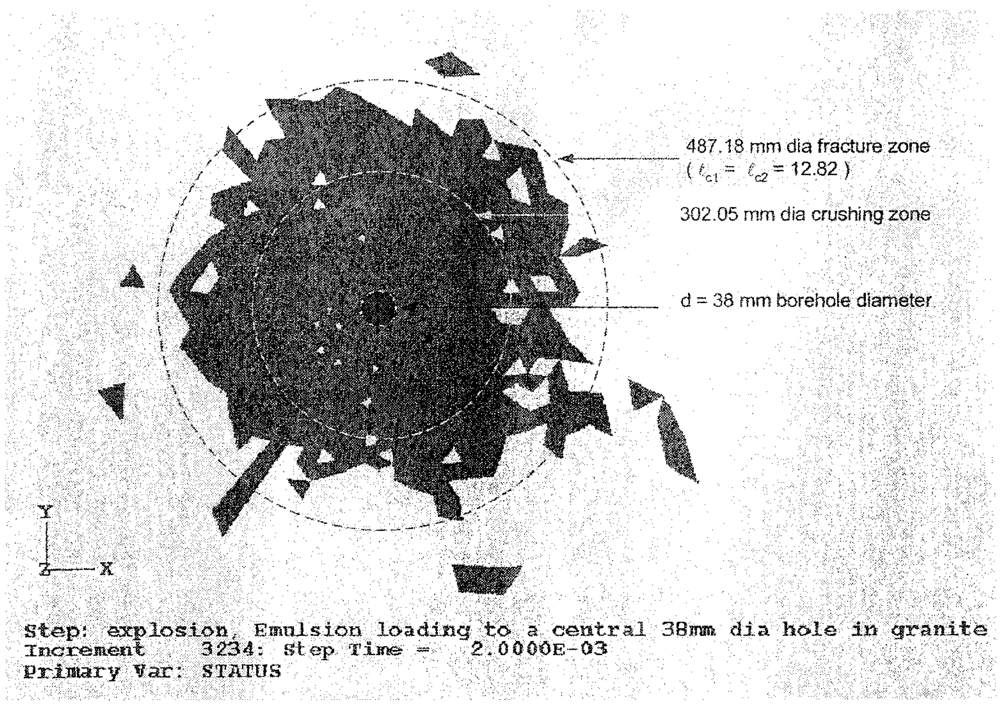

Figure 5.3 – Fracture pattern with no confinement for emulsion type explosive

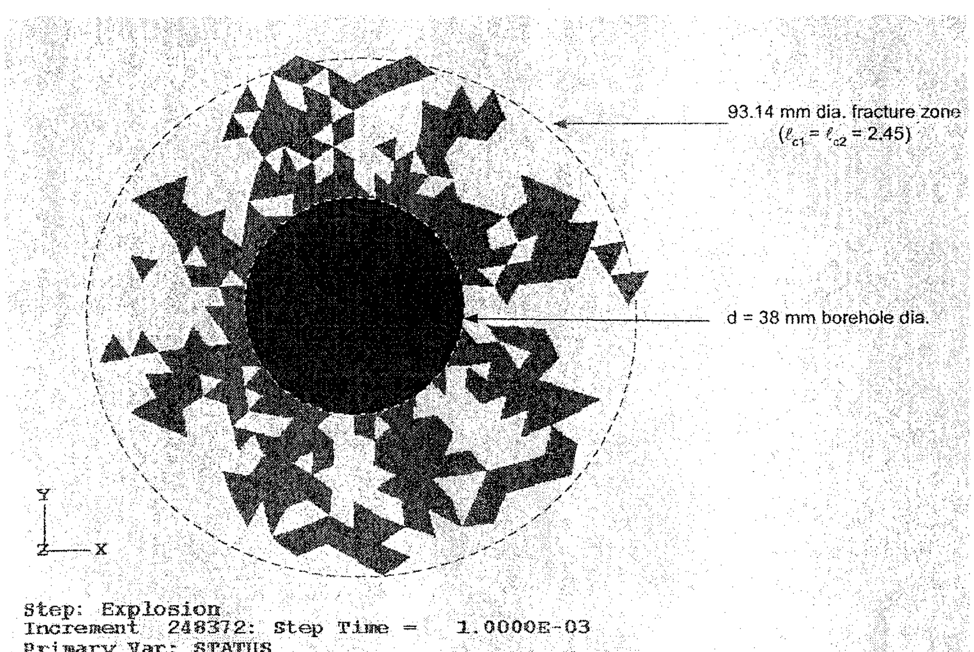

Figure 5.4 – Fracture pattern with the 200 MPa confinement for emulsion type explosive

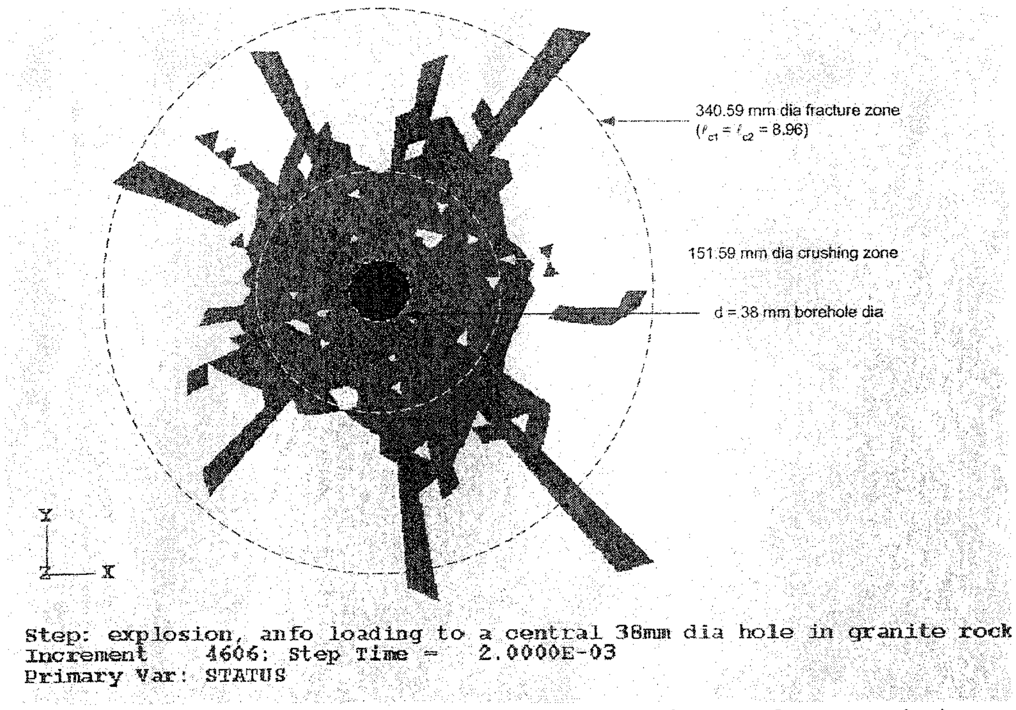

Figure 5.5 – Fracture pattern with no confinement for ANFO type explosive

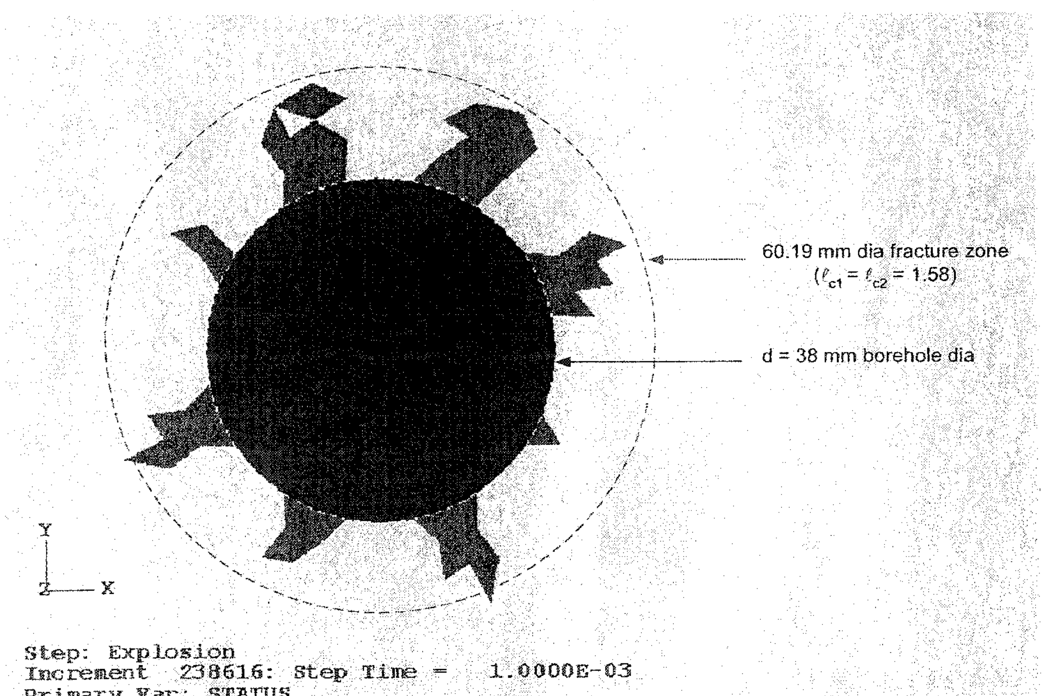

Figure 5.6 – Fracture pattern with 200 MPa confinement for ANFO type explosive

Schatz et al. (1987a) used soft rock-like materials (hydrostone, hydrocal, etc.) and the other two experiments (McHugh, 1983 and Deanhke et al., 1997) involved Plexiglas. Also, the techniques used in their numerical analyses did not have provisions for distinctly accounting for crushing and cracking phenomena associated with rock blasting.

The current research is a major shift from the earlier reported numerical modelling studies. The newly developed procedure does not require pre-specification of the fractures and it is also easy to distinctly accounts for crushing and cracking phenomena. Application of explosion pressure and evolution of fracture growth proceed explicitly in a dynamic fashion similar to the field blasting. Also, the selected confinement stresses are commensurate with the stress levels observed for deep hard rock mines. The material model in the current research also represents brittle rock behaviour.

The following conclusions can be drawn from the results presented in Figures 5.2 to 5.6.

(i) Confinement has a significant impact on the extent of the fracturing length. This impact is more pronounced in the case of shock loading provided by the emulsion type explosive. The reduction in the fracture lengths due to confinement observed in this case is about 3 compared to fracture lengths with no confinement. This observation concurs with the earlier observations in terms of the trends showing the reduction in the extent of fracturing. It is evident that more explosive energy will be needed to obtain longer fractures with an increase in confinement level. Higher energy requirements mean larger borehole diameters are a required for deep hard rock mines.

(ii) The crushing zone diminishes abruptly under the influence of increase in confinement as it can be observed from Figures 5.3 to 5.6. The fracture pattern is reduced to discrete fracture networks rather than an initial crushing zone followed by the cracking zone. Also, number of fractures generated is greater in the case of the emulsion type explosive than the ANFO type explosive.

5.3.2 Effect of Stress Anisotropy

The vertical stress confinement (σ_v) of 100 MPa is considered in the plane stress models of the current research. Stress anisotropy is applied with the application of stress ratio, k = 0.5, 1., 1.5 and 2.0. Thus the horizontal stress (σ_h) applied is equal to 50 MPa, 100 MPa, 150 MPa and 200 MPa. One additional set of simulation with a vertical stress of 50 MPa and a horizontal stress of 100 MPa are also considered in the current analyses in order to find out the effect on the fracture propagation direction from the stress reversal of similar levels (100 MPa vertical to 50 MPa horizontal and vice versa). Material model characteristics and explosive loading characteristics for the two types of explosive loading considered remain the same as described earlier. Dynamic model runs are made for both explosive types established earlier. Results of these simulations are presented in the form of a graph in Figure 5.7. A few typical plots from the output results are also presented in Figures 5.8 to 5.11 in order to illustrate the effect on fracture propagation direction from the stress reversal. The following information can be inferred from Figures 5.7 to 5.11.

Analysis of the results

Rock stresses in the earth's crust are always anisotropic. Commonly encountered stress ratios (stress ratio, $k = \sigma_h/\sigma_v$) range from 0.5 (for the South African mines working at 3000m depth) to 2.0 (for Canadian mines at depth of 500m). Only one study is reported that considered the k up to 4.0 (Schatz et al., 1987a). As reported in the preceding section, Schatz et al. (1987a) used a maximum of 13.8 MPa stress on the soft rock-like materials for their laboratory experiments and used a static finite difference code to model propagation of the pre-placed fractures. Three effects are noticed in their studies. First, the fractures aligned in two fractures sets, namely, fractures in the major principal stress direction (termed as the main fractures) and fractures perpendicular to the major principal stress direction

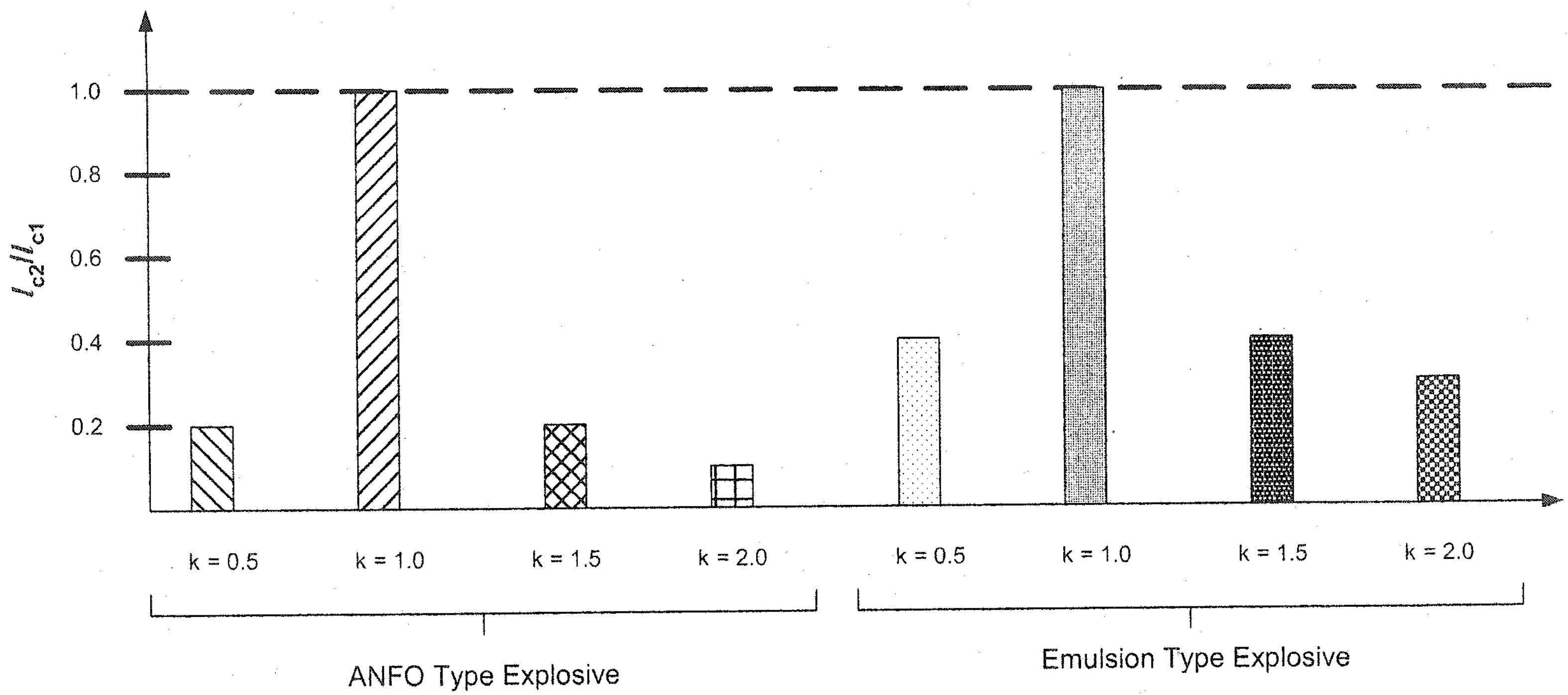

Figure 5.7 – Effect of stress anisotropy on the extent of fractures (for σ_v= 100 MPa)

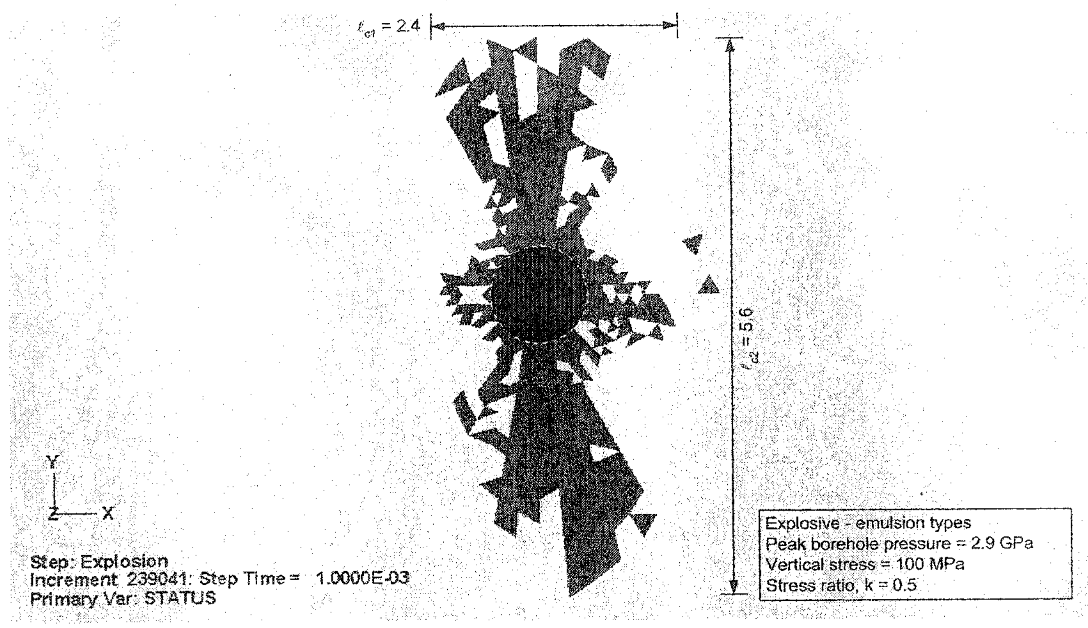

Figure 5.8 – Fracture pattern with emulsion type explosive (σ_v = 100 MPa; σ_h = 50 MPa)

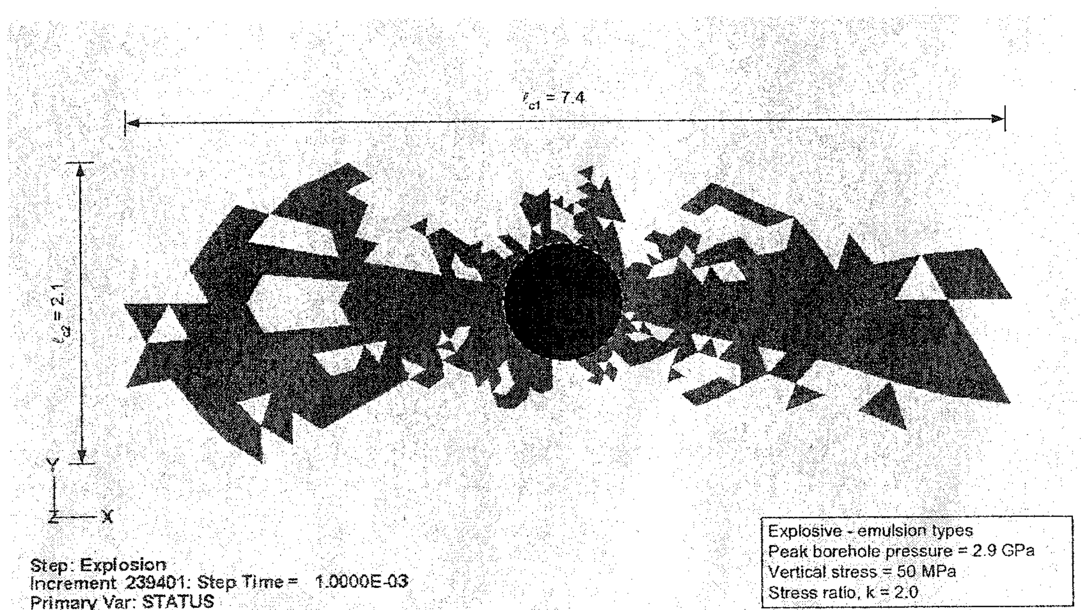

Figure 5.9 – Fracture pattern with emulsion type explosive (σ_v = 50 MPa; σ_h = 100 MPa)

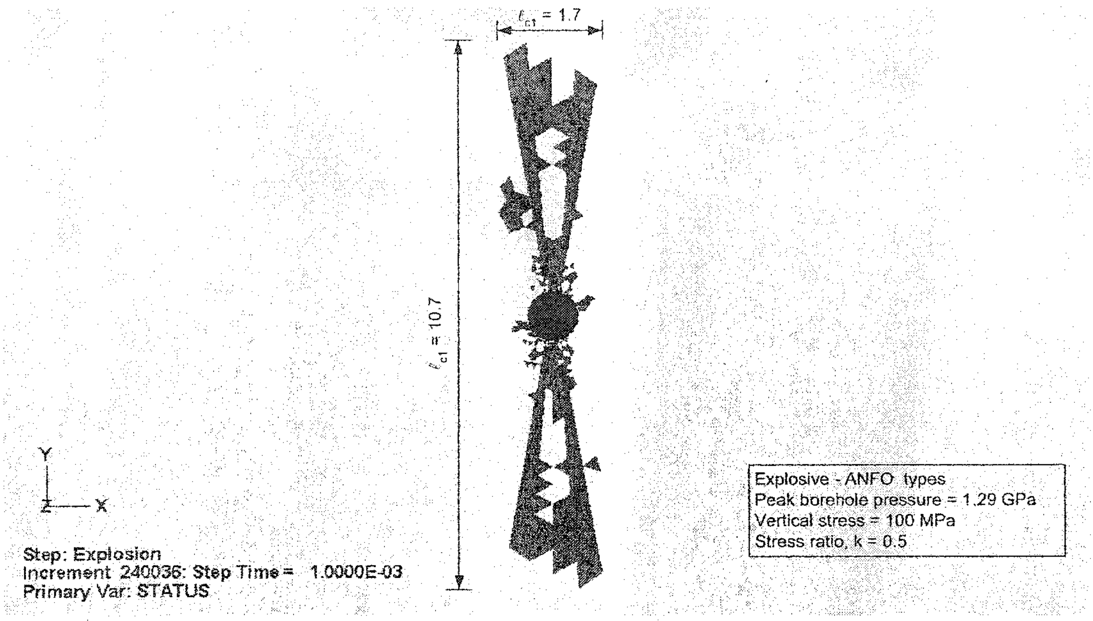

Figure 5.10 – Fracture pattern with ANFO type explosive (σ_v = 100 MPa; σ_h = 50 MPa)

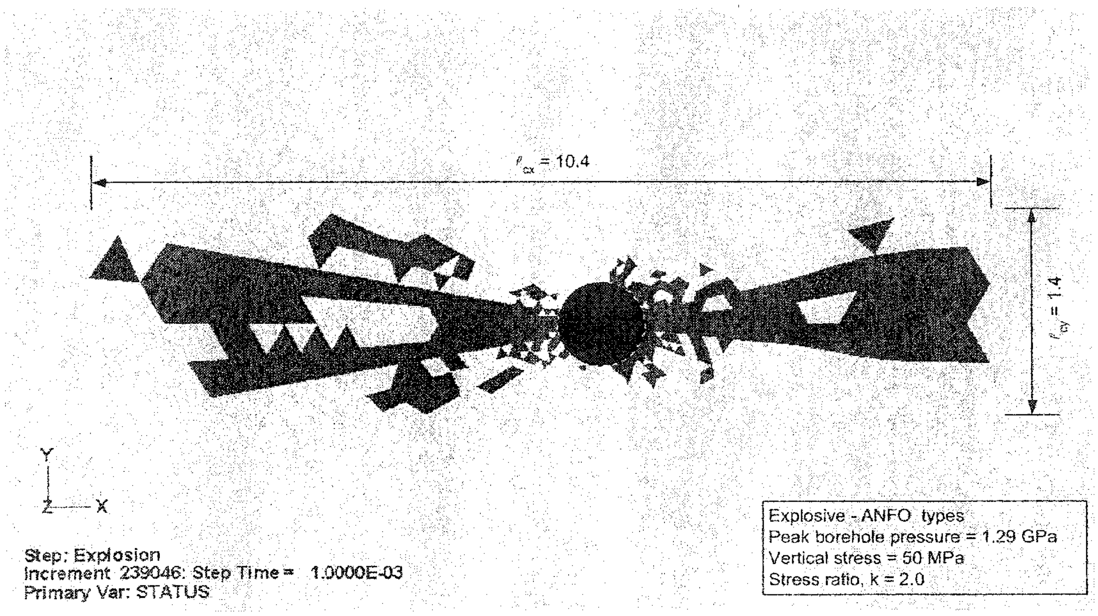

Figure 5.11 – Fracture pattern with ANFO type explosive (σ_v = 50 MPa; σ_h = 100 MPa)

(termed as cross-cutting fractures). Second, the length of the main fractures was reported to be twice the cross-cutting fractures. Third, it was more difficult to get the cross-cutting fractures with quasi-static loading than with shock loading. Based on the numerical modelling results, Schatz et al. (1987a) also reported that cross-cutting fracture lengths of 50 times the borehole diameter can be achieved with the quasi-static loading. However, their own laboratory experiments didn't confirm their numerical results.

Following conclusions can be drawn from the results presented in Figures 5.7 to 5.11.

(i) Figure 5.7 indicates that the ratio of ℓ_{c2}/ℓ_{c1} decreases from 2.3 to 0.3 in the case of the emulsion type explosive while the reduction is from 6.3 to 0.1 in the case of the ANFO type explosive. This trend explains two difficulties associated with the application of destress blasting. First, the longer fractures are aligned with the major principal stress direction. This alignment is irrespective of the applied direction of the major principal stress as can be learnt from Figures 5.8 to 5.11. It was apprehended in Chapter 1 that this alignment is not amenable to destressing. Second, the fracturing extent is reduced with the increase in confinement level as reported also in the previous section. This indicates more difficulty in extending the fracture lengths at greater depths from the surface.

(ii) The fractures are aligned with the applied two principal stresses. The length of fractures along the major principal stress direction is much longer than the other direction. This concurs with observations made by Schatz et al. (1987a). Also, as pointed out just above, the tendency of longer fractures to develop along the major principal stress direction is not propitious to stress relaxation.

5.3.3 Effect of Stress Level

It is a well-known fact that a high stress level is one of the causes fof rockbursts (kindly refer to Chapter 1 and 2 for references). It is also known that rocks have higher strength under confinement (e.g., Weibuls and Cook, 1968; Mogi, 1972; Haimson and Chang, 2000). Therefore, simulations are planned for investigating the fracturing extent withhigh stress environment typical for a mine at a 2000 m depth in the Canadian Shield. Tang and Mitri (2001) made a detailed analysis of representative destress blasting patterns used during drift developments in deep hard rock mines. It has been reported in their analyses that the drift excavation face could have the major principal stress values from 120 MPa to 240 MPa. The drift development case analyzed was at a 2150 m depth from the surface and the material model represents a stiff high strength rock. The present study considers rock properties described in the previous chapter and a value of k = 1.65 which is the observed value for the Canadian Shield at the above mentioned depth (Arjang and Herget, 1997). The major principal stress is in the horizontal direction for deep Canadian mines and in the following simulations this is considered perpendicular to the excavation front in order to assess the worst-case scenario. The horizontal stress value of 150 MPa (which is in the range reported by Tang and Mitri, 2001 and below the uniaxial strength of the rock) and 300 MPa (which is near the bi-axial strength value as reported by Haimson and Chang, 2000) is considered for the simulations. The simulations are conducted for both types of the explosive characteristics established earlier.

The results obtained from the different numerical simulations are shown in Figures 5.12 to 5.15.

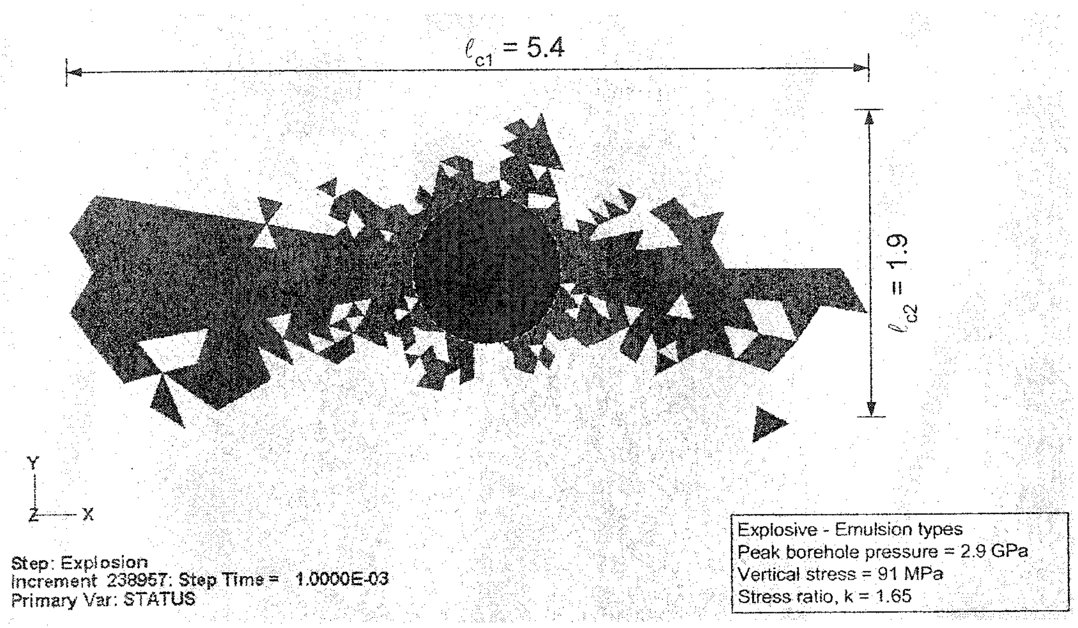

Figure 5.12 – Fracture pattern with σ_h = 150 MPa for the emulsion type explosive

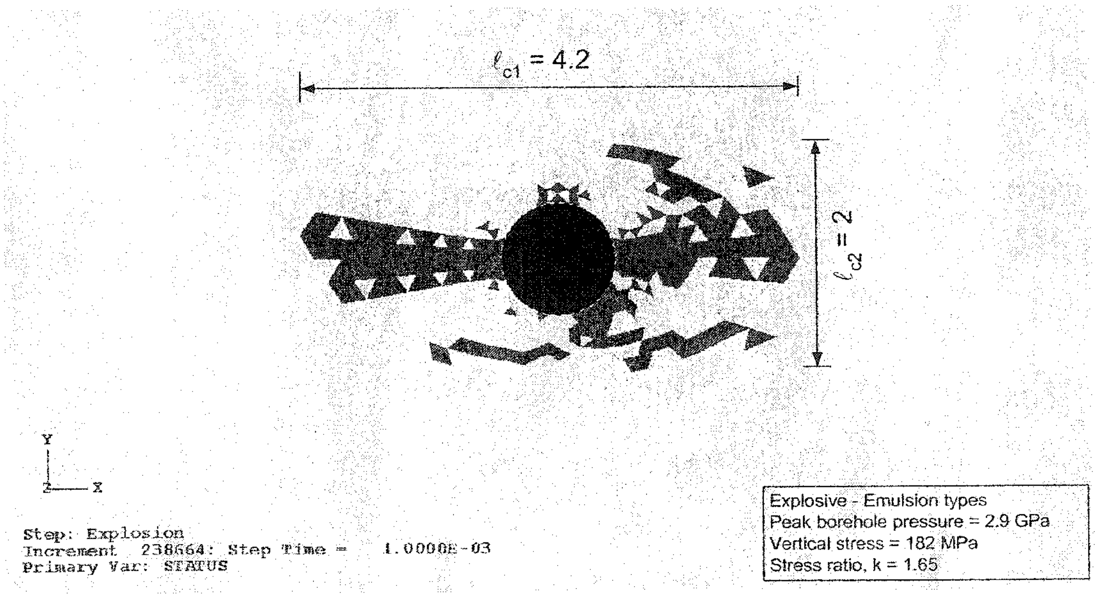

Figure 5.13 – Fracture pattern with σ_h = 300 MPa for the emulsion type explosive

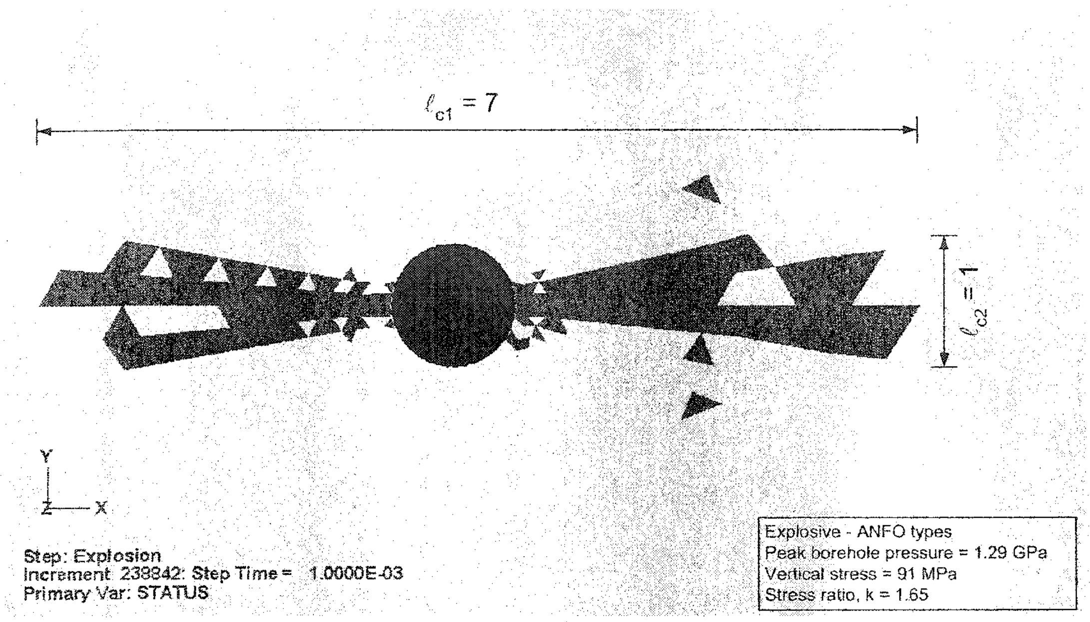

Figure 5.14 – Fracture pattern with σ_h = 150 MPa for the ANFO type explosive

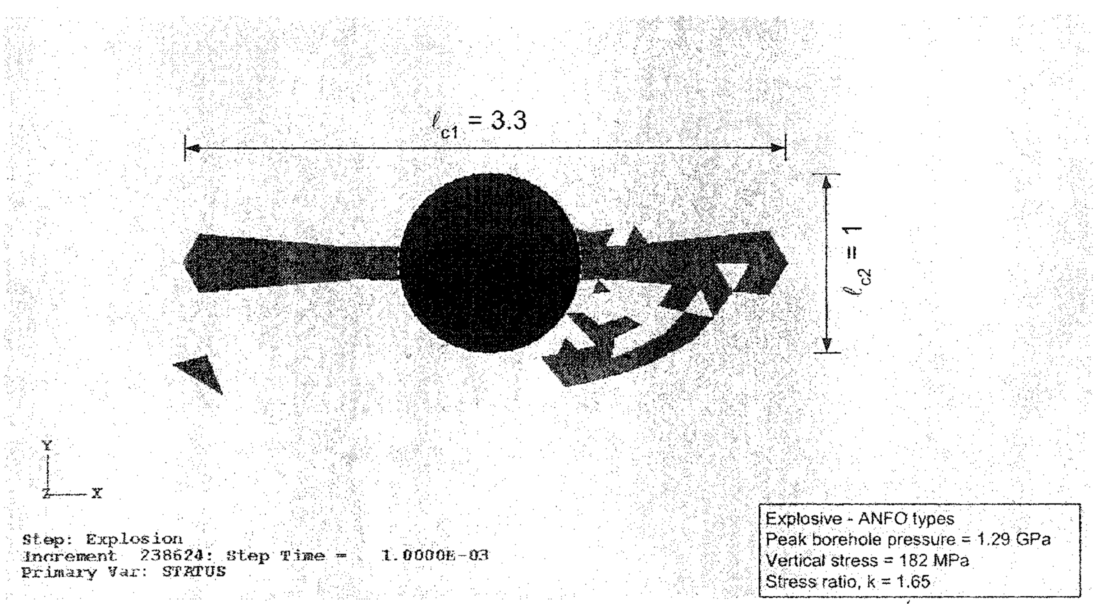

Figure 5.15 – Fracture pattern with σ_h = 300 MPa for the ANFO type explosive

Analysis of the results

The following observations are made in light of the analyses carried out.

(i) Primarily, the fractures are aligned with the major principal stress direction irrespective of the explosive types. This alignment is similar to the previously obtained observations and as reported earlier that it is in the undesired direction with respect to stress relaxation.

(ii) The fracture length decreases under the influence of an increase in the stress level. As can be seen from Figures 5.12 to 5.15, normalized fracture lengths towards the major principal stress are reduced from 5.4 to 1.9 in the case of the emulsion type explosive while the reduction is from 7 to 1 in the case of the ANFO type explosive. Reduction is more prominent for the ANFO type explosive. This behaviour predicts a poor destress blasting practice where it is needed the most. Longer fractures are desired under higher confinement for better effectiveness but such an increase in confinement inhibits fracture growth.

5.3.4 Effect of Borehole Spacing

Based on ground penetrating radar (GPR) studies, CSIR Miningtek, South Africa proposed a borehole spacing of 1.5 m for destress blasting with 38 mm diameter boreholes (Toper et al., 1997). This same reference indicates a borehole spacing of 3.0m based on the studies by Giltner (1992). Borehole spacing of 1.5m is a standard practice for deep South African hard rock mines. The most recent Canadian experiment for destress blasting considered a 2.6 m borehole spacing for 165 mm diameter boreholes (Andrieux et al., 2003). Mitri (2000) and Tang and Mitri (2001) present field case studies where boreholes are being placed at 0.75m spacing for drifts development. Further, it is possible that few boreholes align with the major principal stress direction and a few others with the intermediate principal stress direction with the same borehole spacing during field application of destress blasting. Therefore, simulations are planned with two-borehole (each 38 mm diameter) blast simulations, placed at 0.75 m spacing, to identify the effectiveness of the borehole spacing on the fracturing extent. Also, the two-borehole scheme considered in the study has two spatial arrangements. In one set of simulations, the boreholes are aligned with the major principal stress and the other set has boreholes aligned with the intermediate principal stress. The major principal stress is considered in the horizontal direction as found in the Canadian Shield and considered perpendicular to the excavation front in order to consider the worst case scenario. Also, a 300 MPa magnitude is chosen for the major principal stress as success of destress blasting is more critical for a higher stress level. The boreholes are simulated with a 1 millisecond delay detonation. A schematic of the simulation set-up is shown in Figure 5.16. The results of the analysis are presented in Figures 5.17 to 5.20.

Analysis of the results

The following observations are made from the analyses.

(i) Figures 5.17 through 5.20 indicate that there is little extension in the fracture lengths only for the case when the holes are aligned with the major principal stress direction and charged with the emulsion type explosive. This extension is ineffective to meet fractures in between the holes and is also in the undesired direction as pointed out earlier.

(ii) It is evident from the results presented in Figures 5.17 to 5.20 that the fracture network is largely uninfluenced by the neighbouring borehole detonation when placed at 0.75 m spacing irrespective of their alignments with respect to the principal stresses. Since their behaviour is similar to the isolated borehole detonation presented in the preceding sub-section, it can be concluded that it is difficult to achieve destressing with the prevalent destress blasting practice.

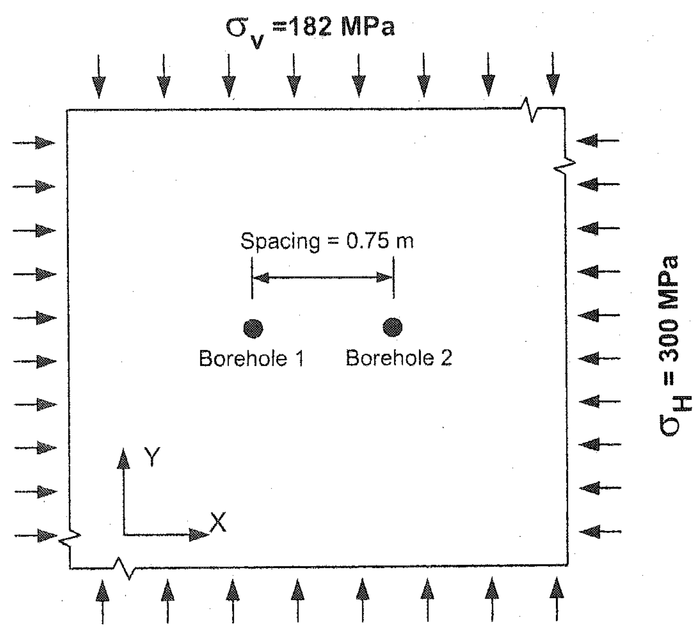

(a) Boreholes aligned horizontally

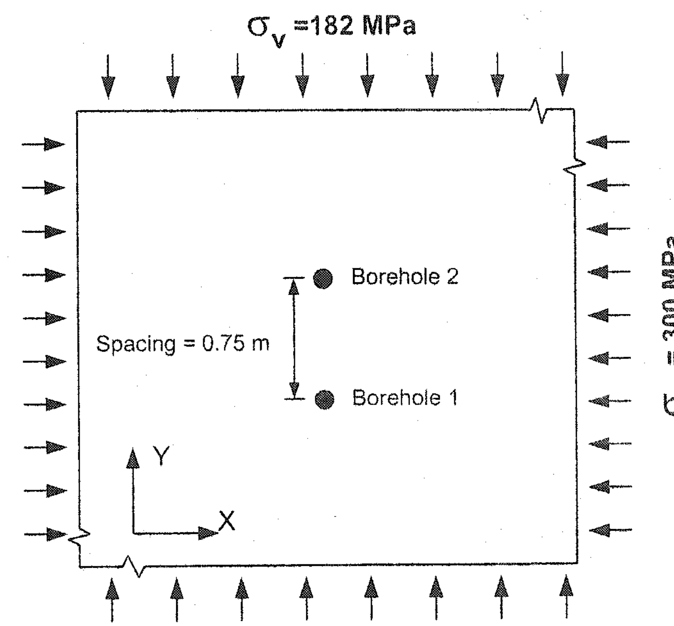

(b) Boreholes aligned vertically

Figure 5.16 – Schematic arrangement for the two-borehole models studies

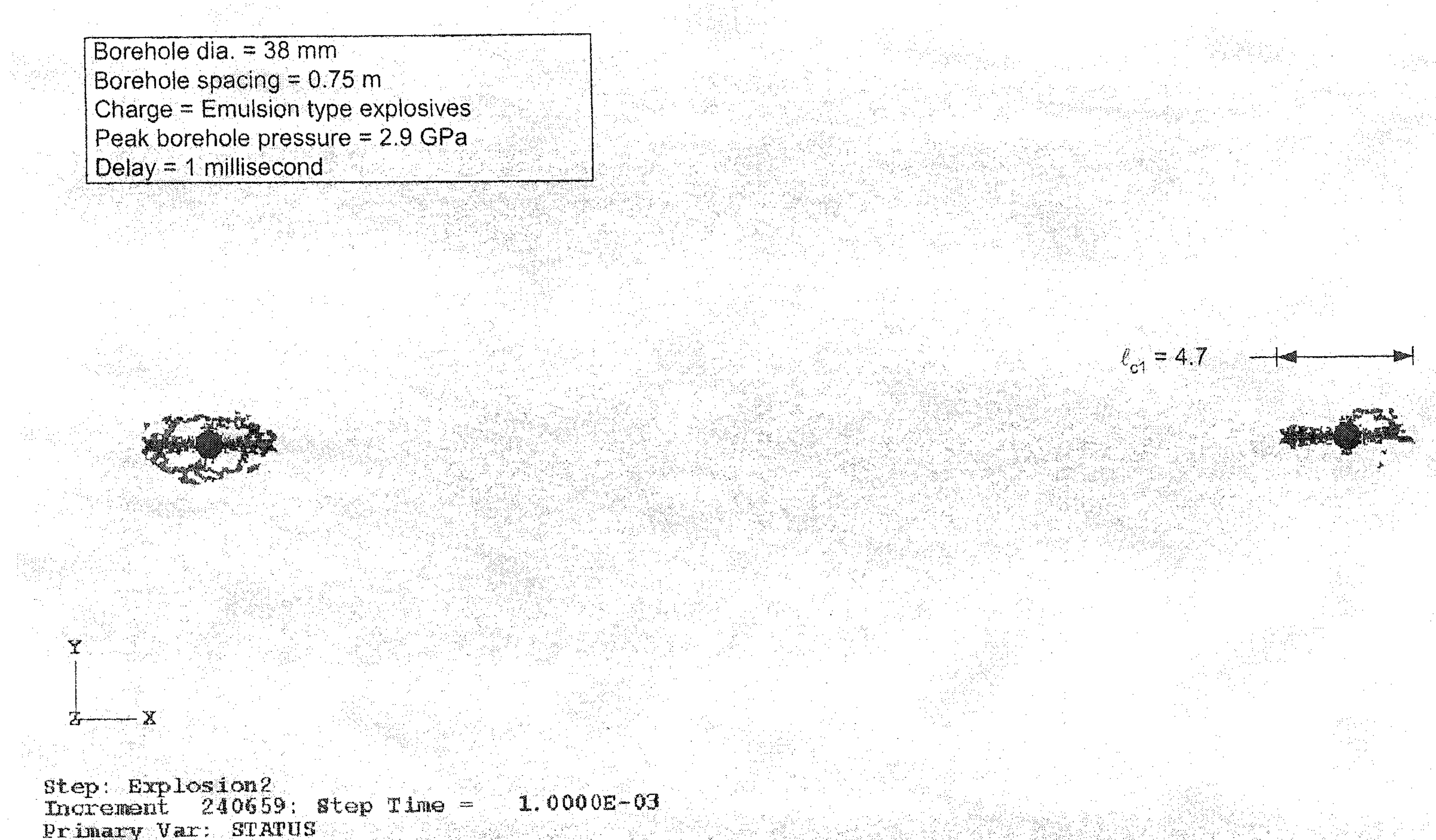

Figure 5.17 – Fracture pattern from the two-borehole model aligned with the major principal stress direction for emulsion type explosive

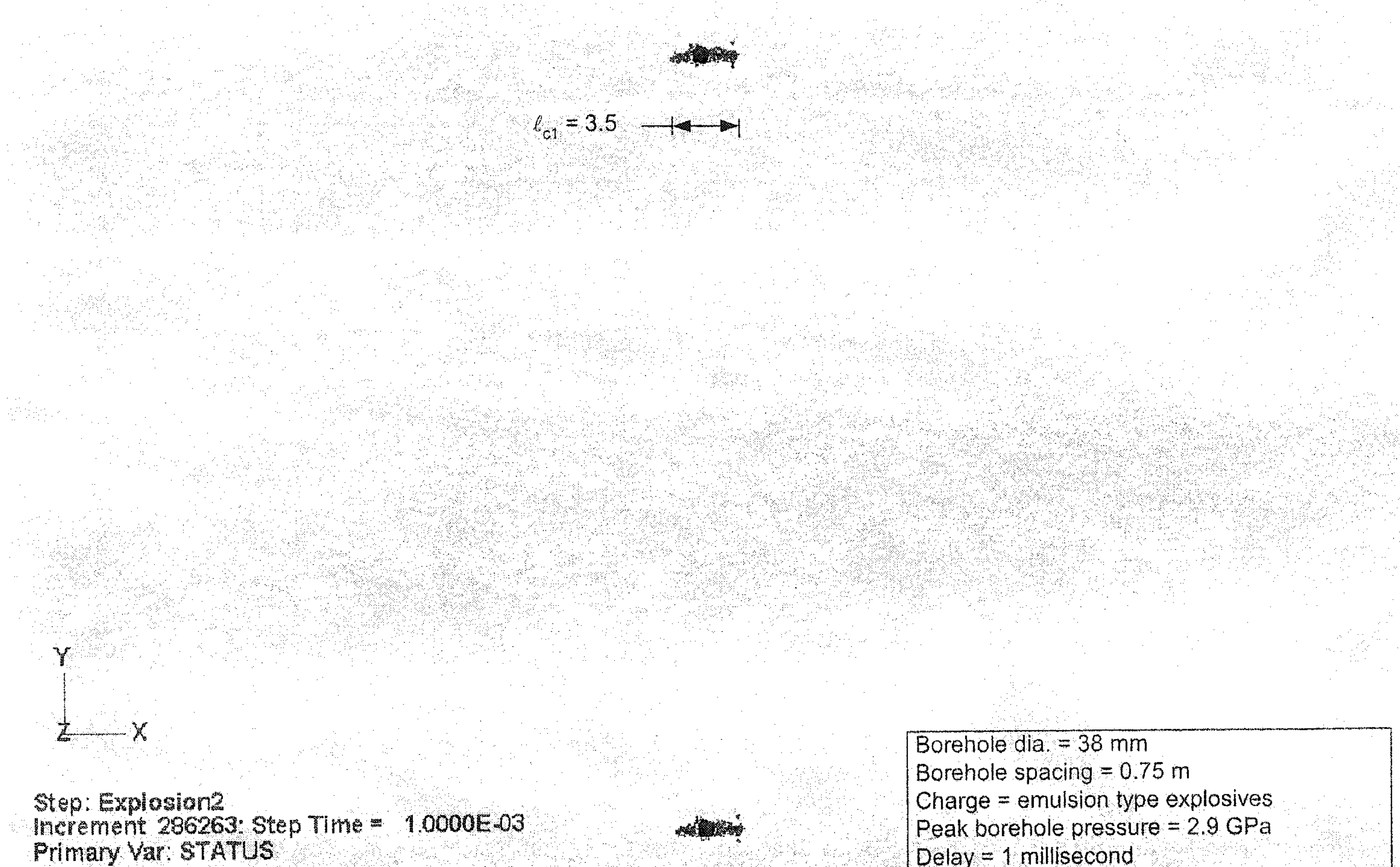

Figure 5.18 – Fracture pattern from two-borehole model aligned with the intermediate principal stress direction for emulsion type explosive

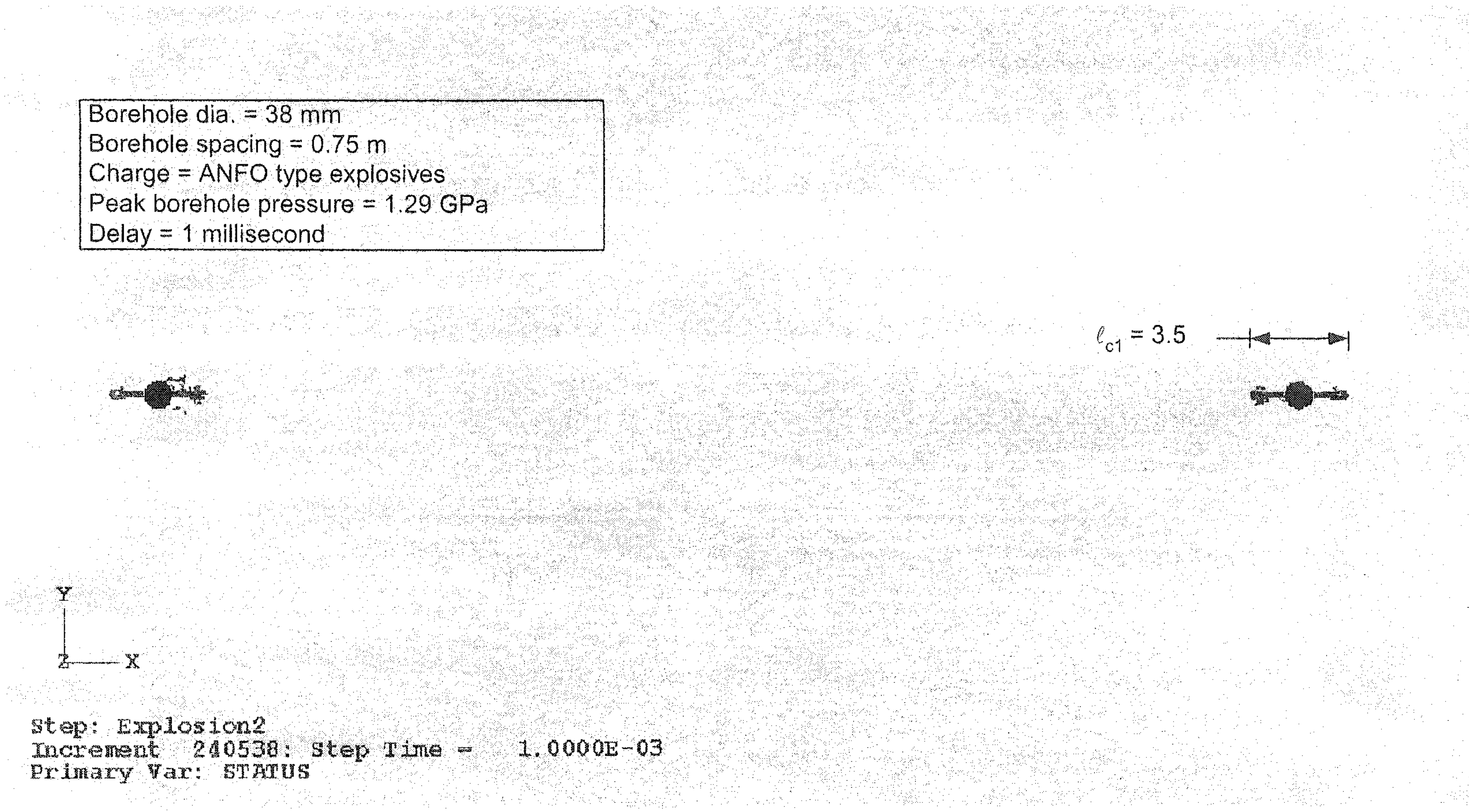

Figure 5.19 – Fracture pattern from two-borehole model aligned with the major principal stress direction for ANFO type explosive

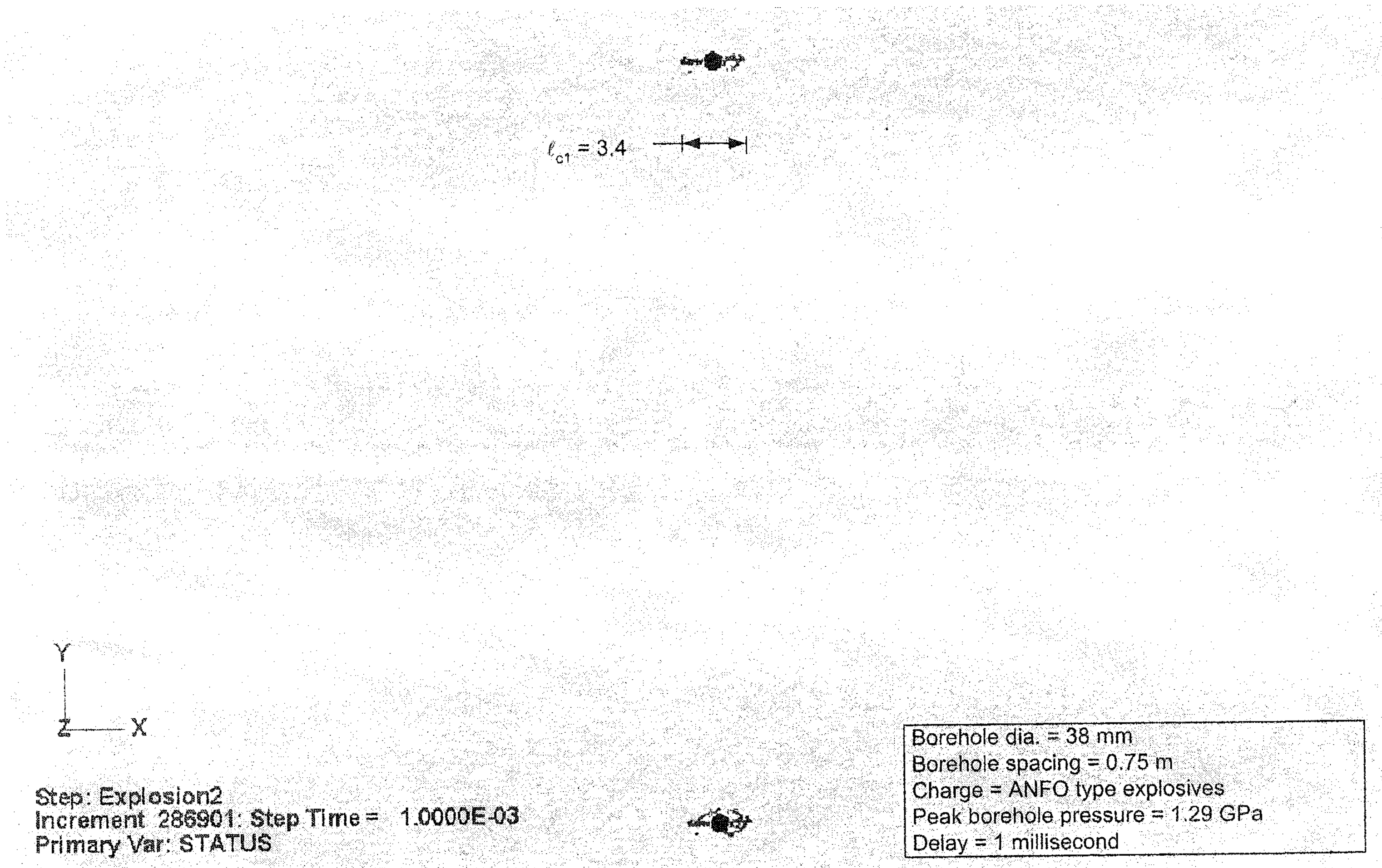

Figure 5.20 – Fracture pattern from two-borehole model aligned with the intermediate principal stress direction for ANFO type explosive

5.3.5 Effect of Young's Modulus

Young's modulus of elasticity of rock is of an engineering importance to rock mechanics studies but has measurement limitations for rockmass. Several empirical relations are proposed and are in use to overcome the limitations (e.g., see for compilation - Singh and Goel, 1999). Studies conducted by Mohammad et al. (1997) and Reddish et al. (2003) indicate that the equation proposed by Mitri et al. (1994) is superior to the others. The effect of rock mass stiffness is explored in the current research in order to identify fracture growth behaviour under different rock mass stiffness values. The Young's modulus is changed from 30 GPa to 60 GPa in increment of 10 GPa. The rock confinement is similar in magnitude and direction as described in the preceding sub-section. Analyses are conducted for both the explosive types established earlier. The results of the analyses are presented in Figures 5.21 through 5.28.

Analysis of the results

Engineering intuition indicates that the fracture length should increase with a decrease in the rock's stiffness (Young's modulus). Only one study by Schatz et al. (1987a) is traced which found negligible effects on fracture length with variations in the rock's modulus of elasticity.

The following observations are made from the results.

(i) There is a negligible difference in terms of fracture length with the reduction in the modulus values as can be seen in Figures 5.21 through 5.28 irrespective of the explosives characteristics. This concurs with the laboratory experiment observations by Schatz et al. (1987a).

(ii) Shock wave loading of emulsion type explosives shows a tendency of fracturing enhancement towards the intermediate principal stress direction. It appears that the reduction in the modulus in conjunction with shock loading leads towards squeezing rock mass behaviour where the stress anisotropy has negligible role. However, such behaviour cannot be corroborated in the absence of any previous study on this subject.

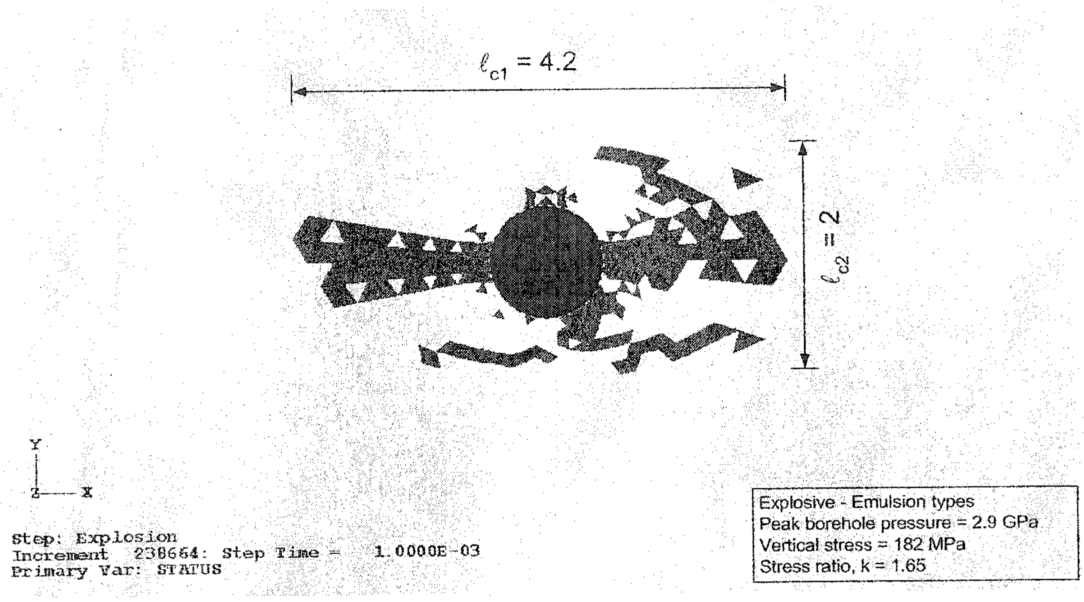

Figure 5.21 – Fracture pattern with Young's modulus = 60 GPa for emulsion type explosive

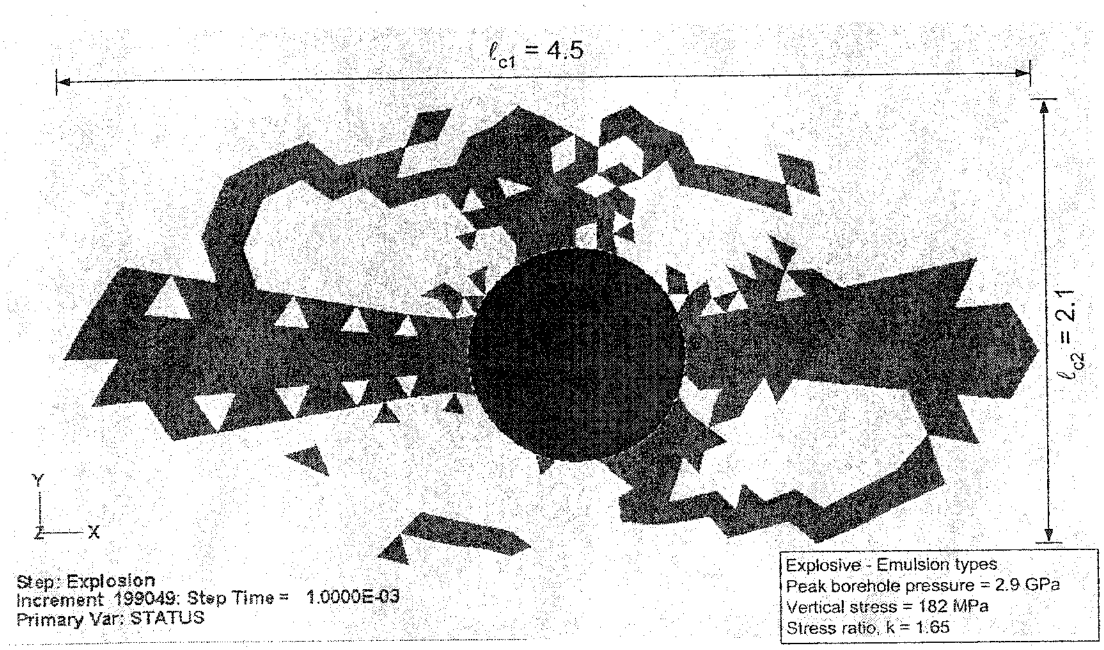

Figure 5.22 – Fracture pattern with Young's modulus = 50 GPa for emulsion type explosive

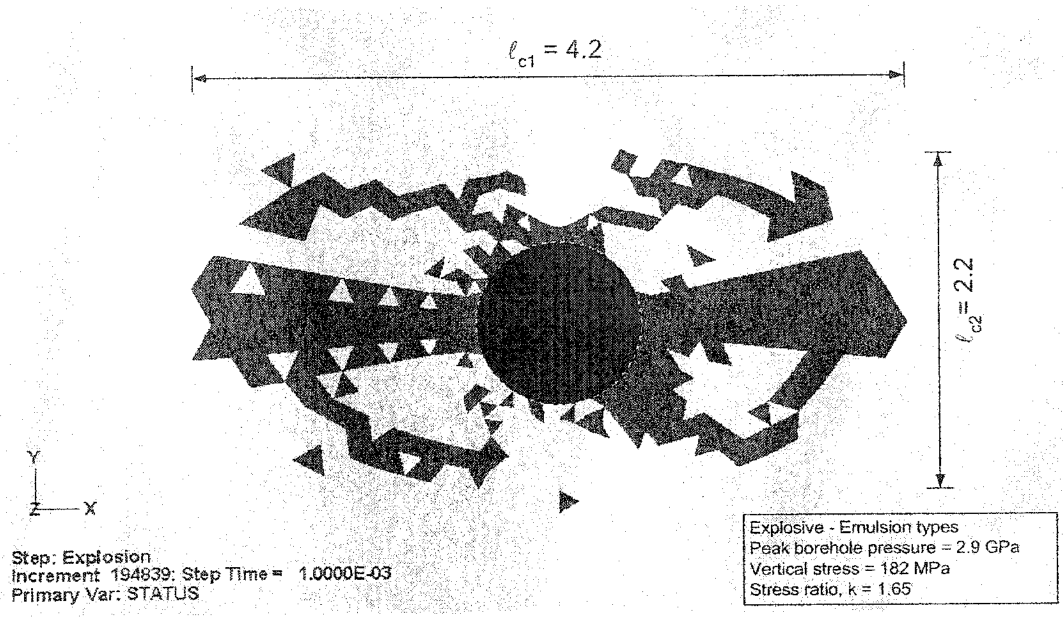

Figure 5.23 – Fracture pattern with Young's modulus = 40 GPa for emulsion type explosive

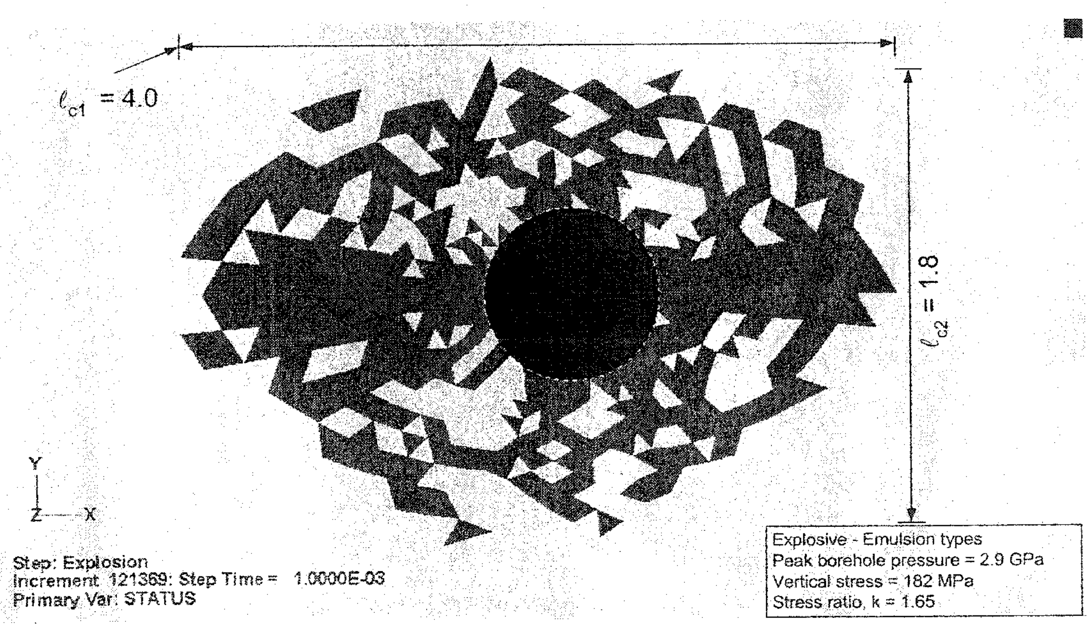

Figure 5.24 – Fracture pattern with Young's modulus = 30 GPa for emulsion type explosive

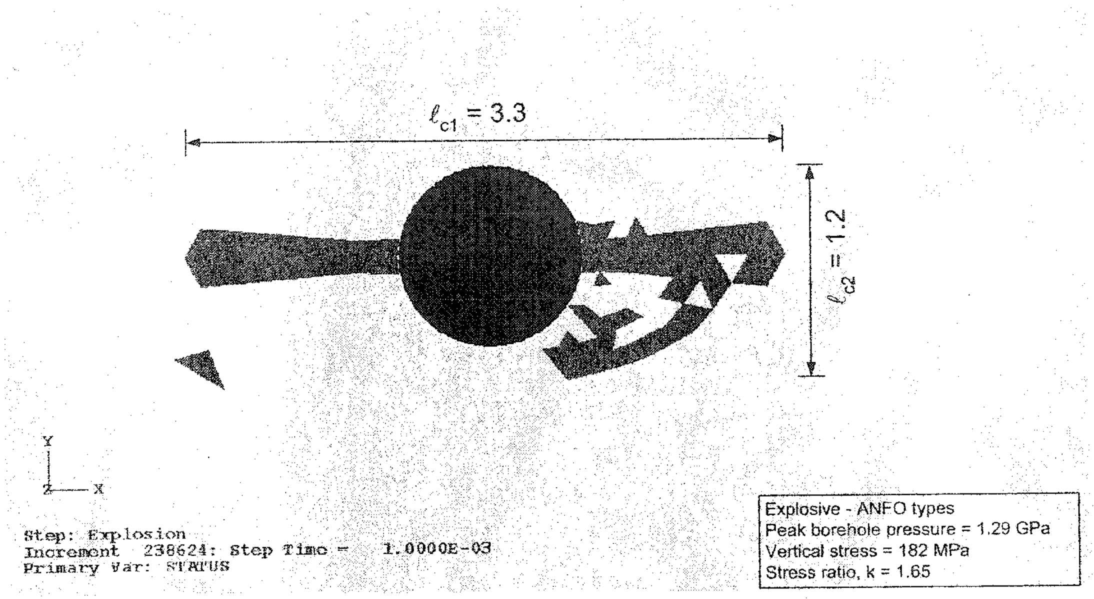

Figure 5.25 – Fracture pattern with Young's modulus = 60 GPa for ANFO type explosive

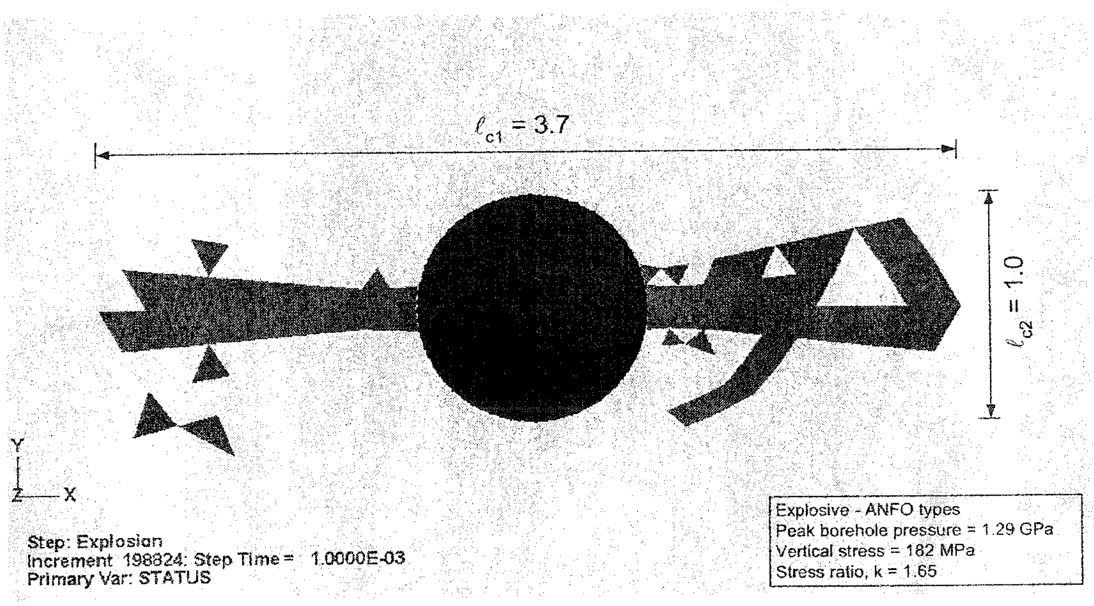

Figure 5.26 – Fracture pattern with Young's modulus = 50 GPa for ANFO type explosive

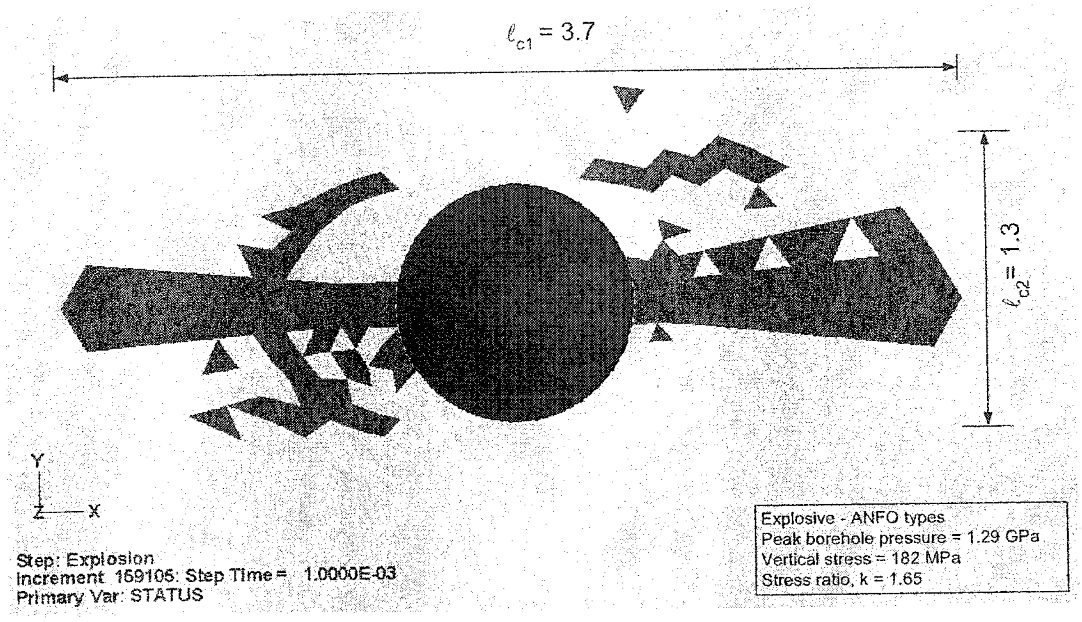

Figure 5.27 – Fracture pattern with Young's modulus = 40 GPa for ANFO type explosive

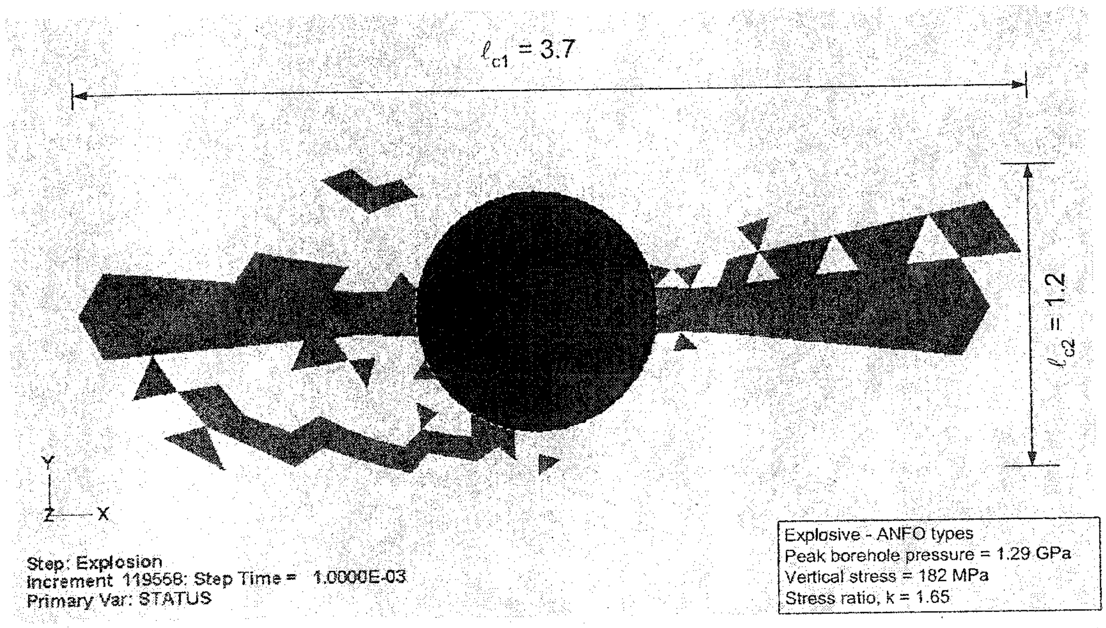

Figure 5.28 – Fracture pattern with Young's modulus = 30 GPa for ANFO type explosive

5.3.6 Effect of Static Tensile Strength

Tensile strength is the other parameter that controls rock fracturing. Several analyses are carried out to determine rock fracturing behaviour under a variation of static tensile strength values. The tensile strength values are changed from 5 MPa to 15 MPa in increments of 5 MPa. The analyses are done for both the explosive types established earlier. The stress confinement provided is also similar in magnitude and direction as described in the preceding sub-section. Other model parameters remain the same as earlier. The results obtained with the tensile strength variation are presented in Figures 5.29 to 5.32 for both the explosive types.

Analysis of the Results

It is evident from the comparison of Figure 5.29 with Figure 5.30, and Figure 5.31 with Figure 5.32, that the change in the static tensile strength value has an insignificant impact on fracture growth behaviour. This observation concurs with the laboratory experiments by Schatz et al (1987a). This typical behaviour can be explained by the rate dependant behaviour of the rock model as observed in Chapter 4 (section 4.3). Rock materials exhibit rate dependant properties and cracking initiates at a much higher stress level than the static tensile strength. The explosive loses almost all of its energy by the time the load level reaches the rock's static tensile strength value. No change in the fracture pattern with changes in the static tensile strength values re-confirms the rate dependant material model behaviour, though such properties are not specified as the input parameters.

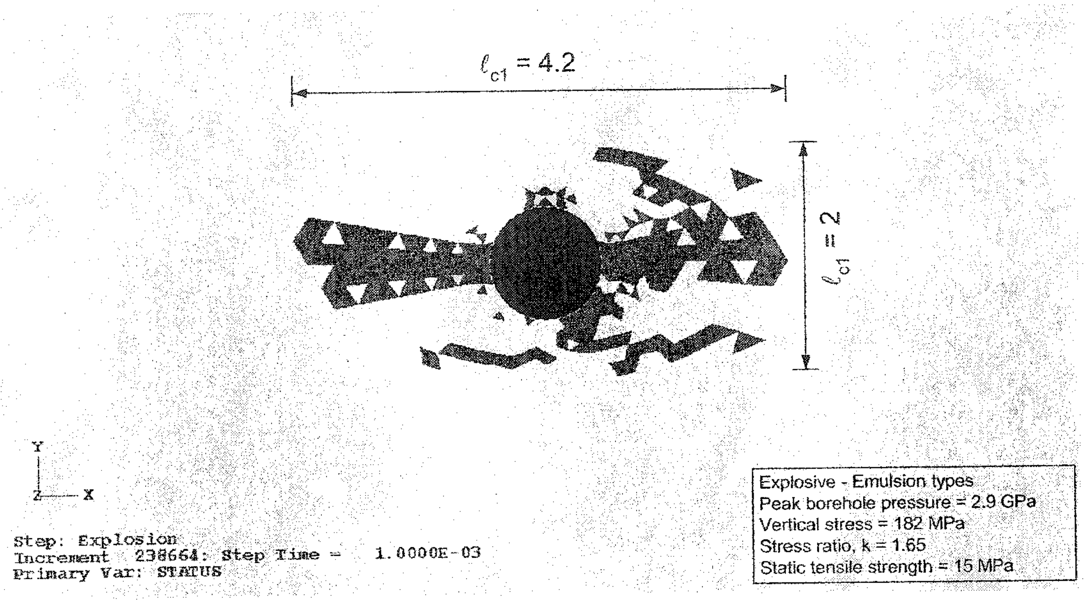

Figure 5.29 – Fracture pattern with static tensile strength = 15 MPa for emulsion type explosive

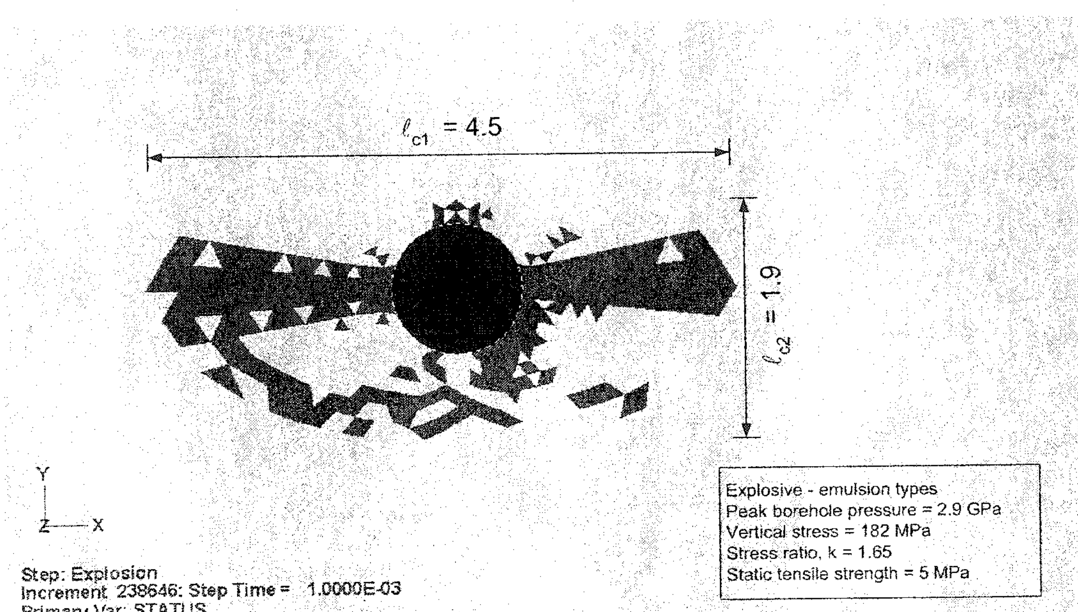

Figure 5.30 – Fracture pattern with static tensile strength = 5 MPa for emulsion type explosive

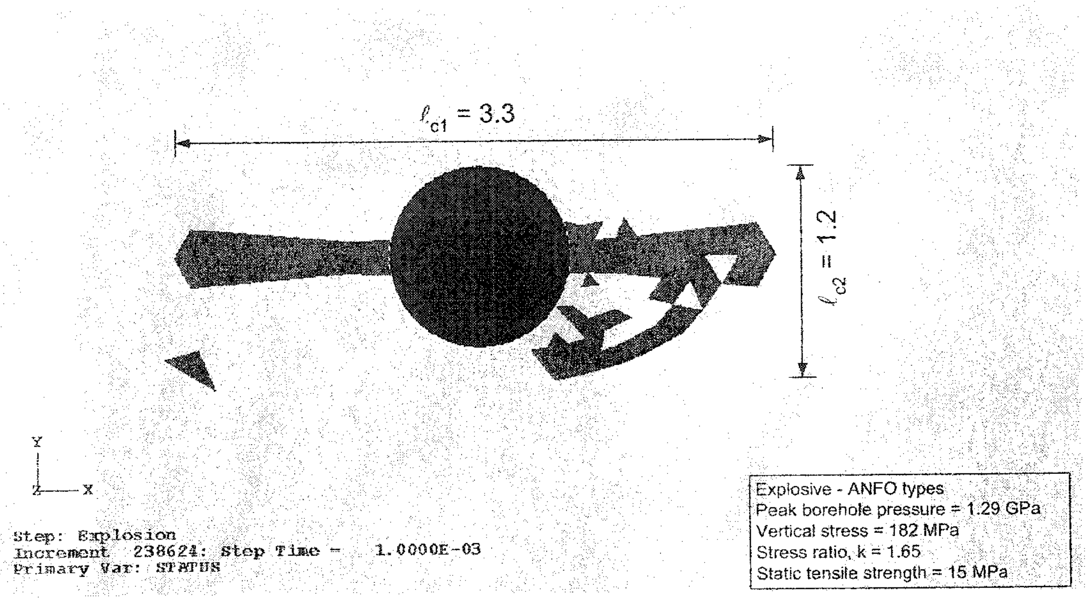

Figure 5.31 – Fracture pattern with static tensile strength = 15 MPa for ANFO type explosive

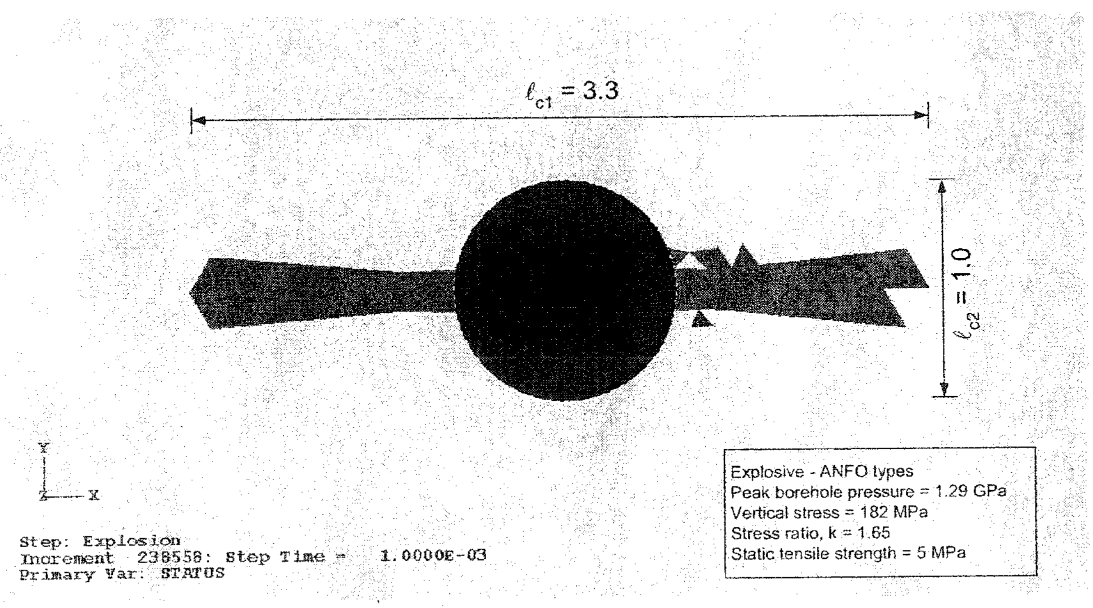

Figure 5.32 – Fracture pattern with static tensile strength = 5 MPa for ANFO type explosive

5.3.7 Effect of Explosive Energy Characteristics

Many researchers (see Chapter 1, sub-section 1.2) advocate ANFO type explosives for destress blasting with the argument that the higher gas content in such explosives helps in obtaining/extending longer fractures. However, controversies exist about the respective role of stress wave energy and gas energy in generating/extending fractures (see Chapter 3, sub-section 3.2 and 3.4). Further, researchers who advocate for ANFO type explosives also report the successful use of emulsion type explosives. Also, there is no concrete evidence about how the fractures grow when rock under confinement is blasted with the different types of explosive.

It was established earlier (see Chapter 3, sub-section 3.2) that the two load characteristics, shock loading by the emulsion type explosives and quasi-static loading by the ANFO type explosives, are the main contributing factors that contributes into fractures propagation, then the amount of gas produced by the respective explosives. It is difficult from a practical point of view to analyze the fracturing produced on account of the explosive energy level as there exists a big difference in the peak-pressure exerted by the different explosives for a similar diameter of borehole, apart from the load characteristics. Therefore, only an assessment can be made regarding the fracture pattern based in the difference of the explosives characteristics. Two numerical models are prepared with the two different explosive types described earlier. The simulations have confinement levels similar to the previous simulations described in the preceding sub-section. The other parameters of the models also remain the same. Results obtained from such simulations are presented in Figures 5.33 and 5.34.

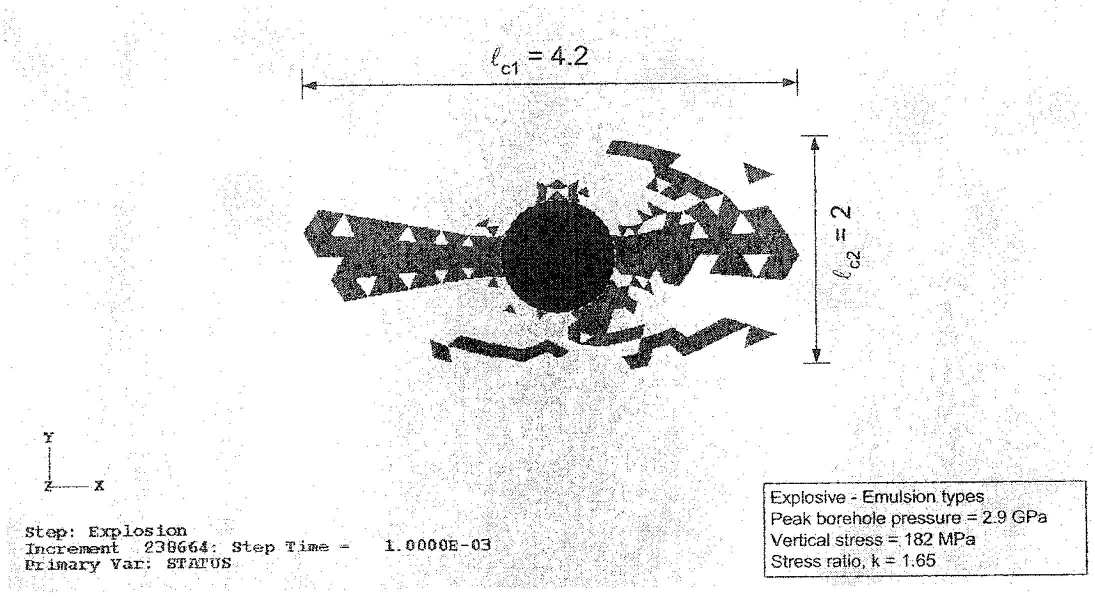

Figure 5.33 – Fracture pattern from emulsion type explosive in 38 mm diameter borehole

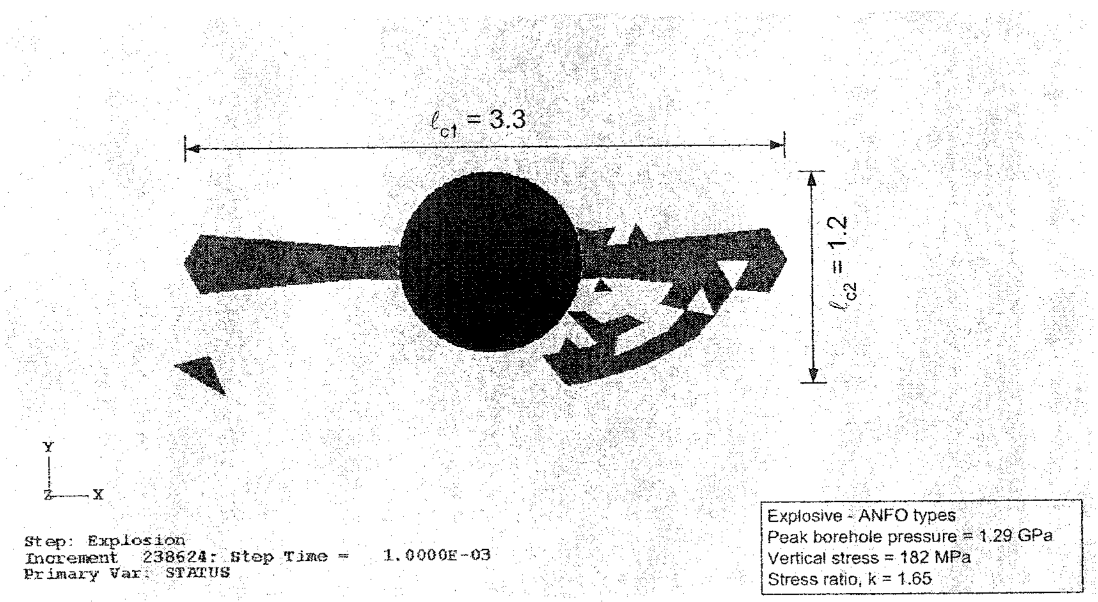

Figure 5.34 – Fracture pattern from ANFO type explosive in 38 mm diameter borehole

Analysis of the Results

The following information can be inferred from the simulations.

(i) Fracture lengths obtained with ANFO type explosive (ℓ_{cl} = 3.3) is 22 per cent smaller than emulsion type explosive (ℓ_{cl} = 4.2). Therefore, the overall effect on destressing with similar borehole diameter will be less from ANFO type explosive due to smaller fractures lengths. These results concur with the analysis made in Chapter 3 (section 3.4), which indicated that higher shock pressure is needed for longer fractures in stiff brittle rocks.

(ii) The peak borehole pressure applied by the ANFO type explosive (P_b = 1.29 GPa) is 45 per cent smaller than the emulsion type explosive (P_b = 2.9 GPa) for 38 mm diameter boreholes but fracture lengths are only 22 per cent smaller. Evidently, the gain in terms of the fracture lengths comes with ANFO with respect to the applied amount of peak pressure. Probably, the quasi-static loading which exerts pressure for a longer duration helps in extending the fracture networks. This observation partly concurs with the belief of researchers who advocate ANFO type explosives. However, the overall fracture length is smaller for the ANFO type explosive due to the fact that such explosives produce a lower peak borehole pressure in comparison to the emulsion type explosives for similar diameter boreholes.

(iii) The characteristics of the fracture pattern obtained with the ANFO type explosive include a narrower fracture band along the major principal stress direction and negligible damage along the intermediate principal stress direction. The focused fracture growth helps in better explosive energy utilization in the case of the ANFO type explosive compared to emulsion type explosive.

5.3.8 Effect of Explosive Energy Magnitude

Different simulations are planned and conducted to identify the increase in fracture length with an increase in explosive energy magnitudes. Larger diameter boreholes are used to increase the energy magnitudes. Four different industry standard borehole diameters, 38 mm, 55 mm, 76 mm and 89 mm, are chosen for the numerical simulations. The simulations are carried out with both the explosive types described earlier. The confinement level and the other model parameters are similar to those employed in the preceding sub-section. The results obtained from the simulations are depicted in Figures 5.35 to 5.43.

Analysis of the Results

The following information is inferred from the results.

(i) The increase in explosive energy magnitudes obtained from an increase in borehole diameters results in a longer fracture pattern irrespective of the explosive type. For most of the cases (except the 89 mm diameter borehole ANFO blast simulation), fracture lengths along the major principal stress direction remain higher than the fracture lengths along the intermediate principal stress. The ratio of ℓ_{c2}/ℓ_{c1} decreases with the increase in the borehole diameter, which indicates a reduction in fracture alignment with the major principal stress. This reduction is more prominent with the ANFO type explosive. The change in the fracture pattern as depicted in Figures 5.36 to 5.43 tends to provide a rock weakening effect akin to large scale fracturing perceived by Roux et al. (1957), but it is still very local.

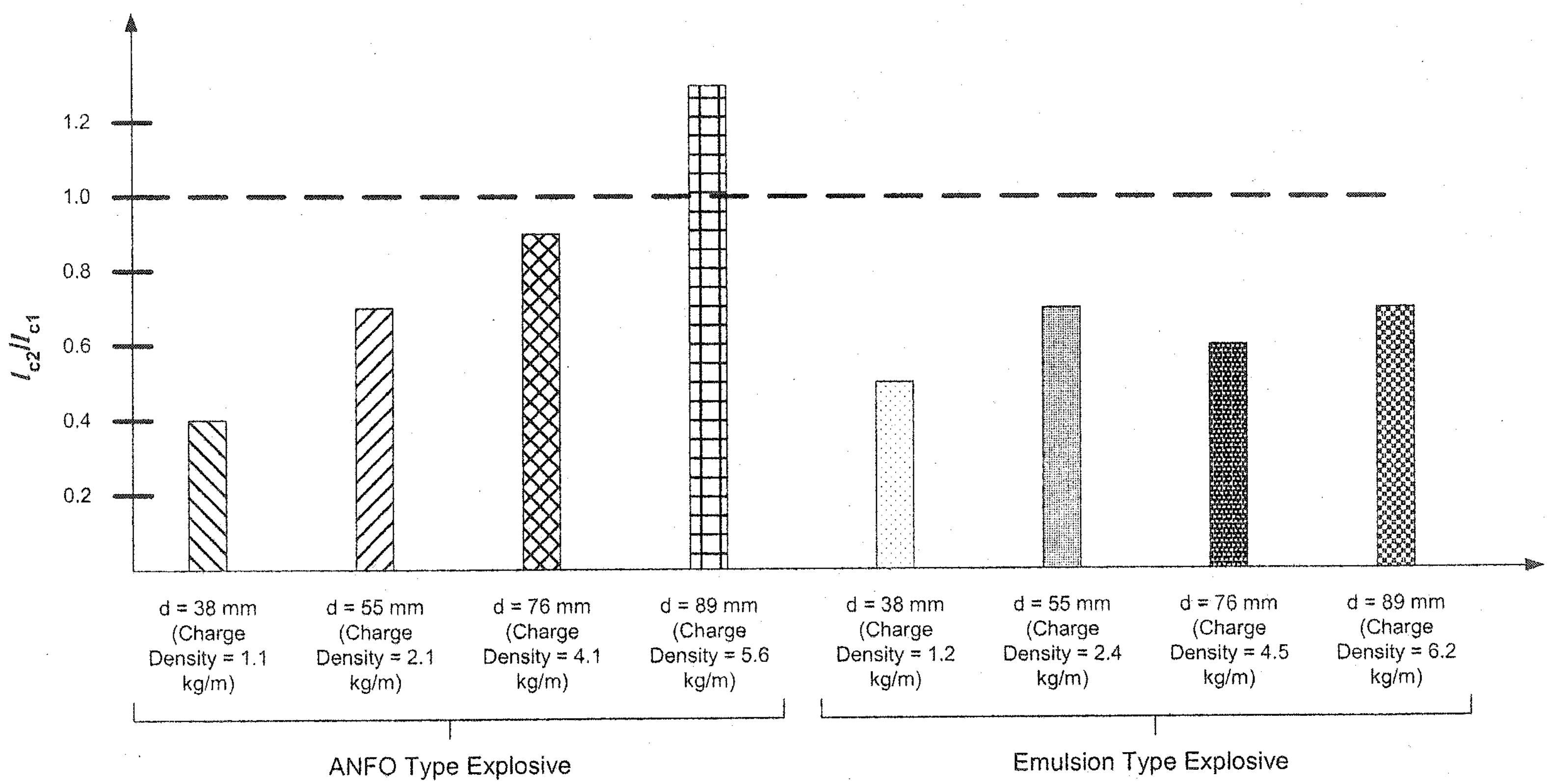

Figure 5.35 – Effect of explosive energy magnitude on the fracturing extent

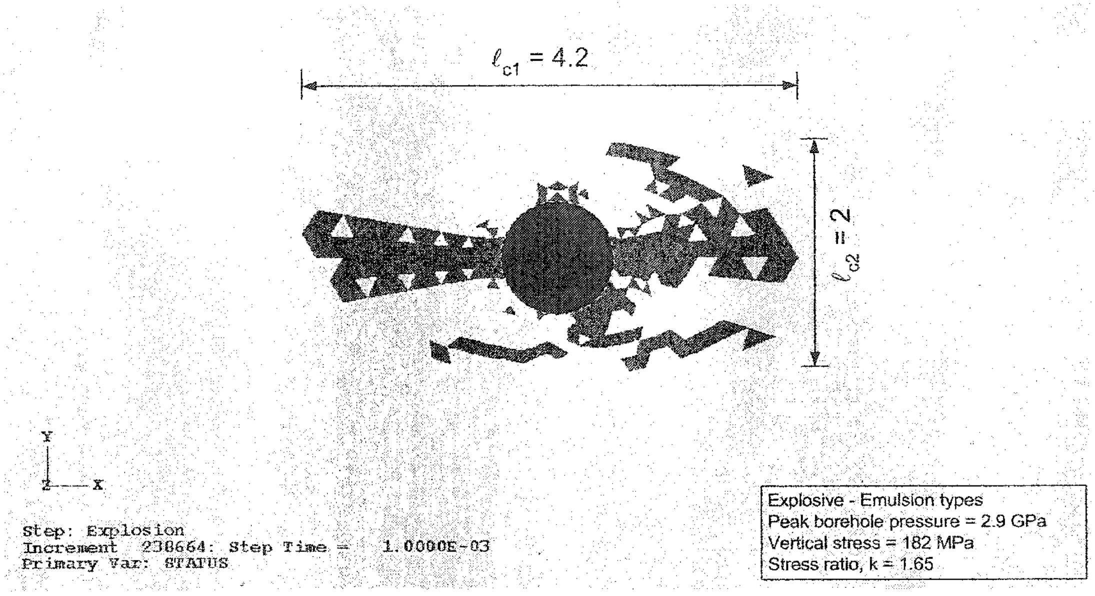

Figure 5.36 – Fracture pattern from emulsion type explosive in 38 mm diameter borehole

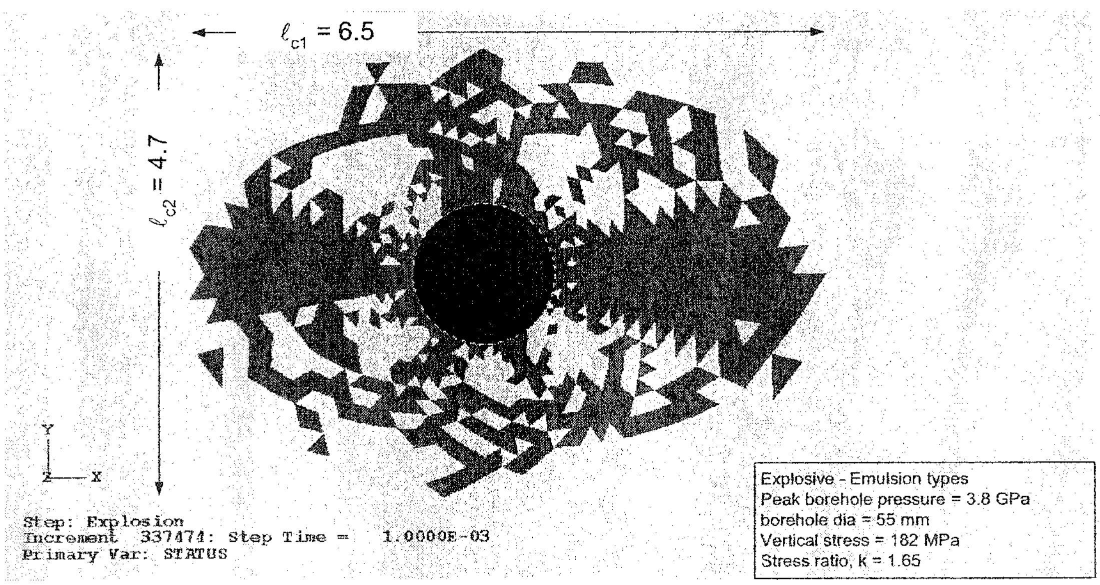

Figure 5.37 – Fracture pattern from emulsion type explosive in 55 mm diameter borehole

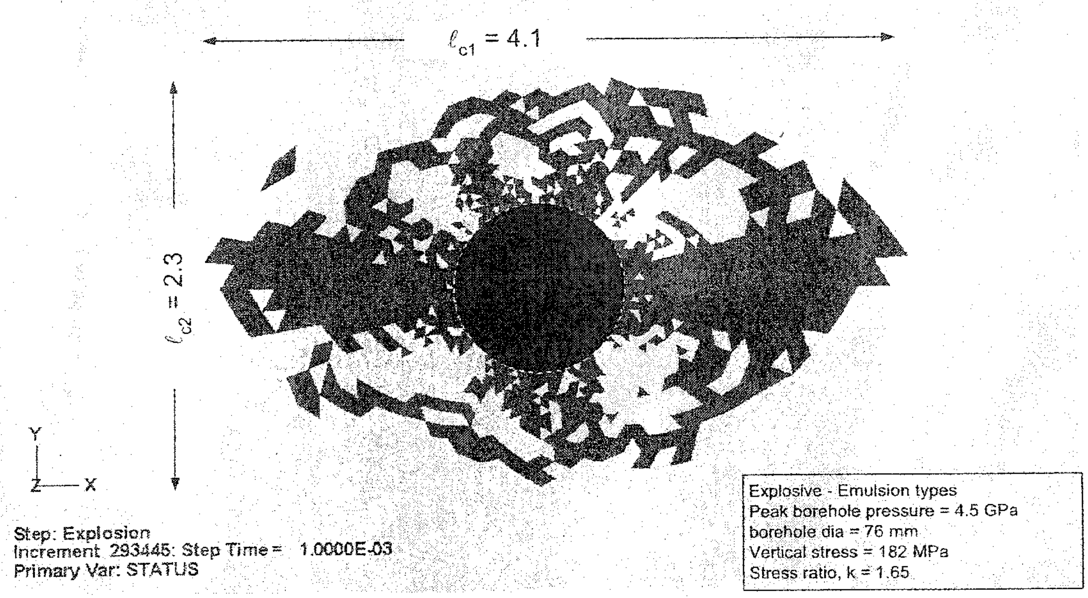

Figure 5.38 – Fracture pattern from emulsion type explosive in 76 mm diameter borehole

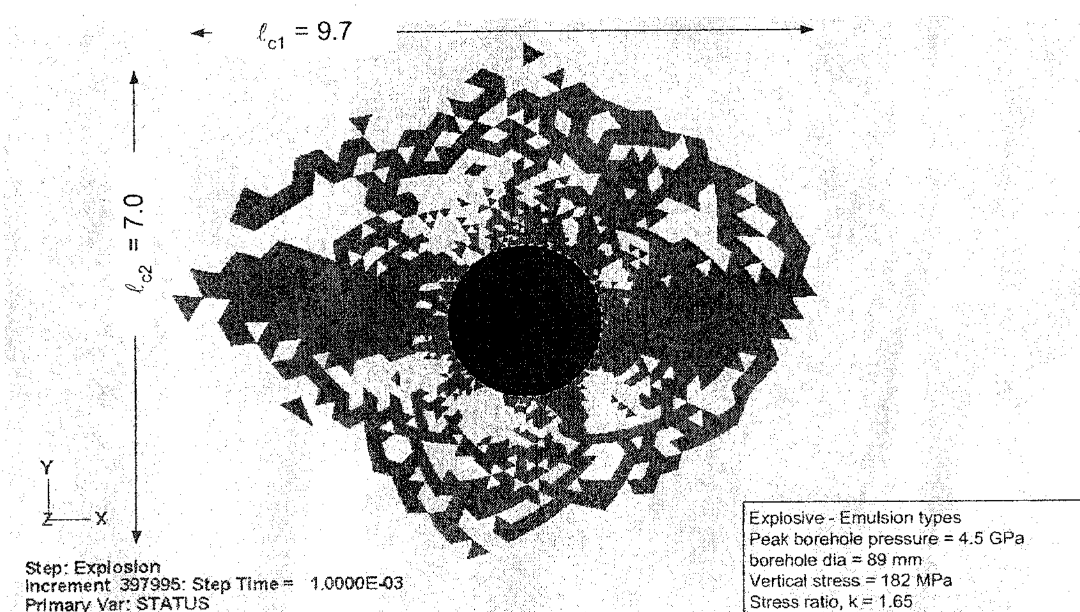

Figure 5.39 – Fracture pattern from emulsion type explosive in 89 mm diameter borehole

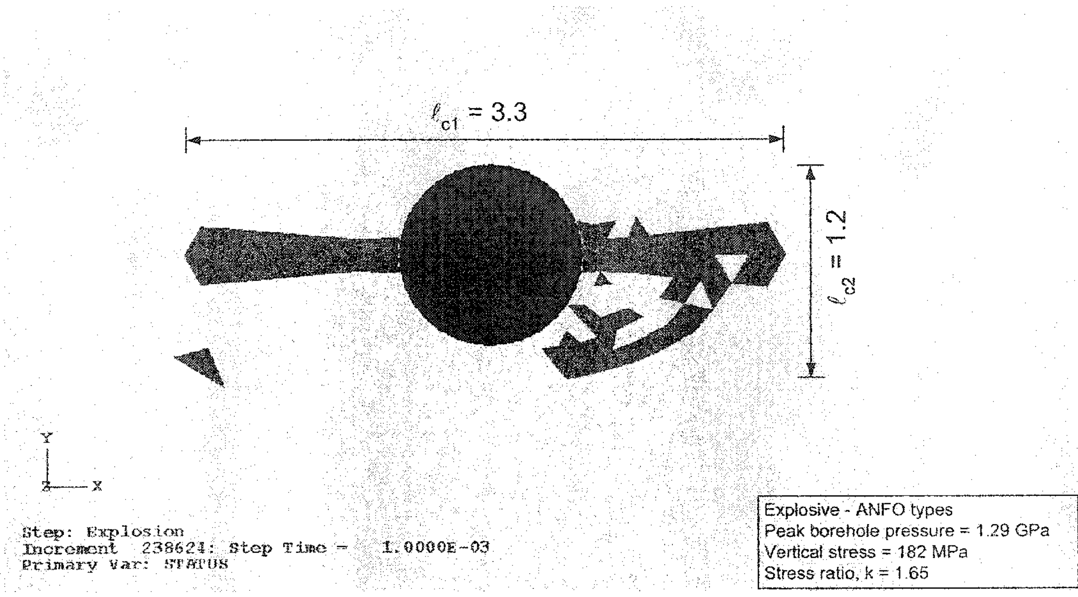

Figure 5.40 – Fracture pattern from ANFO type explosive in 38 mm diameter borehole

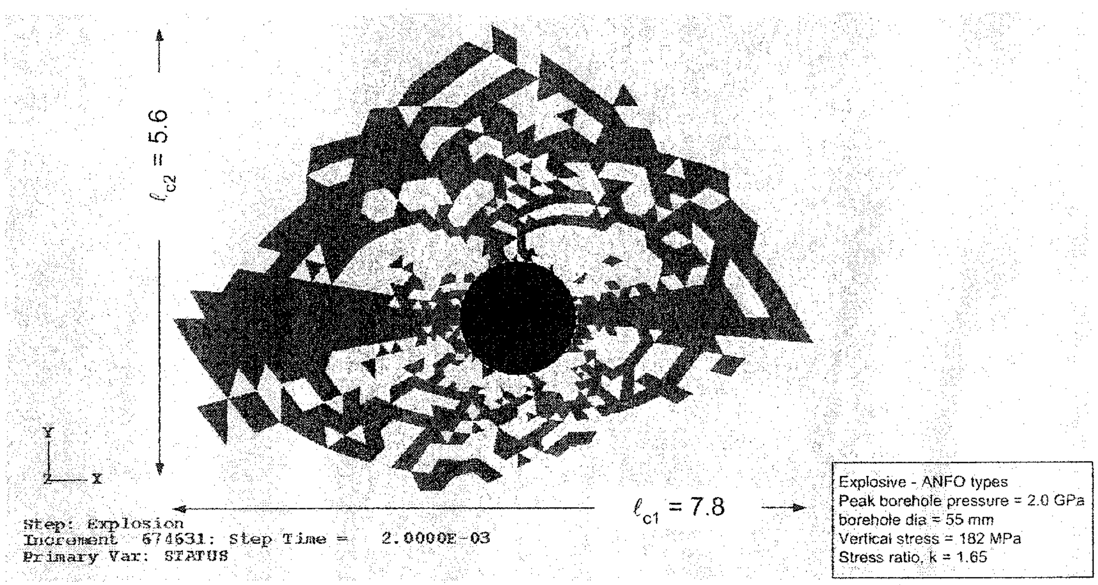

Figure 5.41 – Fracture pattern from ANFO type explosive in 55 mm diameter borehole

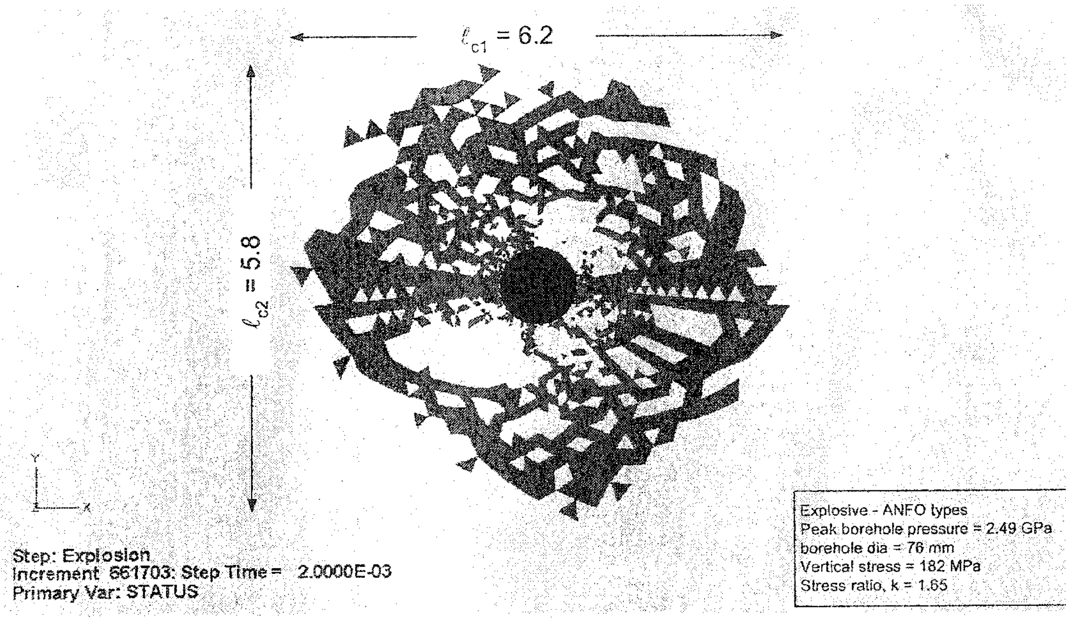

Figure 5.42 – Fracture pattern from ANFO type explosive in 76 mm diameter borehole

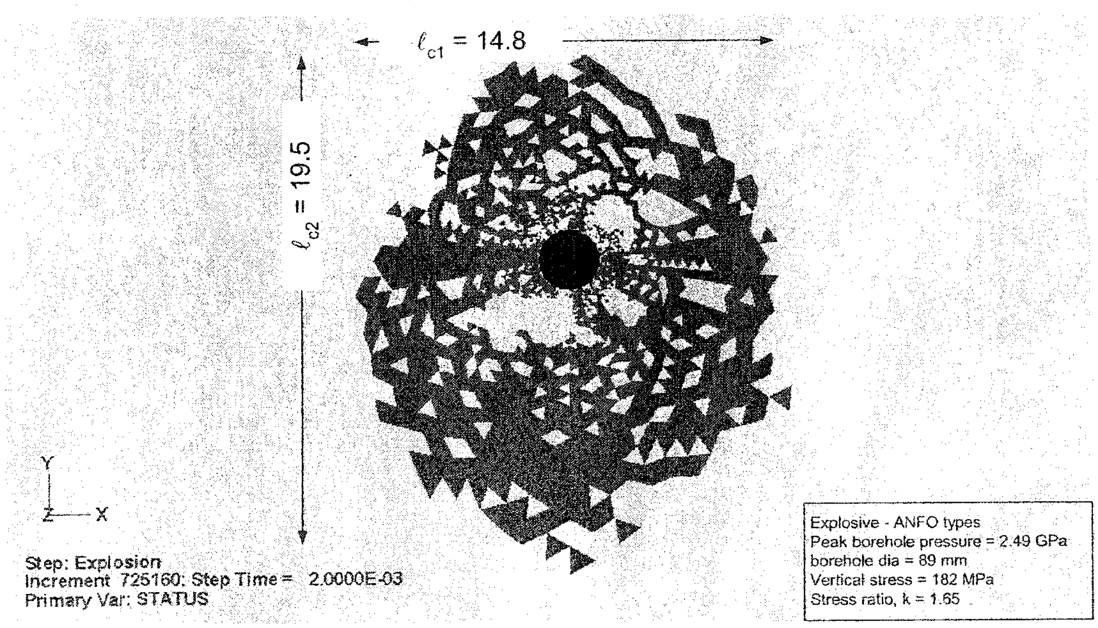

Figure 5.43 – Fracture pattern from ANFO type explosive in 89 mm diameter borehole

5.3.9 Effect of De-coupling of Explosive Charge

The de-coupling of emulsion type charges has been reported as one of the effective techniques to reduce unwanted local damage to the host rock (see Chapter 3, section 3.2 for discussion). Two simultaneous effects are achieved with such a de-coupling – first, the peak pressure is reduced, which helps in reducing the damage and second, the peak borehole pressure remains stagnant for a small period of time (equal to the time needed for expanding gaseous products to fill-up the borehole), which ultimately assists in the extension of the fractures. Three models are prepared and studied to identify such behaviour with 55 mm diameter boreholes. The first model involves no de-coupling of the emulsion type explosive; the second provides 70 per cent de-coupling and the third with 50 per cent de-coupling. The explosion pressure-pulse along with the peak pressure values have been described earlier (Chapter 4, sub-section 4.3.2.4). The confinement applied is similar to the previous simulations and has values of 300 MPa parallel to the X-axis (the major principal stress in the horizontal direction) and 182 MPa parallel to the Y-axis (the intermediate principal stress in the vertical direction). Other model parameters remain the same. Figure 5.44 depicts the concept of de-coupling and the fracture pattern obtained with the three models is presented in Figures 5.45 to 5.47.

Analysis of the Results

The following information is concluded from the analyses.

(i) The application of de-coupling reduces undesired local damage to the host rock as can be seen in Figures 5.45 through 5.47. However, the fracture network aligns itself with the major principal stress direction, which is undesirable with respect to stress relaxation.

(ii) The fracture length along the intermediate principal stress direction doesn't propagate due to the overriding effect of confinement. Therefore, the obtained fracturing does not assist in the destressing mechanism.

(iii) Overall, the effect of confinement is overriding in fracture growth compared to the damage control exercise by de-coupling. A larger de-coupling ratio is barely sufficient to open the fractures towards the major principal stress direction as can be seen from Figure 5.47. A higher peak borehole pressure is necessary to initiate and propagate fracture networks under higher confinement.

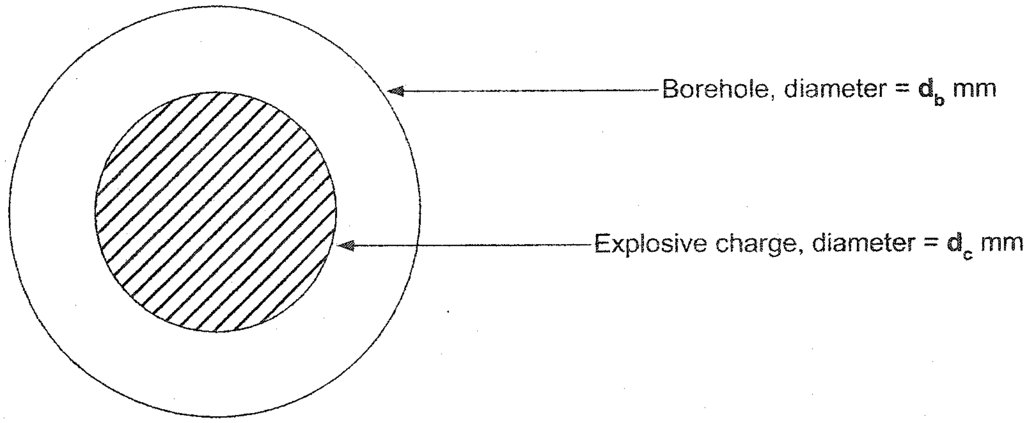

Coupling ratio, $r_c = (\mathbf{d_c} / \mathbf{d_b})$

Figure 5.44 – The concept of de-coupling

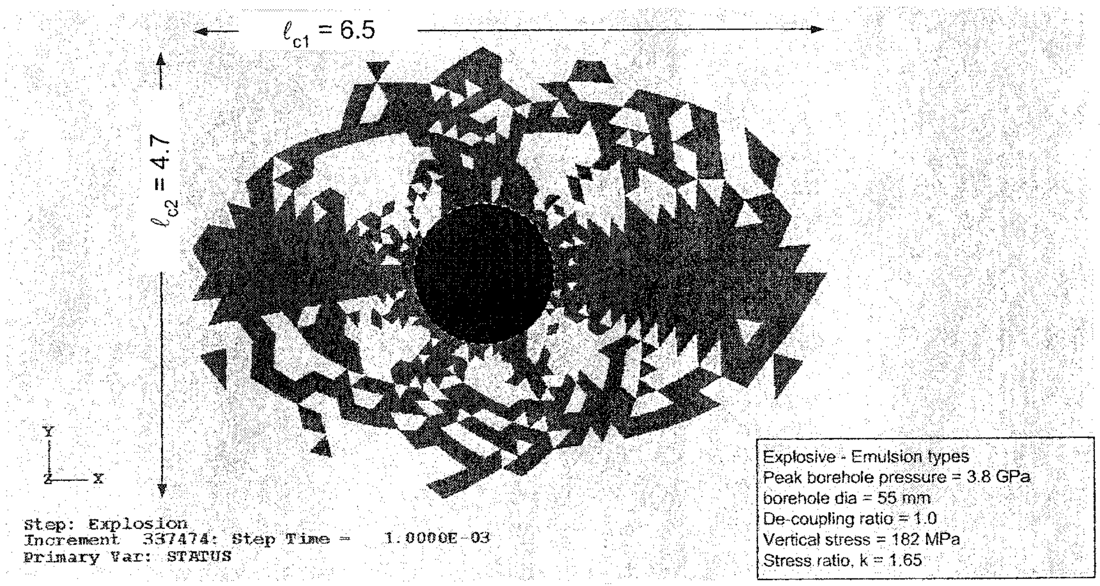

Figure 5.45 – Fracture pattern from fully coupled 55 mm diameter borehole by emulsion type explosive

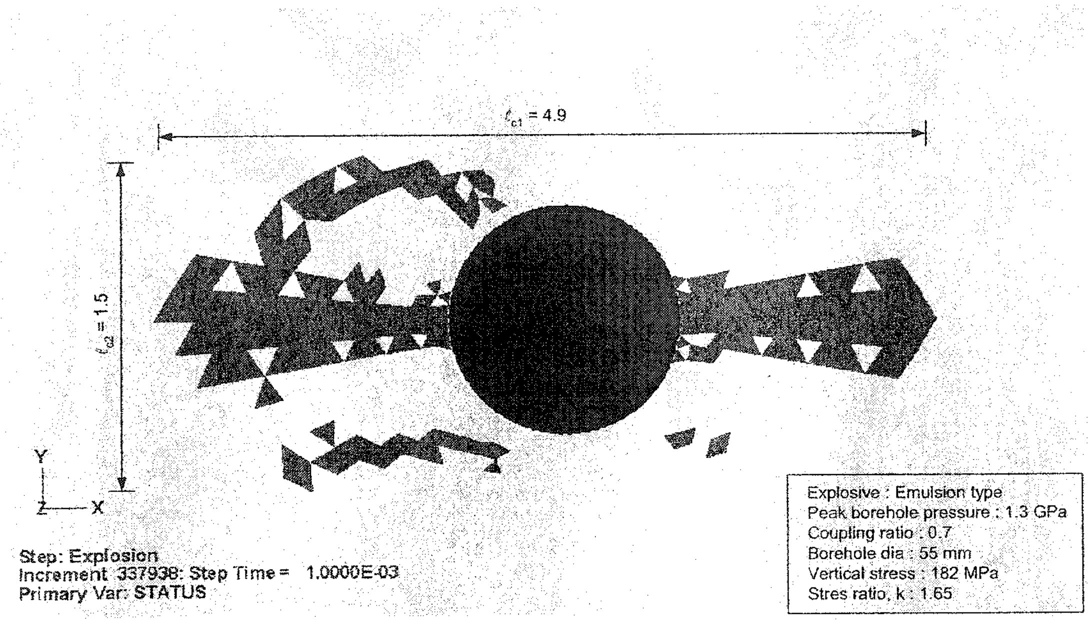

Figure 5.46 – Fracture pattern from 70 per cent coupled 55 mm diameter borehole by emulsion type explosive

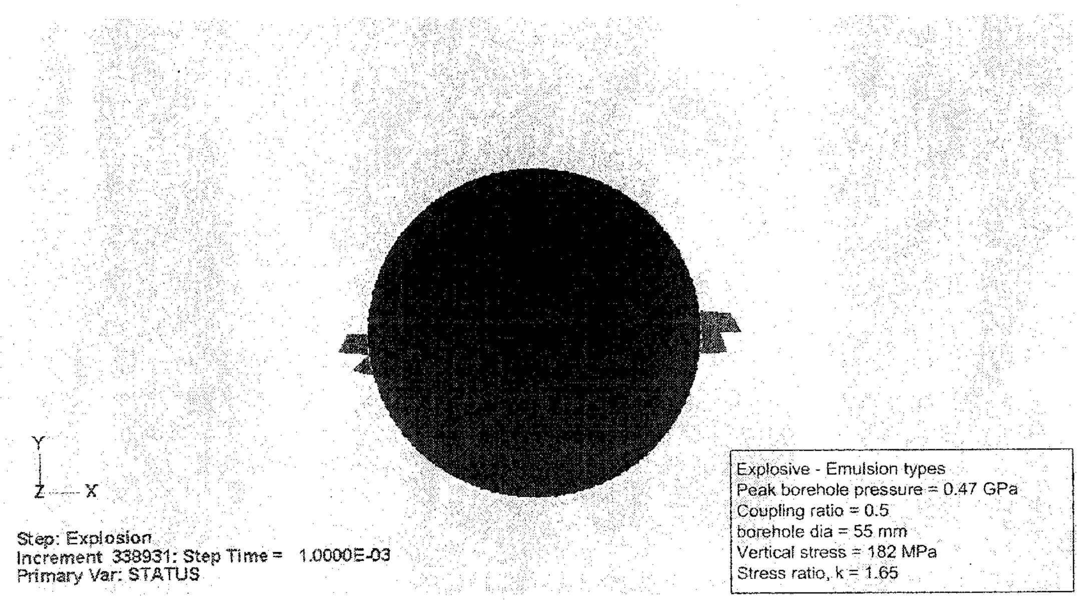

Figure 5.47 – Fracture pattern from 50 per cent coupled 55 mm diameter borehole by emulsion type explosive

5.3.10 Directional Fractures Growth by Notched Borehole

Fourney et al. (1978) report that the ideal fracture control growth requires specification of the fracture initiation points. The notched borehole is one of the techniques experimented for specification of the fracture initiation point (Bhandari and Rathore, 2002; Nakamura, 1999). Holloway et al. (1986) report tools for making notched boreholes for field blasting practice.

It was learnt from the analyses made above that the longer fractures invariably grow along the major principal stress direction due to the overriding effect of confinement. This direction is undesirable in terms of stress relaxation. Therefore, notched borehole models are conceived and simulated in order to achieve directional fracture growths along the intermediate principal stress direction (though this may not be the most desired direction for stress relaxation. It is selected only because it poses the most difficult task.). Two models were simulated to explore directional fracture growth. The first model involved a normal 55 mm diameter borehole. Two identical notches in the intermediate principal stress direction were created in the second model. Figure 5.48 presents the configurations of the notched borehole. Figure 5.49 presents the results of the analysis without the notch. Results obtained from the notched borehole model are presented in Figure 5.50.

Analysis of the Results

The following information is obtained from the simulations:

(i) The notched borehole technique for the directional growth of the fracture network s shows promising results for destress blasting. Fracture growth in the direction of the intermediate principal stress increased from five times the borehole diameter to 15 times the borehole diameter. The results indicate that attempts for directional fracture growth may yield effective destressing provided the desired direction is known.

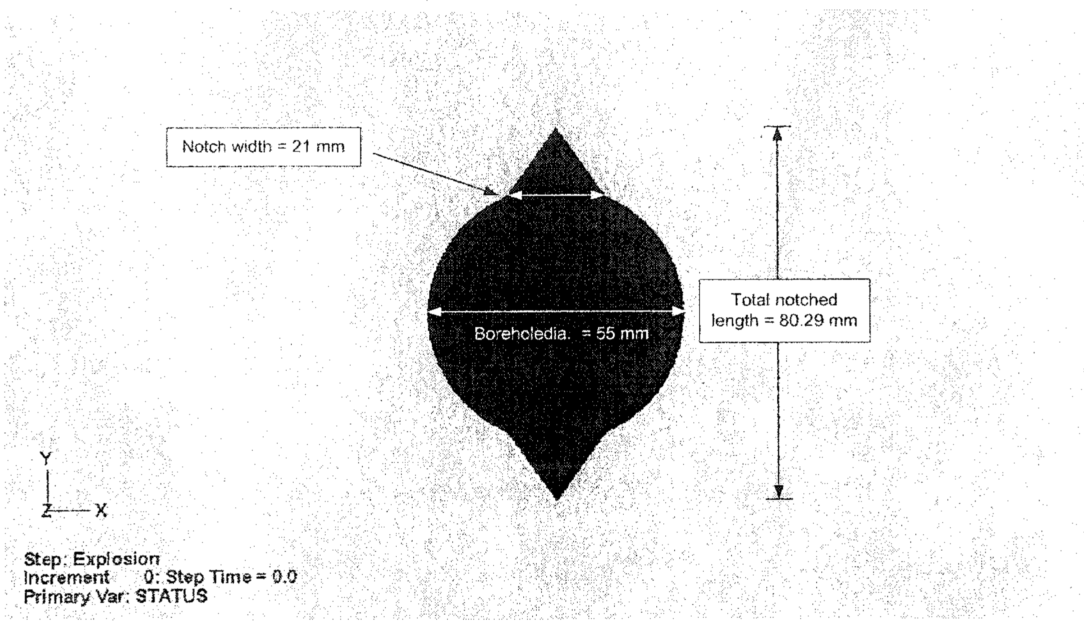

Figure 5.48 – Initial configuration of 55 mm diameter borehole with two notches

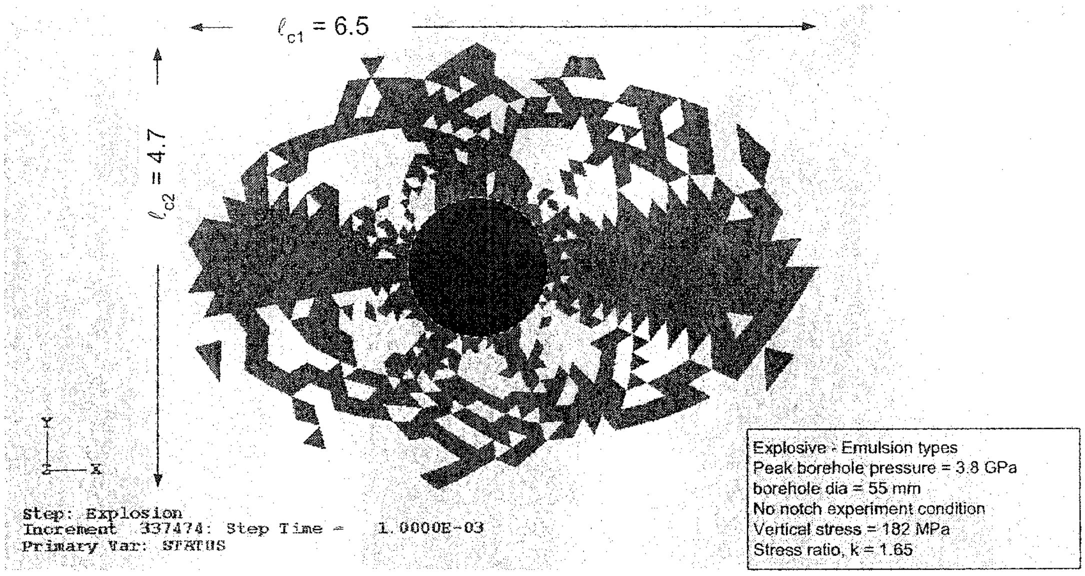

Figure 5.49 – Fracture pattern by 55 mm diameter borehole with no notch and simulated with emulsion types explosive

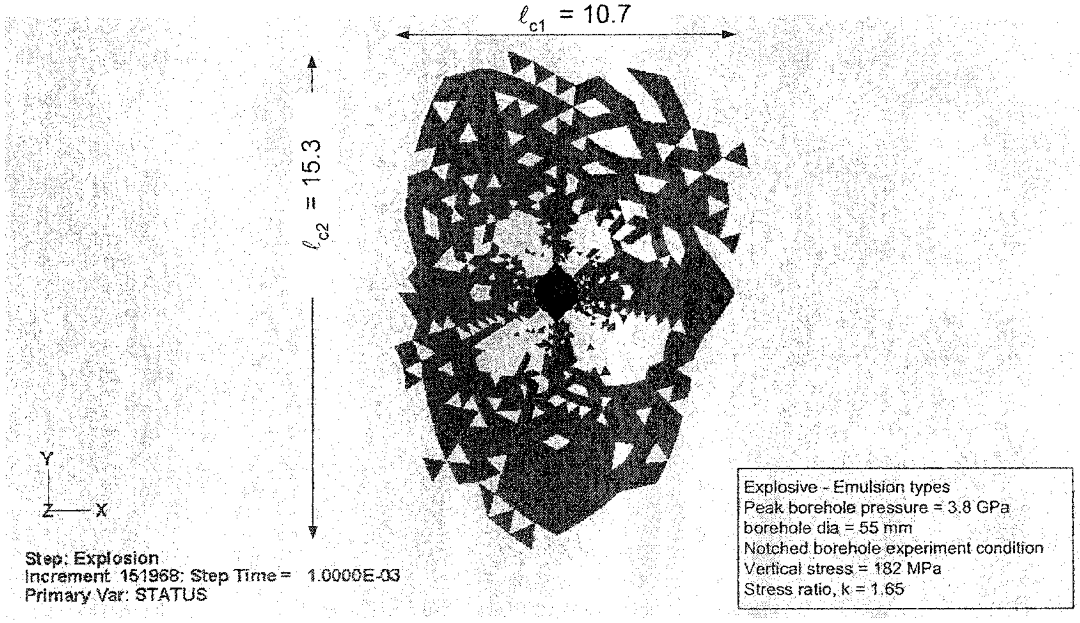

Figure 5.50 – Fracture pattern by 55 mm diameter notched borehole simulated with emulsion type explosive

5.4 SUMMARY

A detailed parametric study is conducted to investigate the quantitative growth of the fracture network initiated due to destress blasting. The fracturing extent is investigated with the introduction of normalized fracture lengths. The results reported here are the first of their kind as destressing concepts are evaluated at the micro-mechanical level. The dynamic pressure pulse used is commensurate with industry standard explosive charges; borehole diameters selected are mostly used with destress blasting; rock properties used are in accordance with the rock properties found in deep hard rock mines and confinement provided for the simulations is similar to the confinement posed by great depth workings. The study identifies the ineffectiveness associated with the practice of destress blasting. It is learnt that higher explosive energy is needed to initiate and propagate fracture network to a sufficient distance with an increase in the confinement level. Only the application of more explosive charges by using larger diameter boreholes can provide this higher demand of explosive energy. Fractures are invariably found to align along the major principal stress direction. It is apprehended that this alignment is not conducive for effective destressing. The study also explores and finds out that directional fracture growth using the notched borehole can assist in achieving longer fractures in a direction other than the major principal stress direction. This simulation provides a platform for exploring an appropriate direction for effective destressing.

Chapter 6

A NOVEL METHOD FOR CHARACTERIZING DESTRESSING

6.1 OVERVIEW

One of the biggest challenges facing destress blasting application in hard rock mines since the first application in early 1930s, is the identification of the effects of destress blasting. Brauner (1994) describes several standardized measures for destress blasting in coal mines such as pulverization, drill cuttings, noise level with drilling, etc. These measures are used to identify locations where destress blasting is required as well as to specify the amount of destressing achieved. However, such methods are not applicable in hard rock mines. Several techniques are in use for destress blasting in hard rock mines but hitherto none of them are predictive.

Microseismic survey (or specifically seismic tomography) is one of the methods relied on for the delineation of destressing. This method proved to be useful in the identification of structures those are potentially in danger of imminent rockbursts. But microseismic data alone is not sufficient for making reliable predictions. Hedley (1992) reports that the maximum possible achievable accuracy from a microseismic survey is ± 5 m. This accuracy level is detrimental in the reliable application of this tool for delineating destressing. The poor accuracy can also be seen from the most recent Canadian destress blasting application (Figure 6.1). Figure 6.1 depicts an intense fractured zone about 5m below the drift floor that experienced heave failure.

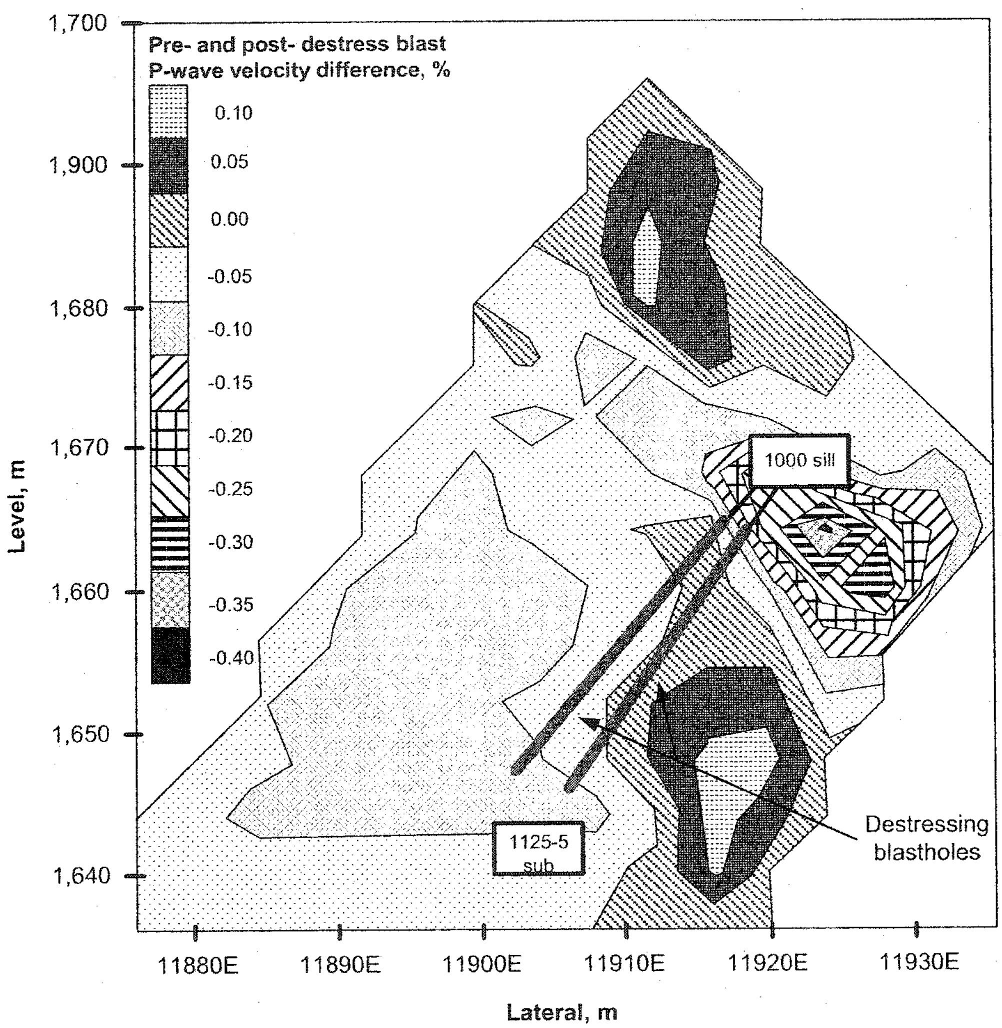

Figure 6.1 – Damage zone identification with the pre- and post- destress blast seismic tomography in the Brunswick Mine, Canada (Longitudinal-section) (Andrieux et al., 2003)

Ground Penetrating Radar (GPR) is another tool used for measuring the extent of fractures of destress blasting. Momayaz et al. (1994) observed that GPR has some limitations when used for fracture mapping in a highly stressed underground environment,as the target (fractured rock) has a low reflectance and fractures are closed by the high stresses. Grodner (2001) apprehends the poor reliability due to several undesirable reflections from the underground mine environment. Further, probably the most severe hindrance comes from the nature of the fractures itself. It was learnt in the previous chapters that mining induced fractures are extensional in nature. These fractures are parallel to the excavation face and not amenable to destressing. A GPR application can only detect characteristic changes with these fractures. Fractures perpendicular to the excavation faces cannot be traced by the GPR studies.

Blake (1972a) proposed the reduction of the Young's modulus of elasticity as a measure of destressing to mimic field observations through numerical modelling. This procedure is adopted based on the perceived belief that destressing involves a change in rock mass stiffness, and is still in use (Andrieux et al., 2003). It was reported in the previous chapter that to date there is no procedure available to measure the rock mass modulus of elasticity. Practitioners rely on empirical equations such as the one proposed by Mitri et al. (1994).

The absence of a measure to characterize destressing has left many questions unanswered. It was observed in Chapter 1 that Toper et al. (1994) and Hakami et al. (1990) reported an increase in the major principal stress magnitudes. Hakami et al. (1990) and Labrie et al. (1997) observed higher Young's modulus values after experimental destress blasts. Such peculiar observations cannot be explained with the prevalent characterizing measures.

A simple yet measurable and reliable parameter is proposed in this work. The following section elaborates on this parameter. The novel parameter adequately explains hitherto inexplicable peculiar measurements.

6.2 "β_{ij}" – THE NEW STRESS RELAXATION PARAMETER

Stress (σ) is the most common engineering parameter known to any engineer working in rock mechanics projects. It is unnecessary to elaborate at this stage that stress at depth can be studied with three principal components (σ_1, σ_2 and σ_3) and that these can be resolved along three Cartesian axes (x, y and z) giving a total of nine magnitudes of interest. Further, the cardinal role of stress as a cause for rockbursts is well acknowledged. Therefore, the parameter selected to represent destressing is the change in stress. This parameter will address the very nomenclature of the technique, "destress". It is proposed to measure change in the stresses, before and after the destress blast, in order to characterize the effect of destress blasting. Tang and Mitri (2001) already laid the foundation in this regard with the introduction of a stress dissipation factor, β. They proposed the following relation to define the stress relaxation factor.

$$\sigma_{(\text{after destressing})} = (1 - \beta) * \sigma_{(\text{before destressing})} \qquad \text{......................} \; (6.1)$$

The above relation does not hold for practical purposes due to the following reasons:

(a) The change in the stress magnitude after destress blasting can never be equal magnitude due to the fact that stresses before blasting are anisotropic for most of the cases.

(b) It was established in Chapter 5 that fractures do not grow radially after blasting in confined rocks. Therefore, an equal reduction in all the directions cannot be achieved.

(c) Finally, such a simple definition is unable to explain the previously mentioned peculiar field observations.

However, the relation 6.1 can be extended to provide a general term. The following expression is proposed to characterize stress relaxation, which can be achieved by destress blasting.

Stress relaxation

$$\beta_{ij} = \left(\frac{(\sigma_{ij} \text{ before destress blasting}) - (\sigma_{ij} \text{ after destress blasting})}{(\sigma_{ij} \text{ before destress blasting})} \right) \text{x } 100, \% \quad \ldots\ldots\ldots\ldots\ldots\ldots (6.2)$$

where,

β_{ij} = Stress relaxation to σ_i at measuring point on the j^{th} Cartesian plane.

σ_{ij} = i^{th} major principal stress at measuring point on the j^{th} Cartesian plane.

i = Principal stress identifier = 1,2,3

j = Cartesian plane identifier = x, y, z

The expression 6.2 is capable of adequately characterizing the effects of destress blasting. The expression may look a complicated assignment as it can be felt that it needs a total of nine values for full characterization. But this is not the case for practical purposes. Only four values are sufficient, for practical purposes, to explain the effects of destress blasting. It was been established in the previous chapters that the bi-axial stress environment is more important to investigate destress blasting immediately ahead to a free face. Therefore, measurements for only two principal stresses is sufficient, which can be made along two perpendicular planes on the face where destress blasting is applied. Fortunately, a free face where destress blasting is used provides the requisite planes. Schematic arrangement for such measurements is depicted in Figure 6.1. The proposed scheme carries one more advantage. As it is evident from Figure 6.1 that the same sampling holes can be used to evaluate β_{ij}, which were drilled for the purpose of deciphering ℓ_{cri} (see Chapter 5, section 5.2). The importance of the ℓ_{ci} has already been established in the previous chapter.

Analyses are made to illustrate the calculations for β_{ij} and the benefits associated with it. Stress values are measured similar to the above proposal and are depicted in Figure 6.2 from the numerical models simulated with the series of simulations presented in Chapter 5, sub-section 5.2.3. The results of β_{ij} measurements are depicted in Figures 6.3 to 6.10.

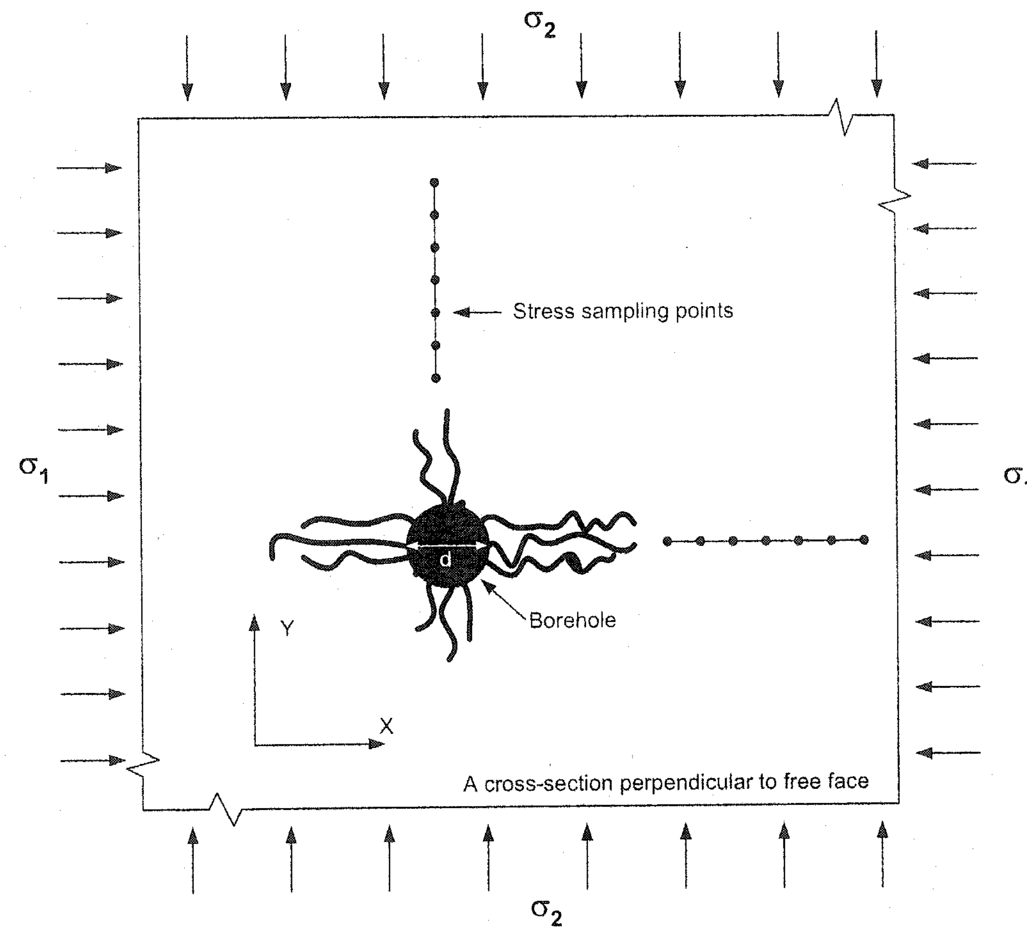

Figure 6.2 – Measurements for the Stress Relaxation parameter, β_{ij} (Schematic, not to the scale)

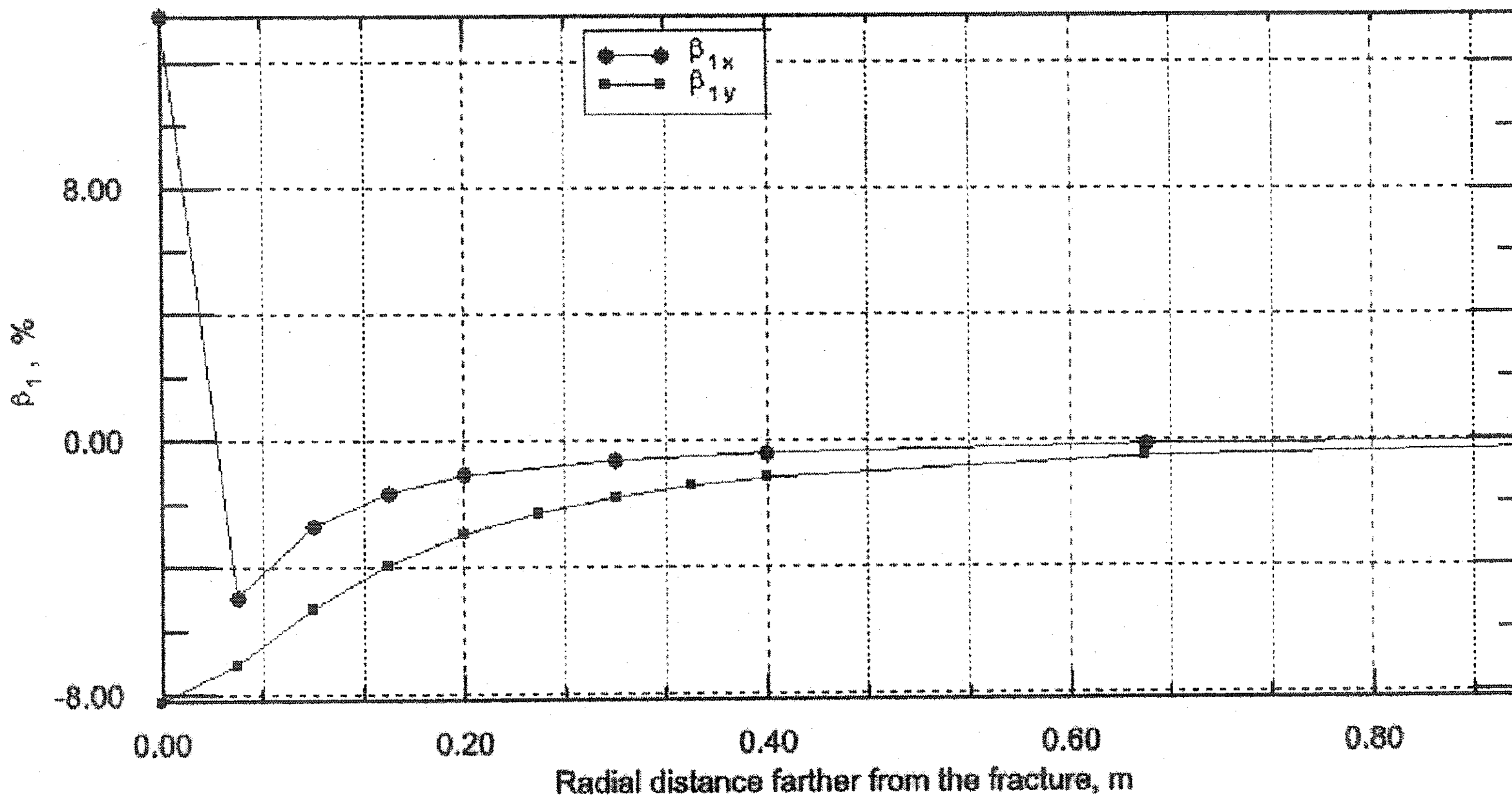

Figure 6.3 – Stress relaxation to the σ_1 with fracture pattern generated by emulsion type explosive destress blast in 38 mm dia borehole

(Applied σ_1 = 150 MPa, σ_2 = 91 MPa; σ_1 applied parallel to the X-axis)

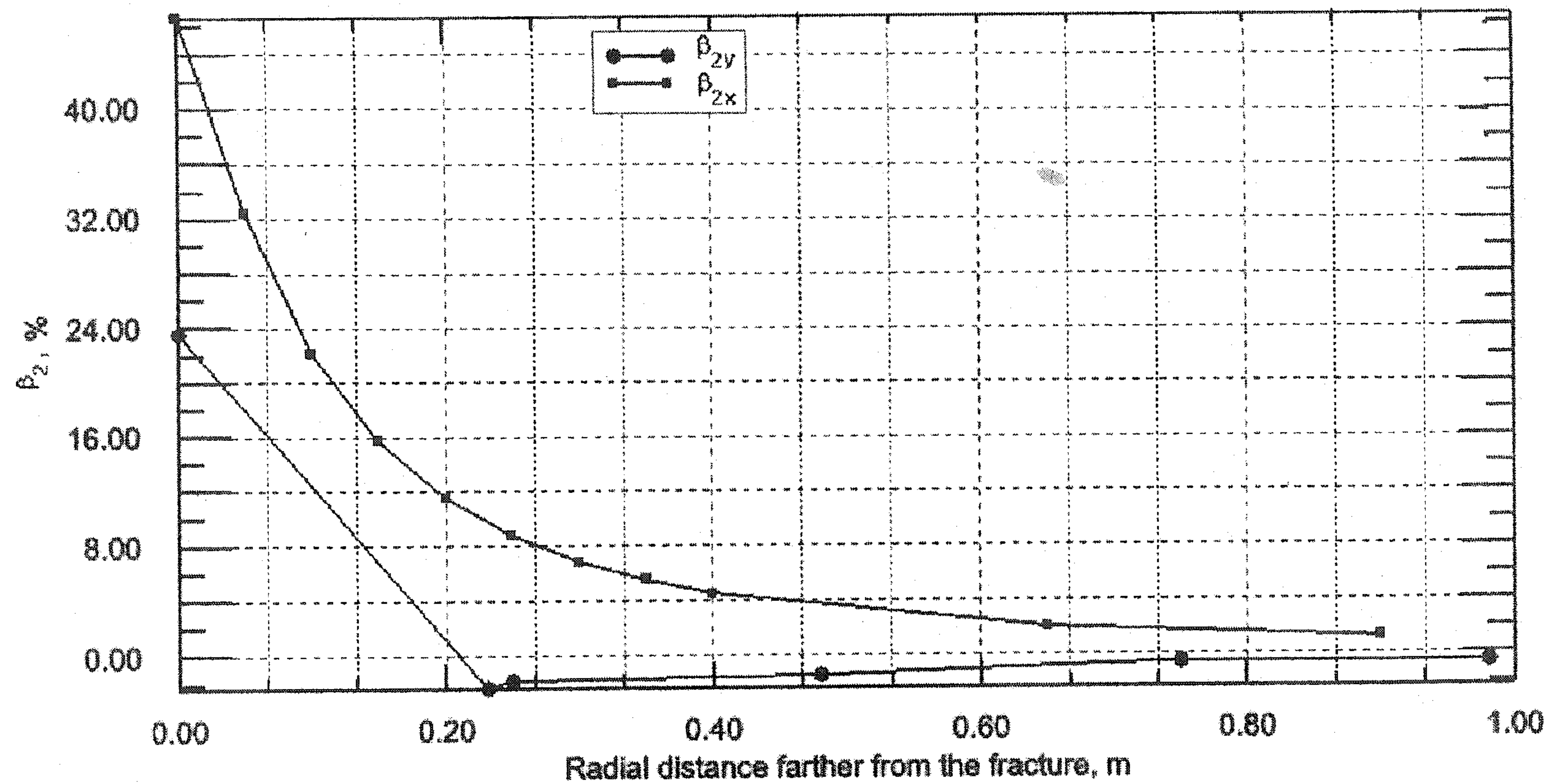

Figure 6.4 – Stress relaxation to the σ_2 with fracture pattern generated by emulsion type explosive destress blast in 38 mm dia borehole

(Applied σ_1 = 150 MPa, σ_2 = 91 MPa; σ_1 applied parallel to the X-axis)

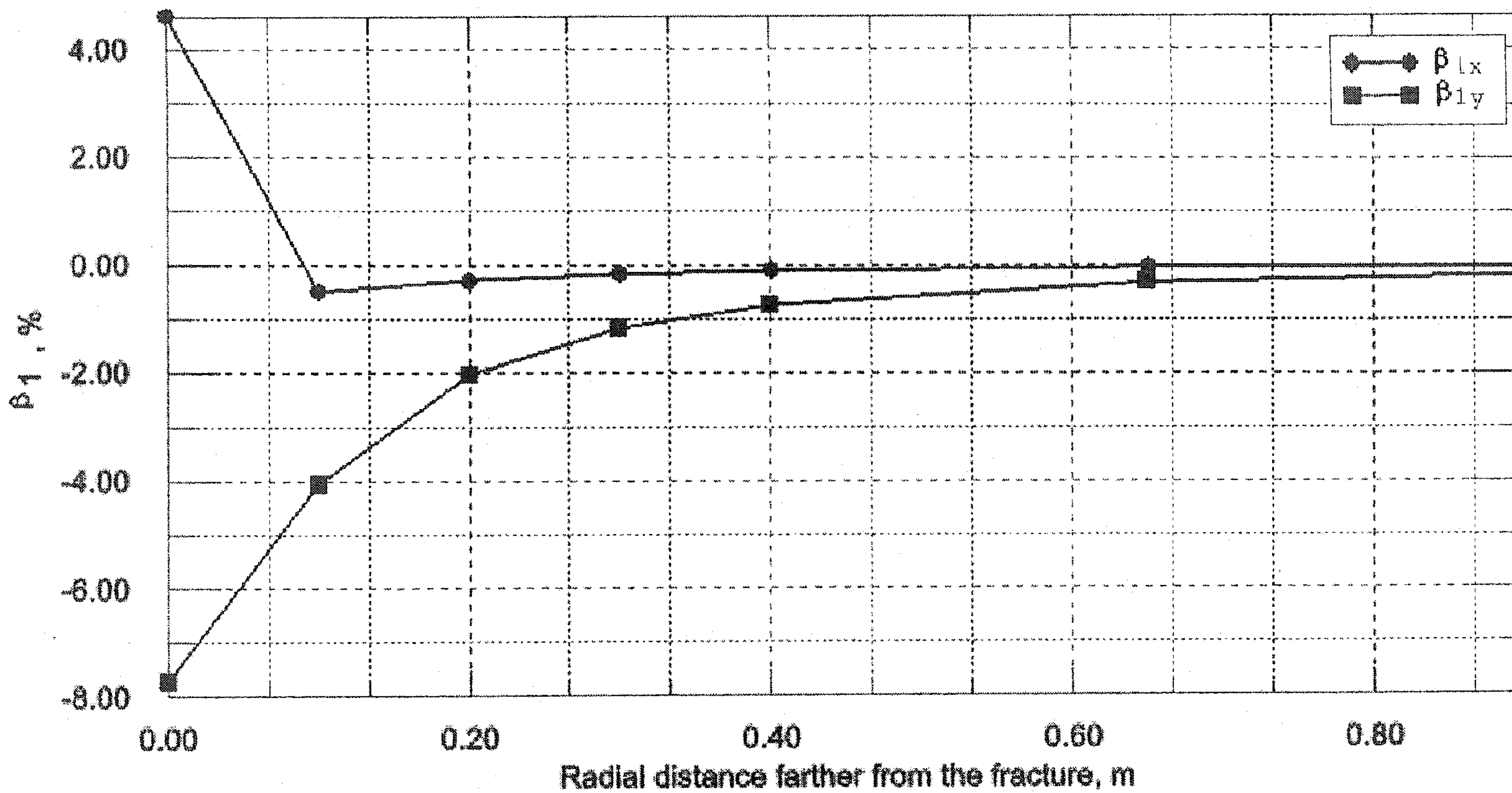

Figure 6.5 – Stress relaxation to the σ_1 with fracture pattern generated by emulsion type explosive destress blast in 38 mm dia borehole

(Applied σ_1 = 300 MPa, σ_2 = 182 MPa; σ_1 applied parallel to the X-axis)

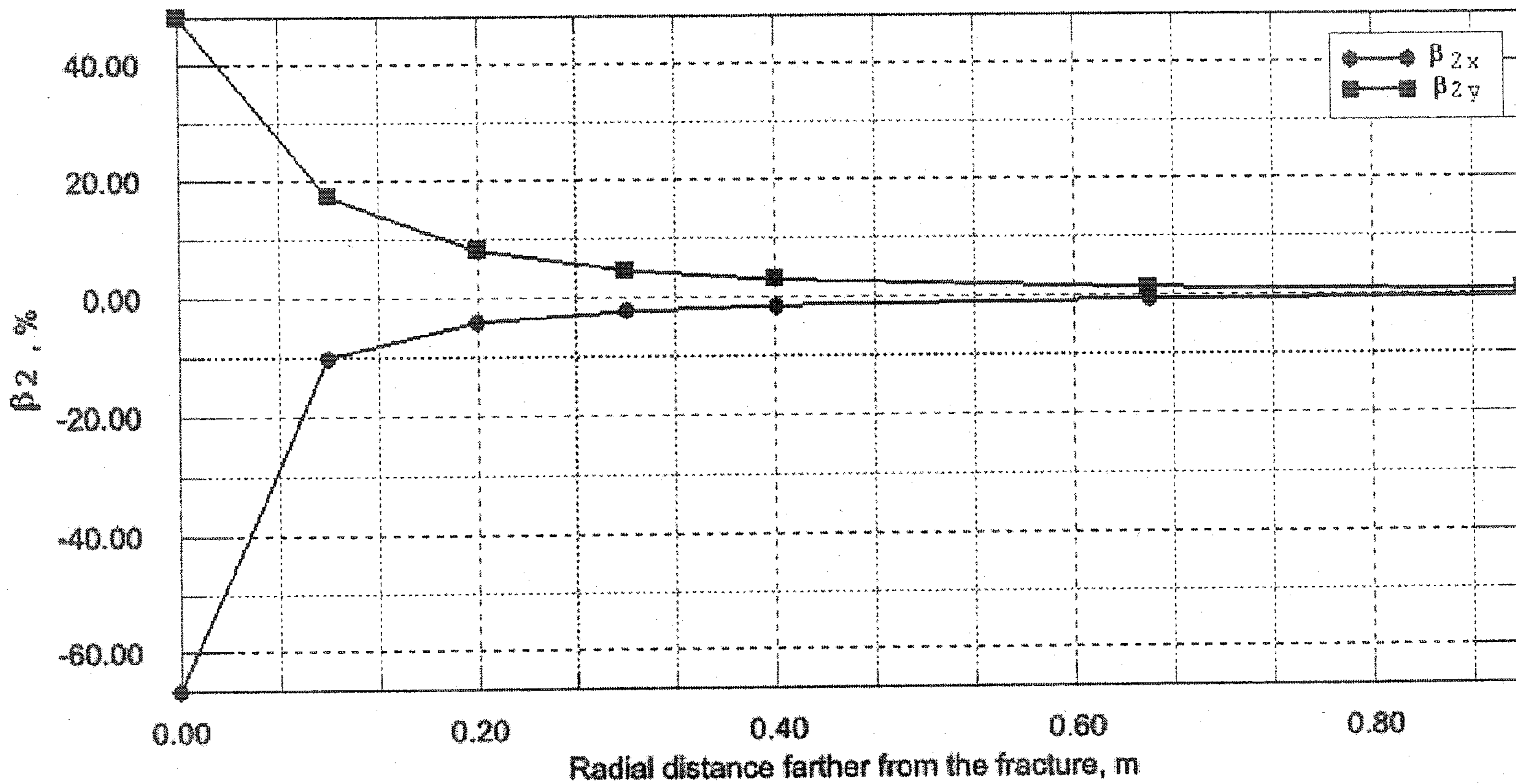

Figure 6.6 – Stress relaxation to the σ_2 with fracture pattern generated by emulsion type explosive destress blast in 38 mm dia borehole

(Applied σ_1 = 300 MPa, σ_2 = 182 MPa; σ_1 applied parallel to the X-axis)

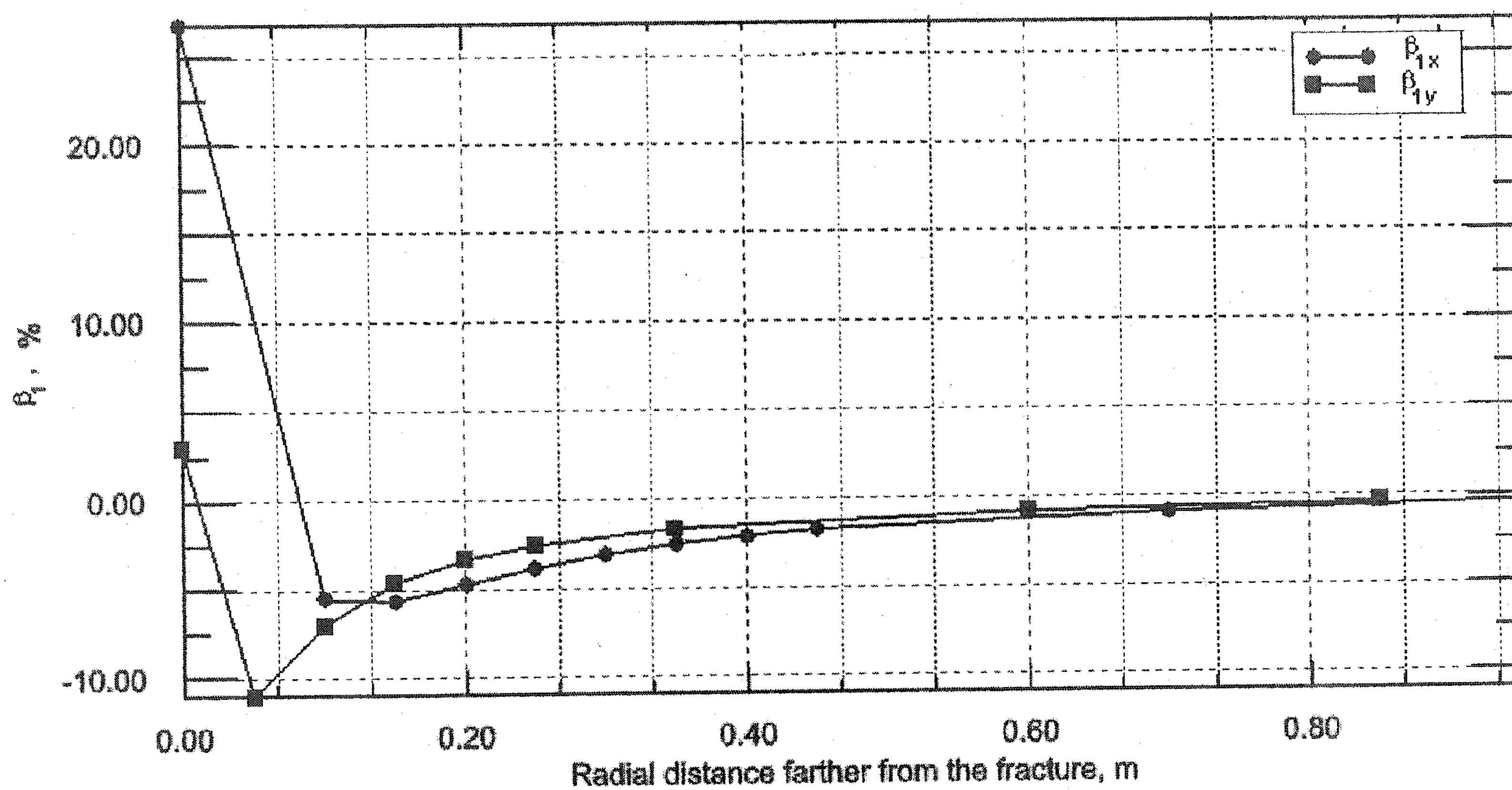

Figure 6.7 – Stress relaxation to the σ_1 with fracture pattern generated by ANFO type explosive destress blast in 38 mm dia borehole

(Applied σ_1 = 150 MPa, σ_2 = 91 MPa; σ_1 applied parallel to the X-axis)

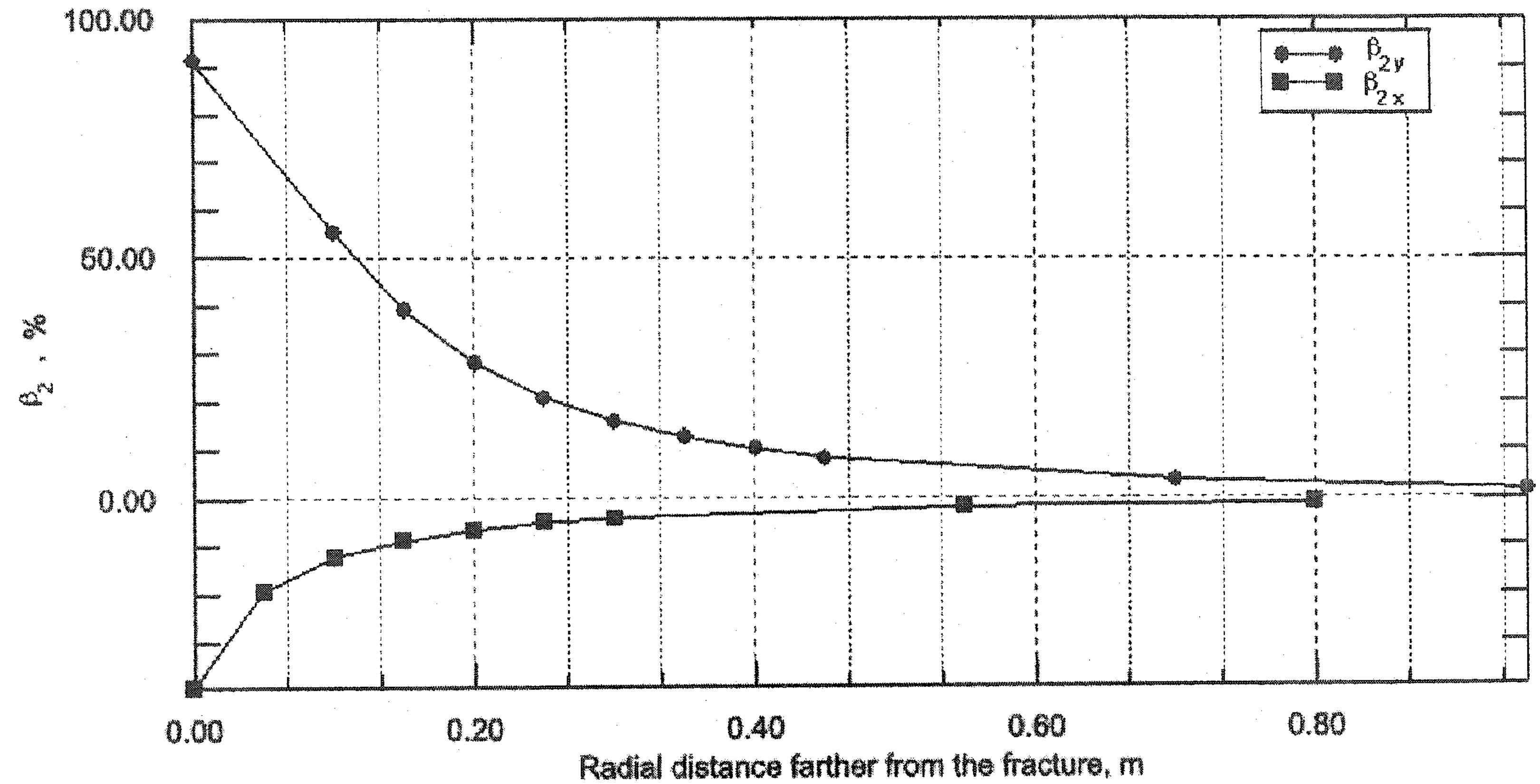

Figure 6.8 – Stress relaxation to the σ_2 with fracture pattern generated by ANFO type explosive destress blast in 38 mm dia borehole (Applied σ_1 = 150 MPa, σ_2 = 91 MPa; σ_1 applied parallel to the X-axis)

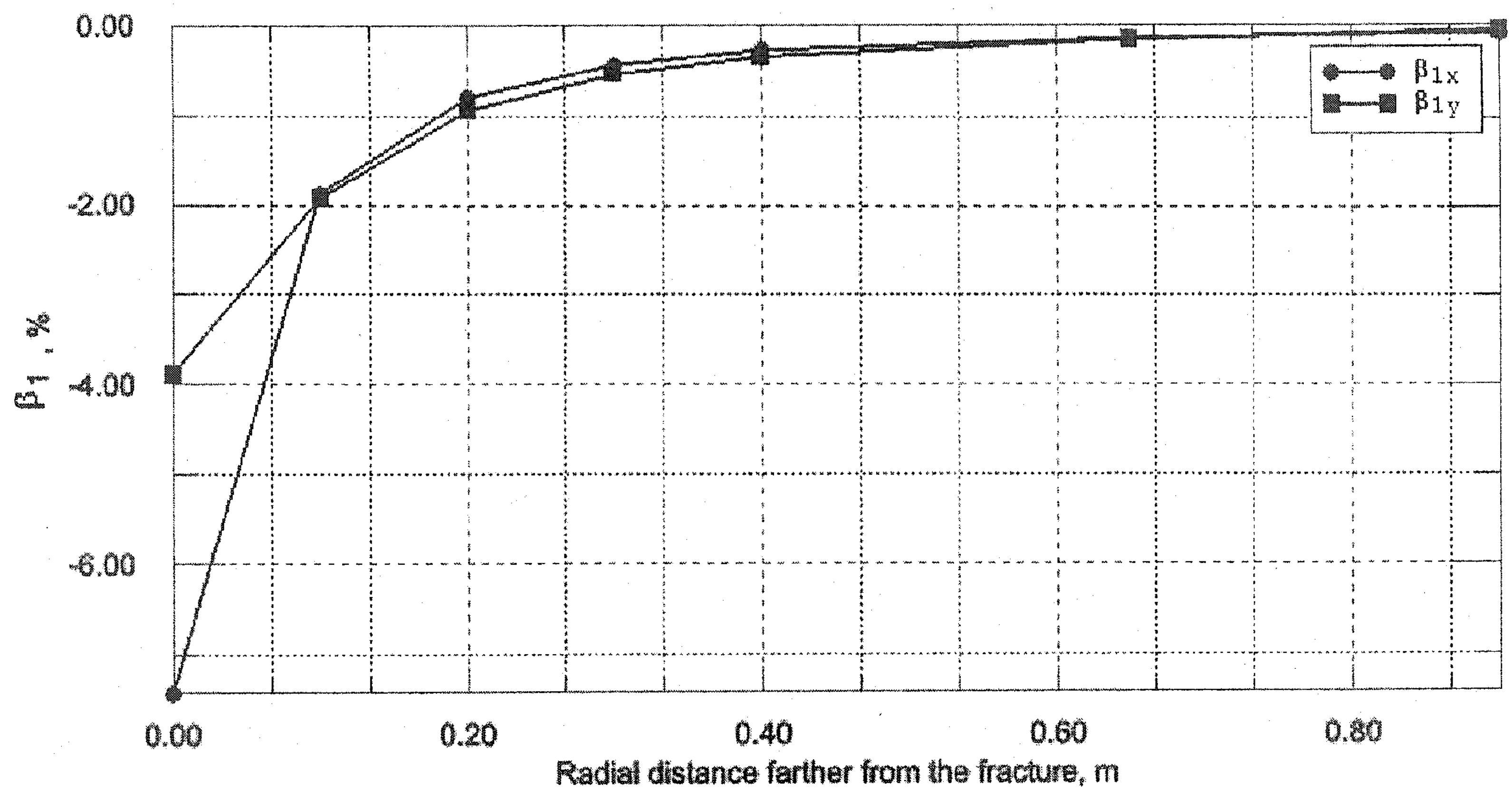

Figure 6.9 – Stress relaxation to the σ_1 with fracture pattern generated by ANFO type explosive destress blast in 38 mm dia borehole

(Applied σ_1 = 300 MPa, σ_2 = 182 MPa; σ_1 applied parallel to the X-axis)

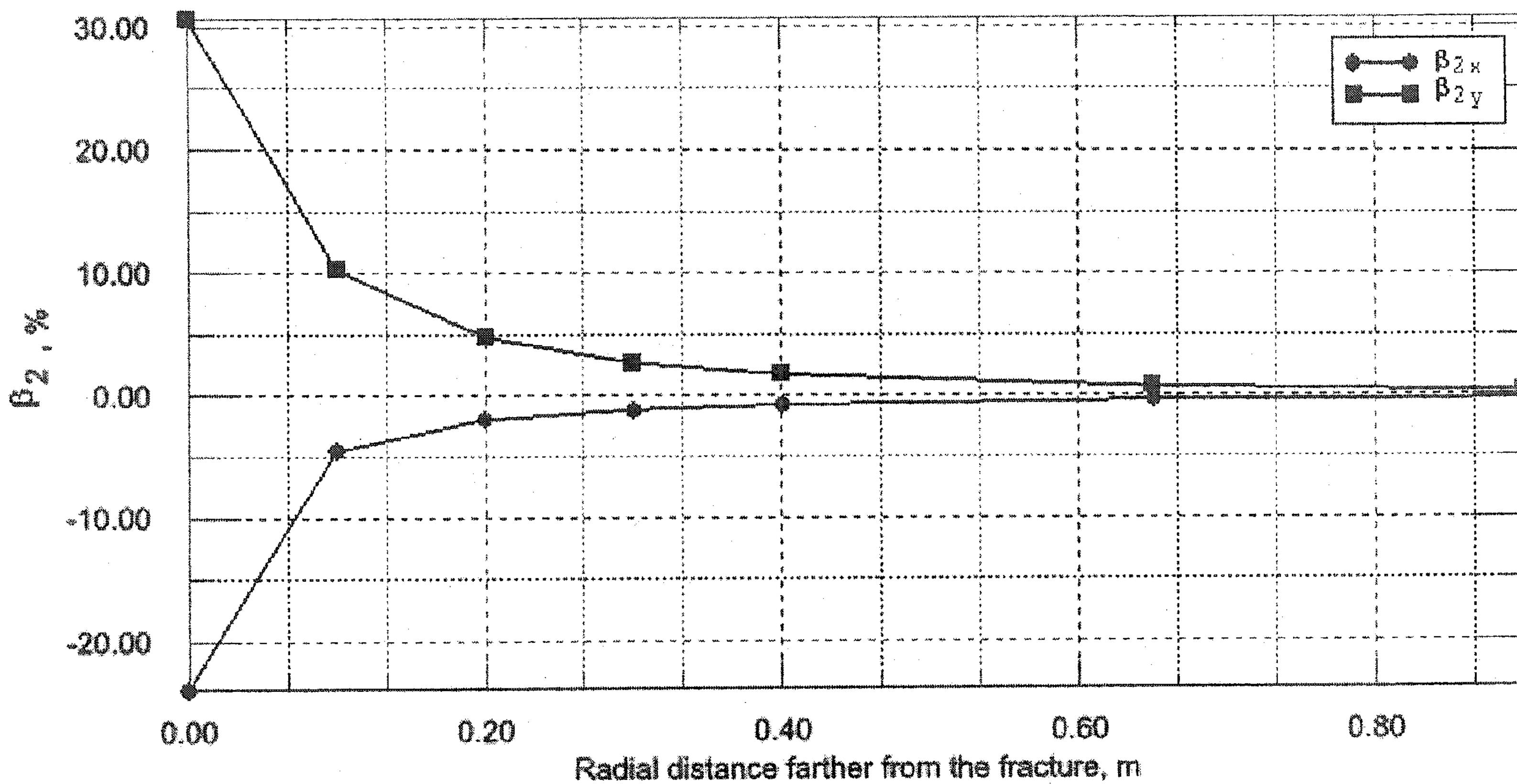

Figure 6.10 – Stress relaxation to the σ_2 with fracture pattern generated by ANFO type explosive destress blast in 38 mm dia borehole (Applied $\sigma_1 = 300$ MPa, $\sigma_2 = 182$ MPa; σ_1 applied parallel to the X-axis)

Analyses of the Results

(i) Figures 6.3 through 6.10 reveal that rock gets more stressed in terms of the major principal stress due to fracture alignment along the major principal direction. The observations are in good conformity with the observations reported by Toper et al. (1994). They reported an increase in the major principal stress value and a reduction in the intermediate principal stress value after experimental destress blasts. Further, the observation presented in Figures 6.3 to 6.10 can explain the inexplicable behaviour observed by CANMET in Sigma I Mine (Labrie et al., 1997) and by SweBeFo in Pyhäsalmi Mine, Finland (Hakami et al., 1990). Post destress blast studies resulted in an increase in the modulus of elasticity in both the studies. Rock stiffening is due to the increase in the major principal stress magnitude, as Figures 6.3 through 6.10 reveal, explains the increase in the elastic modulus. This increased stiffening can be suspected to increase further should fractures grow longer along the major principal stress direction (Compare Figure 6.3 to 6.5 and Figure 6.6 to 6.9).

(ii) Figures 6.3 through 6.10 also indicate that stress relaxation is only achieved in terms of the intermediate principal stress values across the fracture plane (max. stress reduction ≈ 10 per cent at a distance of 0.5 m from away from the fracture zone in Figure 6.8). This relaxation, in conjunction with the increase in the major principal stress value, may result in a differential stress value much higher than the earlier existing ones, leading to stress scenario from bi-axial loading to the uniaxial loading. This change of loading behaviour can induce an even more risky environment than the desired destressing as it is a proven fact that rocks have higher strength in the confinement (for compilation of this behaviour, see Sheorey, 1997).

(iii) Figures 6.3 through 6.10 indicate that the stress increase in the major principal stress magnitude along the fracture propagation direction and the stress relaxation in the intermediate principal stress across the fracture propagation direction is local and confined to a limited distance near the fracture plane. This observation is contrary to the assumption that destress blasting from 38 mm diameter boreholes can reduce face stresses up to 40 per cent of the entire drift of size 4.3 m by 3.7 m as reported by Tang and Mitri, 2001.

6.3 SUMMARY

A new stress relaxation parameter, β_{ij}, is introduced in this chapter. The new parameter addresses the need to characterize the destressing effect. This parameter evaluates change in the principal stresses in a plane, before and after destress blasting. This introduction helped in explaining many phenomena that have hitherto remained unexplained. The parameter adequately explains the reasons for reported increases in Young's modulus with post destress blasting measurements. An increase in the major principal stress magnitude due to fracture growth alignment along the major principal stress direction is found to be the cause. The analyses presented using the β_{ij} for the fracture pattern obtained in Chapter 5 are in good conformity with the field observations by Toper et al (1994).

CHAPTER 7

VALIDITY AND LIMITATIONS OF THE SIMULATIONS

7.1 VALIDITY

The analyses of destress blasting mechanisms presented in the previous two chapters are based on a new numerical procedure, which is developed for the study and it is described in Chapter 4. Brittle rock failure properties obtained from standard laboratory testing (Young's modulus, Poisson's ratio, density and static tensile strength) and the optimized borehole pressure-time profiles are essential requirements for the implementation of the new numerical. The discontinuum nature of discrete fractures generation and their propagation is simulated considering an element elimination technique in a finite element mesh (domain), which essentially remains continuum. The developed numerical procedure is unique and first of its kind. Rigorous proofs are presented for the validation of the developed procedure. To the best knowledge of this researcher, it is the first time that proofs are provided for several important phenomena of rock blasting from a single platform. The important validated phenomena are summarized below.

(i) **Strain rate dependent material response** – The application of the dynamic loads in the 38 mm diameter borehole provided information that the first fracture initiates at 159 MPa for the ANFO type explosive and at 600 MPa for the emulsion type explosive (Figure 4.12, Chapter 4). It is important to mention that the procedure used 15 MPa for the static tensile strength of the rock, which is the criterion for element elimination. The results are in line with the laboratory experiments, which indicate that rocks exhibit much higher strength when subjected to dynamic loading in comparison to the strength obtained by static testing procedures (e.g. Prasad et al., 2000).

(ii) **Distinct fracturing characteristics associated with the different strain rate transient loading** – The application of the dynamic loads in a 38 mm diameter borehole predicted that fracturing by the ANFO type explosive will have a few but longer fractures beyond the crushing zone surrounding the borehole. Contrast to this behaviour, the emulsion type explosive predicted shorter fractures but in large numbers beyond a larger crushing zone surrounding the borehole. Similar behaviour is well documented from laboratory and field observation and is a well-acknowledged phenomenon (e.g. Zhang et al., 2001).

(iii) **Fracturing extent prediction based on the empirical relations** – The application of the dynamic loads in a 38 mm diameter borehole provided results of the fractures zone radius of 487 mm and 341 mm, respectively, for the emulsion type explosive and the ANFO type explosive. The empirical relation provided by Kexin (1995) (Chapter 3, Equation 3.8) predicts 356 mm and 348 mm for the extent of fracture zone radius for the emulsion type explosive and the ANFO type explosive, respectively. The results from the newly developed procedure show close agreement with the predictions of the empirical relation. It is noteworthy to underline that it is easy to obtain the information about the crushing zone and the fracturing zone from the results of the new numerical modelling procedure. Predictions of the crushing zone also show good agreement with the empirical relations provided by Mosinets and Garbacheva (1972) (Equations 3.5 to 3.7, Chapter 3). It is noteworthy to mention that in the developed procedure neither fractures are pre-placed in the domain nor fracture growth sites and paths are pre-specified.

(iv) **Explosive energy consumed in the fracturing** – Numerically, the kinetic energy (provided by the transient loading) change from the peak value of 14.994 kJ to 14.00 kJ for the emulsion type explosive and from 5.97 kJ to 5.80 kJ for the ANFO type explosive (Figure 4.16). This change is due to the energy consumption in the fracturing process. The energy consumption amounts to 6.63 per cent and 2.85 per cent for the emulsion and the ANFO type explosives, respectively. These observations are in line to the observations by Langefors and Kihlstorm (1972) and Nicholls and Hooker (1962). Further, the numerical modelling results validates the well acknowledged fact that very small explosive energy is used for fracturing and a majority of the explosive energy is lost in wave propagation, heat, sound and air-overpressure (Lownds and Du Plessis, 1984). It is important to mention that the newly developed numerical modelling procedure does not incorporate any artificial damping method.

(v) **Inter-relationship of the peak particle velocity with the fracturing extent** - Measurements of the peak particle velocity (PPV) along the wave propagation paths are summarized in Figure 4.18 for both the explosive types simulated with the developed procedure. The correlation of the PPV magnitudes and fracturing extents suggests that the fracturing takes place when the PPV is higher than 1000 mm/sec. The estimation of fracturing zone by PPV measurements is a standard field practice for engineering blasting operations. Several predictor equations are in use for the purpose and the equation by Holmberg and Persson (1979) is the most notable amongst them. Holmberg and Persson (1979) state that the theshold limit for the fracturing in brittle hard rocks is PPV values higher than 1000 mm/sec. Obviously the numerical modelling results are in remarkable agreement with the fracturing zone predictions based on the PPV measurements.

A comprehensive parametric study is made in Chapter 5 by using the validated procedure to investigate basic concepts of destress blasting. The concepts are evaluated with a range of parameters which may largely affect destress blasting in the field. The mining induced stress levels found in drift developments in hard rock mines at 2000 m depth in the Canadian Shield are considered for the analyses. The mining induced stress values considered are in the range of the reported values of a detailed parametric study for drift developments at great depth (Tang and Mitri, 2001). The worst-case scenario is applied to most of the simulations that involve the major principal stress (which is in horizontal direction for the Canadian Shield) and the intermediate principal stress (which is in the vertical direction) perpendicular to the drift development axis. Such assumption is considered the must for the research involving rockbursts hazards in order to avail meaningful information from the worst-case scenario. Further, the critical stress levels considered have value of the major principal stress level close to the bi-axial strength of the brittle rock. This consideration is based on the fact that the confinement ahead to a drift face is bi-axial in nature (Saharan and Mitri, 2003) and the main objective of destress blasting is to relieve from stress concentration, which may have reached to a perilous level (near the bi-axial strength of the rock). Most of the results obtained from the parametric studies are evaluated with the available reported laboratory and field observations made elsewhere. The results are in line to the reported observations. Logical reasonings are presented wherever no previous studies can be traced for the related simulations. Detailed parametric study indicate that the field application of destress blasting involving few small diameter boreholes is not sufficient to achieve the desired destressing, at least for the worst case scenario assumed. Also, proofs are provided with an arrangement involving notched borehole simulations paves the foundation for the possibility to look further development in destress blasting technique for an effective destressing.

Chapter 6 postulates a new stress relaxation parameter, β_{ij}, which provide convincing explanation to the previously inexplicable reported field observations of increase in the major principal stress values (Toper et al., 1994; Hakami et al., 1990) and Young's modulus values (Hakami et al., 1990; Labrie et al., 1997) post to destress blasting experiments. These explanations further cement the validity of the simulations made for the analyses of destress blasting.

7.2 LIMITATIONS OF THE STUDY

Radically different explanations can be propounded to justify the apparent successes with the field application of destress blasting. It is important to note the limitations of the present study. They are listed below.

(i) The rock is considered isotropic in the analyses but in nature it is inherently anisotropic. Therefore, the results may be different from the presented.

(ii) The rock is considered homogeneous in the analyses but in nature it contains microcracks and macrocracks. Destress blasting may generate longer fractures in the presence of such cracks.

(iii) The stress level considered in this research commensurate with the mining induced stresses for a typical mine in the Canadian Shield at 2000 m depth. Many mines are operating at this depth and are faced with rockbursts hazards. Only the worst-case scenario is evaluated in the study, which considered principal stresses to be orthogonal to the drift development axis. The blast-induced fractures are likely to be different than presented here under the lower confinement for shallower depths.

(iv) The principal stresses in the field may be in a direction other than the orthogonal directions to the drift development axis (which was adopted in the thesis). Such consideration may create fractures in a direction that is propitious to stress relaxation.

(v) Another limitations, though not so important (Liu, 1997), arise from the fact that explicit accounting of gas-pressure energy of an explosive is not made in the study. An optimized blasthole pressure profile, similar to a profile obtained from the ANFO type explosives is incorporated in study in order to accommodate direct effect of the gas-pressure energy.

(vi) Due to the demand of the numerical modelling platform, the minimum size of element considered has face length of about 6 mm near the borehole boundary. This means the fractures are represented with this size of elements and the size of elements increases as the distance from the borehole increases. This consideration resulted into representational lapse in the fractures shape and the fracture network appears to be coarser and diverging with the increase in the distance from the boreholes.

Chapter 8

CONCLUSIONS

8.1 CONCLUSIONS

The following conclusions can be drawn from the study:

(1) A critical review of field destress blasting applications presented in Chapter 1, along with the results presented in Chapter 5, indicate that the prevalent destress blasting practice renders more psychological advantages than effective factual destressing. More evidence is available which is an indication for the inability of enough fracturing by blasting in confined brittle rocks.

(2) The literature review presented in Chapter 2, suggests that destress blasting was conceived and first applied in a Canadian coal mine. A few other mines have also reported destress blasting applications before the South African gold mines. These observations are against the common belief that destress blasting evolved in 1950s from the South African gold mines.

(3) Barring any controversies, which exist for the role of different parts of explosive energy in rock fracturing, the analysis in Chapter 3 leads to two distinct observations with respect to the application of destress blasting. First, emulsion type explosives (high shock and low gas content) are required for effective

fracturing of hard brittle rock rather than the ANFO type explosives (low shock and high gas content). Second, de-coupling, air-decking, directional fractures growth techniques, etc. could enhance explosive energy utilization which previously were never considered with destress blasting applications.

(4) Chapter 4 presents the development of a numerical procedure to study rock fracturing by explosive energy. This important development encompasses measurable rock and explosive properties. A noteworthy feature of the developed procedure is that it does not require pre-specification of either the fractures growth sites or the propagation paths. The developed procedure is validated against the established empirical knowledge base and experimental rock behaviour. The fracturing extent predicted by the developed numerical procedure shows remarkable agreement with the empirical equations and a prevalent predictor that uses PPV measurements. The results also show good conformity with the rate dependant material behaviour and damping of explosive energy associated with the rock fracturing though both features are not forced as input parameters. The results presented by the developed procedure are unique and are the first of their kind. The developed numerical procedure provides promising features for the development of better explosive materials, as well as a platform to investigate rock fracturing by explosive energy in order to enhance explosive energy utilization.

(5) Chapter 5 introduces a non-dimensional parameter ℓ_{ci}. The parameter represents the fracturing length along the principal stresses and characterizes the fracturing extent and destressing. Use of the ℓ_{ci} makes it simple to identify the extent of fracturing as well as its impact on destressing. Ratio of ℓ_{c2}/ℓ_{c1} is an indicator about the effectiveness of destress blasting. A higher ratio is needed for effective destressing. The introduction of the ℓ_{ci} is a major shift from the very premise of fracturing by destress blasting, which seeks fracturing of the entire area ahead of an excavation face. Investigations carried out in Chapter 5 confirmed the foundation of the ℓ_{ci}, as fractures due to destress blasting invariably found aligned along the principal stresses. The fracture alignment along the principal stresses

makes it necessary in order to effectively study the destressing phenomena and to look into the directional extent of fractures rather than the amount of fracturing induced. A comprehensive parametric study is presented with Chapter 5 in order to evaluate the fracturing extent with a range of key parameters affecting field destress blasting applications.

(6) The first set of simulations in Chapter 5 investigates the impact of confinement on rock fracturing. It is observed from the analysis of the numerical modelling results that the extent of fractures monotonically decreases with the increase in the confinement level. Numeerical modelling results also revealed that the crushing zone nearly disappears at higher confinements. The observations are the same irrespective of the explosive energy employed. The observations are in good conformity with the reported experimental behaviour.

(7) Analyses of simulations conducted to explore the fracturing pattern involving various differential stresses in Chapter 5, lead to the conclusion that the fractures align along the principal stresses. The extent of fracturing is more along the major principal stress direction. These observations also support previous observations made elsewhere.

(8) The third set of simulations evaluates destress blasting with the confinement commensurate to a 2000 m depth workings in the Canadian Shield. The analyses indicate the ineffective fracturing extent.

(9) Recommended borehole spacing is evaluated in the fourth set of simulations. Reported numerical modelling simulations predict that the extent of fractures is not enough to meet the neighbouring boreholes even at half the borehole spacing suggested by the South African practice.

(10) The fifth and sixth sets of simulations in Chapter 5, relate to exploring the role of rock properties on rock fracturing. The analyses predict that the elastic modulus

and static tensile strength have a negligible role in the extent of fracturing. These results concur with previously documented observations. Also, it is observed that the effects of differential stress on the rock fracturing tend to reduce with the lower Young's modulus values. However, this observation could not be corroborated in the absence of previous studies.

(11) The seventh and eighth sets of simulations in Chapter 5 validate that the emulsion type explosive is better suited for stiff brittle rocks than the ANFO type explosive though explosive energy utilisation is better with ANFO type explosive.

(12) Analyses by the ninth and tenth sets of simulations in Chapter 5 showed that de-coupling and a directional fracture growth technique, notched boreholes, could enhance the explosive energy utilisation for effective destressing. Also, the results showed that longer fractures length, in a direction other than the direction parallel to the major principal stress, can be obtained with the application of directional fractures growth technique, such as notched borehole.

(13) Chapter 6 introduces a non-dimensional parameter β_{ij}. Interesting and important results are obtained with the application of β_{ij} to the simulations conducted in Chapter 5. It could become possible with the obtained results to explain hitherto inexplicable reported field results indicating an increase in the major principal stress values and elastic modulus against the desired relaxation. Measurements by β_{ij} revealed stress relaxation to the intermediate principal stress magnitude across the fractures and stress concentration with the major principal stress magnitude for a limited distance. These results are similar for both the types of explosive characeteristics used in the simulation. These measurements are not only in accordance with the reported field observations, but also, they explain the stress concentration and rock stiffening. Now it can be predictably said that prevalent destress blasting application involving small diameter boreholes in the bi-axial stress confinement would lead to fractures alignment along the principal stress direction. This effect is against the main concept of destressing, which aims for

rock fracturing in a larger area. Noteworthy to mention here, is that this phenomenon is very local. This alignment will lead to stress concentration with the major principal stress magnitude and rock stiffening across the fractures. It has also shown that the increase in the major principal stress magnitude and decrease in the intermediate principal stress magnitude may prove to be more dangerous, as rocks have higher strengths under confinement.

8.2 LIMITATIONS

The study conducted in this thesis is associated with the following limitations:

(1) Blasting is a thermo-mechanical process and only the mechanical behaviour of explosive energy is used in the study. No considerations were made to include the thermal behaviour.

(2) The material model used is suitable only for applications where rock behaves in a brittle manner, i.e., elastic up to the failure point (both in compression and tension) and fails when the tensile stress exceeds the tensile strength (the material model assumes the compressive strength as infinite). This feature was not a limitation to the study. The specific problem investigated in the thesis involves the analysis of rock failure by stresses produced by a dynamic pulse from a circular borehole. The application of this pressure-pulse generates equal amounts of compressive and tensile stresses for any element under question perpendicular to each other and that particular element fails if the tensile strength is violated. Therefore, a material model with an infinite compressive strength and a finite tensile strength had no impact on the accuracy of the results. The material model cannot be applied to cases where rock failure by compressive stresses is important.

(3) The fractures (discontinuum) in the developed numerical procedure are obtained by using a continuum tool and the domain essentially remains continuum.

Therefore, the procedure cannot extend to studies, which result in separate fragments and these fragments interact with each other to form finer fragments.

(4) The study conducted in the thesis represents a specific case of plane stress modelling. The results obtained cannot be applied to explain situations that require either plane strain modelling or 3-dimensional modelling.

8.3 SCOPE OF THE FUTURE RESEARCH

(1) Hopefully, the findings will encourage researchers to build more robust and complex models involving destress blasting between walls and cases for plane strain/3-dimensional modelling in order to further enhance our knowledge of the subject.

(2) A foundation is laid with this study, which makes it appropriate to investigate optimum procedures for stress relaxation by destress blasting.

(3) The logical sequeal of any numerical modelling simulation is verification with laboratory scale studies. Results presented in this thesis need a bi-axial test rig capable of providing accurate confinement, as well as being able to accommodate dynamic blast loads. Such a facility is currently lacking. Endeavours can be made to develop the equipment and re-confirm the model analyses carried out in this thesis before reorganizing field applications.

STATEMENT OF CONTRIBUTIONS

The concept of rock mass fracturing to a larger area (and associated rock mass properties reduction and stress relaxation) by destress blasting has been carried out ever since it was first applied in a Canadian coal mine in the early 1930s, without anyone really challenging it. Since then, the method has been applied across the continents with trial-and-error approach with mixed successes and the method to date lacks a scientific knowledge base. This study took the challenge to investigate this notion at the micro-mechanical level and to identify whether the notion is close to fact or fiction.

A numerical procedure to study rock fracturing by explosive energy was developed in order to accomplish the objectives targeted with the study. The developed procedure is unique and the first of its kind. Neither fracture paths are pre-specified nor fractures are pre-placed. The results obtained with the devloped procedure are in good conformity with the established knowledge base and reported observations. The developed numerical procedure encompasses promising features to investigate rock blasting related issues.

Comprehensive numerical modelling simulations made by using the developed procedure invariably predicted that destress blasting yields fractures aligned along the principal stresses. These observations made it necessary for the introduction of a non-dimensional parameter ℓ_{ci} for evaluating the fracturing extent and destressing. Use of the ℓ_{ci} makes it simple to identify the extent of fracturing, as well as, its impact on the destressing. The ratio of ℓ_{c2}/ℓ_{c1} is an indicator for the effectiveness of destress blasting. A higher ratio is needed for effective destressing. The introduction of ℓ_{ci} is a major shift from the very premise of fracturing by destress blasting, which perceives radial fracturing. Now it can be authoritatively said that it is more important for the effective application of destress blasting to look in the directional extent of fractures rather than remain concerned about the amount of fracturing induced.

Another important development from this thesis is the introduction of a stress relaxation parameter, β_{ij}. The application of β_{ij} made it possible to explain hitherto inexplicable reported field observations of stress concentration and rock stiffening after destress blasting, against the desired relaxation and softening. Now it can be predictably explained that the prevalent destress blasting practice will lead to fracture alignments along the major principal stresses, which will result in the concentration of the major principal stress and rock stiffening across the fractures. The β_{ij} parameter not only offers an explanation to reported field behaviour, but also adequately describes the destressing phenomenon, which is not measurable with the current prevalent techniques.

The literature review made in this study strongly points to the fact that destress blasting evolved in Canada rather than the common belief that it did so from the South African gold mines.

REFERENCES

Abaqus (2003). ABAQUS User's Manuals – Ver. 6.4-1. Abaqus inc., USA.

Aimone, C.T. (1992). Rock breakage: Explosives, blast design. In SME Mining Engineering Handbook (Ed. H.L. Hartman), Society of Mining Engineers, Littleton. 722-746.

Andrieux, P.P., Brummer, R.K., Liu, Q., Simser, B.P. and Mortazavi, A. (2003). Large-scale panel destress blast at Brunswick Mine. CIM Bulletin. 96, 1075. 78-87.

Atlas (1987). Explosives and rock blasting. Atlas Powder Company. Washington, USA.

Adams, D. J., Gay, N. C. and Cross, M (1993). Preconditioning: A Technique For Controlling Rockbursts. In Proc. Rockbursts and Seismicity in Mines (ed. - R. Paul Young), Balkema, Rotterdam. 29-33.

Adams. G. R. and Jager A.J (1980). Petroscopic observations of rock fracturing ahead of stope faces in deep level gold mines. J. of the South African Institute of Mining and Metallurgy. Vol. 80. 204-209.

Adams, G.R., Jager, A., and Roering, G (1981). Investigations of rock fractures around deep-level gold mine stopes. In Proc. 22nd U.S. Rock Mech. Symp, Massachusetts Institute of Technology.

Arjang, B. and Herget, G. (1997). In situ ground stresses in the Canadian hardrock mines: an update. Int. J. Rock Mech. & Min. Sci. 34:3-4. Paper No. 015.

Atchison, T.C. (1968). Fragmentation principles. In Surface mining (Ed. E.P. Pfleider), AIME, New York. 355-372.

Ayres, R.P., Schmidt, M.F.C. and Worsey, P.N. (2000). Effect of boulder geometry on hydraulic fragmentation using small explosive charges. In Proc. 26th annual conf. Explosive and blasting technique. Anthiem, CA, US. 225-232.

Bains, M.J. (1985). On approximate solutions of time-dependent partial differential equations by moving finite element method. Report 85/1, university consortium for industrial numerical analysis.

Barkley, T.L., Lee, R. and Rodgers, J. (2001). A new detonating cord for reducing unwanted damage in controlled blasting. In Proc. 27th annual conf. Explosives and blasting technique, Cleveland, OH, USA. 167-173.

Batzle, M.L., Simmons, G. and Siegfried, R.W. (1980). Microcrack closure under stress: direct observation. Jl Geophy. Research. 85. 7072-7090.

Belytschko, T., Lu, Y.Y. and Gu, L. (1994). Element-free Galerkin methods. Int. Jl. Num Methods in Engg. 37. 229-256.

Bhandari, S. (1997). Engineering rock blasting operations. Rotterdam, Balkema. 375p.

Bhandari, S. and Badal, R. (1990). Post blast study in jointed rocks. Int. J. Eng. Fracture Mechanics. 439-445.

Bhandari, S. and Rathore, S.S. (2002). Comparative study of blasting techniques in dimensional stone quarrying. In Proc. 28th Conf. Explosive and Blasting technique, Society of explosive engineers, Las Vegas, Nevada.

Bhandari, S. and Vutukuri, V.S. (1974). Rock fragmentation with longitudinal charges. In Proc. 3rd Int. Cong. Rock Mech. Denver, US. 1337-1342.

Bickford, W.B. (1994). A first cource in the finite element method. Irwin, USA. 648p.

Biggs, J. M (1964). Introduction to Structural Dynamics. New York: McGraw-Hill.

Bing, Z. and Greenhalgh, S. (1998). A damping method for the computation of the 2.5 green's function for arbitrary acoustic media. Geophysical J. Int. 133, 1. 111-20.

Blair S.C. and Cook, N.G.W. (1998). Analysis of compressive fracture in rock using statistical techniques: Part-I. A non-linear rule-based model. Int. Jl Rock Mech. Min Sci. 35. 837-848.

Blake, W (1972). Rock-burst mechanics, Quarterly of the Colorado School of Mines. Vol. 67, No. 1. pp. 1-64.

Blake, W (1972b). Destressing test at the Galena Mine, Wallace, Idaho, Trans. SME-AIME, September. Vol. 252. 294-299.

Blake, W (1982). Rock preconditioning as a seismic control measure in mines. In Proc. 1st Int. Cong. Rockbursts and Seismicity in Mines, Johannesburg, South African Institue of Mining and Metallurgy. 225-229.

Blake, W (1987). Rockburst occurrences in the Coeur d'Alene mining district, Northern Idaho. In Proc. 6th Int. Conf. Ground Control in Mining, Morgantown, West Virginia.

Blake, W. (1998). Destressing to control rock bursting. In Underground mining methods handbook, SME. Chapter7. 1535-1539.

Board, M.P. and Fairhurst, C. (1983). Rockburst control through destressing, a case example. In Proc. Symp. Rockbursts: Prediction and Control. IMM, London. 91-102.

Boler, F.M. and Swanson, P.L. (1993). Seismicity and stress changes subsequent to destress blasting at the Galena Mine and implications for stress control strategies. USBM-RI 9448. 21p.

Bohloli, B. (1997). Effects of the geological parameters on rock blasting using the Hopkinson split Bar. Int. J. Rock. Mech. Min. Sci. 34, ¾. 630.

Braithwaite, W., Brown, W.B. and Minchinton, A. (1996). The use of ideal detonation computer codes in blast modelling. In Proc. 5th int. sym. rock fragmentation by blasting (FRAGBLAST5) (Ed. - B.Mahanty), Montreal, Quebec, Canada. Rotterdam, Balkema. 37-44.

Brauner, G. (1994). Rockbursts in coal mines and their prevention. Balkema, Rotterdam. 114p.

Brinkmann, J.R. (1987). Separating shock wave and gas expansion breakage mechanisms. In Proc. 2nd Int. Symp. Rock fragmentation by blasting.

Brinkmann, J.R. (1990). An experimental study of the effects of shock and gas penetration in blasting. In Proc. 3rd Int. Symp. Rock fragmentation by blasting, FRAGBLAST3. 55-66.

Brinkmann, J.R., Giltner, S.G. and Gibson, P.A. (1987). Fundamental studies of blasting in narrow-stop gold mines. In Proc. 2nd Int. Symp. Rock Fragmentation by Blasting FRAGBLAST-2. Keystone, Colorado, US. 498-520.

Brown, E.T. (1984). Rockbursts: prediction and control. Tunnels and Tunnelling. April. 17-19.

Brummer, R. K. (1988). Active methods to combat the rockburst hazard in S. African gold mines. In Proc. Conf. on Applied Rock Engineering (CARE 88), Univ. Newcastle-upon-Tyne, Pub. Institute of Mining and Metalurgy, London. 35-43.

Brummer, R.K. and Andrieux, P.P. (2002). A design methodology for destress blasting. In Proc. 5th North American Rock Mech Symp. (NARMS-TAC 2002) - Mining and Tunnelling Innovation and Opportunity (eds. – R. Hammah, W. Bawden, J. Curran and M. Telesnicki). Univ. of Toronto, Canada. Univ. of Toronto press. 165-172.

Brummer, R.K. and Rorke, A.J. (1988). Case studies on large rockbursts in South African gold mines. In Proc. 29th US. Symp. Rock Mech. – Key questions in in rock mech. (Eds. – P.A. Cundall, R.L. Sterling, A.M. Starfield). Minneapolis, Minneapolis, USA. Rotterdam, Balkema. 323-329.

Brummer, R.K. and Rorke, A.J. (1984). Mining induced fracturing around deep gold mine stopes. Research report No. 38/84, Chambers of Mines of South Africa, Johhanesburg.

Bussey, J. and Borg, D.G. (1989). Pre-splitting with the new air-deck technique. J. Explosives engineering. Vol. 6, No. 6. 28-31.

Calder, P. (1977). Perimeter blasting (Chapter 7 – Pit slope manual). CANMET report 77-14.

Camacho, G.T. and Ortiz, M. (1996). Computational modelling of impact damage in brittle materials. Int. J. Solids Structures. 33, 20-22. 2899-938.

Cho, S.H., Miyake, H., Kimura, T. and Kaneko, K. (2003). Effect of the waveform of applied pressure on rock fracture process in one free-face. J. Sc. Tech. Energetic Mat. 64, 3. 116-25.

Christian I.D (1939). Rockbursts at the Teck-Hughes Mines. CIM Bulletin. Vol. XLII, No. 331. 530-567.

Clark, G.B. (1987). Principles of rock fragmentation. John Wiley & Sons Inc., London. 610p.

Cook, J. F. and Bruce, D (1983). Rockbursts at Macassa Mine and the Kirkland Lake mining area. In Proc. Symp. Rockbursts: Prediction and Control, IMM, London. 81-90.

Cook, J. F (1982). Notes on rock burst problems with particular reference to 61-38 stope, Macassa mine. Report of Golder Associates: Consulting Geotechnical and Mining Engineers.

Cook, N.G.W., Hoek, E., Pretorius, J.P.G., Ortlepp, W.D. and Salamon, M.D.G (1966). Rock mechanics applied to rockbursts. Journal of the South African Institute of Mining and Metallurgy. May. 435-528.

Corp, E.L (1981). Rock mechanics research in the Coeur d'Alene mining district. In Proc. Conf. Application Rock Mechanics to Cut and Fill Mining, Lulea, Sweden. Pub. Institute of Mining and Metalurgy. 40-48.

CRRP (1996). A comprehensive summary of five years of collaborative research on rockbursting in hard rock mines. CAMIRO Mining Division, Canadian Rockburst Research Program. Book 1.

Crouch, S.L. and Fairhurst, C. (1973). Analysis of rock deformations due to excavation. In Proc. ASME Symp. On Rock Mech. 26-40.

Crouch, C.L. and Starfield, A.M. (1983). Boundary element methods in solid mechanics. London: GeorgevAllen and Unwin. 322p.

Cruse, T.A. (1969). Numerical solutions in three-dimensional elastostatics. Int. J. Solids Struct., 5. 1259-74.

Cundall, P.A. (1971). A computer model for simulating progressive, large scale movements in blocky rock systems. In Proc. Int Symp. Rock Fracture. Vol. I, paper II-8. ISRM, Nancy.

Cundall, P.A. and Hart, R.D. (1993). Numerical modelling of discontinua. In comprehensive rock engineering (Ed. – Hudson, J.A.). Vol. 2. Pergamon press, Oxford. 231-243.

Curran, D.R., Seaman, L. and Shockey, D.A. (1987). Dynamic failure of solids. Physics reports. 147. 253-388.

Daehnke, A., Rossmanith, H.P. and Knasmillner, R.E. (1996). Blast-induced dynamic fracture propagation. In Proc. 5th Int. Symp. Rock Fragmentation by Blasting, FRAGBLAST5 (Ed. B. Mohanty), Montreal, Canada. 619-626.

Daehnke, A., Rossmanith, H.P. and Napier, A.L. (1997). Gas pressurization of blast induced conical cracks. Int. J. Rock Mech. Min. Sci. Vol. 34, No. ¾. Paper No. 263.

Dally, J.W., Fourney, W.L. and Holloway, D.C. (1975). Influence of containment of the borehole pressures on explosive induced fracture. Int. J. Rock Mech. Min. Sci. & Geomech. Abstr. Vol. 12. 5-12.

Dally, J.W., Fourney, W.L. and Peterson, A.L. (1978). A dynamic photoelastic evaluation of some current practices in smooth wall blasting. Mining Engineering. February. 184-189.

Daniel, R. (2003). Pressure-time history of emulsion explosives. Personal communications.

Desai, C.S. and Zaman, M.M. (1984). Thin-layer element for interfaces and joints. Int. J. Num. Anal. Methods Geomech. 8. 19-43.

Dickhout, M.H (1962). Ground control at the Creighton Mine of the International Nickel Company of Canada Limited. In Proc. 1st Can. Rock Mech. Symp., McGill University, Montreal. 121-139.

Diederichs, M.S. (1999). Instability of hard rockmasses: The role of tensile damage and relaxation. (Unpublished) PhD thesis, University of Waterloo, Canada. 610p.

Diest, F.H. (1973). A new digital method for three dimensional stress analysis in elastic media. Jl. Rock Mech. 5. 189-202.

Donze, F.V., Bouchez, J. and Magnier, S.A. (1997). Modeling fractures in rock blasting. Int. J. Rock Mech. Min. Sci. 34, 8. 1153-1163.

Donze, F.V., Hotiet, N. and Bernasconi, P. (2002). Optimization of the blasting patterns in shaft sinking. In Proc. 5th North American Rock Mech. Symp. - NARMS-TAC 2002 (Eds. – R. Hammah, W. Bawden, J. Curran and M. Telesnicki). Univ. of Toronto press, Toronto, Canada. 999-1005.

Duvall, W.I. (1953). Strain wave shapes in rock near explosions. Geophysics. 18, 2. 310-23.

Edgeston, H.E. and Barstow, F.E. (1941). Further studies of glass fracture with high speed photography. J. the American Ceramic Society. Vol. 24. 131-137.

Etoh, S. Hamashima, H., Murata, K. and Kato, Y. (2002). Determination of JWL parameters from underwater explosion tests. In 12th Int. Detonation Symp. (poster session). San Diego, California.

Fang, Z. and Harrison, J.P. (2002). Development of local degradation approach to the modelling of brittle fracture in heterogeneous rocks. Int. J. Rock Mech. Min. Sci. 39. 447-57.

Fickett, W. and Davis, W.C. (1979). Detonation: 26. Berekeley: Univ. California Press.

Fogelson, D.E., Duvall, W.I. and Atchison, T.C. (1959). Strain energy in explosion-generated strain pulses in rock. U.S. Dep. Inter., Bur. Mines, Report of Invesitigations 5514.

Fotoohi, K. and Mitri, H.S. (1996). Non-linear fault behaviour near underground excavations – a boundary element approach. Int Jl. Num. And Analy. Methods in Geomech. 20. 173-190.

Fourney, W.L. (1993). Mechanics of rock fragmentation by blasting. In Comprehensive rock engineering- principles, practices and projects (ed.-in-chief – J.A. Hudson). Pergamon Press. Vol. 1. 39-70.

Fourney, W.L., Dally, J.W. and Holloway, D.C. (1978). Controlled blasting with ligamented charge holders. Int. J. Rock Mech. Min. Sci. and Geomech. Abstr. 15. 121-129.

Fourney, W.L., dick, R.D., Wang, X.J. and Wei, Y. (1993). Fragmentation mechanism in crater blasting.Int. J. Rock Mech. Min. Sci. & Geomech. Abstr. 30, 4. 413-429.

Freund, L.B. (1990). Dynamic fracture mechanics. Cambridge university press, Cambridge, UK. 563p.

Frantzos, D.C. (1989). Finite element analysis of radial cracking mechanism around blastholes using measured pressure-time curves for low density ammonium nitrate/ fuel oil. (Unpublished) PhD thesis. Dep of Mining Eng, Queen's Univ., Canada. 290p.

Gay, N.G., Spencer, D., Van Wyk, J.J. and Van Der Heever, P.K. (1984). The control of geological and mining parameters on seismicity in the Klerksdrop gold mine district. In Proc. 1st Int. Cong. on Rockbursts and Seismicity in mines (eds. – N.C. Gay and E.H. Wainwright). South African National Group on Rock Mech, SAIMM. Johannesburg. 107-120.

Gemant, A. and W. Jackson (1937). The Measurement of Internal Friction in Some Solid Dielectric Materials. The London, Edinburgh and Dublin Philosophical Magazine and Journal of Science. XXII. 960-83.

Giltneer, S.G. (1992). Proposed method for preconditioning stope faces with small diameter blastholes. COMIRO internal note No. 06/92.

Goodman, R.E., Taylor, R.L. and Brekke, T.L. (1968). A model for the mechanics of jointed rocks. J. Soil Mech. Found. Div. ASCE. 94. 637-59.

Grady, D.E. and Kipp, M.E. (1993). Dynamic fracture and fragmentation (In – High-pressure shock compression of solids; eds. – J.R. Asay and M. Shahinpoor). Springer, N.Y. 265-322.

Grodner, M. (2001). Delineation of rockburst fractures with ground penetrating radar in the Witwatersrand Basin, South Africa. Int. J. Rock Mech. Min. Sc. 38. 885-891.

Hakami, H., Kankkunen, J., O'Flahery, T. and Olsson, M. (1990). Destress blasting experiments at the Pyhasalmi Mine, Finland. SveDeFo, Stockholm, Sweden. Report No. DS 1990:3.

Hanson, D., Malinski, D., Kazakidis, V., Laverdure, L., and Brummer R.K. (1992). The design and evaluation of a destress blast at Strathcona mine. In Proc. 16th Canadian Rock Mech. Symp. Laurantian University, Sudbury. 15 June. 35-42.

Hanson, D., Quesnel, W. and Hong, R (1987). Destressing a rockburst prone crown pillar Macassa Mine. Division Report MRL 87-82(TR), CANMET, Energy, Mines and Resources, Canada.

Hart, R.D. (1993). An introduction to distinct element modelling for rock engineering. In Comprehensive rock engineering, vol. 2 (Ed. – J.A. Hudson). Pergoman Press, Oxpford. 245-61.

He, H., Liu, Z., Nakamura, K., Abe, T., Wakabayashi, K., Okada, K., Nakayama, Y., Yoshida, M. and Fujiwara, S. (2002). Determination of JWL equation of state parameters by hydrodynamically analytical method and cylinder expansion test. Jl. Japan Explosives soc. 63, 4. 197-203.

Hedley, D.G.F (1992). Rockburst handbook for Ontario Hardrock Mines, CANMET Special Report SP92-1 E, ISBN-660-14549-9.

Hill, F.G., and Plewman, R.P (1957). Destressing: a means of ameliorating rockburst conditions: Part2: implementing destressing with a discussion of the results so far obtained. , J. the South African Institute of Mining and Metallurgy (SAIMM). October.

Hilleborg, A., Modeer, M. and Petersson, P.E. (1976). Analysis of Crack Formation and Crack Growth in Concrete by Means of Fracture Mechanics and Finite Elements. Cement and Concrete Research. vol. 6. 773-82.

Haimson, B. C. and Chang, C. (2000). A new triaxial cell for testing mechanical properties of rock, and its use to determine rock strength and deformability of Westerly granite. Int. Jl. Rock Mech. & Geomech. & Min. Sc. 37. 285-96.

Hao, H., Ma, G.W. and Zhau, Y.X. (1998). Numerical simulation of underground explosions. Int. J. Blasting by Fragmentation (FRAGBLAST). 2. 383-95.

Hao, H., Wu, C. and Zhau, Y. (2002). Numerical analysis of blast-induced stress waves in a rock mass with anisotropic continuum damage models, Part I : equivalent material property approach. Rock Mech. Rock Engg. 35, 2. 79-94.

Hazzard, J.F. , Young, R.P. and Maxwell, S.C. (2000). Micromechanical modeling of cracking and failure in brittle rocks. J. Geophy. Res. 105, B7. 16683-97.

Hocking, G. (1976). Three dimensional elastic stress distribution around the flat end of a cylindrical cavity. Int. J. Rock Mech. Min. Sci. 13. 331-37.

Holloway, D.C., Barnholt, G. and Wilson, W.H. (1986). A field study of Fracture control techniques for smooth wall blasting. In Proc. 27th US Symp Rock Mech., Tuscloosa. 456-463.

Holmberg, R. and Persson, P.A. (1979). Design of tunnel perimeter blasthole pattern to prevent rock damage. Tunneling '79. Inst. Min. and Metall., London. 280-283.

Hughes, T.G. and Pritchard, R. (1994). In-situ flat-jack tests matching new mechanical interpretations. 10th int. brick/ block masonary conf., Calgary, Canada.

Hudson, J. A. (1993). The construction process. In Comprehensive rock engineering – principals, practices and projects, vol. 4 (Ed.-in-chief Hudson, J.A.). Pergoman Press. 1-38.

Johnston, J.C. and Einstein, M..H (1990). A survey of mining associated seismicity. In Proc. 2nd Int. Symp. Rockbursts and Seismicity in Mines, Minneapolis, Balkema. 121-128.

Johnson, G.R. and Holmquist, J.J. (1992). A computational constitutive model for brittle materials subjected to large strains, high strain rates, and high pressures. In Proc. Shock-wave and high strain-rate phenomena in materials (eds. – M.A. Meyers, L.E. Murr and K.P. Stuaudhanmel). Marcel Dekker, N.Y. 1075-1081.

Jing, L. and Hudson, J.A. (2002). Numerical methods in rock mechanics. Int. J. Rock Mech. Min. Sci. 39. 409-27.

Jung, W.J., Utagava, M., Ogata, Y., Seto, M., Katsuyama, K., Miyake, A. and Ogava, T. (2001). Effects of rock pressure on crack generation during tunnel blasting. Jl. Japan Explosives Soc. 62, 3. 138-46.

Itasca (2001). FLAC3D 2.0 manuals. Itasca consulting Group Inc. Minneapolis, MN, USA.

Karwoski, W. J., McLaughin, W. C. and Black, W (1979). Rock preconditioning to prevent rock bursts-report on a field demonstration. United States Department of the Interior, Bureau of Mines, Report of investigations 8381.

Kexin, D. (1995). Maintenance of roadways in soft rock by roadway-rib destress blasting. China Coal Society. 20, 3. 311-316.

Khoshrou, S.H. (1996). Theoretical and experimental investigation of wall-control blasting methods. Unpublished PhD thesis, McGill University.

Khoshrou, S.H. and Mohanty, B. (1996). Role of discontinuity on stress-field in wall control blasting. In Proc. 5th int. sym. rock fragmentation by blasting (FRAGBLAST5) (Ed. - B.Mahanty), Montreal, Quebec, Canada. Rotterdam, Balkema. 207-216.

Kikuchi, N. (1983). Remarks on 4CST elements for incompressible materials. Computer Methods in Applied Mechanics and Engineering. 37. 109-23.

Kirby, I.J. and Lieper, G.A. (1985). A small divergent detonation theory for intermolecular explosives. In Proc. 8th Int. Symp. Detonation. Albuquerque, New Maxico.

Kranz, R.I. (1983). Microcracks in rocks: a review. Tectonophysics. 100. 449-480.

Kutter, H.K. (1967). The interaction between stress wave and gas pressure in the fracture process of an underground explosion in rock, with particular application to presplitting. (Unpublished) PhD Thesis. Univ. of Minnesotta, Minneapolis. 234p.

Kutter, H.K. and Fairhurst, C. (1971). On the fracture process in blasting. Int. J. Rock Mech. Min. Sci. Vol. 8. 181-202.

Labrie, D., Plouffe, M., Harvey, A. and Major, C. (1997). Destress blast testing at Sigma Mine: experimentation and results. In 19th session on blasting techniques of the Societe d'Energie Explosive du Quebec, Quebec City. 26p.

Ladegaard-Pedersen, A., Fourney, W.L. and Dally, J.W. (1974). Investigation of pre-splitting and smooth blasting techniques in construction blasting. Univ. of Maryland, Report to the Nat. Sc. Foundation.

Langefors, U. and Kihlstorm, B. (1978). The modern techniques of rock blasting. 3rd edition. John Wiley & Sons Inc., New York. 438p.

Leckie, F.A. and Hayhurst, D.R. (1974). Creep rupture of structures. In Proc. Roy. Soc. London Ser. A. A240. 323-47.

Lee, J. (1996). Theory and implementation of plastic-damage model for concrete structures under cyclic and dynamic loading. (Unpublished) PhD thesis. Civil and Env. Eng., Univ. of Calif., Berkeley. 151p.

Lee, J.S. and Pande, G.N. (1999). A new joint element for media having discrerte discontinuities. Mechanics of Cohesive Frictional Materials. Vol. 4. 487-504.

Lemaitre, J. (1971). Evaluation of dissipation and damage in metals submitted to dynamic loading. In proc. ICM I. Kyoto, Japan.

Lemaitre, J. (1985). A Continuous damage mechanics model for ductile fracture. J. Engrg. Materials Tech. 107. 83-89.

Li, Z. and Reed, M. (1995). A finite element method to model progressive fracturing. Comput. Methods Appl. Mech. Engrg. 120. 303-13.

Lightfoot, N., Goldbach, O.D., Kullmann, D.H. and Toper, A.Z (1996). Rockburst control in the South African deep level gold mining industry. In Proc. The 2nd North American Rock Mech. Symp., NARMS 96 (eds. - Aubertin, Hassani and Mitri), Balkema, Rotterdam. 295-303.

Lima, A.D.R., Romanel, C., Roehl, D.M. and Araujo, T.D. (2002). An adaptive strategy for the dynamic analysis of rock fracturing by blasting. In Proc. Int. Conf . Computational Eng. & Sci . (ICES'02). Reno, Nevada.

Liu, L. (1997). Continuum modelling of rock fragmentation by blasting. (Unpublished) PhD thesis. Department of mining engineering, Queen's university, Kingston, Ontario, Canada. 240p.

Liu, L. and Katsabanis, P.D. (1996). Numerical modelling of the effects of air decking/ decoupling in production and controlled blasting. In Rock fragmentation by blasting, FRAGBLAST 5 (Ed. - B. Mohanty). Montreal, Canada. 319-330.

Liu, L. and Katsabanis, P.D. (1997). Development of a continuum damage model for blasting analysis. Int. J. Rock Mech. Min. Sci. 34, 2. 217-31.

Liu, Q., Blaine, E. and Chung, S. (2003). Advanced blasting technology for large scale destress blast at Brunswick Mine. In Proc. CIM Montreal 2003 Conf. And Exhibition (On CD ROM).

Lownds, C.M. (1986). The strength of explosives. In Proc. The planning and operation of open-pit and strip mines (ed. J.P. Deetlefs), South Africa Institute of Mining and Metallurgy, Johannesburg. 151-159.

Lownds, C.M. and Du Plessis, M.P. (1984). The behaviour of explosives in intermediate-diameter boreholes. In Proc. Inst. Quarrying Trans. December. 709-804.

Lysmer, J. and Kuhlemeyer, R.L. (1969). Finite dynamic model for infinite media. J. Eng. Mech. Div. ASCE. 92, SM1. 65-91.

Massarsch, K.R. (1992). Static and dynamic soil displacements caused by pile driving. In Application of stress-wave theory to piles (ed. – F.B.J. Barends). Balkema, Rotterdam. 15-24.

MacDonald, P., Wiles, T. and Villeneuve, T (1988). Rock Mechanics aspects of vertical retreat mining at 2000 m depth at Creighton Mine. In Proc. CARE 88, Univ. Newcastle-upon-Tyne, Pub. IMM, London. 151-158.

Malan, D.F. and Napier, J.A.L. (1995). Computer modelling of granular material microfracturing. Tectonophysics. 248. 21-37.

McHugh, S (1983). Crack extension caused by internal gas pressure compared with extension caused by tensile stress. Int. J. of Fracture. Vol. 21. 139-145.

McHugh, S. and Keough, D. (1982). Use of laboratory derived data to predict fracture and permeability enhancement in explosive pulse tailored field tests. In Proc. US Symp. Rock Mech., Issues in Rock Mech. 504-514.

McInnes, D., Wilton-Clark, H. and McLachlan, T. (1959). Report of the royal commission on the bump in Springhill No. 2 Mine, October 23, 1958. Ottawa: Queen's printer.

Metzger, D.R. (2003). Adaptive damping for dynamic relaxation problems with non-monotonic spectral response. Int. J. Numer. Meth. in Engng. 56. 57-80.

Mishnaevsky Jr., L., Lippmann, N. and Schmauder, S. (2001). In Proc. IMECE 2001 (Int. Mech. Eng. Cong. Exposition), N.Y. 1-7.

Mishnaevsky Jr., L., Mintchev, O. and Schmauder, S. (1998). FE-simulation of crack growth using a damage paramerter and the cohesive zone concept. In Proc. ECF12 – fracture from defects (12th European conference on fracture; eds. – M.W. Brown, E.R. de los Rios and K.J. Miller). London, EMAS. 2. 1053-59.

Mishnaevsky Jr., L.L. and Schmauder, S. (2001). Continuum mesomechanical finite element modelling in materials development: A state-of-the-art-review. Appl. Mech. Rev. 54, 1. 49-69.

Mitri, H.S. (2002). Lecture notes – Finite element methods in Rock Mech.

Mitri, H.S. (2000). Practitioner's guide to destress blasting in hard rock mines. McGill University.

Mitri, H.S. (1996). Study of rockburst potential at Sigma Mine, Val D'Or, Quebec using numerical modelling. Final report.

Mitri, H.S., Edrissi, R. and Henning, J. (1994). Finite element modelling of cable-bolted stopes in hard rock underground mines. In Proc. Society for Min., Met and Exploration Inc. Reprint No. 94-116.

Mogi, K. (1972). Effect of the triaxial stress system on fracture and flow of rocks. Phy. Earth Planet Interiors. 5. 318-24.

Mohammad, N., Reddish, D.J. and Stace, L.R. (1997). Relation between in situ and laboratory rock properties used in numerical modelling. Int. J. Rock Mech. Min. Sci. 34, 2. 289-297.

Mohanty, B. (2003). Personnel communications.

Momayaz, M., Hara, A., Hassani, F.P. and Sadri, I. (1994). Application of GPR for a more efficient mine planning. In Proc. The 5th Int Conf. Ground Peneterating Radar (GPR'94). Kitchener, Ontario, Canada. 883-94.

Mosinets, V.N. and Garbacheva, N.P (1972). A seismological method of determining the parameters of the zones of deformation of rock by blasting. Soviet Mining Science. Vol. 8, No. 6. 640-647.

Morrison, R.G.K. (1942). Report on rockburst situation in Ontario mines. Trans. Canadian Institute of Mining and Metallurgy. Vol. 45. 225-272.

Mortazavi, A. and Katsabanis, P.D. (2001). Modelling burden size and strata dip effects on the surface blasting process. Int. Jl. Rock Mech. Min. Sci. 38. 481-98.

Moruzi, G.A. and Pasieka, A.R. (1969). Evalaution of a blasting technique for destressing ground subject to rockburting. In Proc. 5th Canadian Symp. Rock Mech., Mines branch, Queen's printer, Ottawa. 185-204.

Nakajima, I. and Watanabe, Y. (1981). Acoustic emission during advance boring associated with the prevention of cola and gas outbursts. In Proc. 3rd Conf. Acoustic Emission/ Microseismic Activity in Geologic Structures and Materials. P.A. State Univ., Univ. Park, Pansylvania, USA. 529-548.

Nakamura, Y. (1999). Model experiments on effectiveness of fracture plane control methods in blasting. Int. J. Blasting and Fragmentation (FRAGBLAST). 3. 59-78.

Nakayama, Y., Matsumura, T., Iida, M. and Yoshida, M. (2001). Propagation of blast waves initiated by a solid explosive in a cylinder. J. Japan Explosives Soc. 62, 5. 244-256.

Napier, J.A.L., Daehnke, A., Dede, T., Hildyard, M.W., Kujipers, J.S.., Malan, D., Sellers, E.J. and Turner, P.A. (1997). Quantification of stope fracture zone behaviour in deep level gold mines. J. the South African Inst. Of Min. and Met. (SAIMM). Vol. 97. 119-134.

Nemes, J.A. and Eftis, J. (1993). Constitutive modelling of the dynamic fracture of smooth tensile bars. Int. J. plasticity. 9. 243-70.

Neumann, M., Makuch, A., Hedley, D. and Blake, W. (1987). Practical applications of pillar destressing at Campbell Red Lake Mine. In Proc. 8th U/G Operators Conf., CIM.

Nicholls, H.R. and Hooker, V.E. (1962). Comparative studies of explosives in salt. U.S. Bur. Mines R.I. 6041. 46p.

Nie, S.L. and Olsson, M. (2000). Study of mechanism by measuring pressure history in blast holes and crack lengths in rock. In Proc. 27th annual conf. Explosives and Blasting Technique. Orlando, US. 291-300.

Obert, L. (1962). Effects of stress relief and other changes in stress on the physical properties of rocks. USBM- RI – 6053. 8p.

Obert, L. and Duvall, W (1967). Rockbursts, Bumps, and Gas Outbursts, chapter 19 in 'Rock Mechanics and the Design of Structures in Rock'. John Wiley and Sons Inc. 582-593.

O'Donnell, J.D.P. (1992). The use of destress blasting at Inco's Creighton mine. In Proc. MASSMIN 92, SAIMM, Johannesburg. 71-74.

Olatidoye, O., Sarathy, S., Jones, G., McIntyre, C. and Milligan, L. (1998). A representative survey of blast loading models and damage assessment methods for buildings subject to explosive blasts. Report by Nichols Research Corporation. Report No. CEWES MSRC/PET TR/98-36. 14p.

Oliver, P., Wiles, T., MacDonald P. and O'Donnell, D (1987). Rockburst control measures at Inco's Creighton Mine. In Proc. 6th Conf. Ground Control in Mining, Morgantown, West Virginia.

Olsson, M., Nie, S., Bergqvist, I. And Ouchterlony, F. (2001). What causes cracks in rock blasting? In Proc. EXPLO2001. Hunter valley, NSW, Australia. 191-196.

Pande, G.N., Beer, G. and Williams, J.R. (1990). Numerical methods in rock mechanics. John Wiley and Sons, England. 327p.

Pandolfi, A. and Ortiz, M. (2002). An efficient procedure for three-dimensional fragmentation simulations. Eng. with computers. 18. 148-159.

Poliakov, A.N.B. (1999). Modelling of tectonic problems with PAROVOZ: examples of lithospheric rifting and buckling. In Proc. Flac and numerical modelling in geomechanics (eds.- Detournay and Hart). Balkema, Rotterdam. 165-72.

Potapov, A. and Campbell, C.S. (1996). A hybrid finite element simulation of solid fracture. Int. J. modern physics. C7, 2. 155-80.

Prasad, U., Mohanty, B. and Nemes, J.A. (2000). Dynamic Fragmentation of Selected Rocks Under Impact Loading. In Proc. 4th North American Rock Mech. Symp., Seattle, Washington, pp. 577-581.

Ramshaw, C.L., Selby, A.R. and Bettess, P. (1998). Computation of the transmission of waves from pile driving. In ground dynamics and man made processes (Ed. B.O. Skipp). T. Telford Pub., London. 115-28.

Reddish, D.J., Stace, L.R. and Whittles, D.N. (2003). Numerical modelling of longwall panels as an aid to mine layout design. In Proc. CIM Montreal 2003 Conf. And Exhibition (On CD ROM).

Repetto, E.A., Radovitzky, R. and Ortiz, M. (2000). Finite element simulation of dynamic fracture and fragmentation of glass rods. Comput. Methods Appl. Mech. Engrg. 183. 3-14.

Rienferg, J. (1991). Statistical evaluation and time series analysis of microseismicity, mining, and rock bursts in a hard-rock mine. United States Dep. of the Interior, Bureau of Mines, RI 9379.

Robertson, N.J., Hayhurst, C.J. and Fairlie, G.E. (1994). Numerical simulation of explosion phenomena. Int J. Computer Appl. Tech. 7, 3-6. 316-29.

Rorke, A J and Brummer, R K (1990). The use of explosives in rockburst control techniques. In Proc. 2nd Int. Symp. Rockbursts and seismicity in mines (Ed.- C. Fairhurst), Minneapolis, Minnesota. A.A. Balkema, Rotterdam. June. 377-386.

Rorke, A.J., Cross, M., Van Antwerpen, H.E.F. and Noble, E (1990). The mining of a small up-dip remnant with the aid of preconditioning blasts. In Proc. Int. Deep Mining Conf., Johannesburg, SAIMM, Symposium Series S10. 765-774.

Roux, A.J.A., Leeman, E.R. and Denkhaus, H.G (1957). Destressing: a means of ameliorating rockburst conditions. Part 1: the concept of destressing and results obtained from its application. South Africa Institute of Mining and Metallurgy. October. 101 -127.

Ryu, C.H. (2002). Computer modeling of dynamic ground motion due to explosive blasting and review of some modeling problems. J. Japan Explosives Society. 63, 5. 217-22.

Saharan, M.R. and Mitri, H. (2003). Analysis of distress blasting techniques: A systematic approach. In Proc. 56th Canadian Geotech. Conf. (paper No. G070 on CD-ROM). Sep. 29-Oct. 1, 2003. Winnipeg, Canada.

Salamon, M.D.G. (1963). Elastic analysis of displacements and stresses induced by the mining of seam or reef deposits –part I. Jl. South African Inst. Min and Metall. 64. 129-149.

Salamon, M.D.G. (1964a). Elastic analysis of displacements and stresses induced by the mining of seam or reef deposits –part II. Jl. South African Inst. Min and Metall. 64. 197-218.

Salamon, M.D.G. (1964b). Elastic analysis of displacements and stresses induced by the mining of seam or reef deposits –part III. Jl. South African Inst. Min and Metall. 64. 468-500.

Salamon, M.D.G. (1964c). Elastic analysis of displacements and stresses induced by the mining of seam or reef deposits –part IV. Jl. South African Inst. Min and Metall. 65. 319-338.

Schatz, J.F., Zeigler, B.J., Bellman, R.A., Hanson, J.M. and Christianson, M. (1987a). Prediction and interpretation of multiple radial fracture stimulations. Final report to Gas Research Insitute, Chicago, Illinois. 290p.

Schatz, J.F., Ziegler, B.J. and Christianson, M. (1987b). Multiple radial fracturing from a wellbore – experimental and theoretical results. In Proc. 28th US symp. Rock Mech (Ed- H.L. Hartman). Tucson, Arizona, USA. 821-829.

Schaefer, H. (1975). A contribution to the solution of contact problems with the aid of boundary elements. Comput. Methods Appl. Mech. Engrg. 6. 335-54.

Scoble, M.J., Cullen, M. and Makuch, A. (1987). Experimental studies of factors relating to destress blasting. In Proc. 28th U.S. Sypm. Rock Mech Ed. – H.L. Hartman). Tucson, Arizona, USA. 901-908.

Scott, A., Cocker, A., Djordjevic, N., Higgins, M. La Rosa, D., Sarma, K.S. and Wedmaier, R. (1996). Open pit blast design – analysis and optimisation. JKMRC monograph serried in mining and mineral processing 1, Julius Kruttschnitt Mineral Research Centre, The University og Queensland, Australia. 338p.

Sheorey P.R. (1997). Empirical Rock Failure Criteria. A. A. Balkema, Rotterdam. Netherlands. 194p.

Shi, G. (1992). Modeling rock joints, blocks by manifold method. In Proc. 33rd US Sym Rock Mech.(Eds. - Tillerson and Wawersik). Santa Fe, New Maxico. Balkema, Rotterdam. 639-648.

Shockey, D.A., Curran, D.R., Seaman, L., Rosenberg, J.T. and Petersen, C.F. (1974). Fragmentation of rock under dynamic loads. Int. J. Rock Mech. Min. Sci. & Geomech. Abstr. Vol. 11. 303-317.

Simon, R. (1999). Analysis of fault-slip mechanisms in hard rock mining. Unpublished PhD thesis, McGill Univeristy.

Sing, B. and Goel, R.K. (1999). Rock mass classification: a practical approach in civil engineering. Elsevier, Amsterdam. 267p.

Singh, D.P. and Sastry, V.R. (1986). Rock fragmentation by blasting – influence of joint filling material. Jl. Explosives engineering. Vol. 3, No. 5. 18-27.

Sochacki, J.R., Kubicheck, R. George, J., Fletcher, W.R. and Smitheson, S. (1987). Absorbing boundary conditions and surface wave. Geophysics. 52. 60-71.

Starfield, A.M. and Crouch, S.L. (1972). Elastic analysis of single seam extraction, new horizons in rock mechanics. In Proc. 14th US Rock Mech Symp.

Stolarska, M., Chopp, D.L., Moes, N. and Belytschko (2001). Modelling crack growth by level sets in the extended finite element method. Int. Jl. Num. Methods in Engg. 51. 943-960.

Sun, C., Later, D.W. and Chen, G. (2001). Analysis of the effect of borehole size on explosive energy loss in rock blasting. Int. j. Rock Fragmentation and Blasting – FRAGBLAST. 5, 4. 235-46.

Sunu, M.Z., Reed, S.M. and Singh, R.N. (1988). Evaluating of rock parameters on surface mine blasting by finite element analysis. Int. J. surface mining and reclamation. 2. 209-15.

Szuladzinski, G. (1993). Response of rock medium to explosive cavity pressure. In Proc. 4th Int. Symp. Rock Fragmentation by Blasting -FRAGBLAST IV (Ed. H.P. Rossmanith). Vienna. Balekma, Rotterdam. 17-23.

Taylor, L.M., Chen, E.P., Kusmaul, J.S. (1986). Micor-crack induced damage accumulation in brittle rock under dynamic loading. Computer Methodology in Applied Mechanics Engineering. 55. 301-20.

Takewaki, I. (2000). Soil-structure random response reduction via TMD-VD simultaneous use. Comput. Methods Appl. Mech. Engrg. 190. 677-90.

Tang, B (2000). Rockburst control using destress blasting. Unpublished PhD thesis, McGill University.

Tang, B. and Mitri, H. (2001). Numerical modelling of rock preconditioning by destress blasting. Ground Improvement. 5, 2. 57-67.

Taube, A., Krauland, N., Outcherlony, F. and Hakami, H. (1991). Destress blasting Centralmine's (Boliden Group) Laisvall orebody. Report DS 1990:3. SveDeFo, Stockholm, Sweden. (in Swedish).

Thorne, B.J., Hommert, P.J. and Brown, B. (1990). Experimental and computational investigation of the fundamental mechanisms of cratering. In Proc. 3rd Int. Symp. Rock fragmentation by Blasting - FRAGBLAST 3. Brisbane, Australia. 412-23.

Toper, A.Z. (1995). Numerical modelling to investigate the effects of blasting in confined rock simulation of a field study. In Proc. 35th US Symp. Rock Mech (eds. – J. J.K. Daemen and R.A. Schultz). University of Nevada, Reno, USA. Balekma, Rotterdam. 541-546.

Toper, A.Z., Adams, D.J. and Janse Van Rensburg, A.L. (1994). The effects of preconditioning blast in confined rock. In Proc. ISRM Int. Symp. on integral approaches to applied rock mechanics. Santiago, Chile.

Toper, A. Z, Grodner, M., Stewart, R. D. and Lightfoot, N (1997). Preconditioning: A rockburst control technique. In Proc. Rockbursts and seismicity in mines (eds. - S. J. Gibowicz and S. Lasocki), Balkema, Rotterdam. 267-272.

Toper, A.Z., Stewart, R.D., Kullmann, D.H. Grodner, M., Lightfoot, N., Janse van, Rensburg, A.L. and Longmore, P.J. (1998). Develop and implement preconditioning techniques. CSIR Division of mining technology, SIMARC report, GAP 336.

Tvergaard, V. (1997). Studies of void growth in a thin ductile layer between ceramics. Comput. Mech. 20. 184-191.

Tvergaard, V. and Hutchinson, J.W. (1988). Effect of T-Stress on Mode I crack growth resistance in a ductile solid. Int. J. Solids Struct. 31, 6. 823-833.

Udy, L.L. and Lownds, C.M. (1990). The partition of energy in blasting with non-ideal explosives. In Proc. 3rd Int. Symp. Rock Fragmentation by blasting, FRAGBLAST3, Brisbane, Australia. August. 37-43.

Valliapan, S., Lee., I.K., Murti, V., Ang, K.K. and Ross, A.H. (1983). Numerical modelling of rock fragmentation. In Proc. 1st Int. Symp. Rock Frag. By Blasting – FRAGBLAST 1(Ed. – O. stephansson). Balkema, Rotterdam. 375-90.

Van De Steen, B., Vervoort, A. and Napier, J.A.L. (2001). Numerical modelling of fracture initiation and propagation in biaxial tests on rock samples. Int. J. fracture. Vol. 108. 165-191.

Wiebols, G.A. & Cook, N.G.W. (1968). An energy criterion for the strength of rock in polyaxial compression. Int. Jl. Rock Mech. Min. Sci. 5. 529-49.

Whittaker, B.N. (1992). Chapter 13: fracture mechanics applied to rock fragmentation due to blasting, In rock fracture mechanics. Elsevier. 443-480.

Willan, J., Scoble, M. and Pakalnis, V. (1985). Destressing practice in rockburst prone ground. In Proc. 4th Conf. Ground Control in Mining. W. Verginia Univ., WV, USA. 135-147.

Williams, T.J. and Cuvellier, D.J (1988). Report on a field trial of an underhand longwall mining method to alleviate rockburst hazards. In Proc. 2nd Int. Symp. Rockbursts and Seismicity in Mines, Minneapolis, A.A. Balkema, Rotterdam. 349-354.

Winzer, S.R., Anderson, D.A. and Ritter, A.P. (1983). Rock fragmentation by explosives. In proc. 1st Int. symp. Rock frag. By blasting, FRAGBLAST1. Lulea, Sweden. 225-249.

Worsey, P.N., Farmer, I.W. and Matheson, G.D. (1981). The mechanics of pre-split blasting to rock slopes. In Proc. 22nd US Symp. Rock Mech. MIT, Boston, Masschusetts. 205-210.

Xia, L., Shih, C.F. and Hutchinson, J.W. (1995). A computational cell approach to ductile crack growth under large scale yielding conditions. J. Mech. Phys. Solids. 43, 3. 389-413.

Xu, X.P. and Needleman, A. (1994). Numerical simulations of fast crack growth in brittle solids. J. Mech. Phy. Solids. 42. 1397-1434.

Yang, R., Bawden, W.F. and Katsabanis, P.D. (1996). A new constitutive model for blast damage. Int. J. Rock Mech. Min Sci. Geomech Abstr. 33. 245-254.

Zhang, Z.X., Yu, J., Kou, S.Q. and Lindqvist, P.A. (2001). Effects of high temperatures on dynamic rock fracture. Int. J. Rock Mech. Min. Sc. 38, 2. 211-225.

Zienkiewicz, O.C. and Best, B. (1970). Analysis of nonlinear problems in rock mechanics with particular reference to jointed rock systems. In Proc. 2nd ISRM congress. Belgrad. 3. 501-09.

Van De Steen, B., Vervoort, A. and Napier, J.A.L. (2001). Numerical modelling of fracture initiation and propagation in biaxial tests on rock samples. Int. J. fracture. Vol. 108. 165-191.

Wiebols, G.A. & Cook, N.G.W. (1968). An energy criterion for the strength of rock in polyaxial compression. Int. Jl. Rock Mech. Min. Sci. 5. 529-49.

Whittaker, B.N. (1992). Chapter 13: fracture mechanics applied to rock fragmentation due to blasting, In rock fracture mechanics. Elsevier. 443-480.

Willan, J., Scoble, M. and Pakalnis, V. (1985). Destressing practice in rockburst prone ground. In Proc. 4th Conf. Ground Control in Mining. W. Verginia Univ., WV, USA. 135-147.

Williams, T.J. and Cuvellier, D.J (1988). Report on a field trial of an underhand longwall mining method to alleviate rockburst hazards. In Proc. 2nd Int. Symp. Rockbursts and Seismicity in Mines, Minneapolis, A.A. Balkema, Rotterdam. 349-354.

Winzer, S.R., Anderson, D.A. and Ritter, A.P. (1983). Rock fragmentation by explosives. In proc. 1st Int. symp. Rock frag. By blasting, FRAGBLAST1. Lulea, Sweden. 225-249.

Worsey, P.N., Farmer, I.W. and Matheson, G.D. (1981). The mechanics of pre-split blasting to rock slopes. In Proc. 22nd US Symp. Rock Mech. MIT, Boston, Masschusetts. 205-210.

Xia, L., Shih, C.F. and Hutchinson, J.W. (1995). A computational cell approach to ductile crack growth under large scale yielding conditions. J. Mech. Phys. Solids. 43, 3. 389-413.

Xu, X.P. and Needleman, A. (1994). Numerical simulations of fast crack growth in brittle solids. J. Mech. Phy. Solids. 42. 1397-1434.

Yang, R., Bawden, W.F. and Katsabanis, P.D. (1996). A new constitutive model for blast damage. Int. J. Rock Mech. Min Sci. Geomech Abstr. 33. 245-254.

Zhang, Z.X., Yu, J., Kou, S.Q. and Lindqvist, P.A. (2001). Effects of high temperatures on dynamic rock fracture. Int. J. Rock Mech. Min. Sc. 38, 2. 211-225.

Zienkiewicz, O.C. and Best, B. (1970). Analysis of nonlinear problems in rock mechanics with particular reference to jointed rock systems. In Proc. 2nd ISRM congress. Belgrad. 3. 501-09.